University of Huddersfield Repository

Hassin, Osama A.A.

Condition Monitoring of Journal Bearings for Predictive Maintenance Management Based on High Frequency Vibration Analysis

Original Citation

Hassin, Osama A.A. (2017) Condition Monitoring of Journal Bearings for Predictive Maintenance Management Based on High Frequency Vibration Analysis. Doctoral thesis, University of Huddersfield.

This version is available at http://eprints.hud.ac.uk/id/eprint/34161/

CONDITION MONITORING OF JOURNAL BEARINGS FOR PREDICTIVE MAINTENANCE MANAGEMENT BASED ON HIGH FREQUENCY VIBRATION ANALYSIS

OSAMA A. A. HASSIN

A thesis submitted to the University of Huddersfield
in partial fulfilment of the requirements for the degree of
Doctor of Philosophy

School of Computing and Engineering

May 2017

CONTENTS

COPYRIGHT

Copyright statement

DECLARATION

I hereby declare that I am the sole author of this thesis.

No portion of the work referred to in this thesis has been submitted in support of an application for another degree or qualification at this or any other university or other institute of learning.

(Osama Hassin)

DEDICATION

بِسْمِ اللَّهِ الرَّحْمَنِ الرَّحِيمِ

In the Name of Allah, the Most Beneficent, the Most Merciful.

وَمَا تَوْفِيقِي إِلاَّ بِاللَّه

''My Success is only by Allah'' *(The Holy Quran, 11:88)*

The road to success comes through faith, hard work, determination, sacrifice and good supervision.

To my *Fathe*r, *Mother* and *Wife*

To all my relatives and friends

whose affection, love, encouragement and prayers to achieve much success and honour.

ACKNOWLEDGEMENT

All praise and thanks are to **ALLAH** the Almighty for guidance to the right path and for helping me to complete this thesis on time.

I would like to express my sincere gratitude to my supervisors **Prof. Andrew Ball** and **Dr. Fengshou Gu** for the supervision, guidance, advice, patience, motivation, enthusiasm and immense knowledge that they have afforded from the beginning stage of my research up to submission stage.

Also my thanks to all **colleagues** and **visitor researchers** at the Centre for Efficiency and Performance Engineering and many thanks to **staff members** and **technicians** at university of Huddersfield.

I would like also to convey my thanks to **LIBYAN** government for sponsoring and supporting.

Last but not least, my special, profound, and affectionate thanks are due to my **parents** and my partner of this journey, my **wife**. Also, I would especially like to thank and dedicate this thesis to my **brother**, **sisters, uncles and aunts.**

ABSTRACT

Journal bearings are widely used as rotor supports in many machinery systems such as engines, motors, turbines and huge pumps. The journal bearing is simply designed, highly efficient, has a long life, low cost and doesn't fail easily. Based on preventive maintenance strategies, many monitoring techniques are developed for monitoring journal bearings such as lubricant analysis, vibration analysis, noise and acoustic emission analysis. Vibration monitoring techniques have been developed and it can be implemented online or offline without interrupting the machine operations. The vibration phenomena in a journal bearing is complicated which combined between different types of signals created by different sources. To understand this phenomenon, a vibration model is established for fault diagnosis, which includes not only conventional hydrodynamic forces but also excitations of both asperity collisions and churns. However, mis-operations and oil degradation in the journal bearings might cause unexpected and sudden failure which is risky in machines and operators. Consequently, clustering technique is used to investigate into vibration responses of journal bearings for identifying different lubrication regimes as categorised by the classic Stribeck curve. High frequency clustering allows different lubricant oils and different lubrication regimes to be identified appropriately, providing feasible ways for online monitoring of bearing conditions. Additionally, modulation signal bispectrum magnitude results represent the nonlinear vibration responses with two distinctive bifrequency patterns corresponding to instable lubrication and asperity interactions. Using entropy measures, these instable operating conditions are classified to be the low loads cases. Furthermore, average MSB magnitudes are used to differentiate the asperity interactions between asperity collisions and the asperity churns. In addition, the oil starvation of a journal bearing has been found by MSB analysis that the instable frequency can affect the measured vibration responses. Moreover, the structural resonances in the high frequency range can better reflect the separation of different oil levels under wide operating conditions. Finally, As a result of worn bearings, shaft fluctuation increases and asperity collisions decreases. Thus a worn bearing is not all the time good because of instability.

LIST OF FIGURES

LIST OF TABLES

LIST OF FLOWCHARTS

LIST OF ABBREVIATIONS

AC	Alternating current
AR	Autoregressive
BL	Boundary lubrication regime
BM	Bearing modulus
CB	Conventional bispectrum
CBM	Condition based maintenance
CM	Condition monitoring
CP	Power spectrum
cP	Centipoise
cSt	Centistokes
DAS	Data acquisition system
DC	Direct current
DE	Drive end
DFT	Discrete Fourier transform
EN	Entropy
FDT	Failure detection threshold
FFT	Fast Fourier transform
FMECA	Failure mode, effects and criticality analysis
FTA	Fault tree analysis
HL	Hydrodynamic lubrication regime
HOS	Higher order spectra
HP	Horse power
HRC	Hard rubber coupling
HUMS	Health and usage monitoring systems
Hz	Hertz
ISO	International organization for standardization
JG	Jackson and Green
ML	Mixed lubrication regime
MSB	Modulation signal bispectrum
NDE	Non-drive end
OEE	Overall equipment effectiveness
PDF	Probability density function
RB	Rolling bearing
RCM	Reliability-centred maintenance
REM	Review of equipment maintenance

RMS	Root mean square
Rpm	Revolution per minutes
RUL	Remaining useful life
SB	Sliding bearings
SISO	Signal-input signal-output
STFT	Short time Fourier transform
TAN	Total acid number
TBN	Total base number
TPM	Total productive maintenance
TSA	Time synchronous average
TVE	Trust valued estimation
VG	ISO viscosity grade

LIST OF NOTATIONS

C_{ij}	Oil damping	N/m/s
C_{xx}, C_{yy}	direct damping	N/m/s
C_{xy}, C_{yx}	cross-coupled damping	N/m/s
E'	Equivalent elasticity modulus	Pa
E_1, E_2	Young's moduli	Pa
F_a	Asperity collision force	N
F_e	Ecstatic force	N
F_o	Oil force	N
F_p	Asperity churning force	N
F_r	Radial force	N
F_t	Tangential force	N
F_u	Unbalance force	N
F_x	Force x direction	N
F_y	Force y direction	N
K_{ij}	Oil stiffness	N/m
K_{xx}, K_{yy}	direct stiffness	N/m
K_{xy}, K_{yx}	cross-coupled stiffness	N/m
N	Number of data	dimensionless
O_b	Bearing centre	dimensionless
O_j, O_s	Journal or shaft centre	dimensionless
R_a	Roughness surface RMS	m
$R_{v,1}$, $R_{v,2}$	Asperity diameter	m
S	Sommerfeld number	dimensionless
T	Torque	Nm
U	Linear velocity	m/s
U_i	Energy	Nm
$\dot{U}_i$	Power	Nm/s
V_r	Radial velocity	m/s
V_t	Tangential velocity	m/s
W	Static load	N
W_1	Tangential load	N
W_2	Radial load	N
a_i	Asperity diameter	m
c	Radial clearance	m
c_{ij}	Oil damping	dimensionless

c_{xx}, c_{yy}	direct damping	dimensionless
c_{xy}, c_{yx}	cross-coupled damping	dimensionless
D	Distance between surfaces	m
E	Eccentricity	m
e_x	Eccentricity x direction	m
e_y	Eccentricity y direction	m
F	Friction coefficient	dimensionless
f^*	Critical force ratio	dimensionless
h_{max}	Maximum oil film	m
h_{min}	Minimum oil film	m
h_θ	Oil film thickness	m
k_{ij}	Oil stiffness	dimensionless
k_{xx}, k_{yy}	direct stiffness	dimensionless
k_{xy}, k_{yx}	cross-coupled stiffness	dimensionless
L	Journal length	m
m_b	Bearing mass	Kg
m_h	Housing mass	Kg
m_s	Shaft mass	Kg
P	pressure distribution	Pa (N/m^2)
r_b	bearing radius	m
r_j	Journal radius	m
T	Time interval	s
v	Asperity sliding velocity	m/s
v1, v2	Poisson ratios	dimensionless
w^*	Critical interference ratio	dimensionless
$\bar{x}$	Mean of data	any
$x(t)$	Signal in time domain	mV or m/s^2
x_i	Data in particular index	any
z_1, z_2	Heights of asperity summits	m
Λ	Film parameter	dimensionless
δ	Deformation of an asperity	m
ε	Eccentricity ratio	dimensionless
η	Viscosity	Pa.s
θ, Θ	Circumferential angle	rad
ρ	Oil density	Kg/m^3
σ	Standard deviation	any
τ	Shear stress	N/m^2
τ_B	An asperity shear stress	N/m^2
ϕ	attitude angle	rad
Ω	Rotational speed	rad/s

LIST OF PUBLICATIONS

[1] **Hassin, O.**, Yao, A., Gu, F. and Ball, A.(2016) 'Journal Bearing Condition Monitoring based on the Modulation Signal Bispectrum Analysis of Vibrations'. In: the International Congress of Power Transmissions, ICPT 2016, Octoper 27-30 Chongqing, P.R. China.

[2] **Hassin, O.**, Yao, A., Zhang, H., Gu, F. and Ball, A.(2016) 'Monitoring Oil Levels of Journal Bearings based on the Analysis of Vibration Signals'. In: 29th International Congress of Condition Monitoring and Diagnostic Engineering Management, COMADEM, August 20-22 Xi'an, Shaanxi, China.

[3] **Hassin, O.**, Wei, N., Towsyfyan, H., Gu, F. and Ball, A.(2015) 'Journal bearing lubrication monitoring based on spectrum cluster analysis of vibration signals'. In: 28th International Congress of Condition Monitoring and Diagnostic Engineering Management, COMADEM, Buenos Aires, Argentina.

[4] Towsyfyan, H., **Hassin, O.**, Gu, F. and Ball, A.(2014) 'Characterization of Acoustic Emissions from Mechanical Seals for Fault Detection'. BINDT Manchester, UK.

[5] **Hassin**, **O** (2013). 'Different Signal Processing Techniques for Predicting the Condition of Journal Bearings'.

Educational Qualifications:

Master degree (MEng) from University Kebangsaan Malaysia at 2005-2007, grade Excellent

Bachelor degree (BSc) from Tripoli (Al-Fateh) University in Libya at 1995-2000, grad Good

CHAPTER ONE

INTRODUCTION

This chapter presents a general background of condition monitoring in industrial. In addition, it contains research motivations aims, and objectives. Finally, the thesis organisation is outlined.

1.1 Background

The dictionary defines maintenance as : the work of keeping something in proper condition [1]. Also, according to European Standard EN 13306 defines maintenance as: ''the combination of all technical, administrative and managerial actions during the life cycle of an item intended to retain it in, or restore it to, a state in which it can perform the required function [2].'' Maintenance is several taken actions to prevent a plant or component from failure, or to repair degraded equipment. Furthermore, maintenance can be classified into three areas: corrective maintenance, preventive maintenance and predictive maintenance or condition based maintenance [3].

Condition Based Maintenance (CBM) is a technology that attempts to find incipient faults before they become critical, this offers more accurate planning of the preventive maintenance [4]. Additionally, CBM may be defined as maintenance actions based tests, operating, inspection, condition measurement and monitoring. Condition based maintenance is a process that requires technologies and technical skills. Condition indicators such as diagnostic and performance data, operator and maintenance data and design information are integrated to make appropriate decisions about timely maintenance requirements of important equipment [5].

Several philosophies have been developed to establish appropriate maintenance strategies for defined failures. The most important strategy to diagnose the faults before the machine breakdown is condition monitoring. Monitoring is defined as: "Activity, performed either manually or automatically, intended to observe the actual state of an item [6]." Condition monitoring is based on monitoring the performance of a machine within normal operating conditions and analysing the collected information and data either online or offline. Therefore, the main purpose of condition monitoring is to sense a fault that has reached a certain symptomatic level, by providing an exclusive warning before breakdown occurs [7]. Additionally, Condition Monitoring defends faults through high-tech equipment with measurements like pressure, temperature, vibration, etc. CM avoids catastrophic component failure and damages.

Vibration condition monitoring is an affective technique of condition monitoring used to detect a fault in a bearing and a degradation process that have reached a certain damage. Therefore, time domain and frequency domain analyses the vibration signal to predict the

journal bearing faults. High amplitude probably indicates that the component nearly touches failure point.

In industry, there are two common types of bearing widely used; ball bearing and journal bearing. A journal bearing called a sleeve bearing is simply designed containing lubrication which raises the rotating element to prevent metal to metal contacts. Many researchers have studied vibration condition monitoring of ball and roller bearings but limitation studies of journal bearing vibration has been published.

1.2 Research Motivation

A rotating shaft is always the key element of industry, such as pumps and turbines. Journal bearings are used to guide and support shafts to minimise friction. Due to oil starvation, oil contamination, mass centre and mis-operating conditions use of the bearings, defects such as misalignment, unbalance, looseness, friction and wear will develop. There are many techniques used to monitor journal bearing conditions. Accordingly, the most commonly used techniques for monitoring journal bearings is lubrication analysis. Oil analysis techniques are often applied to provide an indication of an unhealthy lubrication. This particular technique allows for offline detection faults. Also it needs special equipment to detect lubrication faults such degradation, oil contamination, improper oil consistency and oil deterioration [3].

The challenge of the condition monitoring is to choose an appropriate technique capable of detecting, classifying and recognising a fault at earlier stages. Also the challenge remains to monitor the system online with low equipment costs.

The first motive is that using online and offline condition monitoring of journal bearings instead of only offline condition monitoring. The vibration signals analysis is the online technique for monitoring journal bearings and it is cost-effective and easy to deployment. In contrast, conventional condition monitoring of journal bearing such as oil analysis causes stopping running the machine, requires especial device, costly and often produce unreliable results due to improper handling of offline samples.

The second motive is to prove that not only low frequency of vibration signals are effective for diagnosing mechanical problems as previous steadies but also the utilisation of high

frequency band vibrations for more accurate detection and diagnosis of incipient problems such as lube oil changes in the journal bearings.

The third motive is to establish a mathematical model of journal bearings to simulate the internal and external excitations of vibration mechanisms. Most of published mathematical model of journal bearings consider only external excitations caused by the shafts.

The fourth motive is that using a proper vibration technique to identify lubricant regimes instead of using limitation methods such as measuring oil film thickness.

The fifth motive is that applying advanced vibration technique to detect mis-operating conditions that cause instable operations and excessive friction of journal bearing.

The sixth motive is to prove that vibration signal analysis is an effective technique to detect a number of simulated faults occurring commonly in journal bearings.

1.3   Research Aim and Objectives

The aim of this research is to develop vibration condition monitoring techniques for an on line predictive maintenance system, which is capable of detecting and diagnosing common mechanical faults present in journal bearings. To achieve this aim the main objectives have been set as follows:

Objective 1: To review maintenance management strategies and discuss condition monitoring techniques and their applications to journal bearings.

Objective 2: To review and evaluate potential vibration signal processing techniques and their parameters of detecting and diagnosing journal bearing faults.

Objective 3: To understand the fundamentals of journal bearing components, operating characteristics and their failure modes.

Objective 4: To establish a mathematical model of journal bearing vibrations to take into account fluid churns and asperity collusions and any likely excitations that correlate with bearing health conditions.

Objective 5: To design and build comprehensive tests rig to test journal bearings with different faults under different lubrication regimes and operating conditions.

Objective 6: To investigate journal bearing vibrations under different operating conditions to discover key characteristics using both conventional methods and the state of the techniques such as clustering and MSB analyses.

Objective 7: To detect and diagnose lubricant starvation of a journal bearing under different operating conditions with proposed analysis methods.

Objective 8: To detect and diagnose worn bearings under different operating conditions with proposed analysis methods.

1.4   Thesis Organization

The thesis is organised into ten chapters which are logically connected to address the research objectives. The contents of each chapter are briefly described below:

Chapter One: This chapter is the introduction which contains background, research motivation, research aim and objectives and thesis organization.

Chapter Two: It begins by discussing the importance of maintenance strategies and management for industrial processes. Additionally, it emphasises condition based maintenance and condition monitoring. Finally, this chapter reviews monitoring techniques of a journal bearing, the subject of this research.

Chapter Three: This chapter introduces some of conventional diagnostic techniques as a method of condition monitoring. It reviews time domain, frequency domain and their features of the vibration signal. In addition, it introduces the concepts of clustering techniques. Also, it investigates waveform signals in time-frequency domain STFT, and in frequency-frequency domain CB and MSB.

Chapter Four: It describes the different types of journal bearing. In addition, this chapter emphasises self-aligning spherical journal bearings that are the subject of this research. Also, it presents journal bearing failure modes.

Chapter Five: It presents the operational principle of journal bearings. In addition, this chapter discusses various new sources of vibrations in journal bearings. Furthermore, it contains the free body, equation of motion and state space method. Finally, it presents natural mode frequency and mode shape of the vibration.

Chapter Six: This chapter describes the experimental facilities; mechanical components of a journal bearing test rig along with measurement instrumentations and assistant devices.

Chapter Seven: This chapter investigates the vibration behaviour of the journal bearing at different operating conditions. Time domain, frequency domain and frequency-frequency domain are used to investigate the bearing vibration. Spectrum clustering technique of vibration signals have been differentiated between different lubricant regimes. Furthermore, MSB has been detected the instable operations and high friction operations.

Chapter Eight: This chapter introduces fault detections that are caused by oil starvation. Vibration signals have been analysed by time, frequency and doubled frequency domains. Mean values of MSB at specific frequency band positively detect starvation of lubricant.

Chapter Nine: This chapter introduces detections of a worn journal bearing. Wear of journal bearing reduces the vibration but on the other hand shaft fluctuating increases. MSB technique confidently diagnoses worn journal bearings.

Chapter Ten: It presents the conclusions and reviews the achievements of the project against the aim and objectives. These are followed by the contribution to knowledge made by the research, novelties and future works.

CHAPTER TWO

CONDITION MONITORING BASED MAINTENANCE

This chapter aims to provide a review of maintenance management and strategies. Additionally, to express condition based maintenance and condition monitoring techniques. Finally, it presents a review of journal bearing monitoring techniques such as human senses, temperature monitoring, lubrication analysis and vibration investigation which is the most important technique in this research.

2.1 Introduction

Several definitions of maintenance have been suggested in literature. Traditionally, maintenance is described as the process of repairing broken objects. Furthermore, maintenance is known to keep equipment performance and systems' efficiencies in order during the lifetime of the incorporated components [8]. Moreover, through regular maintenance, a system is able to achieve the required availability, reliability, product quality, and safety requirements. Equipment reliability plays an important role not only in achievement generation and safety goals, but also in the reduction of production costs and helps to avoid catastrophic failures that require extensive downtime and labour/parts costs.

Maintenance management includes the planning, organisation, monitoring and evaluation of the required activities and their costs. A good maintenance management system necessitates knowledgeable and experienced staff, together with appropriate condition monitoring techniques. It can provide a higher quality of asset life by reducing the number of breakdowns and operating costs. In general, maintenance management includes five different strategic aspects, namely, the maintenance methodology, support processes, organisation and work structuring, comparable culture and general management policy [9].

2.2 Maintenance Strategies

Three basic types of maintenance plans, namely: corrective, preventive and predictive maintenance have been described. Preventive and predictive maintenance represent two proactive actions by which equipment breakdowns can be avoided. This is can be achieved by adding an advanced maintenance strategy to maintenance programs [10].

2.2.1 Corrective Maintenance

The corrective maintenance is a measure undertaken, when a breakdown or a clear fault in the machine has occurred. The terminology standard SS-EN 13306 (2001) defines a corrective maintenance, as maintenance carried out after fault recognition and intended to put an item into a state in which it can perform a specific function. Corrective maintenance can be delayed if the consequences of a fault on some items have no impact on the complete plant. Furthermore, corrective maintenance is applied when the fault items are small costs, non-critical, no safety risk, quickly recognized, and fast and easy repair. Minimal planning is required for corrective maintenance and the process is simple due to that fewer staff are

required. Because of unpredictable failure, the process poses a safety risk to employees and other assets.

2.2.2 Preventive Maintenance

The preventive maintenance type has been defined as (SS-EN 13306, 2001) maintenance carried out at predetermined intervals or according to some prescribed criteria. This type of maintenance is intended to reduce the probability of failure or the degradation of the functioning of an item. Moreover, preventive maintenance prevents a system from faults or breakdowns on items that have direct effected on the overall system function. Furthermore, any fault that might be hazardous to safety, environment, or any other specified maintenance rules must be immediately maintained.

The first category of preventive maintenance includes periodic maintenance, which may be done at calendar intervals (i.e. after a specified number of operating cycles) or after a certain number of operating hours. These intervals are planned based on the manufacturers' recommendations and industry operating experience [5]. In general, preventive maintenance can be considered as the following:

- time based preventive maintenance,

In a time-based maintenance strategy, assets are periodically inspected, serviced and cleaned, with parts replaced in an effort to prevent sudden failure. It doesn't require extensive training and lower long term costs compared with breakdown maintenance. In contrast parts are often replaced before end of life, which costs more than waiting until they fail.

- condition based maintenance

Condition monitoring is the process of determining the condition of an asset while it is in operation, through techniques. Condition monitoring of assets is essential to minimising the failure and downtime Problems with components can be identified prior to failure and repairs can be carried out on assets to keep them running with minimal disruption to productivity. Long-term costs are very low compared with the cost of failure.

- predictive maintenance

In a predictive maintenance strategy, engineers predict when equipment failure might happen, and then perform maintenance to keep machines in operation. Predictive

maintenance uses a process to check the status of assets on a regular basis. It keeps the cost and time of machine downtime minimum. Probability of failure is reduced and reliability improved, nevertheless, higher cost than more basic maintenance strategies [11].

2.3   Maintenance Management Strategies

There are several techniques identifying appropriate maintenance management strategies. The most common approaches are Fault Tree Analysis (FTA), Failure Mode, Effects and Criticality Analysis (FMECA) and Reliability-Centred Maintenance (RCM) [12]. Another recently developed technique is the Review of Equipment Maintenance (REM) [13] and Total Productive Maintenance (TPM).

2.3.1   Fault Tree Analysis

FTA is an analytical technique that is used for reliability, maintainability and safety analysis. Clemens stated that FTA is a pathway graphic of a system that leads to a predictable and undesirable loss event [14]. The pathways use standard logic symbols to connect events and conditions together. The FTA method uses a full mathematical modelling process to analyse the whole system on a top down to combine a series of lower events. From the top event to the next levels of events, the basic causes are identified.

2.3.2   Failure Modes, Effects, and Criticality Analysis

FMECA is used to help with the safety and reliability of products in a wide range of applications [15]. FMECA is usually used to evaluate the reliability of a system by considering the possible failure modes and assessing their effects on the performance of complex electrical and mechanical systems [16]. The result of performing FMECA leads to the development of optimal preventive, predictive and proactive maintenance strategies [13]. Moreover, FMECA process depends on the operator experience and/or failure history details. The application of FMECA upon a system is divided into four main steps. The first step is to describe the functions of that system. The second step is to perform each function by assessing the reliability of every mode of each function in order to determine the different modes of operation. The third step is to determine how each failure mode affects the failure modes of other items in the plant. The final step is to evaluate the severity, frequency and cost of each failure mode and the corresponding critical values [13].

2.3.3   Reliability of Centred Maintenance

RCM is known as the maintenance requirement of any physical asset to continue achieving its planned operating functions [17]. RCM is a method for developing and selecting maintenance design alternatives based on safety and operational and economic criteria [17]. Essentially, the RCM investigates the system, failures of the system functions, and prevents these failures. The RCM methodology structure establishes the criticality of the defined failure modes for each plant item.

2.3.4   Review of Equipment Maintenance

REM has been developed to ensure that the application of revised maintenance practices such as condition monitoring are aligned with the company's business objectives to deliver a maximum cost benefit [18], [13]. The aim of REM is to develop an optimised maintenance plan by reviewing the existing maintenance schedule and history.

2.3.5   Total Productive Maintenance

Total Productive Maintenance (TPM) is one of the maintenance programmes that aims to increase production and safety [13]. TPM has two goals: zero breakdowns and zero defects. The TPM maintenance approach seeks to improve equipment performance and to avoid equipment failures [10]. Availability, performance and quality rate are typical measures of the improvements or not of the machine. TPM does not only consider maintenance, but also takes an essential and important approach towards the improvement of industrial plants [19]. The performance of a TPM is indicated by the Overall Equipment Effectiveness (OEE) as,

$$OEE = Availability \times Performance \times Quality\ Rate \tag{2.1}$$

2.4   Maintenance Optimisation

Plant maintenance optimisation is a plan to generate a work environment that optimises the use of resources, maintenance processes, employee skills and the technology for meeting the maintenance objectives [5]. Therefore, plant maintenance optimisation is important to inspect the maintenance processing, management methodology, work culture, skill set, the work force motivation and the effectiveness of technology.

2.4.1   Management and Business Culture

A positive work environment can potentially increase the levels of optimisation in plant maintenance. This can be realised through setting goals, providing strong leadership, promoting good communication, therefore establishing an organisation where roles and responsibilities are clearly identified and assigned [5].

2.4.2   Maintenance Processes

By using the industry's best maintenance practices, it is possible to minimise the impact on production and to maximise the workforce utilisation, which both contribute to the optimisation of plant maintenance. These goals are usually accomplished by good time management skills so that maintenance can be prioritised, planned and executed. The work carried out must be documented clearly to be reviewed later for prevention purposes. These processes are applicable to daily works, both planned and unplanned outage works and works arisen from proactive activities such as engineering projects [5].

2.4.3   People Skills and Work Culture

By having a qualified and skilled workforce, together with a safe work environment, the plant maintenance optimisation can be further strengthened. This can be achieved by providing an effective staff training programme and implementing a human performance initiative that entail positive behaviours and values [5].

2.4.4   Technologies

By the uptake and utilisation of cost effective technologies, plant maintenance can be further optimised. This is achieved by the maximisation of the maintenance process efficiencies, providing periodic information on equipment conditions and artificially learning from the mistakes made. The adoption of such technologies can enable access to multiple plants and department data sources and allow for the findings, recommendations and corrective actions to be shared. The common technology tools include process data, enterprise wide clouding software and numerous condition monitoring technologies [5].

2.5   Condition Based Maintenance

In the past, maintenance techniques were time-based with scheduled running schemes. Later on, modern maintainers attempted to change the maintenance technology from a time-based to a condition-based approach [20]. The condition-based maintenance (CBM) involves a set an of maintenance actions that are based on real-time or near real-time monitoring and assessment of the equipment condition. The input data is often provided by embedded sensors and/or from external tests using portable measurement equipment [20]. CBM, in general, aims to determine whether there are any problems and tries to assess the severity of the problem and how the system can continue its operation without failure. The assessment can go down to components level for a more detailed diagnosis of the failure causes [6]. In general, CBM is a more accurate planning technique than the preventive maintenance [3].

CBM is a maintenance programme, which depends on the collected information by the condition monitoring system. Condition monitoring encompasses a huge range of technologies and can be used to detect failure symptoms that would otherwise go undetected [13]. The main goal of CBM is to predict the system's performance capability without failure. This is realised through continuous detection of the system's current state [21]. Moreover, CBM executes maintenance only when required to prevent system failure and plant shutdown. As a result, CBM can minimise the time-consuming and expensive maintenance procedures by reducing the unnecessary planned maintenance tasks. Furthermore, CBM can make a more efficient use of the equipment and improve the equipment's performance and service lifetime [22].

In order to realise a robust CBM strategy, it is imperative to have an understanding of the failure behaviours in a particular equipment. The time taken for a potential failure (P) to develop into a functional failure (F) is called the P-F interval. Figure 2.1 shows an exemplary P-F curve, demonstrating the fault behaviour of a particular parameter. In this curve, the start point of the failure is shown by point (P), which is practically difficult to detect. Therefore, point (P_1) is usually considered as the indicator for a potential failure. The point at which system failure occurs is commonly referred to as the functional failure point and is shown by (F) in Figure 2.1. As a result, almost all of the necessary analysis and maintenance duties are confined to the range 'P_1-F' [23]. Within the resulting *P-F*

interval, there exists other failure indication points, $(P_2 \rightarrow P_n)$, for which there are many algorithms that can be developed to detect them.
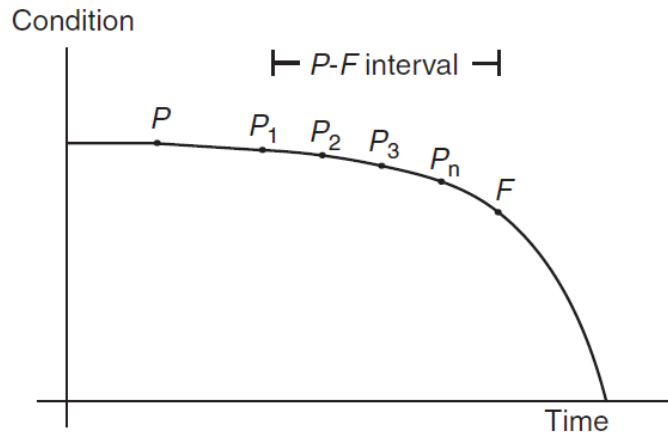
Figure 2.1 P-F curve

The failure detection threshold (FDT) is another critical point that can be used in detection and determination of system failure. In FDT-based scheme, the percentage of a component's elapsed service lifetime is calculated and used as a trigger point for an approaching failure. For example, a processed FDT value of 0.7 implies that there is only a probability of 0.3 for a failure to occur over system's lifetime. Since this parameter is largely related to the underlying system characteristics, it can therefore vary from one system to another [23].

2.6 Condition Based Maintenance System Architectures

The condition-based maintenance system architecture was initially developed to address the need for a standard, which could handle the flow of information between different software components in a system. In this architecture, there are seven different layers, all representatives of the functional capabilities, which can be specified as:

1. Sensor Module,
2. Signal Processing,
3. Condition Monitor,
4. Health Assessment (diagnosis),
5. Prognostics,
6. Decision Support,
7. Presentation.

The sensor module feeds the system with signals, which are processed into features in the signal processing block. The condition monitor detects abnormal features, which are classified in the health assessment module. The prognostic module then predicts the remaining useful life. By taking into consideration all of the tasks mentioned so far, the decision support module can take the right decisions to schedule the maintenance actions.

Another, yet similar, architecture for condition-based maintenance is the so-called prognostic system, in which focus has been put on diagnostics and prognostics. In such a system, the output is a time-to-failure parameter that can be utilised in order to perform the condition-based maintenance actions. The diagnostician assesses the real condition of an item through an on-line sensor measurement. Its purpose is to decide about the existence of impending or incipient failure conditions [12].

2.6.1   Data Collection

Data collection involves the process of gathering all the system function information. The main stream of system information is sourced by the relevant data that are acquired either online or offline. The data are usually collected by using the process control system, vibration measurements, oil sampling and other methods. There are also two other types of data that are gathered during data collection, namely, the failure data and the process data. The failure data are the direct-address failure modes of a system component including vibration features and lubrication oil constituents. On the other hand, process data that are related to components such as pressure, flow and temperature, can be used to identify the mode of failure.

2.6.2   Data Processing Analysis

The data can be analysed by direct comparison methods, by looking at outstanding behaviour or by other methods, depending on the failure modes. Furthermore, two types of models are used for analysing the data; analytical and statistical models. Analytical models or cause-effect models are failure mode expressions, whereas statistical models estimate the probability of failure and the expected time to failure by analysing historical data [12].

The main part of a CBM programme, the process of data collection from the physical components and saving them appropriately. The collected data are classified into two main groups of event data and condition monitoring data. Event data includes the historical

information such as installation, breakdown, overhaul, etc. and the causing factors and/or a record of what has been done to the targeted asset, such as, minor repair, preventive maintenance, oil change, etc. [24]. In contrast, the condition monitoring data is used to identify the current state or condition of the physical asset's health [24].

Through advances in computer and sensor technologies in the recent years, data acquisition for CBM has become more plausible to achieve. In a CBM application, both event data and condition monitoring data are equally important [24]. However, in practice, more attention is usually given to the collection of condition monitoring data, and in some cases, totally neglecting the event data collection [24].

Upon the collection of the required data, a sequence of data processing steps are conducted. The first step is data cleaning to avoid any errors due to data anomalies. Then, the clean data is used for analysis and modelling purposes. In the case of event data, the error can stem from a number of sources including the human factor. In contrast, condition monitoring data errors are caused as a result of faulty or inaccurate sensors. The data cleaning algorithms are usually complex and require significant amounts of computational power. The next step in the sequence is data analysis, which is largely dependent on the type of data being analysed. Researchers have developed various models and advanced algorithms that are particularly useful in understanding and interpretation of different datasets [24].

2.6.3 Diagnostics

Diagnostic is a process used to detect the failure mode and the failing component in a system. Furthermore, the goal of a diagnostic is to measure a certain indication of the failure function. Diagnosis is done after or during the process of fault occurring. Therefore, by conducting fault diagnosis, it is possible to improve the system's reliability and availability. Fault diagnosis provides a more detailed insight into the nature and locality of the failure. The obtained information can be used to reduce system downtime and help schedule an adequate maintenance procedure [25]. By running a fault diagnosis at an early stage, it is possible to avoid any sudden failure of the overall system.

Machine fault diagnostic involves the transfer of the information obtained in the observation and/or features space into machine fault space [24]. The transition process between the spaces is usually referred to as pattern recognitions. Pattern recognition uses

graphical tools such as power spectra, phase spectra, spectrum graphs, AR spectra, spectrograms, wavelet spectrograms, wavelet phase graphs and many others. These techniques are usually time consuming. Therefore, automatic pattern recognition algorithms are more desirable, which can be achieved by sorting the signals according to the information and/or features extracted from them.

2.6.4 Prognostics

Prognostic is the process of predicting the remaining useful lifetime of a component or estimating the probability of failure of that component [26]. In order to achieve a zero-downtime performance more efficiently, prognostic approaches are preferred to diagnostics [24]. Moreover, to predict the future failure of a system, prognostic tools are employed to analyse the current and previous history of the system's operating conditions. Also, the rate of deviation in the operating conditions from the normal conditions can be closely monitored to realise a prognostic tool.

Some of the major challenges in any system prognosis are the time-to-failure or remaining useful life (RUL) prediction, condition monitoring interval prediction and trust valued estimation (TVE) [23]. The RUL is often used to predict how long the component can operate before a failure occurs. On the other hand, condition monitoring interval is applied to predict the probability of a machine to operate with no fault nor failure up to a certain time in future.

Prognostic is different to a CBM in a sense that CBM determines any impending failure based on the physically measured indicators installed on the equipment, whereas, prognostic has the additional capability of predicting the equipment's RUL. Furthermore, prognostic tends to factor any external stress factors such as environment causes when calculating the RUL. This is considered as another way of enhancing the condition-monitoring information. A prognostic system is able to predict a failure well in advance, when compared to the predictions made by the current state condition of the equipment [20].

2.6.5 Decision Making

A decision is made based on the data collection and data analysis. These decisions may change in operating routines or in maintenance planning, which may result in a need for

additional data collection and analysis. Upon the completion of a decision, reports can be generated and archived for future references, and evaluations can be performed if required [26].

2.6.6 Usage-based Modelling

The concepts of CBM was developed in parallel to Health and Usage Monitoring Systems (HUMS). HUMS can detect an early fault and the need for maintenance actions, through processing of signals from sensors and inspections [27]. The RUL of a component can be predicted through usage-based models. In this approach, the model verification process plays an important role in developing and deploying the usage-based model [23].

Flowchart 2.1 shows the maintenance strategies and shows that CBM implementation will develop the management of the maintenance system.
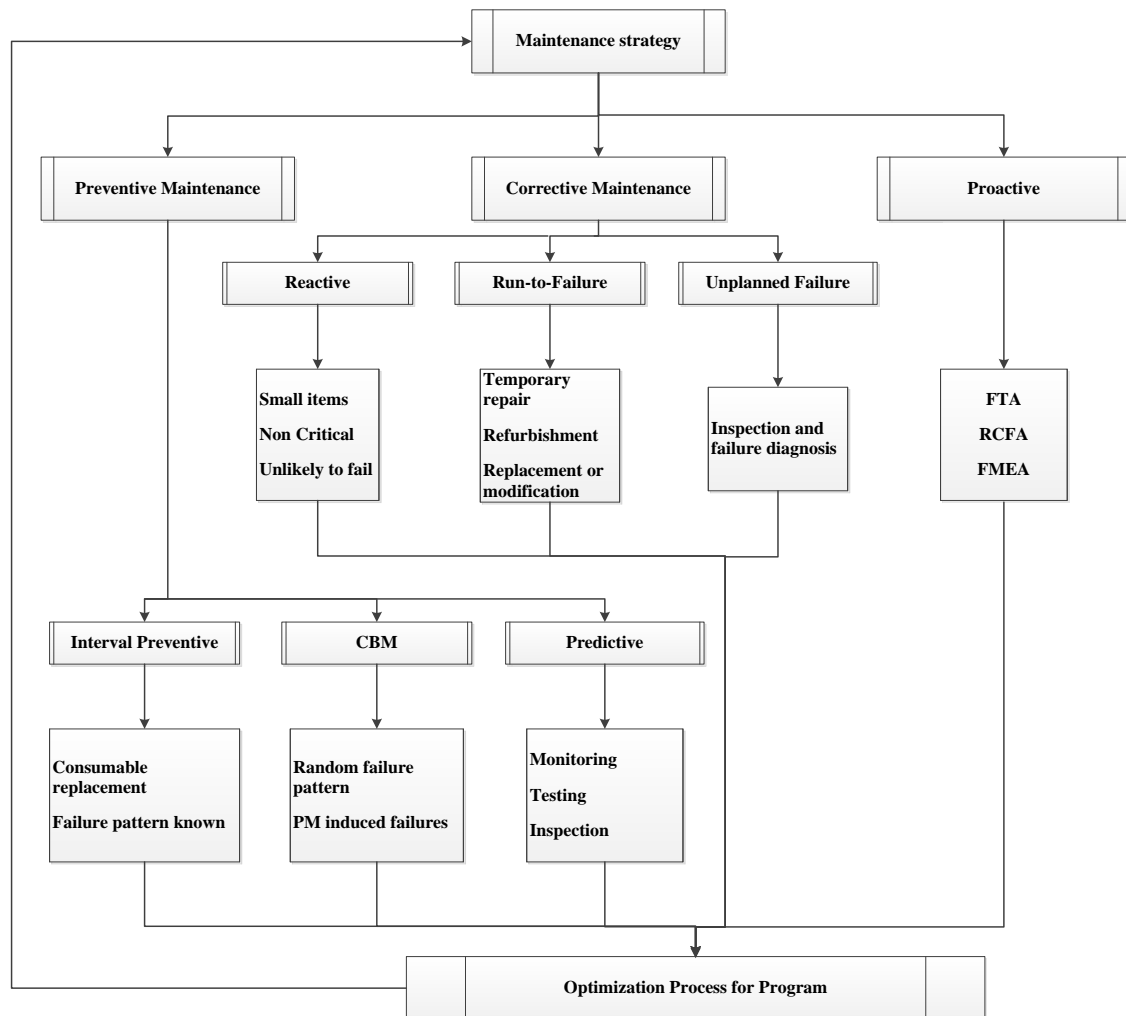
Flowchart 2.1 Maintenance strategies

2.7   Condition Monitoring

The condition monitoring includes the monitoring of the operating behaviour of a system and analysing the gathered information and data. Furthermore, by making analysis of failure symptoms, CM identifies when and how the item is probable to fail. Condition monitoring encompasses a huge range of technologies and can be used to detect failure symptoms that would otherwise go undetected [9]. The condition monitoring serves a main purpose, to detect faults or degradation processes that have reached a certain characteristic threshold. By producing an indication of the type and severity of the fault in advance, the condition monitoring prevents any functional breakdown during the operation.

2.7.1   Temperature Measurement

Temperature measurement techniques such as, temperature-indicating paint and thermography are employed to detect potential temperature-related failures in equipment. A temperature change in a healthy equipment can be associated with several problems, such as, excessive mechanical friction (e.g., faulty bearings, inadequate lubrication), degraded heat transfer (e.g., fouling in a heat exchanger) and poor electrical connections (e.g., loose, corroded or oxidized connections) [3].

2.7.2   Dynamic Monitoring

In contrast to condition monitoring, dynamic monitoring makes use of techniques such as spectrum analysis and shock pulse analysis to measure and interpret the energy emitted from the equipment in the form of a vibration, pulse or acoustic wave. By analysing the vibration characteristics of particular mechanical equipment, faults and damages caused by wear, imbalance and misalignment can be detected [3].

2.7.3   Oil Analysis

Oil analysis techniques such as ferrography and particle counter testing are often applied on different types of oil (e.g. lubrication, hydraulic or insulation oils) to provide an indication of an unhealthy machine. This particular technique allows for the detection of faults such as degradation, oil contamination, improper oil consistency and oil deterioration. The research carried out on oil analysis can be categorised into one of the following areas:

- Fluid Physical Properties (Viscosity, appearance).

- Fluid Chemical Properties (TBN, TAN, additives, contamination, % water).

- Machine Health (wear metals associated with plant components) [3].

2.7.4 Corrosion Monitoring

Corrosion monitoring techniques include coupon testing and corrometer testing, which are useful in detection of the extent, rate and state (i.e. active or passive) of corrosion in a particular material [3].

2.7.5 Non-destructive Testing

Non-destructive procedures such as X-ray and ultrasonic are online tests that are considered as non-invasive and can be implemented whilst the equipment is under operation [3].

2.7.6 Electrical Testing and Monitoring

Electrical condition-monitoring techniques include high potential testing and power signature analysis. These methods involve measuring and analysing various electrical properties of a system, such as, resistance, conductivity, dielectric strength and potential variations. Subsequently, the results can be used to detect problems related to insulation deterioration, broken motor rotor bars and shorted motor stator laminations [3].

2.7.7 Observation and Surveillance

Observation and surveillance techniques rely heavily on human sensory capabilities to carry out visual, audio and touch inspections. These methods can be employed to enhance the performance of other condition-monitoring techniques. By using the observation and surveillance techniques the following problems can be identified:

- Loose/worn parts,

- Leaking equipment,

- Poor electrical/pipe connections,

- Steam leaks,

- Pressure relief valve leaks,

- Surface roughness changes [3].

2.8 Condition-Monitoring Data Category

There are three main categories of condition monitoring data. First one is value-type data, which is the data collected at a specific time intervals and are single-valued. Examples of this type of data include oil analysis data, temperature, pressure and humidity [24]. The second category includes time-series data, which are known as waveform-type data. Examples of such data-type include vibration and acoustic data [24]. The final data-type is multidimensional variables that are collected at specific times. The most common examples of such data-type are image data from infrared thermographs, X-ray images and visual images [24]. The data processing for waveform and multidimensional data-types may also be referred to as signal processing in literature. Signal processing techniques allow for an improvement of current diagnostic and prognostic tools.

2.9 Review of Journal Bearing Monitoring Techniques

In industry there are many monitoring techniques are used for monitoring bearings. Beside the human senses, the most common techniques used to detect the fault symptoms in journal bearing are lubricant analysis, acoustic emission, acoustic and vibration response [28].

2.9.1 The Human Senses Monitoring

The human sensory capabilities of touch, vision, smell and hearing are the first simple methods used to monitor the bearing. These simplest techniques can help detect bearing problems such as oil leakage, looseness, and worn parts. Because of the fact that human senses are able to detect large faults, a maintenance manager should increase the personnel ability to sense the changeable between healthy and faulty conditions [29]. Mobley argued that this method should be included in modern monitoring systems even though the human senses cannot detect small faults [30].

2.9.2 Temperature Monitoring

Temperature is one of the most important measured parameters that can monitor the bearing conditions. Additionally, Temperature provides acquiring information on bearing situation and operating conditions for understanding all phenomena affecting bearings. Temperature fluctuates very fast during machine startup and shutdown, thus temperature monitoring

during these actions is very useful for obtaining information on machine performance [31]. In industry, most bearings are designed to operate well under certain temperature thus if measured temperature accessed this certain value the warning message appears.

2.9.3   Lubrication Analysis

Lubricant monitoring system is one of the important method of predictive maintenance. Many early failure symptoms of machine and its components can be detected by Lubricant contamination analysis and lubricant film measurement. In hydrodynamic journal bearing lubricant the oil film thickness measurement is a clue factor, thus film thickness measurement is a great method to monitor bearing condition. In practice, it is very difficult to measure the lubrication oil films less than 0.1 micron by general method [32]. Moreover, lubricant particular analysis is a vital method to detect the bearing conditions by counting the number of contamination such as, dust, fibre, water, metal worn away from machine components. Furthermore, a laser technology now days is used to count and identify the lubricant particulars and present images to show the size of this contamination. Q230 is a one of the laser device used to know the types, numbers and sizes of contamination, more details in Chapter 5. Additionally, high temperature, water contamination concentration and long-time running are influenced the lubricant viscosity, thus monitoring viscosity is a general parameter used for lubricant monitoring analysis. Viscosity analysis such as Total Acid Number (TAN), Total Base Number (TBN) and water contaminant concentration test are useful methods but they usually are implemented offline with costly instruments.

2.9.4   Vibration Analysis

In the mid-1950s, modern vibration monitoring has been established with the development and application of basic vibration sensors [33]. World Industry depends on vibration analysis to prevent a comprehensive information to identify various defects. Because machine faults produce certain signals, a good vibration condition monitoring program can diagnose and predict a variety of problems [7]. Also it helps to identify the cause and allows appropriate corrective maintenance before equipment failure.

Condition vibration monitoring is to understand signals, which are generated during machine operating. Vibration generated from a machine contains vital information on the health of the machine and can be used to identify developing problems. Appling condition vibration monitoring over the bearing can detect initial faults at an early stage [34].

Frequent vibration monitoring can detect deteriorating or defective bearings, worn bearing, mechanical looseness, misalignment and unbalance of a rotor [35].

Vibration analysis technique is capable to detect, diagnose and prognoses faults within the bearing. The vibration measurements are expressed as displacement, velocity or acceleration based on which transducers are in use. Mobley stated the accelerometer is the best vibration transducers for determining the vibration force of a machine [30]. Piezoelectric accelerometer transducers, nowadays, are the most widely used for vibration measurements of stationary machine elements. The benefits of accelerometers are linearity over a wide frequency range from a few Hz to tens of kHz, dynamic ranges, stable over a long period of time, don't need a power supply and they are not affected by hazardous environments. Finally, they are comparatively strong and reliable and their output signals can be integrated to give velocity and displacement.

Vibration analysis is one of the most commonly used condition monitoring techniques in industry to diagnose different faults such as unbalance, misalignment, looseness, rolling bearing defects, electrical faults, cavitation and surface cracks. The raw measurement of a vibration sensor displays the data as a function of time and amplitude. The amplitude is measuring the severity of vibration in the bearing. Thus a certain value of amplitude is used as a safety limit to warn of

 the risk if the vibration reaches this boundary [28]. Fast Fourier Transform was developed as an effective function for quickly mimicking the frequently changed signal. The frequency domain indicates the source of the vibration. Many applications in industry, the frequency could tell which component of a machine has failed whereas each source has a unique hertz. For example, each components of ball bearing or gear box generate a unique calculated frequency which related to geometry and rotational speed [36, 37]. Journal bearings are simply designed as they contain only journal rotating inside stationary component. Due to that, there aren't any calculated frequencies except low frequency related to rotating speed. Many vibration monitoring investigations of journal bearing focused on mechanical instabilities such as unbalance, misalignment and looseness in rotor bearing systems which are the most commonly faults have been studied by many researchers [38, 39]. However, limited works have been found addressing the diagnostics of journal bearings itself.

The main external excitation force in rotating part of a journal bearing is mechanical unbalance which causes a pure sinusoid and therefore generates a peak at 1 time rpm. Unbalance is a centrifugal force that occurs when the shaft mass in not centred. Misalignment is the most common vibration problem. Unlike unbalance and misalignment, their vibration symptom frequencies related to shaft frequency and its harmonics. Furthermore, looseness occurs when the hydrodynamic forces throw the journal away from the stationary bearing. Thus, high clearance causes looseness of bearing which generates more of a square wave than a sinusoid wave [38, 39]. From looseness vibration signals, shaft frequency and some harmonics will appear in spectrum analysis of vibration signal. In cases of severe looseness, it is stretched all the way across the spectrum and half-harmonics are even generated (1 time, 2 times, 3 times, 4 times, 5 times, 6 times, etc.) rpm [38]. Moreover, in reality the journal has a noncircular shape which leads to kinematic constraints regarding the movement of the shaft journals on the oil film of the sleeve bearings and therefore excite the rotor dynamic system to vibrate [40]. Moreover, fluid instabilities such as oil whirl and whip are common faults in journal bearings [41]. Furthermore, oil whirl frequency is between 0.38 to 0.48 rpm [42]. At hydrodynamic regime, thick oil film, journal bearings vibration sources would be generated by mechanical problems touch the rotating shaft and stationary bearing [43].

The sources of journal bearing vibration are not only from rotor system but also at boundary and mixed regimes, thin oil film, asperity churns and collisions cause random vibration. Two frictional effects, surface asperity collision and viscos shearing are sources to produce random high frequency of vibration responses [28]. High random frequency bands of the vibration signals are occurred by topography surfaces of shaft and bearing [44]. Parno stated that wear and asperity collisions response to produce high frequencies from 1000Hz to 10,000Hz [45]. He found that the mean value of vibration signals for the high frequency band (6kHz-40kHz) is a promising method of detecting scratched journal bearing because vibration responses are well related to micro asperity collisions [28]. Additionally, Parno et al (2010) found experimentally that vibration signals in low frequency range (< 2000Hz) contains useful information for monitoring journal bearing and that distant vibration sources [46].

Finally, the interaction between periodic responses and resonant responses produce modulation signals. Modulation signal bispectrum (MSB) is an advanced technique used

to analyse the vibration of composite signals which are a combination of the information and the carrier signals. In this research it is found that, MSB magnitude of specific frequency band is useful to identify vibrations caused by internal and external excitations.

Different monitoring techniques are developed to detect, diagnose bearing faults at early stages so that preventive maintenance actions can be taken timely to avoid any possible major failures. The commonly techniques for condition monitoring of journal bearings are lubricant analysis, temperature measurement, and vibro-acoustic analysis. However, the vibration techniques can provide more timely detection results.

2.10 Summary

Maintenance is a key to not only improving the availability and reliability of equipment, but also increasing the product and safety measure qualities. Moreover, maintenance can help reduce production costs that might arise from catastrophic failures, which will bring the production process into a halt until repair has been carried out. Maintenance optimisation is as important. It allows for an enhancement of the work environment and optimise the utilised resources by motivating the workers' skills and improving their skills [5]. This is accomplished by turning from time-based maintenance to condition-based maintenance.

The tasks undertaken by condition-based maintenance methods can be planned in advance by using the condition data collected from a system to help detect incipient failures and avoid system shutdown. The process of data collection and analysis is called condition monitoring, whose goal is to enable a better understanding of the causes and effects of different failure mechanisms and their deterioration patterns [6].

CBM is a form of condition-based monitoring that takes on a proactive approach to maintenance by foreseeing incipient failures [20]. The CBM approach to maintenance combines the predictive and measures usually taken by traditional calendar- or run-based maintenance programmes with real-time monitoring techniques to significantly optimise the utilisation and efficiency of the available resources.

CHAPTER THREE

VIBRATION ANALYSIS BASED CONDITION MONITORING

This chapter provides an overview of vibration signal processing techniques commonly used for the condition monitoring of journal bearings. First, it presents different types of signals together with key waveform or time domain parameters such as RMS, kurtosis, histogram, entropy and hierarchical clustering approaches in measuring complicated vibration signals from the bearing. Then it reviews methods implemented in the frequency domain, and more advanced ones including joint time-frequency and frequency-frequency (bispectrum) analysis.

3.1 Introduction

Vibration based condition monitoring refers to the use of transducer for detection and investigation of system characteristics in the time, frequency or coupled domains [47]. Vibration analysis is one of the main techniques used to diagnose and predict various defects [3]. Each faults in industry machine produces an unique signal which can be monitored by certain monitoring techniques [7]. Vibration analysis offers vital information about machinery faults for future monitoring purpose and appropriate maintenance procedure. A component vibration in a machine provides real information on the health of the machine and these vibration signals can be used to detect developing problems. Regular vibration monitoring can detect misalignment and unbalance of a rotor, mechanical looseness, worn bearing etc.

Condition vibration monitoring is to understand signals, which generate during machine operating. Whenever operating conditions change, the signal changes too. Appling condition vibration monitoring over the bearing can detect faults at an early stage. As the result of bearing condition monitoring, breakdown or catastrophe of the machine can be avoided by indicating the occurrence of such failures. Vibration monitoring used to detect a fault in a self-aligning journal bearing, or a degradation process, that has reached a certain symptomatic level and to provide an indication of the abnormality in time before the breakdown occurs [48].

As reviewed earlier, high periodic vibration is induced by rotating journal inside stationary bearing. Moreover, high random vibration is encouraged by direct contact of shaft and bearing surfaces. Furthermore, the combination between periodic and random signals will generate modulation signals.

3.2 Signal Types

A signal is a time history used to convey information of a physical phenomenon. Signals examples such as human speech, temperature, voltage, pressure, vibration and etc. are indicated as a function of time. The examination physical phenomenon is often translated into an electrical voltage or current by a transducer. Mathematically, signals are functions of one or more independent variables [49]. Examples of independent variables used to represent signals are time, frequency, time-frequency or frequency-frequency domains.

Various signals generated by machine components in healthy and faulty condition. Flowchart 3.1 presents the common types of signals.

Signal types
Stationary — Non-Stationary
Deterministic — Random — Continuous — Transient
Periodic — Quasi-Periodic
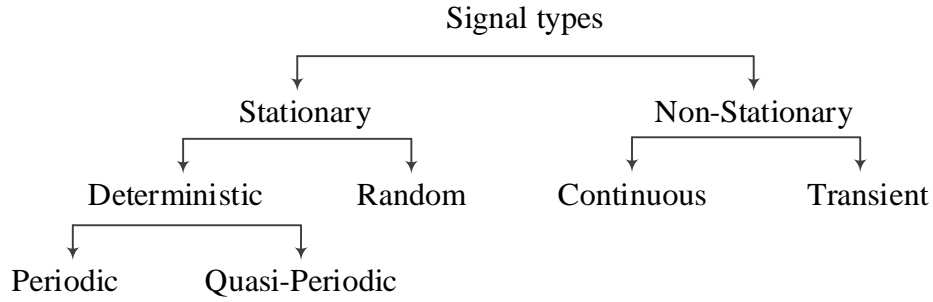
Flowchart 3.1 Classification of signals [50]

3.3   Vibration Responses of a Self-Aligning Journal Bearing

The journal bearing effect the vibration responses and produce periodic and random signals. Periodic signal is correlated to angular speed of the shaft. Common faults in journal bearing such as misaligning, looseness, oil whirl and whip and unbalance are deterministic signals. Otherwise, the most random signals mainly come from asperity collisions and fluid shear [51]. Coupling between different types of signal produce modulation signals.

3.3.1   Linear: Summation of Periodic and Random

Periodic signals are defined as those whose waveform repeats exactly at regular time intervals [52]. The mathematical definition of periodic signal *x(t)* is expressed as

$$x(t) = x(t + nT_0) \quad n = \pm 1, \pm 2, \pm 3, ... \tag{3.1}$$

at all-time *t* and for some positive constant T_0.
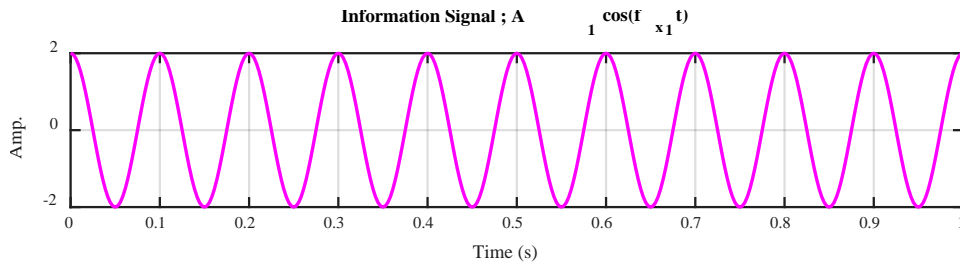
Figure 3.1 Periodic signal

Conversely, random signals are values cannot be expected their behaviour [49]. Random signals cannot be modelled accurately [49]. Random signals are commonly characterized by statistical values such as standard deviations, means, kurtosis, root mean square and etc. [49].

Carrier Signal ; Random Signal
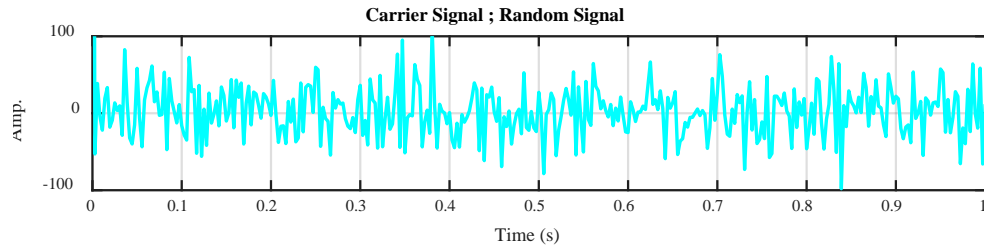
Figure 3.2 Random signal

Linear Signal ; Information Signal + Carrier Signal
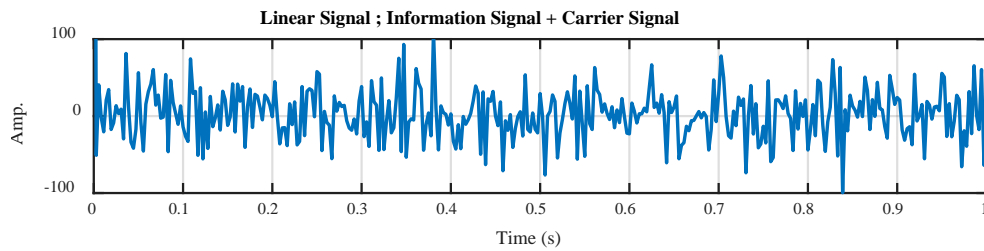
Figure 3.3 Summation of periodic and random signals

3.3.2 Nonlinear: Multiplication of periodic and Random

Modulation is the process of involving low frequency information signal such as shaft frequency, into a high frequency, carrier wave such as fault frequency by changing the characteristics of either its amplitude, frequency, or phase angle.

Amplitude Modulation Signal ; Information Signal * Carrier Signal
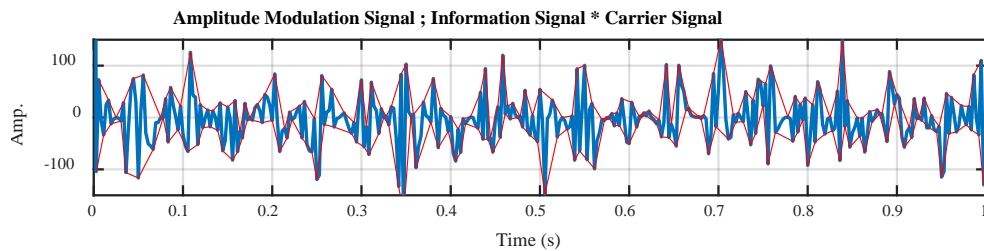
Figure 3.4 Modulation signal

3.4   Waveform Analysis

The vibration signals and acoustic emissions are the most common waveform data in condition monitoring. Other waveform data are ultrasonic signals, motor current, partial discharge, etc. The categories of waveform data analysis are time domain analysis, frequency domain analysis, time–frequency analysis and frequency-frequency analysis [24].

3.4.1   Time Domain Analysis

Time domain is the analysis of raw signals data with respect to time. Time-domain analysis is directly based on the time waveform itself. Figure 3.2 and Figure 3.3 show how a signal changes with time. Vibration data plotted as amplitude versus time is referred to as a time domain data profile [53]. Because time domain analysis gives the behaviour of the signal over time, a prediction signal can be modulated. Furthermore, traditional time domain features determine signals characteristics such as descriptive statistics (peak, mean, peak to peak interval and high order statistics such as skewness, root mean square, kurtosis, etc.). Baydar et al. researched the use of a multivariate statistical technique for analysis of the time waveform signals in gear fault diagnostics [54]. Time synchronous average (TSA) is one of the most popular time-domain analysis approaches using the ensemble average of the raw signal over a number of evolutions. The purpose of using TSA is to enhance the signal components of interest by removing or reducing noise and effects from other sources [24]. Additionally, there are many other time domain analysis techniques to analyse waveform data for machinery fault diagnostics. Wang et al. discussed three non-linear diagnostic methods for fault diagnosis of rotating machine, known as 1) pseudo-phase portrait, 2) singular spectrum analysis and 3) correlation dimension [55], which show certain effectiveness in discriminating different fault conditions in rolling bearings.

3.4.2   Waveform Parameters

3.4.2.1   Root Mean Square

RMS is a statistical parameter of the magnitude of a varying quantity. It is especially useful when varieties are positive and negative and when mean value equals zero. The root mean square (RMS) value of a vibration signal is a time analysis feature that is the measure of the power content in the vibration signature. It is a good indicator of the energy amount

contained in the vibration signal and it measures the overall intensity of wide-band vibration. Even though it is good for tracking faults in a machine, this feature does not provide any information about which part in a machine has failed [56]. The following equation is used to calculate the root mean square value of a vibration signal:

$$RMS = \sqrt{\frac{1}{N} * \sum_{i=1}^{N} \left(x_i - \overline{x} \right)^2} \qquad (3.2)$$

3.4.2.2 Kurtosis

Kurtosis is a common statistic parameter used in condition monitoring to detect symptoms of machine faults because it is sensitive to sharp variant signals, such as impulses. The larger value of kurtosis means the impulse signal is great. Kurtosis is defined as the fourth moment of the distribution and measures the relative peakedness or flatness of a distribution as compared to a normal distribution. Kurtosis provides a measure of the size of the tails of distribution and is used as an indicator of major peaks in a set of data. The equation for kurtosis is given by:

$$K_u = \frac{1}{N} \sum_{i=1}^{N} \left[\frac{x_i - \overline{x}}{\sigma} \right]^4 - 3 \qquad (3.3)$$

where x_i is the raw time series at point n, $\overline{x}$ is the mean of the data, σ is the standard deviation of the data, and N is the total number of data points [56].

3.4.2.3 Probability Density Functions

The concept of probability density function (PDF) is to distribute the expected amplitudes of the data. This amplitude distribution may be described by its mean ($\overline{x}$) and standard deviation (σ). The true density function (f) of the underlying data (x) may be achieved by substituting x and σ into the expression for the normal distribution given by:

$$f(x) = \frac{1}{\sigma\sqrt{2\pi}} e^{\left(\frac{-(x_i - \overline{x})}{2\sigma} \right)^2} \qquad (3.4)$$

The probability of the raw data is given by the integral of this variable's density over a particular range. Moreover, the probability is given by the area under the density function distribution but it should limit by vertical lines between the lowest and highest value of the range. The probability density of a healthy bearing signal takes shape of Gaussian

distribution (bell shaped), whereas a faulty bearing signal results in non-Gaussian distribution with dominant tails due to increasing in level of acceleration. Therefore, a PDF has two fundamental properties, it is larger than or equal to zero and the integral of a PDF over its limited range equal one. In practical applications, the PDF estimate the proportion of amplitudes of a data signal which is known amplitude density estimation.

$$Pr[a \leq X \leq b] = \int_a^b f(x)\,dx \quad and \ f(x) \geq 0\,for\ all\ x \tag{3.5}$$

3.4.3   Histogram and Entropy

Entropy value is used in various engineering applications to measure uncertainty of a random variable data [57]. The Shannon entropy is in fact the expected value of the information content in bit of information. It is also equivalent to the average missing information when the value of the random variable is unknown [58]. The entropy H_x of a signal variable x with continuous probability $f_x(x)$ is defined as:

$$H_x = -\int_{-\infty}^{+\infty} f_x(x) log f_x(x)\,dx \tag{3.6}$$

3.5   Spectrum Analysis

Frequency domain is a method used to analyse data. Frequency domain data are achieved by adapting time domain data using a mathematical technique known as Fast Fourier Transform (FFT). The Fast Fourier Transformation is used to convert any shape signal into infinite number of sinusoidal waves. FFT allows each vibration component of a complex spectrum to be shown as a discrete frequency peak. Frequency domain graph shows how much of the signal lies within each given frequency band over a range of frequencies.

A Fast Fourier Transform (FFT) is an algorithm to compute the discrete Fourier transform (DFT) and it's inverse. A Fourier transform converts time to frequency and vice versa.

Continuous-Time Fourier Transform:

$$F(j\omega) = \int_{-\infty}^{+\infty} f(t)\,e^{-i\omega t}\,dt \tag{3.7}$$

Discrete- Time Fourier Transform:

$$X\left(e^{i\omega t}\right) = \sum_{n=-\infty}^{+\infty} x[n]e^{-i\omega t} \tag{3.8}$$

3.5.1   Spectral Centroid

The spectrum centroid is obtained by evaluating the centre of spectrum using the Fourier transforms' frequency and magnitude information. The individual centroid of a spectral frame is defined as the average frequency weighted by amplitudes, divided by the sum of the amplitudes;

$$Centroid = \frac{\sum_{n=1}^{N} f(n) X(n)}{\sum_{n=1}^{N} X(n)} \tag{3.9}$$

3.6   Hierarchical Cluster Technique

Cluster analysis techniques are used to characterise the complicated data sets. Cluster scheme represents a large data set, easily understood by grouping data into small subsets that provide a brief description, similarities and differences, of the data patterns were provided [59]. There are many approaches in implementing cluster analysis. A hierarchical clustering method is a more popular one that works by grouping data set into a tree of clusters [60]. A common agglomerative hierarchical clustering method starts by placing each object in its own cluster and then merges these atomic clusters into larger and larger clusters, until all the objects are in a single cluster or until certain termination conditions are satisfied. The single (complete) linkage algorithm measures the similarity between two clusters as the similarity of the closest (farthest) pair of data points belonging to different clusters, merges the two clusters having the minimum distance and repeats the merging process until all the objects are eventually merged to form one cluster. The Ward's minimum variance algorithm is often used to merge the two clusters that will result in the smallest increase in the value of the sum-of-squares variance. At each clustering step, all possible mergers of two clusters are tried. The sum-of-squares variance is computed for each and the one with the smallest value is selected. This means that cluster analysis allows a set of representative signals to be determined based on only incomplete knowledge of signal mechanisms.

3.7 Time-Frequency Analysis

Time–frequency analysis investigates waveform signals in both time and frequency domain at same time. Time–frequency analysis has been developed for non-stationary waveform signals which are very common when machinery faults occur.

The most popular time–frequency analysis is short-time Fourier transform (STFT) or spectrogram (the power of STFT) [24]. Another transform for time frequency analysis is the wavelet transform. Wavelet theory has been rapidly developed in the past decade and has wide application [24].

$$STFT\left(t',u\right)=\int_{t}\left[f\left(t\right).W\left(t-t'\right)\right].e^{-i2\pi ut}\ dt \tag{3.10}$$

A window should be narrow enough to make sure that the portion of the signal falling within the window is stationary.

Wide window → good frequency resolution, poor time resolution.

Narrow window → good time resolution, poor frequency resolution.
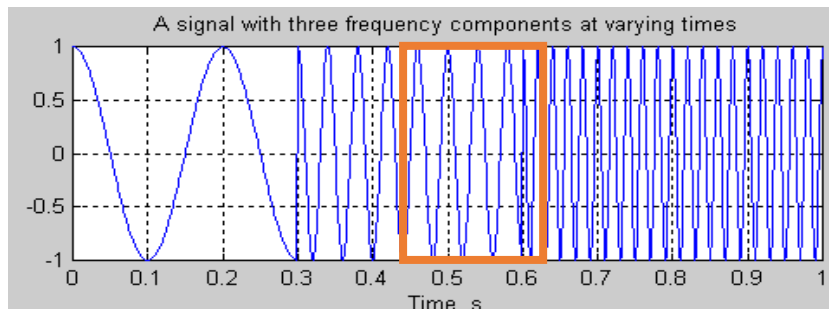
Figure 3.5 STFT window is stationary portion of the signal [61]

3.8 Bispectrum Analysis

3.8.1 Conventional Bispectrum

Many researchers have been used the higher order spectra (HOS) since 1980. Conventional bispectrum analysis is common technique used to take the measurements of the third order of signal statistics.

$$B(f_c, f_x) = E\left\{ X(f_c)X(f_x)X^*(f_c + f_x) \right\} \tag{3.11}$$

where f_x is information frequency; f_c is the carrier frequency, $f_c + f_x$ is the higher sideband frequency.

The third order measure is a complex quantity, in that it contains both magnitude and phase information about the original time signal $x(t)$.

$$b^2{}_{CB}(f_x, f_c) = \frac{|B_{MS}(f_x, f_c)|^2}{E\left\langle |X(f_c)X(f_x)|^2 \right\rangle E\left\langle |X(f_c + f_x)|^2 \right\rangle} \tag{3.12}$$

3.8.2 Modulation Signal Bispectrum

Understandably, high forces of external and internal excitation will generate massive vibration responses. Mechanical problem will produce vibration with low frequency correlated to shaft rotational speed. Contrast, random asperity collisions will produce high band frequency. Due to a low frequency, information signal, is superimposed on a high frequency, carrier signal, modulation signal of vibration will be generated in journal bearing. Figure 3.6 up to Figure 3.9 show the concept of modulation signal.
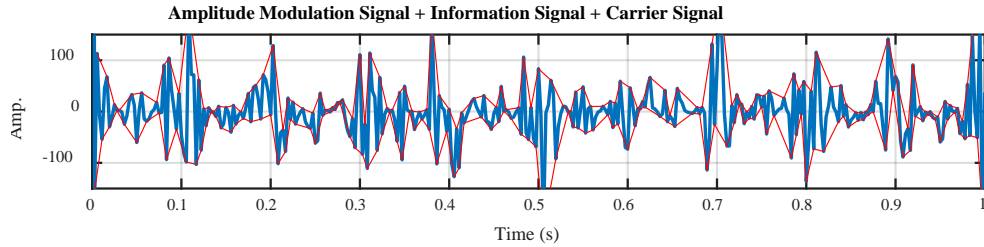
Figure 3.6 Time domain of modulation signal
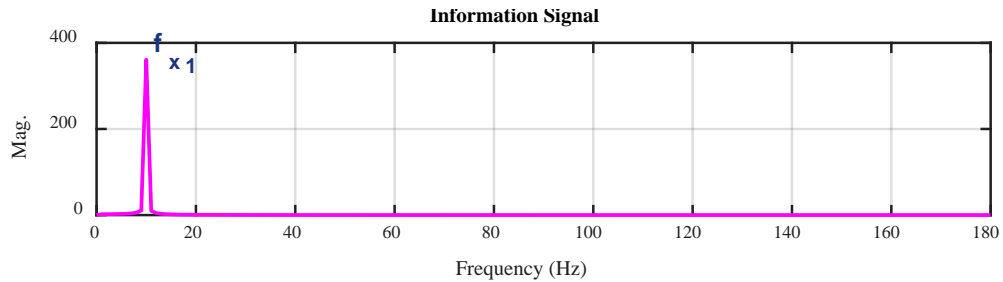
Figure 3.7 Frequency domain of information signal
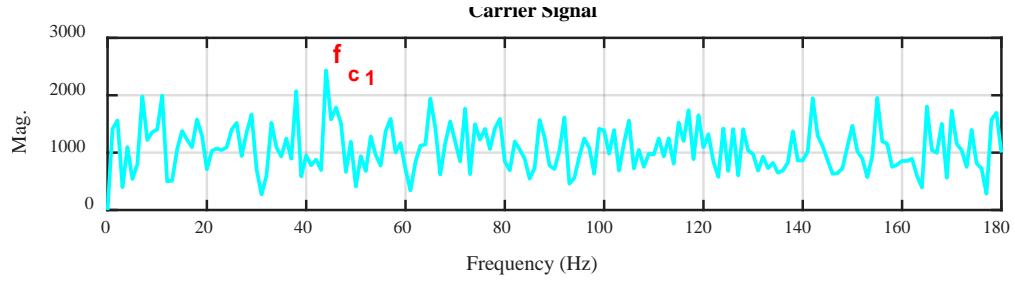
Figure 3.8 Frequency domain of carrier signal
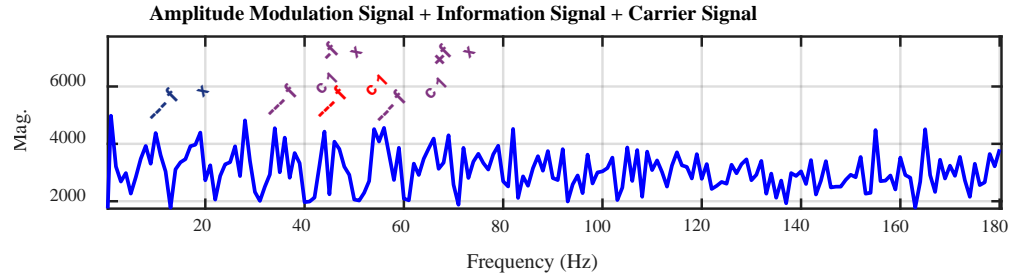
Figure 3.9 Frequency domain of modulation signal

Bispectrum is a non-linearity signal generated when two waves interact. MSB is used to detect a coupling signal between shaft frequencies and the wideband compounds.

The modulation signal of vibration is formed two components, periodic and random signal. Thus, it is anticipated that bispectrum can give a more accurate representation of the vibration signal for mis-operating diagnosis. [62]

The Discrete Fourier Transform (DFT) $X(f)$ of a vibration signal $x(t)$ is defined in the form of Modulation Signal Bispectrum (MSB),

$$B_{MS}(f_x, f_c) = E\left\langle X(f_c + f_x)X(f_c - f_x)X^*(f_c)X^*(f_c)\right\rangle \tag{3.13}$$

The phase relationship of MSB is

$$\begin{aligned}\varphi_{MS}(f_x, f_c) &= \varphi(f_c + f_x) + \varphi(f_c - f_x) - \varphi(f_c) - \varphi(f_c)\\ &= \varphi(f_x) + \varphi(-f_x)\end{aligned} \tag{3.14}$$

where f_x is information frequency; f_c is the carrier frequency, $f_c + f_x$ and $f_c - f_x$ are the higher and lower sideband frequencies respectively. It takes into account both $f_c + f_x$

and $f_c - f_x$ simultaneously in Equation (3.13) for quantifying the nonlinear effects of modulation signals. If they are due to the modulation effect between f_c and f_x, a bispectral peak will be at bifrequency $B_{MS}(f_x, f_c)$. On the other hand, if these components such as various noises are not coupled but have random distribution, their magnitude of MSB will be close to zero. In this way, the wideband noise and periodic components of vibration signals can be suppressed effectively so that the discrete components relating modulation effects can be represented sparsely and characterised more accurately.

A normalized form of MSB, also named as modulated signal bicoherence, is introduced as,

$$b^2{}_{MS}\left(f_x, f_c\right) = \frac{|B_{MS}(f_x, f_c)|^2}{E\left\langle|X\left(f_c\right)X\left(f_c\right)X^*\left(f_c\right)X^*\left(f_c\right)|^2\right\rangle E\left\langle|X\left(f_c + f_x\right)X\left(f_c - f_x\right)|^2\right\rangle} \quad (3.15)$$

It is to measure the degree of coupling between four components against noise influences, in the same way as the conventional bicoherence. [63] [64]

3.9   Summary

Vibration generated from the journal bearing contains vital information on the causes and affective of bearing vibration. When the journal bearing is operating it creates certain vibration signals that reflect its case. Thus, vibration analysis can detect bearing failure modes such as wiping, scoring, fatigue and wear.

This chapter provides the concept of condition monitoring vibration signal processing of journal bearings. First, it presents different types of signals and further parameters. Also it presents the vibration response concept and equations of journal bearing in time domain, frequency domain, time-frequency domain and frequency-frequency domain. additionally, it has focused to show the idea of modulation signals and MSB technique which used to decompose this type of signals.

CHAPTER FOUR

JOURNAL BEARING TYPES, APPLICATIONS AND COMMON FAULTS

This chapter provides a review of journal bearing classifications and its basic operating mechanisms. More details are presented to the self-aligning spherical journal bearing which is a case of this research for its ease of modifications with less influence of shaft errors. In addition, it presents different types of common failure modes occurring in journal bearings.

4.1   Introduction

A bearing is an important component of a machine used to allow rotation at a certain part, also for supporting radial and axial loads. The bearings are used in rotating machinery to minimise friction between shaft and bearing surfaces. There are many types of bearings. Basically, the classifications of bearings are sliding bearings (SB) and rolling bearing (RB). Furthermore, a sliding bearing is a bearing that does not contain any rotating element as rolling bearing shown in Figure 4.1. It reduces friction through lubricating oils between the bearing and the shaft, rather than the rolling elements of the roller bearing.
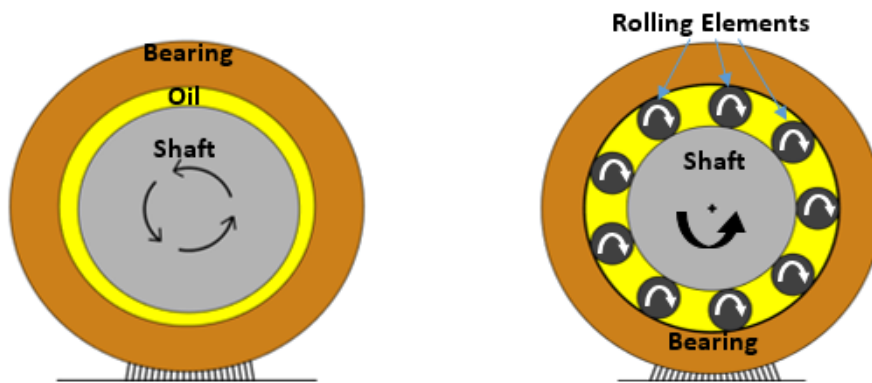
Figure 4.1 A) Sliding bearing B) Rolling bearing

This thesis focuses on a sliding bearing named as plain, sleeve or journal bearing. The journal is the part of the shaft supported by a bearing seen Figure 4.2.
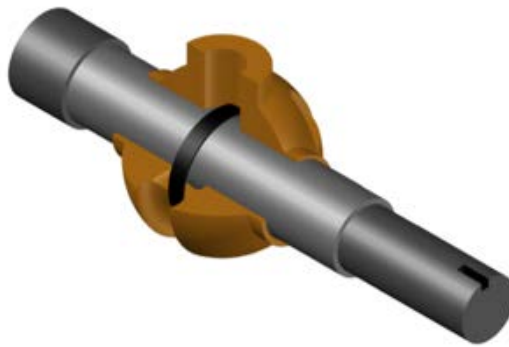
Figure 4.2 Journal bearing section

4.2   Types of Journal Bearings

The simplest type of plain bearing is a hole in a machine to support the rotated shaft in it, Figure 4.3. However, the plain bearings can be divided into plain radial bearings, plain

thrust bearings, combination radial and thrust bearings, tilting pad bearings and self-aligning spherical journal bearings, which are the subject of this research.
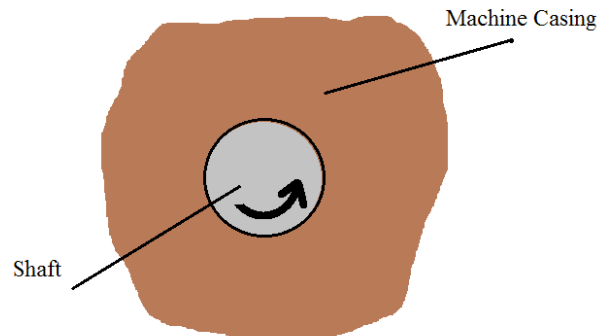
Figure 4.3 Simplest journal bearing [65]

4.2.1 Plain Radial Bearings

A cylinder or tube bearings (bush) is the modest type of plain bearings as shown in Figure 4.4 and Figure 4.5. The methods of making them are casting a solid material or wrapping a strip of the bush material into a cylinder. Bushes are made from bronze and other softer material. Also, they are easy to replace if excessive wear occurs.

Figure 4.4 Machined or cast bushes [66]   Figure 4.5 Wrapped bushes [67]

Another type of bush bearings are a split bearing (two halves), it is used where a one-piece bush cannot be fitted, Figure 4.6 The split bearings are designed to support radial loads only and it is used in larger power transmission devices. The split bearings help to reduce noise, vibration, friction and the maintenance required. Most split bearings have two halves; also there are multi-part more than two parts.

Figure 4.6 Split bearing [68]

4.2.2   Plain Thrust Bearings

A thrust journal bearing is used to support a shaft in an axial load as shown Figure 4.7. Also, Plain thrust bearings have a pad, or pads, on which a shoulder or the end of the shaft can push.
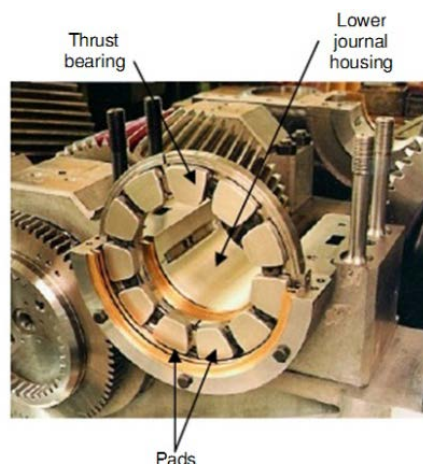
Figure 4.7 Thrust axial bearings [65]

4.2.3   Combination Bearings

Some bearings are designed to support radial and thrust loads such as a flanged bush. Figure 4.8 shows a pair of flanged bushes.
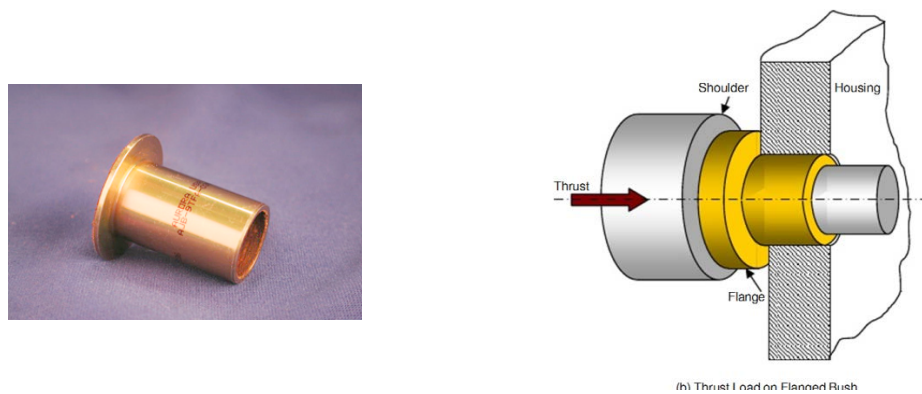
Figure 4.8 Flanged bush [65]

4.2.4 Tilting-pad Bearings

Tilting-pad bearings are a more developed design of a plain bearing. Also, the lubrication system is better. In Figure 4.9 presents examples of three types of tilting-pad bearings. They are designed for high-speed operation and low or medium loads [65].
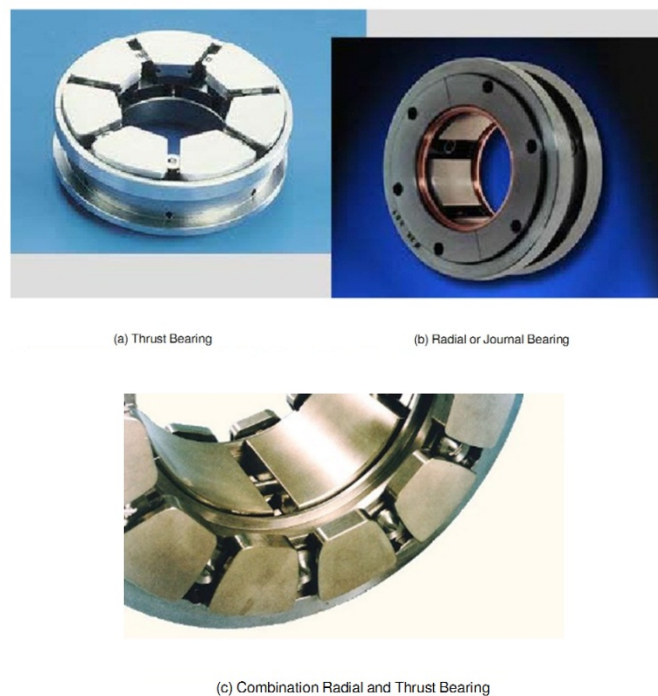
Figure 4.9 Tilting-pad bearings [65]

4.3 Self-aligning Plain Bearings

The main issue of this research is a self-aligning spherical journal bearing designed for high speeds such as fans and similar applications. Figure 4.10 shows the components of a

self-aligning spherical journal bearing. A journal bearing has a spherical part that allows some movement to adjust bearing's position, this is why it is called self-aligning. Bearing housing holds the journal bearing in place, which has a hole where the shaft fitted. Also the ring oil, surrounds the shaft, spreads the lubricant into the gap between the shaft and the bearing [69].
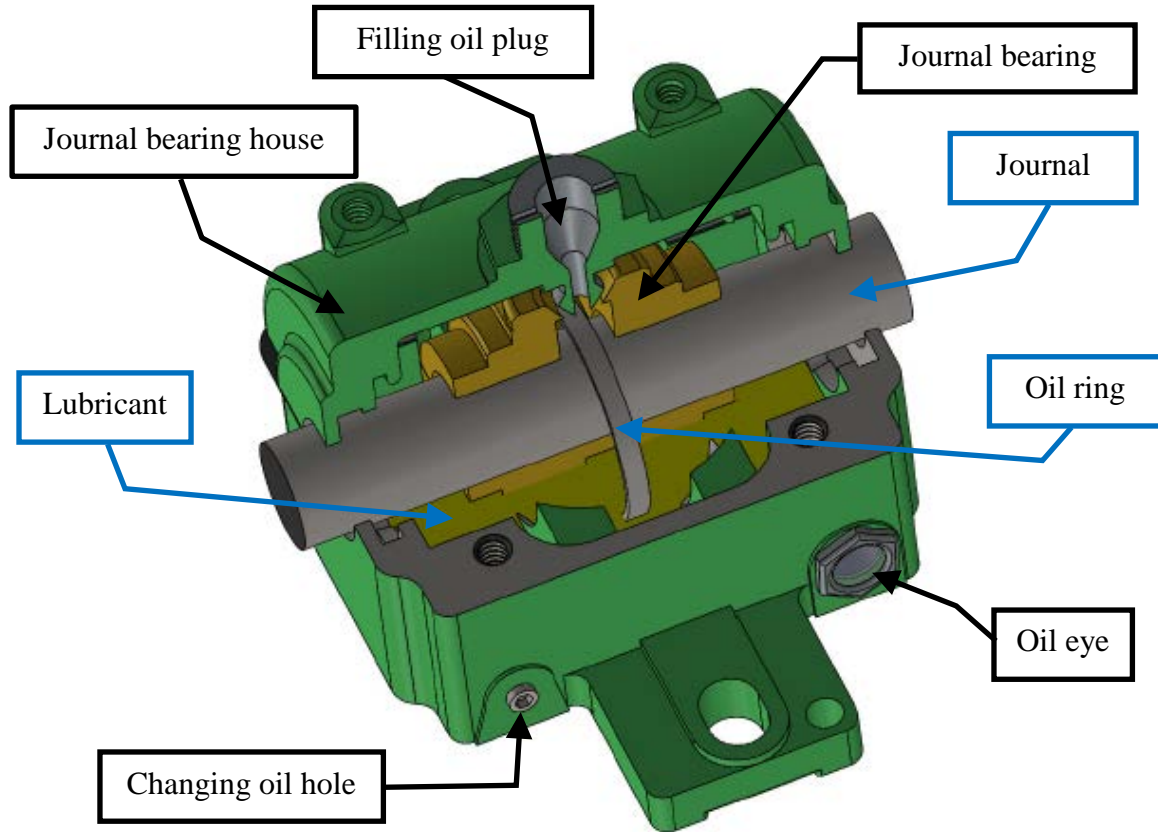
Figure 4.10 Self-aligning spherical journal bearing section

The self-aligning spherical journal bearing does three main jobs. Figure 4.11 and Figure 4.12 illustrate that the journal bearing locates the moving part and guides its motion, and supports the weight of the moving part. Figure 4.13 shows how a Journal bearing allows for some bending of the shaft as a result of misalignment [65].
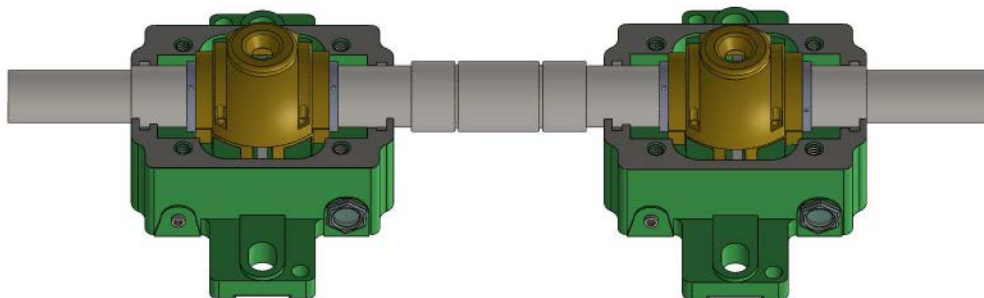
Figure 4.11 Journal bearing uses to locate and guide
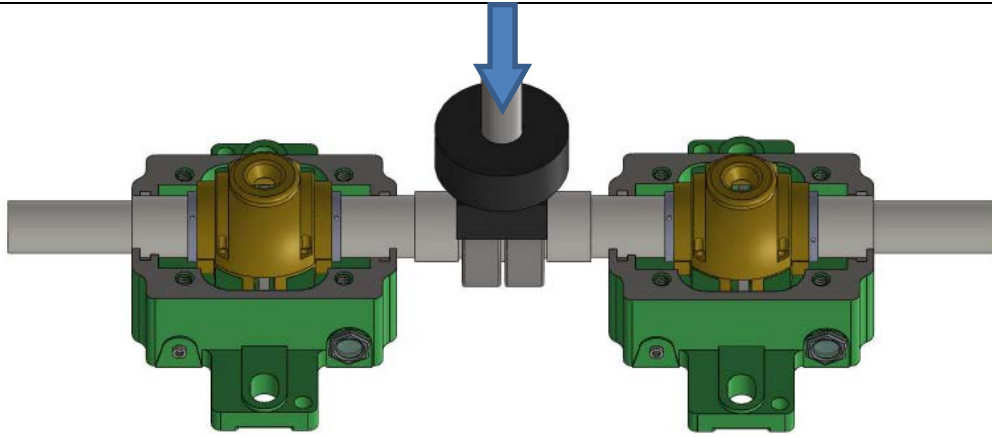
Figure 4.12 Journal bearing supports loads
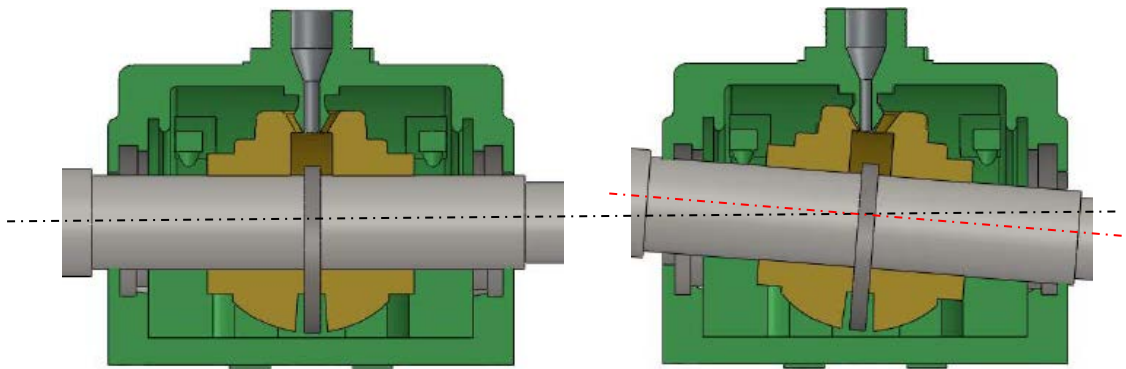
Figure 4.13 Journal bearing reduces misalignment

4.4   Material Selection of Journal Bearing

Journal bearing materials must have a low coefficient of friction to reduce wear and its hardness must be softer than the shaft hardness to wear away the bearing surface before it wears the shaft. Furthermore, there are other characteristics of plain bearing materials that must be considered: density, melting point, conductivity, strength, corrosion resistance and fatigue resistance. Two other special properties that are used only for plain-bearing materials are: Embeddability is the ability to allow small particles of dirt, etc., to be embedded or sink into the material so that they do not scratch the shaft. Softer materials have better embeddability than harder materials and conformability is the ability of the material to adjust to very slight misalignment of the shaft. Softer materials also have better conformability than harder materials. Most plain bearings are made of metals, but some are made of polymers (plastic materials) or have parts made of these materials. It is not possible to get one material that has all the properties needed for a bearing. For this reason, it is important that the material has the properties most needed for the conditions under which the bearing operates. Two important operating conditions are radial load and running speed.

Metals used in a plain bearing can be divided into two main types' pure metals such as iron, copper, zinc and tin and alloys such as brass, bronze and white metal. Other metal alloys used for bearings are aluminium, tin alloys and copper or bronze lead alloys.

A self-aligning spherical journal bearing material is LG2 Leaded Gunmetal Bronze, offering excellent machinability, excellent wear resistance at normal lubrication, high resistance to seizure and good corrosion resistance. Also known as red brass [69].

4.5   Lubricant Selection of Journal Bearing

The proper lubricant selection is a key to avoid failure in the journal bearing and to extend bearing's live. Journal bearings is designed to be lubricated by a fluid lubricant that gives appropriate film thickness between the bearing and the shaft surfaces. To determine the correct viscosity, detailed information is needed on, (for example) shaft speed, temperature and pressure loading. [70].There are a number of tables that can be used for ISO viscosity lubricant selection for a journal bearing. Table 4.1 offers an ISO viscosity lubricant selection based on rotating speed, operation temperature and medium pressure about 20.7 to 35 Mpa [70]. The machinery requires higher viscosity if the operating temperature is higher.

Table 4.1 Viscosity selection for medium pressure [70]

Shaft Speed (rpm)	Operating Oil Temperature (Cº)			
	20-50	60	75	90
800	ISO 68	ISO 100	ISO 150	-
1200	ISO 46	ISO 68	ISO 100-150	-
1800	ISO 32	ISO 46	ISO 68-100	ISO 150
3600	ISO 32	ISO 32	ISO 46-68	ISO 68-100
10000	ISO 32	ISO 32	ISO 32	ISO 32-46

Figure 4.14 shows the appropriate absolute lubricant viscosity (cP) based on shaft linear speed (m/s) and bearing radial load (kPa or kN/m2). At industry, the lower of the lubricant viscosity needed when the shaft speed is higher at low radial load.
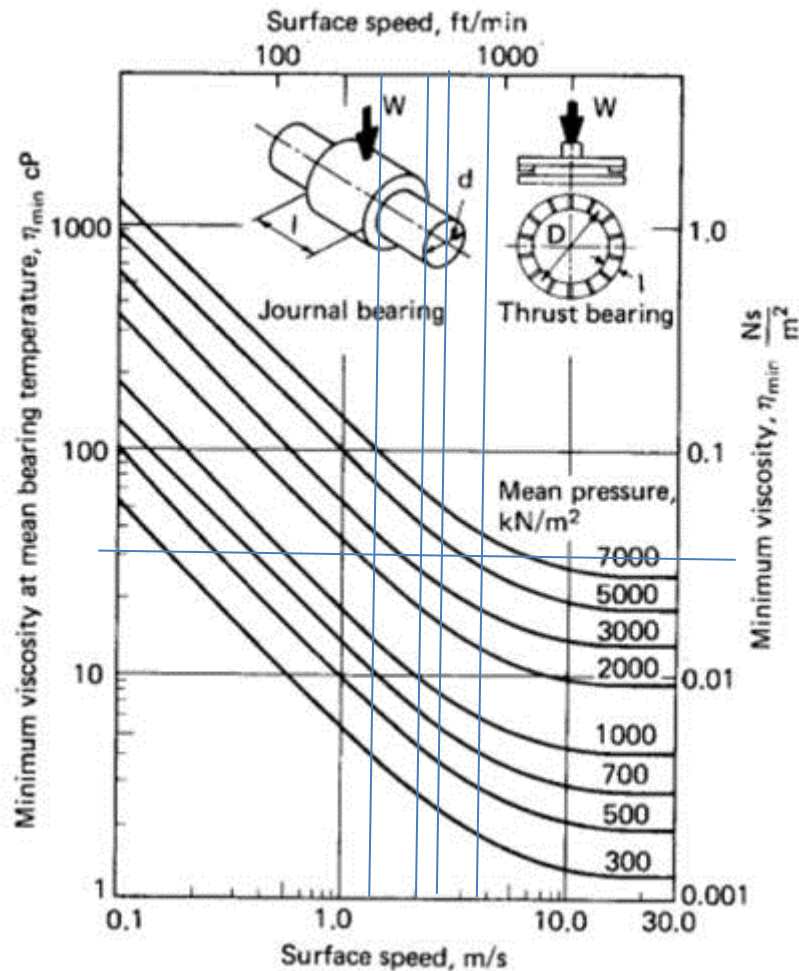
Figure 4.14 Selection of lubricant viscosity [71]

4.6 Lubrication Mechanisms of Journal Bearing

A journal bearing is designed to use lubricant, this keeps the sliding surfaces of the bearing and the shaft apart and reduces friction. Although the bearing surfaces are made of materials that have low coefficients of friction, direct contact between shaft and bearing still causes the bearing to wear quickly. Although the main purpose of using lubrication in a journal bearing is to reduce friction, lubricant also reduces wear, removes heat, prevents corrosion and removes dirt. Lubricants change sliding friction in a plain bearing to fluid friction, which is less aggressive and therefore prolongs the life of the bearing. Lubricant is supplied to the bearing through a hole in the housing or from one end of the bearing. The self-aligning spherical journal bearings have grooves at each side to help distribute the lubricant over the bearing surface. Moreover, the journal bearing has a ring for bringing the oil up from the oil reservoir to the rotating surface. Figure 4.15 shows self-aligning spherical journal bearing with lubricant groove, oil ring and surface of contact.
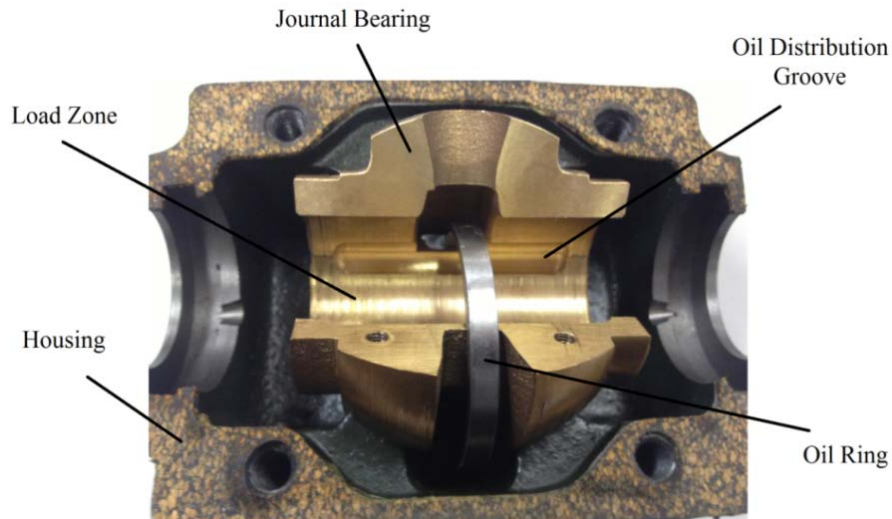
Figure 4.15 Lubrication system in self-aligning spherical journal bearing

4.7 The Lubrication Regimes of Journal Bearing

In 1846, Stribeck reported the results of a journal bearing experiment. He found that the friction coefficient was inversely proportional to speed. Thus, he presented the characteristic curve of the coefficient of friction versus speed. Figure 4.16 illustrations the Stribeck curve, this shows the relationship between the coefficient of friction and the bearing parameter or modulus $\eta N/p$, where η is the absolute viscosity of the lubricant in kg/m.s, N is the shaft speed in rpm and p is the pressure on the projected area in Pa. The Stribeck curve shows how the coefficient of friction changes with lubrication regime: boundary lubrication, mixed-film lubrication and hydrodynamic lubrication. The coefficient of friction of a bearing is very importat, because it determines the life time of bearing.

The optimum point of the curve is when the coefficient of friction passes through a minimum point from mixed to hydrodynamic lubrication. Also, the coefficient of friction passes through a maximum, this is known as the transition point from boundary to mixed lubrication [72]. It is well known that, journal bearings are designed to operate at hydrodynamic lubrication regimes, and for there to not be any metal-to-metal contact. Shigley stated that a certain characteristic number is considered as an optimum value for a journal bearing, above this number a bearing will work in a hydrodynamic lubricant regime that means there is not any asperities contact. When the bearing works under the optimum number means there is contact in asperities thereby friction will be generated [73].
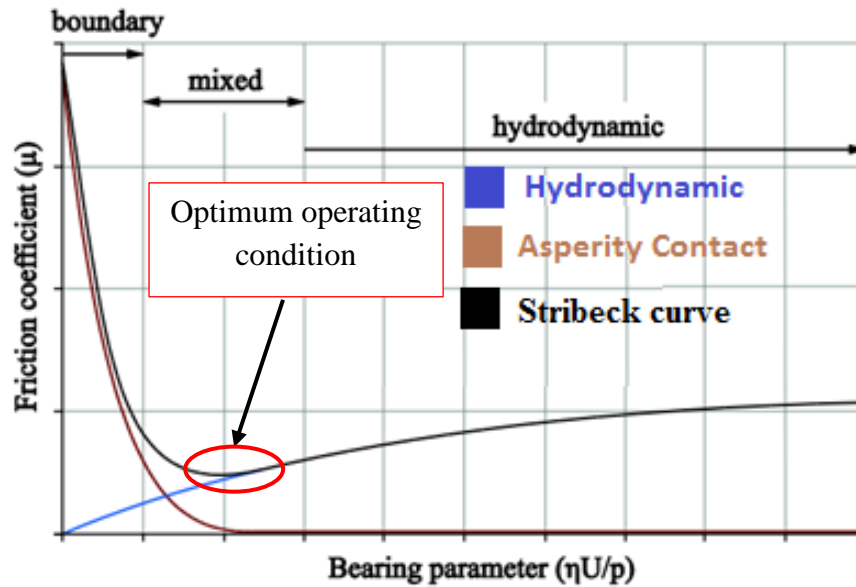
Figure 4.16 The Stribeck curve presents lubrication regimes [74]
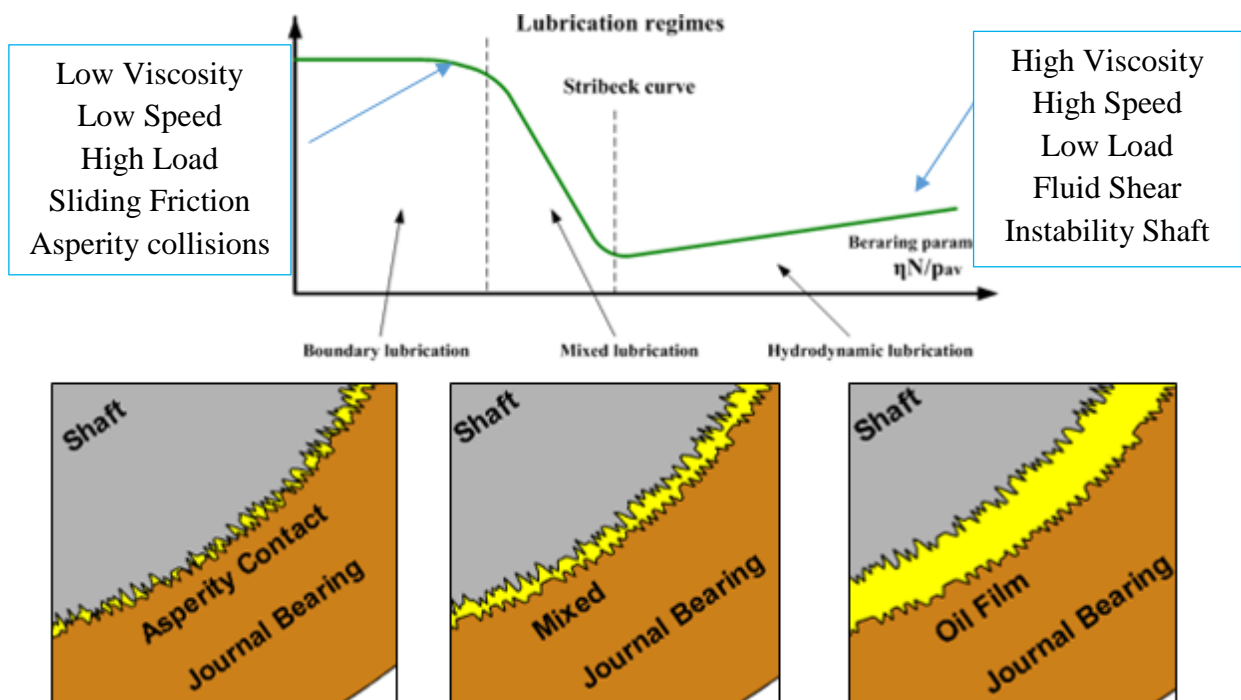
Figure 4.17 The Stribeck curve presents lubrication regimes [75]

Many parameters influence the friction coefficient such as the operating conditions (speed, pressure), the material properties (roughness of surface) and the viscosity of the lubricant. Burwell reported the critical speed was influenced by the surface roughness, cited by [76]. The coefficient of friction for a full lubricated journal bearing is a function of bearing modulus depend on the absolute viscosity of the lubricant, angular speed and bearing

pressure (Khurmi and Gupta, 2005) cited by [28]. Also, the McKee brothers in 1932 demonstrated that the coefficient of friction depends on the oil viscosity in the boundary or the mixed lubrication regimes [76]. Lu and Khonsari (2005) concluded that in mixed or boundary lubrication regime, a high temperature creates a great friction coefficient. A high load causes a smaller friction coefficient in the hydrodynamic lubricant regime [76]. Later, the Stribeck curve application extended to a number of tribology components other than just a journal bearing. For example, ball bearing, seals and wet clutches have applied the Stribeck curve idea.

4.7.1   Hydrodynamic Regime ($h_{min} > R_a$)

Hydrodynamic lubrication regime, the surfaces are separated by stable thick oil film and this will prevent any metal-to-metal contact, as in Figure 4.18. By rotating the journal, the oil film pressure developed around it to lift the radial load. In this regime, wear is at its minimum and slide friction displays limited vibration. The oil film thickness (h_{min}) is greater than the average of the roughness surfaces (R_a).
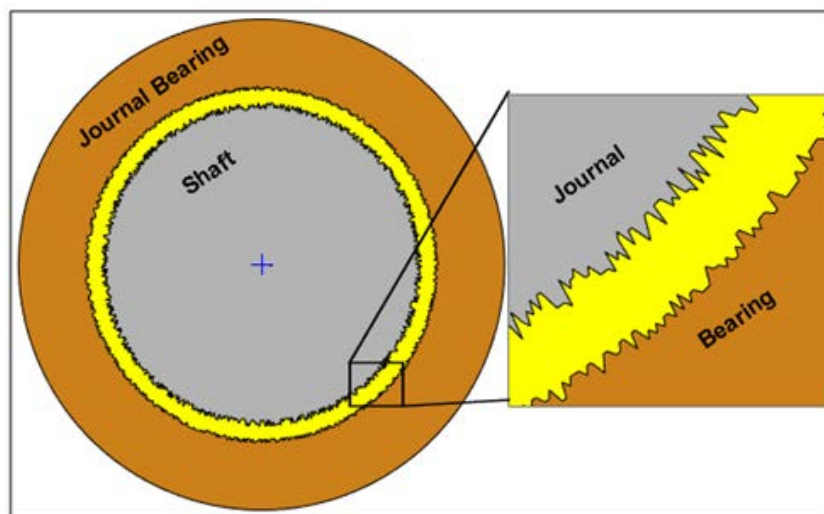
Figure 4.18 Hydrodynamic lubricated regime

Hydrodynamic lubrication condition at the Stribeck curve is when the bearing operates between point C and D due to the fluid friction being directly proportional with speed and viscosity and inversely proportional with load, as shown in Figure 4.19.
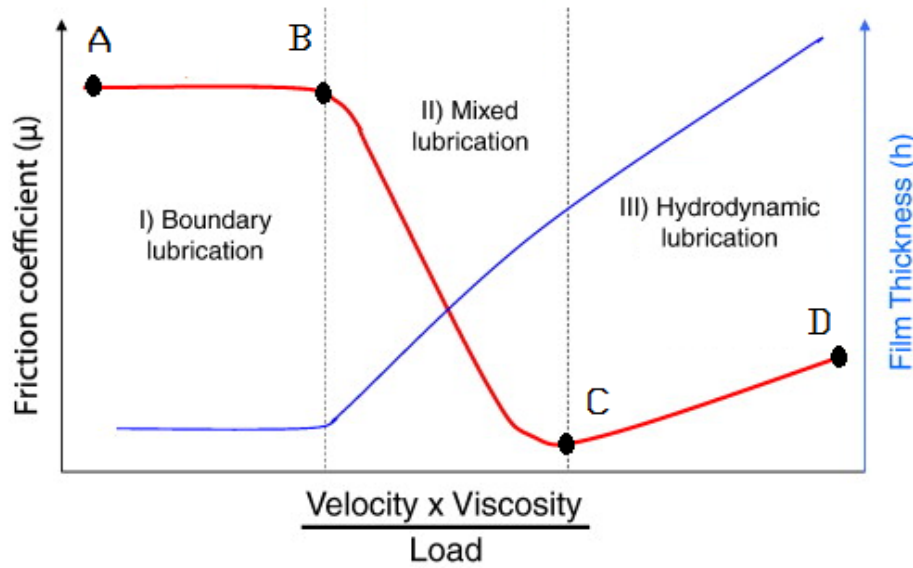
Figure 4.19 Low friction coefficient at optimum point C [77]

Based on bearing modulus and hydrodynamic lubrication regime, any increases in rotating speed or lubricant viscosity produce more fluid friction thereby increasing the time rate and the forces needed to shear the oil film. The operating conditions in point C, in Figure 4.19, are either low viscosity with high speed or high viscosity with low speed, at a given load. At the hydrodynamic lubrication regime, the friction coefficient at point C is around 0.001 [78]. ''Further reductions in bearing load do not produce corresponding reductions in the bearing friction drag force. Thus the bearing coefficient of friction $\mu = f / F$, which is the ratio of friction drag force to radial load F, increases'' [79]. Moreover, heat has been generated if the fluid shear force is high. This heat will result in the production of low friction because the temperature decreases the oil viscosity.

The Friction Characteristics of Hydrodynamic Lubrication Regime

In hydrodynamic lubricated condition: one surface is moving with velocity (U) and another is stationary, these are separated by thick film of lubricant (h) which prevents any metal-to-metal contact.

The lubricant film will be sheared such that the layer in contact with the moving plate will move at the same velocity of the plate and the layer in contact with the stationary plate will remain stationary. The intermediate layers will have velocities proportional to their distance (y) from the stationary plate [73].
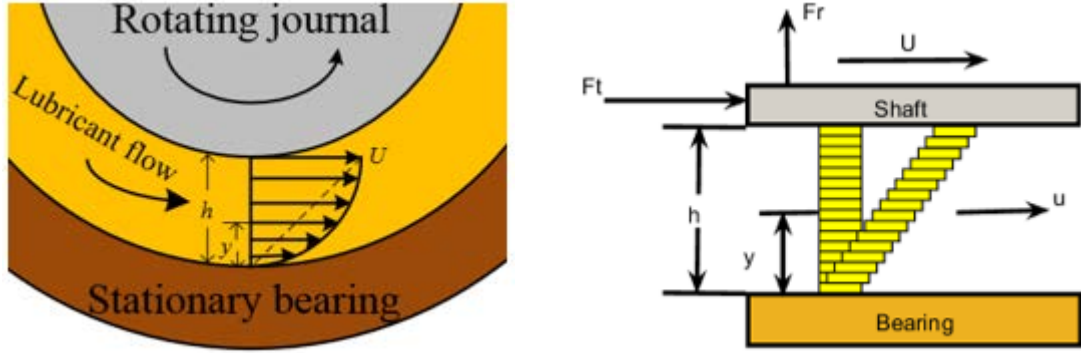
Figure 4.20 Friction model of sheared lubrication at hydrodynamic regime [73]

Newton viscous effect states that the shear stress in the fluid is proportional to the velocity gradient. Thus it is written:

$$\tau = \frac{F}{A} = \eta \frac{du}{dy} \tag{4.1}$$

where η, the dynamic (or absolute) viscosity, is the constant of proportionality

For Newtonian fluids the velocity gradient is constant; $\dfrac{du}{dy} = \dfrac{U}{h}$ (i.e., linear increase)

Thus,

$$\tau = \mu \frac{U}{h} \tag{4.2}$$

The Petroff equation gives the coefficient of friction in journal bearings. It is based on the assumption that the shaft is concentric. Consider a shaft of radius (r) rotating inside a bearing with rotational speed (N), and the clearance between the shaft and sleeve (c) is filled with oil (leakage is negligible).

From Newton's viscosity equation:

$$\tau = \frac{F}{A} = \eta \frac{U}{h} = \eta \frac{2\pi r N}{c} \tag{4.3}$$

$$A = 2 \pi r l \tag{4.4}$$

Torque $T = F.r$
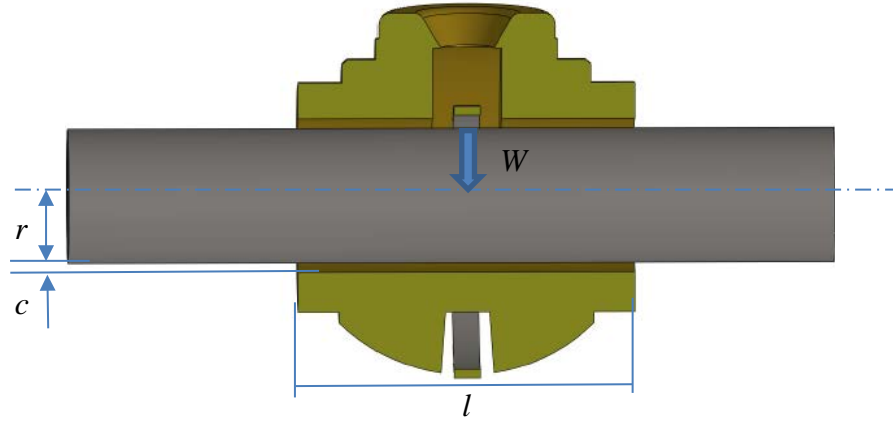
Figure 4.21 Section of journal bearing

The projected area; $= 2rl$

$$F = \eta \frac{2\pi r N}{c} \times 2\pi r l \tag{4.5}$$

$$T = \frac{4\eta \pi^2 r^3 l N}{c} \tag{4.6}$$

The pressure on the projected area is;

$$P = \frac{W}{2 r l} \tag{4.7}$$

where W is load (N). The torque created by the frictional force is:

$$T = fWr \tag{4.8}$$

where f is the coefficient of friction.

$$T = f W r = f2rlP \, r = 2 \, r^2 \, f \, l \, P \tag{4.9}$$

$$\frac{4\eta \pi^2 r^3 l N}{c} = 2 \, r^2 \, f \, l \, P \tag{4.10}$$

$$f = 2 \, \pi^2 \frac{\eta N}{P} \frac{r}{c} \quad \text{known as Pitroff's equation} \tag{4.11}$$

Bearing characteristic is known as Sommerfeld number

$$S = \frac{\eta N}{P} \left(r/c \right)^2 \tag{4.12}$$

4.7.2 Mixed Regimes ($h_{min} \sim R_a$)

Mixed lubrication regime means the surfaces partially separated by thin film of lubricant. Even though the surfaces are detached by thin oil film, some high asperities collisions exist,

Figure 4.22. The fluid film thickness h_{min} is marginally larger than the surface roughness Ra, thus the surfaces affect each other. Because of this intermittent contact, the wear of a bearing surface is mild [80] [28]. Mixed lubrication conditions at the Stribeck curve is when the bearing operates between point B and C due to summation of the fluid friction and slid friction, as shown in Figure 4.16 and Figure 4.19.
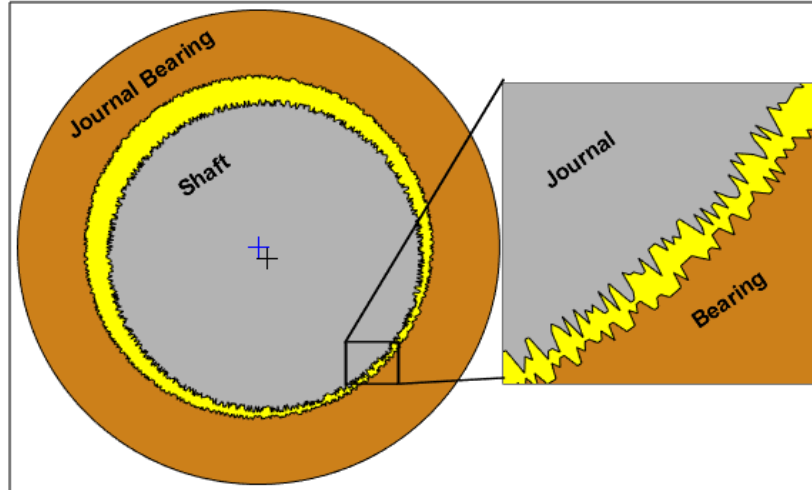
Figure 4.22 Mixed lubricated regime

4.7.3 Boundary Regimes ($h_{min}<R_a$)

Boundary lubrication regime occurs when the lubricating thickness h_{min} is very thin and almost the same as the surface roughness (R_a). Because the gap between surfaces is very tiny, direct asperity collision occurs. This regime is an unwanted operation for a journal bearing, because it generates friction, wear, losses energy and damages material. Even though, the journal bearings are designed to not work in this regime, most of them see the boundary regime during the start-up and shutdown the machine. Boundary lubrication regime factors are as follows: the speed of the shaft is slow, less amount of lubricant separates the surfaces, increases in the bearing radial load, a decrease in the oil viscosity, or an increase in the lubricant temperature resulting in drop in viscosity, and may stop to format a thick oil film and to establish metal-to-metal contact extensively.

Boundary lubrication condition at Stribeck curve is when the bearing operates between point A and B due to asperity collision, as shown in Figure 4.19. Under these critical conditions, hydrodynamic pressure developed is inadequate to support the load thus metal-to-metal contact occurs [78]. Wear is the maximum in this case and friction induced more vibration[81].
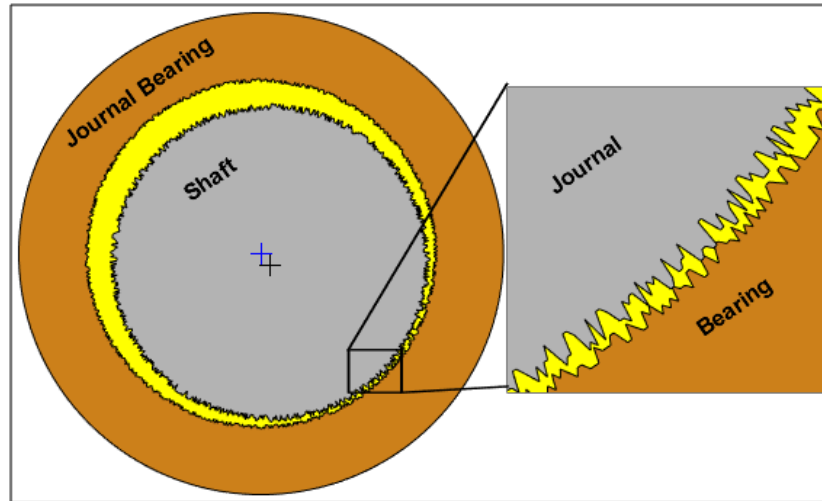
Figure 4.23 Boundary lubricated surface

At the boundary and mixed films, the friction coefficient (ratio of friction force to normal force) rises from 0.03 to 0.1, while dry sliding coefficient of friction may reaches 0.2 to 0.4 [78]. Further increases in bearing load, result in an increase in bearing friction, therefore the friction change from fluid friction to some sliding friction. In order to prevent boundary and mixed conditions, the bearing should operate with a ηv/p at least three times the minimum value of the bearing modulus [78].

The friction characteristics of boundary lubrication regime

Boundary lubrication lubricant in the oil film thickness is reduced to be very thin. A small minimum film thickness leads to excessive bearing temperature and increased susceptibility to wear from contamination and misalignment. Too large a minimum film thickness might provide poorer vibration stability.
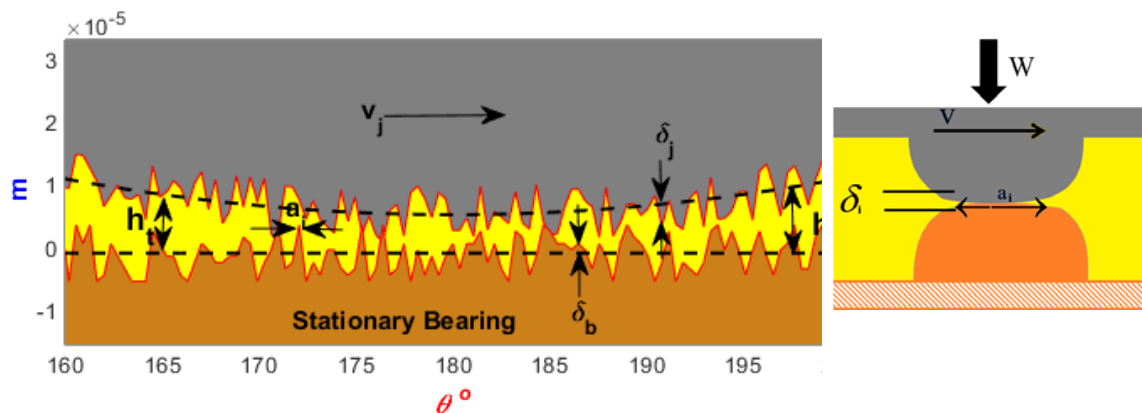
Figure 4.24 Contact of a pair asperity

the friction force in BL regime is calculated as the sum of all friction forces present in each micro-contact [82].

$$F_{f,BL} = \sum_{i=1}^{N} \iint_{A_{ci}} \tau_{Bi} dA_i \tag{4.13}$$

where τ_{Bi} is the shear stress at the ith asperity contact; A_i is the contact area of the ith asperity contact; N is the number of micro-contacts. Furthermore, the number of contacting asperities is proportional linearly with the normal load. The coefficient of friction at boundary lubricant regime is calculated as flowing Equation:

$$f_{Bi} = \frac{F_{f,BL}}{W} = \frac{\tau_{Bi}}{P_{Bi}} \tag{4.14}$$

Lu and Khonsari stated that the definition of film parameter Λ can show which regime the journal bearing at specific operating condition [76]. It is assumed that Λ equal 3 for Gaussian distribution. R_s and R_b are RMS of roughness surfaces of shaft and bearing. The ideal operation occurs when the mating surfaces are so smooth that no contact exists between their asperities, with no wear and minimum friction, point C. Under the operating conditions of high surface roughness, low speed, high load and low viscosity chief direct full contact of asperities, thereby increasing the friction. The range of lubrication regime is defined as: Hydrodynamic lubrication: $5 \leq \Lambda \leq 100$, Partial lubrication: $1 \leq \Lambda \leq 5$, and Boundary lubrication: $\Lambda < 1$. Λ factor is calculated as:

$$\Lambda = \frac{h_{min}}{\left(R_s^2 + R_b^2\right)^{1/2}} \tag{4.15}$$
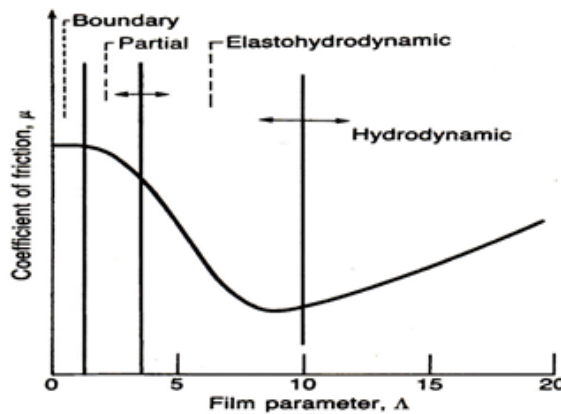
Figure 4.25 The variation of the friction coefficient with the film parameter Λ [78]

4.8   Failure modes

A journal bearing is simply designed, has high efficiency, long life and is low costly. Nevertheless, unusual operating conditions in the journal bearings may cause unexpected sudden failure which is risky in machines and operators. Additionally, a good maintenance technic does not just find a worn or broken component and replace it; it knows why it is worn and why it has broken. If you replace a damaged component without finding out what has caused the damage, you will probably find the same problem again in a few weeks or months. The maintenance is looking for the root cause of the damage: not just what has happened but why has it happened. The maintenance technicians have to act like a doctor or a detective looking for symptoms (signals) to find out what has happened and how to detect the faults. Almost all the bearing damage occurs during startup and shutdown. ''It is important to understand that the rotating shaft is not centred in the bearing shell during normal operation'' [83]. The common types of damage and their causes are described.

4.8.1   Wiping

Wiping happens when the surface of a plain bearing melts. It is dragged by the rotating shaft and re-solidifies at a cooler part of the bearing. If the metal has melted, it must have become hot. Thus, the most likely cause of too much heat at a bearing is too much friction due to too little lubricant or the oil has become so hot has reached the melting temperature. Another cause can happen during high-speed rotation. Furthermore, a heavy load on the bearing or slow form of the lubricant film, can cause wiping on start-up. Too many loads can make the lubricant too hot or break down the film. Plus the lubricant film is slow to form if the lubricant viscosity is too high [65].
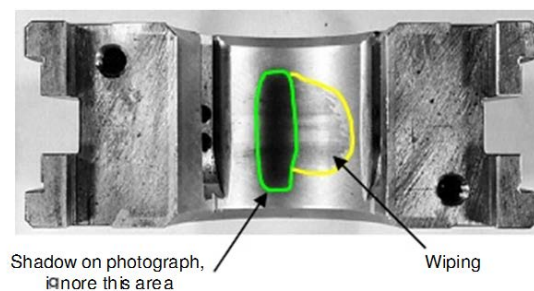
Figure 4.26 Start-up wiping [65]

4.8.2   Scoring

Scoring (scratching) happens when there are solid particles of dirt, for example that get between the bearing and the shaft. This is caused by hard solid particles that are bigger than the minimum film thickness of the lubricant. Scoring can also be caused by dirt in the oil. This occurs by inadequate filtering of the oil or failure to change the oil when necessary [65].

Figure 4.27 Heavy scoring of a journal bearing [65]

4.8.3   Fatigue

Fatigue is caused by a continuously changing load over a long period of time. The first signs of fatigue damage in soft materials are small cracks on the surface. These cracks can be in any direction are often described as surface crazing [65].

Figure 4.28 Fatigue failure [65]

4.8.4   Corrosion

Corrosion and deposits form as a result of chemical reactions in the lubricant. Chemical reactions may result from using the wrong lubricant or from contamination of the lubricant, often by the product being processed in the equipment. High lubricant temperatures increase the problem. Corrosion and deposits can cause high spots on the bearing surface.

High spots will carry more loads than low spots and the lubricant film can break down where the load is greatest [65].
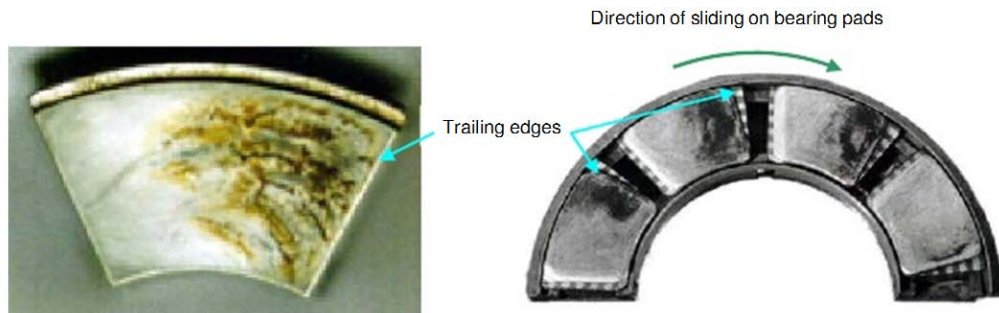
Figure 4.29 Lubricant oxidation [65]

4.8.5 Friction

In general, friction is the force that tries to stop one surface sliding on another and where there is friction there is always wear, heat and oxidation. When the shaft rotates, the shaft and/or the journal bearing will wear. Journal bearings are designed to reduce friction as much as possible, but they cannot remove it completely. Fine surfaces, materials selection and lubrication viscosity help to reduce friction in journal bearings. Smooth surfaces have a lower friction force and a lower coefficient of friction than rough surfaces. Direct contact between shaft and journal bearing causes quick wear and high temperature, even though the journal bearing surfaces are fine and made of materials that have low coefficients of friction. Using lubricants reduces the amount of friction, as well as reducing unwanted heat. Lubricant is supplied to the sliding surface between shaft and the bearing. Furthermore, the friction in a plain bearing varies with the rotational speed but is practically constant for a rolling bearing as shown in Figure 4.30 [84].

Failure mode for journal bearing is normally messy. A journal bearing will not fail gently, they either work or don't. The most common failure mode will be the loss of lubricant. Since the shaft rides on a thin film of oil that could be as thin as .0005 at the minimum film thickness, loss of lubricant will result in the shaft and bearing making contact. If this occurs, a tremendous amount of heat is generated due to the sliding friction between the shaft and liner which results in a major failure in a very short time [85].
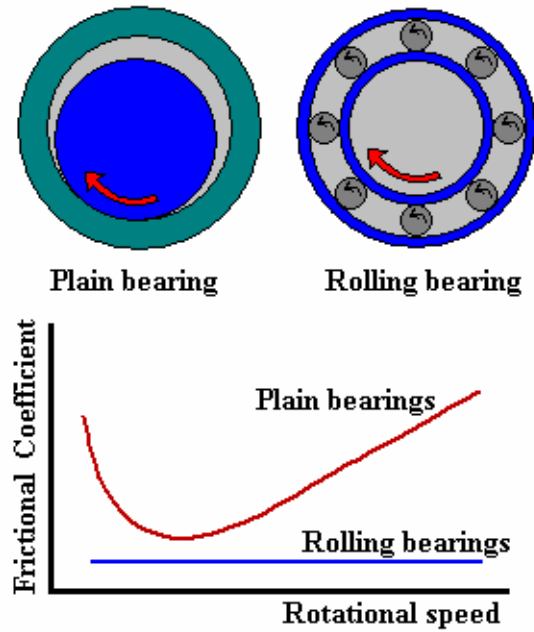
Figure 4.30 Frictional behaviour of plain and rolling bearings [86]

4.8.6   Wear

Wear of bearings may be defined as the removal of surface material. The friction between shaft and journal bearing causes wear on the bearing material surface. Wear marks can be made by the rolling elements on the raceways. Wear mark is not only important to be able to recognize damage, it is just as important to know what a bearing should look like if it is in good condition. The mark on the Journal bearing surface depends on the direction and type of load. Self-aligning spherical journal bearings do not suddenly fail, as a rolling element but wear extremely slowly. Moreover, vibration in bearings and/or misalignment can also cause excessive wear [65].
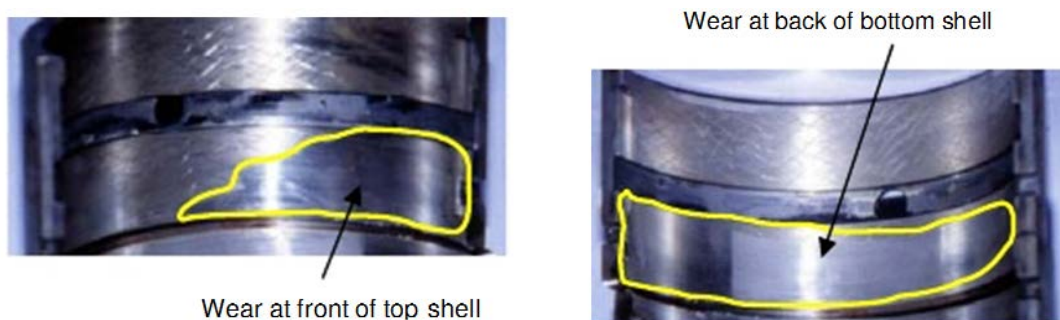
Figure 4.31 Wear of journal bearing [65]

4.9 Summary

In this chapter, different journal bearing types based on their functions have been presented. In general, the journal bearing is used for supporting radial and/or axial load. Furthermore, each type of journal bearings has been designed for special job with discernible in mind of operating conditions, material and lubricant type. Unfortunate, many resonances make a journal bearing fail such as wiping, scoring, fatigue, friction and wear.

CHAPTER FIVE

MATHEMATICAL MODELS OF JOURNAL BEARING VIBRATIONS

To develop vibration based monitoring techniques, a vibration model is established in this chapter with taking into account micro asperity collisions and churns for more comprehensive understanding the vibration mechanisms and characterising vibration responses of a journal bearing under different operating status. Firstly, it presents the operational principle of journal bearing. Then, it provides a detailed analysis of the vibration responses to both external dynamic effects such as unbalanced rotors, and internal excitations including micro asperity collisions and churns. Finally, resonances of a bearing system are investigated by considering both the fluid film and surface asperity effects.

5.1   Introduction

In journal bearings the vibration occurring is caused mostly by mechanical problems such as misalignment, looseness and unbalanced forces. It can also be caused by fluid film forces which throw the shaft away from the bearing. Furthermore, asperity contact between the journal and the bearing surfaces can cause random vibrations spreading over a wide frequency band.

To understand the vibration phenomena in a journal bearing, the vibration model was developed to include variable excitation forces. Unbalance (F_u) creates an external excitation force. When unbalance occurs, the journal fluctuates inside the bearing and causes low frequency correlated into shaft frequency and its harmonics. The hydrodynamic (F_o) generate self-excitation force correlated to oil coefficients. Asperity contact (F_a) produces an internal self- excitation force. This random force causes corresponding high frequency vibration responses.

Self-exited vibration of machinery rotors can take the form of fluid induced (oil, steam, or gas) or rotor internal (material) hysteresis induced whirl or whip. The energy to sustain these vibrations is often drawn from the rotational motion of the rotor. For fluid whirl or whip, the constant source of energy is shaft rotation, and the energy converter is fluid dragged into circumferential motion by friction. The response frequency of self-excited vibration is very close to one of the system's natural frequencies [87].

5.2   Principle of Journal Bearing Operation

The journal central positions displace within the bearing clearance based on operating condition parameters. The eccentricity, distance between journal and bearing centres, approaches the radial clearance for large loads, low shaft speeds or light lubricant viscosity and it is aligned with the radial loads. For small loads, high speeds or large lubricant viscosities (large Sommerfeld numbers), the journal travels towards the bearing centre and its position is orthogonal to the applied load. Due to different eccentricity, Figure 5.1 shows the travelling path of the journal central positions inside stationary bearing. This peculiar behaviour is the source of rotor dynamic instability.
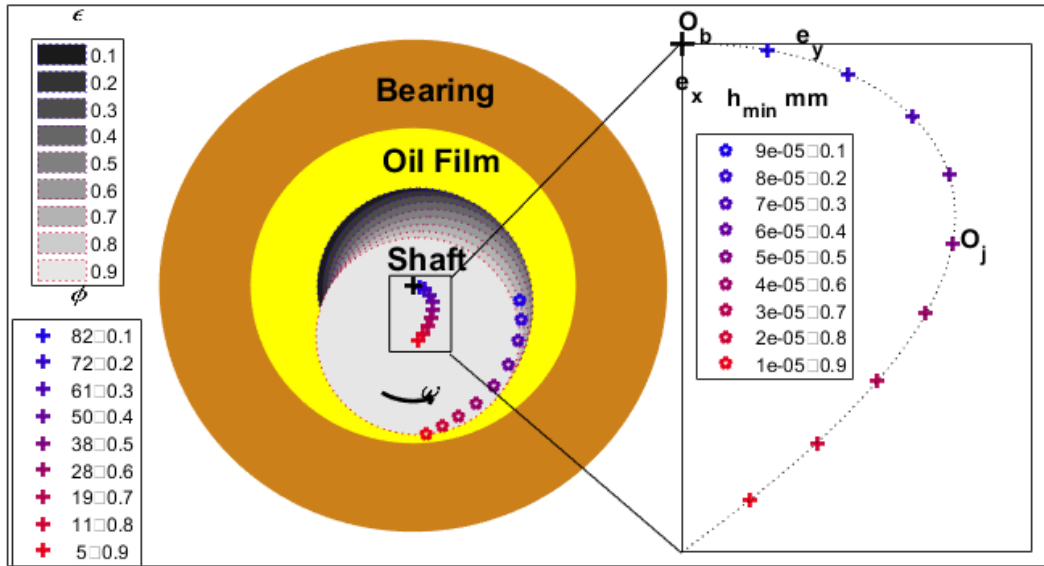
Figure 5.1 Locus of the equilibrium states of journal centre

5.2.1 Eccentricity Ratio in Journal Bearing

Eccentricity ratio (journal eccentricity/radial clearance) is a function of operating condition parameters (speed, load and oil viscosity). For example, if the eccentricity is too high there is a sign of asperity collisions and high slide friction. And if the eccentricity is too low, this means the journal centre is nearing the bearing centre then the machine could more easily become unstable. The optimum value of eccentricity ratio is close to 0.7 [88]. The journal eccentricity and attitude angle defining the static performance of the journal bearing are shown as functions of operating speed, lubricant viscosity and applied load.

In Appendix B the minimum ratio of film thickness and eccentricity ration are plotted against the Sommerfeld Number with variable bearing ratio (length/diameter). Also, for bearing design, the sector between the two dashed lines might be considered a desirable values of oil thickness and eccentricity ratio [73]. Due to that, the optimum eccentricity ration for journal bearing subject of study is between 0.5 to 0.85 [78, 89].

Figure 5.2 describes the journal eccentricity ratio versus the Sommerfeld number. Great Sommerfeld numbers (Hydrodynamic lubricant regime), represented by a small radial load, a high rotating speed, or a large lubricant viscosity, determine small operating journal eccentricities or O_j and O_b are almost overlapped. Due to that, the journal eccentricity e is nearly perpendicular to the applied load.

Small Sommerfeld numbers (Boundary lubricant regime), represented by a large radial load, low speed, or low lubricant viscosity, determine large journal eccentricities, determine great operating journal eccentricities or eccentricities are almost equal radial clearance. That is, the journal eccentricity *e* is nearly parallel to the applied load.
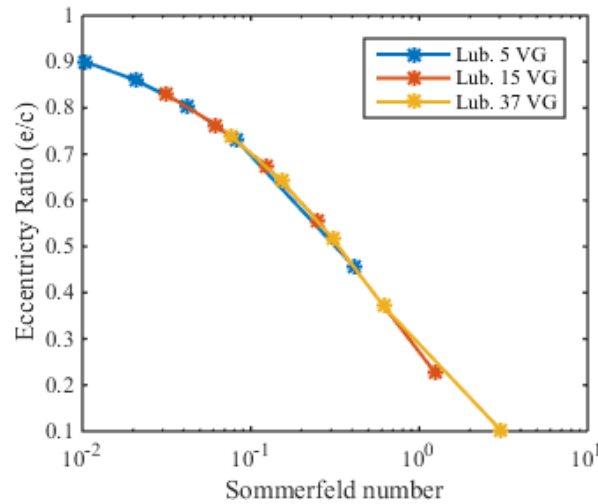
Figure 5.2 Eccentricity ratio vs. Sommerfeld number

5.2.2 Reynolds Equation

In the majority of hydrodynamic journal bearings, the shaft is moving with rotational speed (*U*) and the bearing is stationary, both surfaces are separated by thick film of lubricant (*h*) due to avoiding any metals contact.

The lubricant film will be such that the layer in contact with the moving plate will move at the same velocity of the plate and the layer in contact with the stationary plate will stay stationary. The intermediate layers will have the velocities (*u*) proportional to their distance (*y*) from the stationary plate [73], as shown in Figure 4.20.

Reynolds equation describes the generation of hydrodynamic pressure (*P*) within the bearing. This equation describes the relation between the pressure and film shape as a function of the viscosity and the velocity.
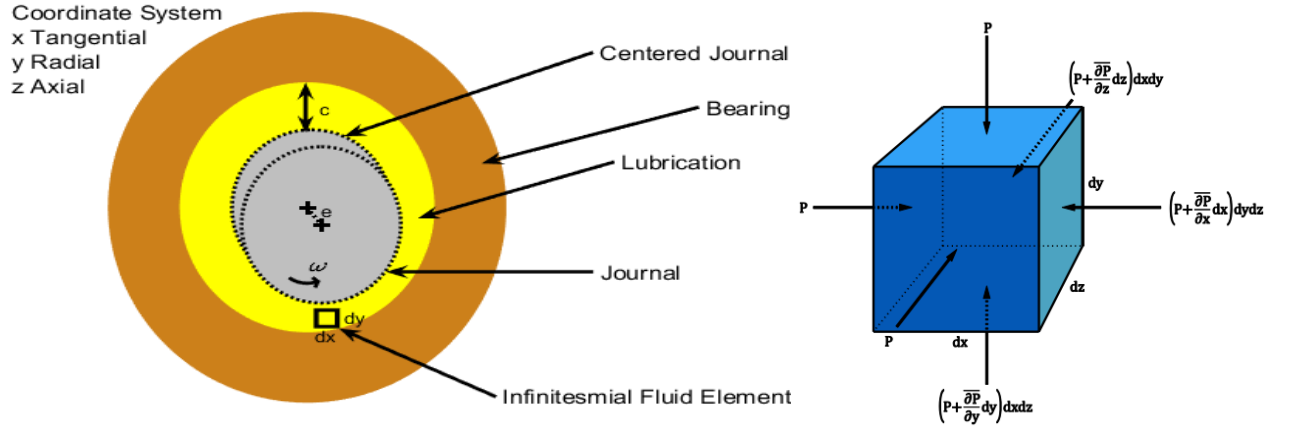
Figure 5.3 Illustration of a journal bearing and an infinitesimal fluid element

$$\overbrace{\frac{\partial}{\partial x}\left(\frac{\rho h^3}{\eta}\frac{\partial p}{\partial x}\right)}^{\substack{\text{Pressure}\\ \text{in}\\ \text{circumferential direction } \theta}} + \overbrace{\frac{\partial}{\partial z}\left(\frac{\rho h^3}{\eta}\frac{\partial p}{\partial z}\right)}^{\substack{\text{Pressure}\\ \text{in}\\ \text{axial direction } z}} = \overbrace{6U\frac{\partial(\rho h)}{\partial x}}^{\substack{\text{Wedge}\\ \text{relative to}\\ \text{tangential velocity}}} + \overbrace{6\rho h\frac{\partial U}{\partial x}}^{\substack{\text{Stretch}}} + \overbrace{12\frac{\partial(\rho h)}{\partial t}}^{\substack{\text{Squeeze}\\ \text{relative to}\\ \text{radial velocity}}}$$

$$(5.1)$$

where U *is* the velocity of the shaft movement ωr_j, x equals $r_j\Theta$ or $r_j\theta$, z $-0.5L \le z \le 0.5L$, t time, p pressure, h film thickness, ρ oil density, η oil viscosity.

There are three possibility generate pressure in the gap between the shaft and bearing. The first term is referred to as the wedge term the second as the stretch term and the last as the squeeze term, $p(\Theta\, or\, \theta, z, t)$. The stretch term is omitted.

The remaining Reynolds equation:

$$\frac{\partial}{\partial x}\left(\frac{h^3}{\eta}\frac{\partial p}{\partial x}\right) + \frac{\partial}{\partial z}\left(\frac{h^3}{\eta}\frac{\partial p}{\partial z}\right) = 6U\frac{\partial h}{\partial x} + 12\frac{\partial h}{\partial t} \qquad (5.2)$$

$$\frac{1}{r_j^2}\frac{\partial}{\partial\Theta}\left(h^3\frac{\partial p}{\partial\Theta}\right) + \frac{\partial}{\partial z}\left(h^3\frac{\partial p}{\partial z}\right) = 6\omega\eta\frac{\partial h}{\partial\Theta} + 12\eta\frac{\partial h}{\partial t} \qquad (5.3)$$

or

$$\frac{1}{r_j^2}\frac{\partial}{\partial\theta}\left(h^3\frac{\partial p}{\partial\theta}\right) + \frac{\partial}{\partial z}\left(h^3\frac{\partial p}{\partial z}\right) = 6\omega\eta\frac{\partial h}{\partial\theta} + 12\eta\frac{\partial h}{\partial t} \qquad (5.4)$$

where $0 \le \theta \le 2\pi$

5.2.3 Pressure Distribution
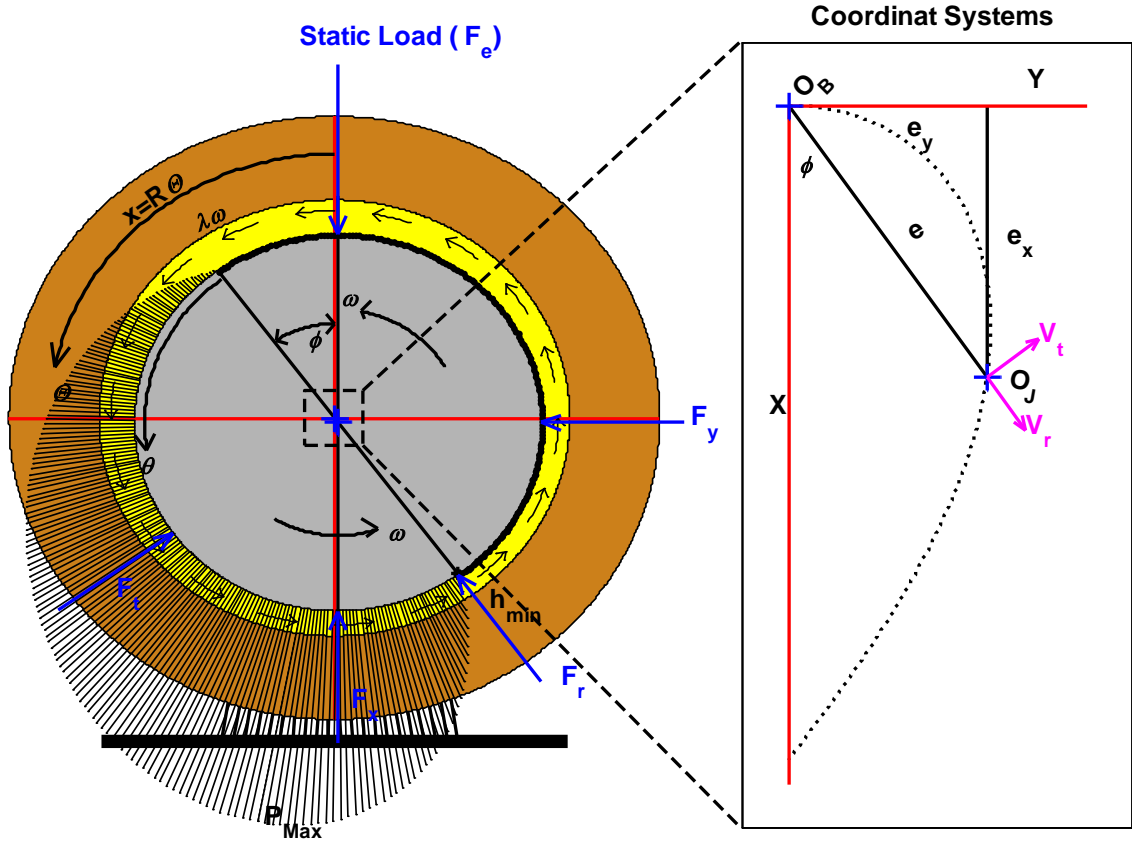
Figure 5.4 Steady state equilibrium of journal bearing

By assuming that [90] no lubricant flow occurs in the axial direction, it is not squeezed; and omit stretch term, the squeeze term is omitted as well, the Equation 5.1 is simplified as,

$$\frac{1}{r_j}\frac{\partial}{\partial\theta}\left(\frac{h^3}{\eta}\frac{\partial p}{\partial\theta}\right) = 6U\frac{\partial h}{\partial\theta} \tag{5.5}$$

The pressure distribution of a journal bearing is given by [91]:

$$p = \frac{6\eta U r_j}{c^2}\frac{\varepsilon(2+\varepsilon cos\theta)sin\theta}{(2+\varepsilon^2)(1+\varepsilon cos\theta)^2} \tag{5.6}$$

where c radial clearance, ε eccentricity ratio, $\varepsilon = e/c$, e absolute bearing eccentricity, θ circumferential angle.

Note that as the journal eccentricity $\varepsilon \to 0$, $\phi \to 90^o$, while $\varepsilon \to 1$, $\phi \to 0^o$. ϕ is known as the attitude angle. $p = 0$ when $\theta = 90^o, 180^o$ and 360°, seen Figure 5.5.
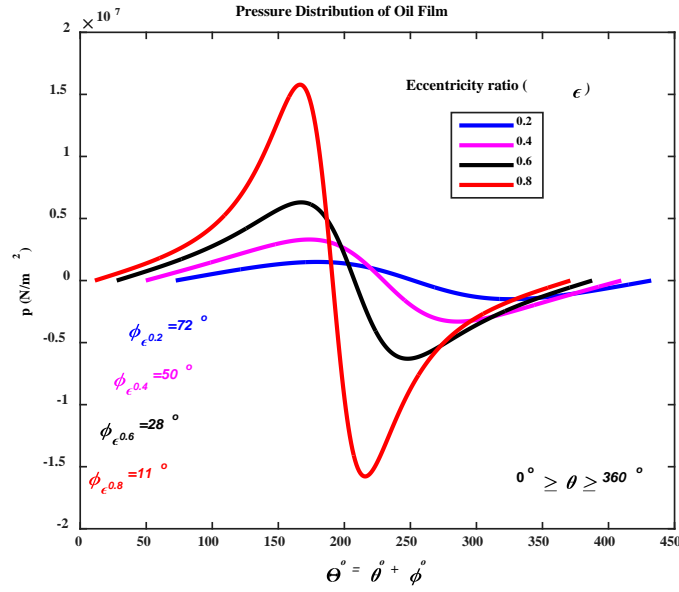
Figure 5.5 Lubricant film pressure distribution

5.2.4   Oil Wedge Thickness
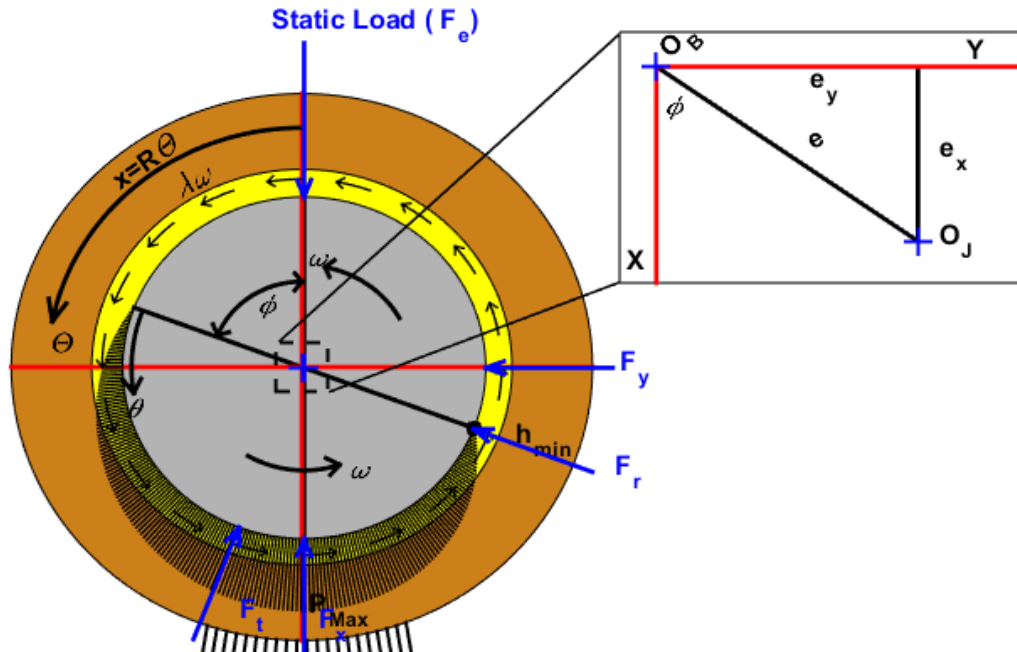
Figure 5.6 Hydrodynamic lubricated bearing

The centre of the journal (O_j) is relatively moved to the bearing centre (O_b) as in Figure 5.1. Most journal bearings operate under steady conditions in the range from $\varepsilon = 0.6$ to $\varepsilon = 0.8$ [92] [89]. The distance O_b-O_j is the eccentricity, e, and the dimensionless eccentricity ratio, ε, is defined as:

$$\varepsilon = \frac{e}{C} \tag{5.7}$$

The attitude angle ϕ is defined as:

$$\tan(\phi) = \frac{\pi\sqrt{\left(1-\varepsilon^2\right)^2}}{4\varepsilon} \tag{5.8}$$

$$e_x = e\cos(\phi) \tag{5.9}$$

$$e_x = e\sin(\phi) \tag{5.10}$$
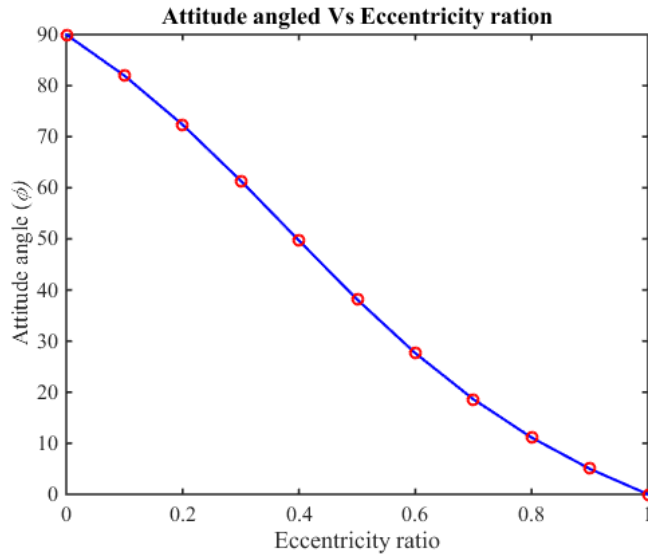
Figure 5.7 Journal eccentricity versus attitude angle

The lubricant film thickness (h) is converging along the region from $\theta = 0$ to $\theta = \pi$. The minimum film thickness h_{min} at $\theta = \pi$. Then the clearance is diverging along the region from $\theta = \pi$ to $\theta = 2\pi$, where the maximum oil film h_{max} when coordinate $\theta = 0$ and 2π, as seen Figure 5.8. The most important design detail is to make oil film thickness h_{min} much higher than the size of surface roughness[88].

$$h(\theta) = c\left(1 + \varepsilon \cos\theta\right) \tag{5.11}$$

$$h_{min} = c\left(1-\varepsilon\right) \tag{5.12}$$

$$h_{max} = c\left(1+\varepsilon\right) \tag{5.13}$$
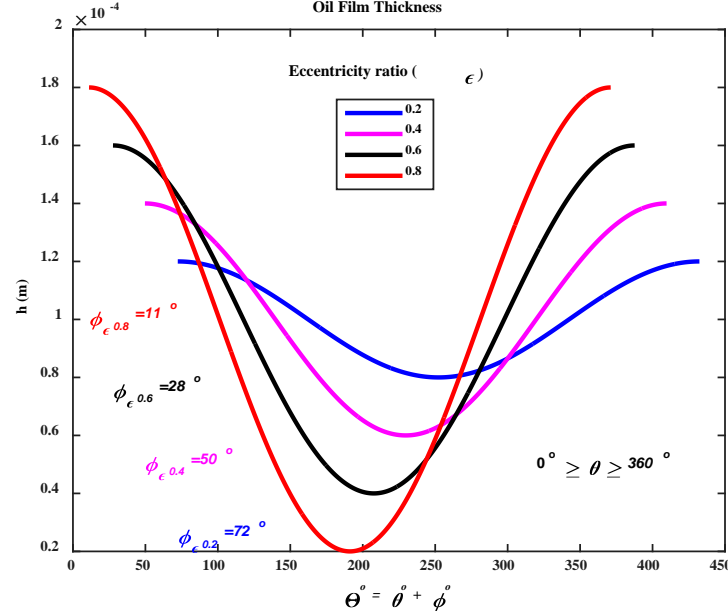
Figure 5.8 Oil film thickness at different eccentricity ration

The distance between bearing centre and journal centre is titled (e), so the eccentricity components in the (*X, Y*) fixed coordinate system are[90, 93]:

$$e_x = ecos\left(\phi\right) \tag{5.14}$$

$$\dot{e}_x = \dot{e}cos\phi - e\dot{\phi}sin\phi; \; \dot{e}_x = V_t cos\phi - V_r sin\phi \tag{5.15}$$

$$e_y = esin\left(\phi\right) \tag{5.16}$$

$$\dot{e}_y = \dot{e}sin\phi + e\dot{\phi}cos\phi; \; \dot{e}_y = V_t sin\phi + V_r cos\phi \tag{5.17}$$

$$\left. \begin{array}{l} V_t = \dot{e} \\ V_r = e\dot{\phi} \end{array} \right\} \tag{5.18}$$

The radial and tangential components of the journal translational velocity [93].

$$\begin{bmatrix} \dot{e}_x \\ \dot{e}_y \end{bmatrix} = \begin{bmatrix} cos\phi & -sin\phi \\ sin\phi & cos\phi \end{bmatrix} \begin{bmatrix} \dot{e} \\ e\dot{\phi} \end{bmatrix} = \begin{bmatrix} cos\phi & -sin\phi \\ sin\phi & cos\phi \end{bmatrix} \begin{bmatrix} V_r \\ V_t \end{bmatrix} \tag{5.19}$$

$$h = c + ecos(\Theta - \phi) \tag{5.20}$$

$$h = c + e(\cos\Theta cos\phi + sin\Theta sin\phi) \tag{5.21}$$

$$h = c + e_x cos\Theta + e_y sin\Theta \tag{5.22}$$

$$\frac{\partial h}{\partial\Theta} = -e_x sin\Theta + e_y cos\Theta \tag{5.23}$$

$$\frac{\partial h}{\partial t} = \dot{e}_x cos\Theta + \dot{e}_y sin\Theta \tag{5.24}$$

Substitution of the film thickness gradients into Reynolds Equation (5.3) gives the following lubrication equation for an incompressible and isoviscous fluid [93]:

$$\frac{1}{r_j^2}\frac{\partial}{\partial\Theta}\left(h^3\frac{\partial p}{\partial\Theta}\right) + \frac{\partial}{\partial z}\left(h^3\frac{\partial p}{\partial z}\right) = 6\omega\eta(-e_x sin\Theta + e_y cos\Theta) + 12\eta(\dot{e}_x cos\Theta + \dot{e}_y sin\Theta) \tag{5.25}$$

An alternative form of Reynolds equation arises when using the angular coordinate (θ). This angle starts from the location of maximum film thickness.

$$h = c + ecos\theta \tag{5.26}$$

$$\frac{\partial h}{\partial\theta} = -e_x sin\theta \tag{5.27}$$

$$\frac{\partial h}{\partial t} = \frac{\partial e}{\partial t}cos\theta + e\frac{\partial\theta}{\partial t}sin\theta \tag{5.28}$$

$$\frac{\partial h}{\partial t} = \dot{e}cos\theta + e\dot{\phi}sin\theta \tag{5.29}$$

$$\frac{\partial h}{\partial t} = V_r cos\theta + V_t sin\theta \tag{5.30}$$

$$\frac{1}{r_j^2}\frac{\partial}{\partial\theta}\left(h^3\frac{\partial p}{\partial\theta}\right) + \frac{\partial}{\partial z}\left(h^3\frac{\partial p}{\partial z}\right) = 6\omega\eta(-e_x sin\theta) + 12\eta(\dot{e}cos\theta + e\dot{\phi}sin\theta) \tag{5.31}$$

$$\frac{1}{r_j^2}\frac{\partial}{\partial\theta}\left(h^3\frac{\partial p}{\partial\theta}\right) + \frac{\partial}{\partial z}\left(h^3\frac{\partial p}{\partial z}\right) = 12e\eta\left(\dot{\phi} - \frac{\omega}{2}\right)sin\theta + 12\eta\dot{e}cos\theta \tag{5.32}$$

5.2.5   Bearing Reaction Forces

Once the pressure field is obtained, fluid film forces acting on the journal surface are calculated by integration of the pressure field acting on the journal surface. An equal

opposing force acts on the bearing as well. The bearing reaction forces are expressed in the fixed (X, Y) coordinate system as [93];

$$\begin{bmatrix} F_x \\ F_y \end{bmatrix} = \int_0^L \int_0^{2\pi} p(\Theta, z, t) \begin{bmatrix} cos\Theta \\ sin\Theta \end{bmatrix} r_j d\Theta dz \tag{5.33}$$

and (r, t) coordinate system as;

$$\begin{bmatrix} F_r \\ F_t \end{bmatrix} = \int_0^L \int_0^{2\pi} p(\theta, z, t) \begin{bmatrix} cos\theta \\ sin\theta \end{bmatrix} r_j d\theta dz \tag{5.34}$$

The relationship between the fluid film forces in both coordinate systems is given by:

$$\begin{bmatrix} F_x \\ F_y \end{bmatrix} = \begin{bmatrix} cos\phi & -sin\phi \\ sin\phi & cos\phi \end{bmatrix} \begin{bmatrix} F_r \\ F_t \end{bmatrix} \tag{5.35}$$

The fluid film forces are generic functions of the journal rotational speed (ω) and the journal centre translational velocities, i.e.

$$F_i = F_i \left(\dot{e}, e[\dot{\phi} - \frac{\omega}{2}] \right); i = x, y \text{ or } r, t \tag{5.36}$$

5.2.6 Bearing Capacity

There are several factors influencing radial load such as speed, viscosity, bearing geometry and shaft eccentricity. The shaft does not move directly with the load direction but always moves at an angle inclined with the load direction, as illustrated in Figure 5.4.

Hydrodynamic journal bearings are designed (and implemented) to support a static load F_e, hereafter aligned with the *X* axis for convenience. At the equilibrium condition, denoted by a journal centre eccentric displacement *e* with an attitude angle ϕ, the hydrodynamic bearing generates a reaction force balancing the applied external load at the rated rotational speed ω. The equations of static equilibrium are [90]

$$F_e + F_x = 0; \quad -F_e = F_x = F_r cos\phi - F_t sin\phi \tag{5.37}$$

$$F_y = 0; \quad F_y = F_r sin\phi - F_t cos\phi \tag{5.38}$$

For static equilibrium, V_t and $V_r = 0$. By substitute in Equation (5.31), the static radial and tangential film reaction forces are [93]

$$F_r = \frac{-\mu r_j l^3 \omega}{c^2} \frac{\varepsilon^2}{(1-\varepsilon^2)^2} \qquad (5.39)$$

$$F_t = \frac{\mu r_j l^3 \omega}{c^2} \frac{\pi \varepsilon}{4(1-\varepsilon^2)^{3/2}} \qquad (5.40)$$
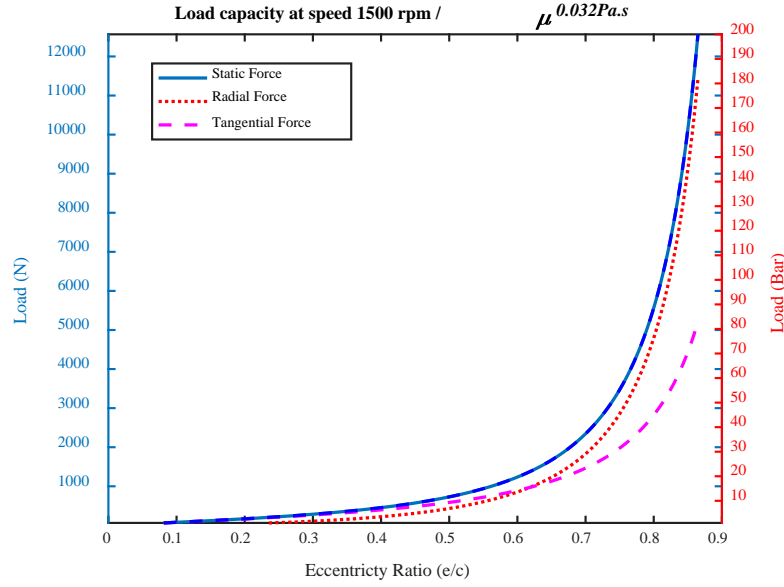
Figure 5.9 Load capacity, radial and tangential forces

The external load F_e is balanced by the fluid film reaction forces [90, 94]. Thus

$$F_e = (F_r^2 + F_t^2)^2 = \eta \omega r_j \frac{l^3}{c^2} \frac{\varepsilon}{4} \frac{\sqrt{16\varepsilon^2 + \pi^2(1-\varepsilon^2)}}{(1-\varepsilon^2)^2} \qquad (5.41)$$

W is journal bearing capacity (*N*), *U is* linear speed of shaft (*m/s*), η is absolute viscosity (*P.as*), *l* is the length of bearing (*m*), *c* is clearance (*m*), ε is eccentricity ratio.

Figure 4.14 shows that the maximum load on ajournal bearing depends on multiple variables: such as rotating speed, oil veiscosity and bearing geometry. The journal bearing increases its capacity of supporting radial load by increasing those variables. Thus the maximum load at 1500, 1200, 900, 600 rpm are around 10, 8, 6, 4kN while bearing contains rocommended lubrication viscosity.

5.3   Vibration Mechanisms

External and internal excitation forces generate vibration of the journal. In Figure 5.10, brown, blue, green and red arrows present unbalance force, oil forces, asperity churns forces and asperity collision forces, respectively. And, black arrow is static radial load. To describe the vibration phenomena of journal bearing more clearly the vibration equations were developed to include variable forces. One of these forces cause external excitations is unbalance force (F_u). Unbalance causes the shaft rotation disturb inside the bearing and causes low frequency correlated into shaft frequency. In addition, by the rotating motion of the shaft inside the bearing, self-excited vibration occurs. This phenomenon is called oil whirl instability [95] cited from [96]. This type of instability occurs when the lubricant is trapped in a wedge between shaft and bearing surfaces. Furthermore, self-excitations generated from the fluid film forces (F_o) are correlated with oil stiffness and damping coefficients. These forces affect the journal whirling frequency. Finally, forces between asperity contacts (F_a) are sources of self-excitations and random forces cause high frequency vibration responses as shown in Figure 5.10. Appendix A presents different vibration sources in a journal bearing.
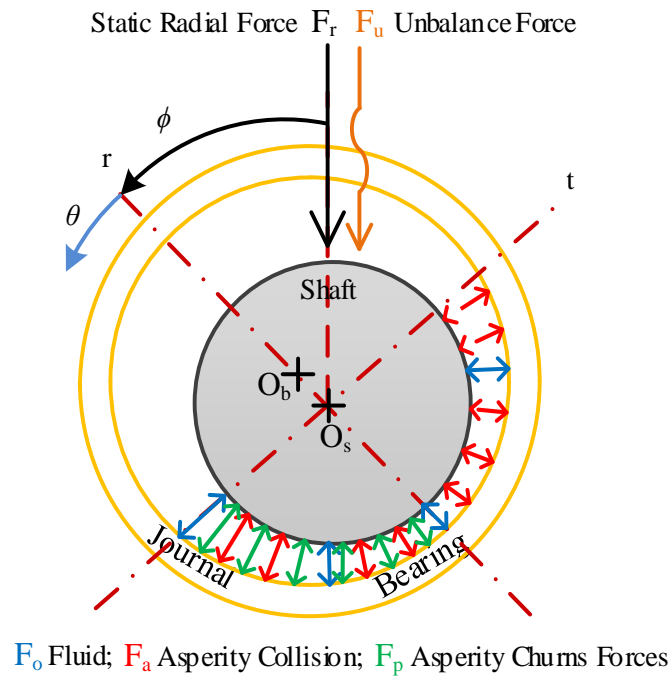
Figure 5.10 Free body diagram of different forces of journal bearing

The equations for small amplitude motions of the rotor-bearing system in *X* direction and *Y* direction are, [93, 97]

$$m\ddot{x} + F_{ox} = F_{ux} + F_e \tag{5.42}$$

$$m\ddot{y} + F_{oy} = F_{uy} \tag{5.43}$$

where m is the mass of the shaft, F_{ox} and F_{oy} are oil film forces at *x* and *y* directions, F_e is static load at *x* direction only, and F_{ux} and F_{uy} are unbalance forces at *x* and *y* direction. By adding asperity collision forces F_{ax} and F_{ay}, Equations (5.42) and (5.43) become;

$$m\ddot{x} + F_{ox} + F_{ax} = F_{ux} + F_e \tag{5.44}$$

$$m\ddot{y} + F_{oy} + F_{ay} = F_{uy} \tag{5.45}$$

$$m\begin{bmatrix} \ddot{x} \\ \ddot{y} \end{bmatrix} + \overbrace{\begin{bmatrix} F_{ox} \\ F_{oy} \end{bmatrix}}^{\text{Viscous Friction Force}} + \overbrace{\begin{bmatrix} F_{ax} \\ F_{ay} \end{bmatrix}}^{\text{Asperity Friction Force}} = \overbrace{\begin{bmatrix} F_{ex} \\ 0 \end{bmatrix}}^{\text{Static Force}} + \overbrace{\begin{bmatrix} F_{ux} \\ F_{uy} \end{bmatrix}}^{\text{Unbalance Forces}} \tag{5.46}$$

5.3.1 Unbalance Excitation

The excited force of journal bearing vibration signal is unbalance force, Figure 5.11. The unbalance occurs when the journal centre mass is not at the centre of the journal O_j.

$$\begin{bmatrix} F_{ux} \\ F_{uy} \end{bmatrix} = m\delta\omega^2 \begin{bmatrix} cos(\omega t) \\ sin(\omega t) \end{bmatrix} \tag{5.47}$$

in which the distance between the journal centre and the shaft centre is $\delta = I_j O_j$.
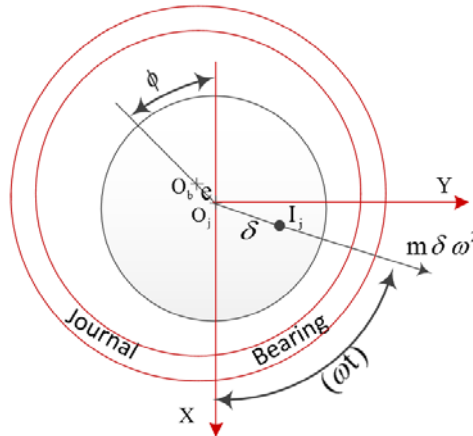
Figure 5.11 Vibration caused by unbalance force

5.3.2 Fluid Stiffness and Damping Coefficients

Fluid-film forces may be expanded in a Taylor series about the static equilibrium position[93].

$$F_x = F_{x0} + \frac{\partial F_x}{\partial x}\Delta x + \frac{\partial F_x}{\partial y}\Delta y + \frac{\partial F_x}{\partial \dot{x}}\Delta \dot{x} + \frac{\partial F_x}{\partial \dot{y}}\Delta \dot{y}$$

$$F_y = F_{y0} + \frac{\partial F_y}{\partial x}\Delta x + \frac{\partial F_y}{\partial y}\Delta y + \frac{\partial F_y}{\partial \dot{x}}\Delta \dot{x} + \frac{\partial F_y}{\partial \dot{y}}\Delta \dot{y}$$

(5.48)
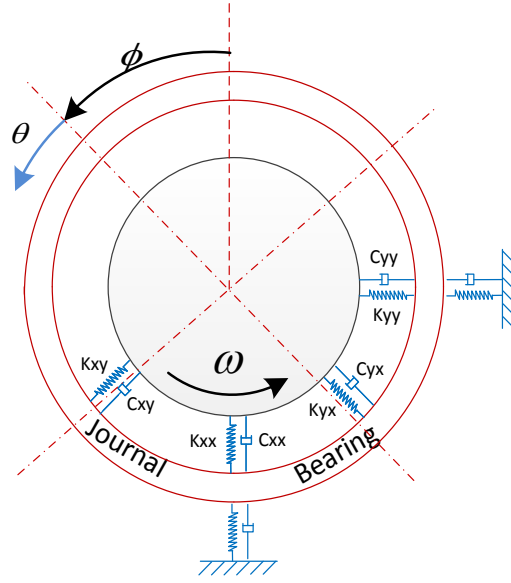
Figure 5.12 Fluid coefficients model

Fluid film bearing stiffness K_{ij}, $ij = X, Y$ and damping C_{ij}, $ij = X, Y$ force coefficients are defined as

$$K_{ij} = \frac{-\partial F_i}{\partial x_j}$$

(5.49)

$$C_{ij} = \frac{-\partial F_i}{\partial \dot{x}_j}; \quad i, j = x, y$$

(5.50)

For example, $K_{xy} = \partial F_x / \partial y$ corresponds to a stiffness produced by a fluid force in the X direction due to a journal static displacement in the Y direction. By definition, this coefficient is evaluated at the equilibrium position with other journal centre displacements and velocities set to zero. The negative sign in the definition ensures that a positive magnitude stiffness coefficient corresponds to a restorative force [90].

$$F_x = F_{x0} + K_{xx}\Delta x + K_{xy}\Delta y + C_{xx}\Delta \dot{x} + C_{xy}\Delta \dot{y}$$
$$F_y = F_{y0} + K_{yx}\Delta x + K_{yy}\Delta y + C_{yx}\Delta \dot{x} + C_{yy}\Delta \dot{y}$$

(5.51)

The force coefficients (K_{xx}, K_{yy}) are known as the direct stiffness terms, while (K_{xy}, K_{yx}) are referred as cross-coupled stiffness. Figure 5.12 provides a pictorial representation of the bearing force coefficients as mechanical parameters.

With these relationships, one finally obtains after transformation the following relationships for the stiffness and damping coefficients of the short circular bearing.

$$k_{ij} = K_{ij}\frac{c}{F_e}; \quad c_{ij} = C_{ij}\frac{c\omega}{F_e}$$

(5.52)

where F_e is the static load applied on a bearing in the X direction. c and ω are radial clearance and rotational speed, respectively. k_{ij} and c_{ij} are the dimensionless stiffness and damping coefficients, respectively. They are given by [93]

$$k_{xx} = \frac{f_{ro}}{\varepsilon(1-\varepsilon^2)}(f_{ro}^2 + 1 + 2\varepsilon^2)$$

(5.53)

$$k_{yy} = \frac{f_{ro}}{\varepsilon(1-\varepsilon^2)}(f_{to}^2 + 1 - \varepsilon^2)$$

(5.54)

$$k_{xy} = \frac{f_{to}}{\varepsilon(1-\varepsilon^2)}(f_{ro}^2 + 1 + 2\varepsilon^2)$$

(5.55)

$$k_{yx} = \frac{f_{to}}{\varepsilon(1-\varepsilon^2)}(f_{ro}^2 - 1 + \varepsilon^2)$$

(5.56)

$$c_{xx} = \frac{2f_{to}}{\varepsilon(1-\varepsilon^2)}((2+\varepsilon^2)f_{ro}^2 + 1 - \varepsilon^2)$$

(5.57)

$$c_{yy} = \frac{2f_{to}}{\varepsilon(1-\varepsilon^2)}((2+\varepsilon^2)f_{to}^2 - 1 + \varepsilon^2)$$

(5.58)

$$c_{xy} = c_{yx} = \frac{2f_{ro}}{\varepsilon(1-\varepsilon^2)}((2+\varepsilon^2)f_{to}^2 - 1 + \varepsilon^2)$$

(5.59)

$$f_{ro} = \frac{4\sigma\varepsilon^2}{(1-\varepsilon^2)^2}$$

(5.60)

$$f_{to} = \frac{\pi\sigma\varepsilon}{(1-\varepsilon^2)^{3/2}}$$

(5.61)

$$\sigma = \frac{(1-\varepsilon^2)^2}{\varepsilon\sqrt{(16\varepsilon^2 + \pi^2(1-\varepsilon^2))}} \qquad (5.62)$$
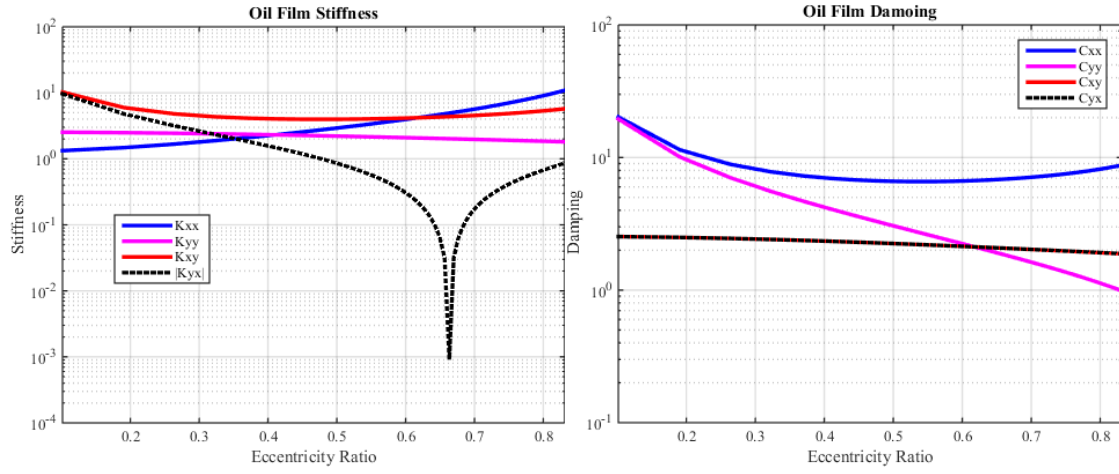
Figure 5.13 Dimensionless stiffness and damping coefficients
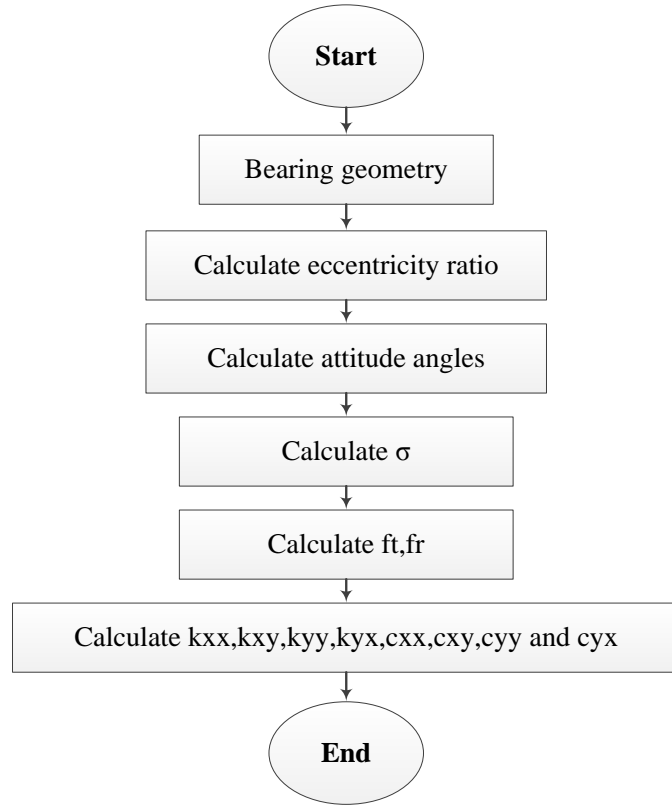
Flowchart 5.1 Fluid stiffness and damping coefficients

5.3.3 Vibration Excitations of Lubricated Surfaces

Signal simulation of the vibration produced by asperities is a significant and effective tool to understand vibration behaviour of journal bearings. Signals simulation can also aid to an improved understanding of the asperity generation mechanisms for understanding fault vibration symptoms. Simulations of asperity vibration can be used to characterise the performance of journal bearing and diagnostic techniques under the influence of asperity.

Almost no-studies currently present the vibration mechanism of asperities in journal bearings. This study presents a concept of vibration excitations by asperity interactions. Three different vibration mechanisms associated with asperity effects have been created for studying the dynamic effects on journal bearing, which are asperity collisions, asperity churns, and compressed asperities.

Simulated impact time signals is generated for each asperity based on their deflections. The impulse response function is given as [98]:

$$x(t) = Ae^{-\alpha t} cos(2\pi ft); \quad t > 0 \tag{5.63}$$

where f is the structural resonance frequencies of either the journal or the shaft, which is considered between (3-6) kHz and α is the damping ration which considered as random between (0.01-0.1). where A is the impulses amplitude which is considered based on maximum deflection of each asperities. The transient signature of the defective asperities can be modelled as:

$$u(t) = \sum_{i=1}^{n} A_i e^{-\alpha_i t} cos(2\pi f_i t) \tag{5.64}$$

n is the number of the impulses which also the number of asperities in contacts.

5.3.3.1 Asperity Collision Excitation

A journal bearing is designed to operate under the hydrodynamic regime. Unfortunately, it often operates under mixed or boundary regimes due to abnormal operating conditions during transient operations and fault cases like oil leakages, oil degradations, worn surfaces etc. In these two regimes asperity collisions occur and results in increased vibration. Figure 5.14 illustrates that asperity contact can be expressed as a source of vibrations in journal bearing. It shows that one of the asperity pairs has a larger degree of collisions, which

produces higher transient vibrations; whereas the smaller contact produces lower transient responses.
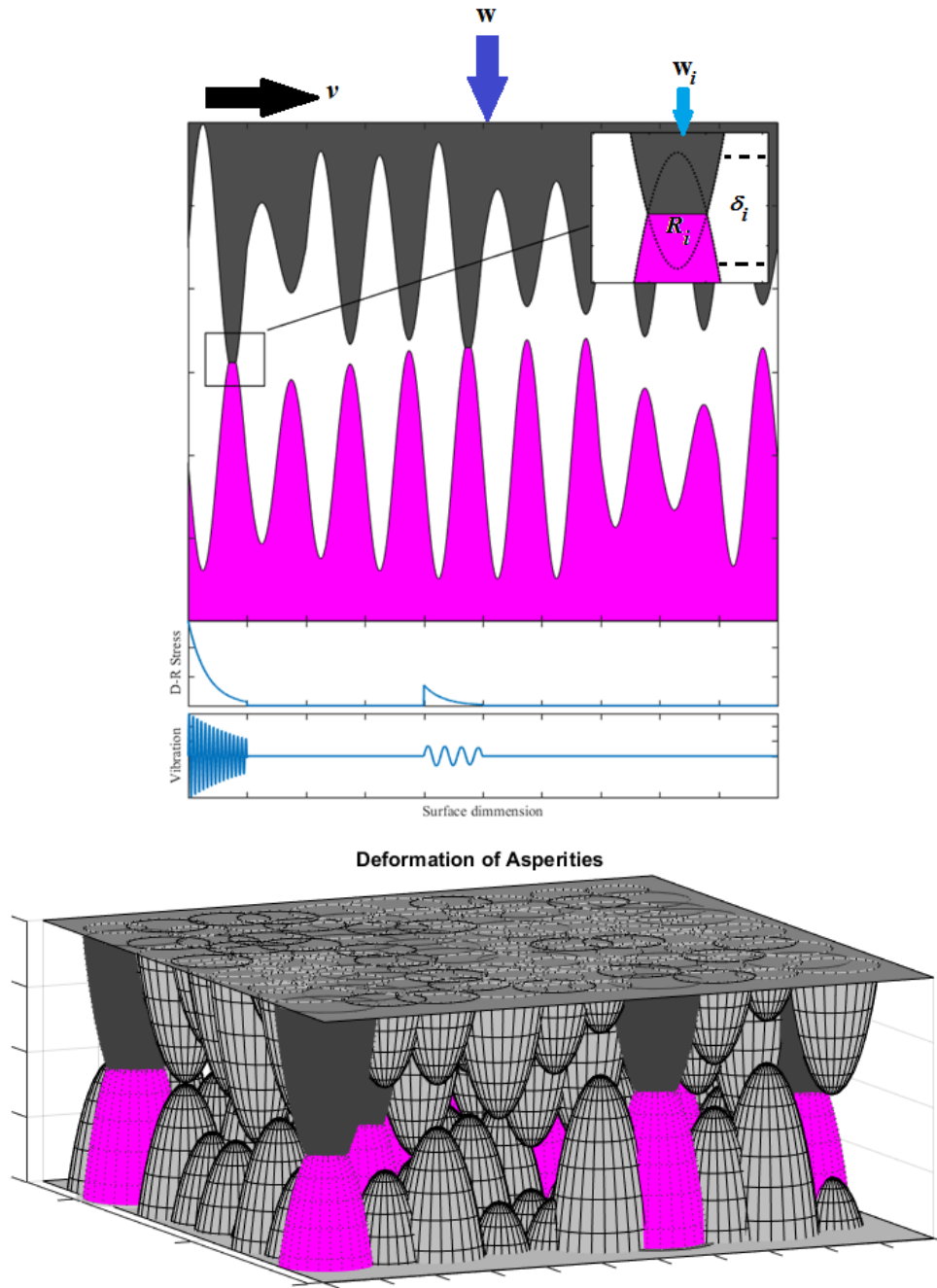
Figure 5.14 Asperity deformation caused by collisions

The pressure undertaking by a asperity pair can be expressed as

$$p = \frac{w}{A} \tag{5.65}$$

The contact area A between the shaft and bearing is nearly summation of asperity areas A_i at contact zone.

$$\sum_{i=1}^{n} A_i \cong A \tag{5.66}$$

where n is the number of asperity pairs in contact per unit area. To simplify the modelling of such collision effects, all the asperity summits are assumed to be spherical, which are more close to realistic cases after the running-in phase, thus any asperity area can be expressed as:

$$A_i = \pi a_i^2 \tag{5.67}$$

At boundary lubricant regime, radial load w is high and cause asperity collisions. And by assuming that the radial load distributed uniformly over the contact area

$$\sum_{i=1}^{n} w_i = w \tag{5.68}$$

The maximum deflection δ_i of asperity pair can be expressed as a function of elastic modulus, total load, and dimension of each asperity.

$$\delta = f(E, w, R) \tag{5.69}$$

Based on Hertz theory the maximum deflection δ_i in the contact area of each asperity pair can be expressed as [99]

$$\delta_i = \left(\frac{w_i^2}{E'^2 R_1} \right)^{1/3} \tag{5.70}$$

where E' is the equivalent elastic modulus for two different solid materials, it depends on the Poisson ratio and the modulus of elasticity for the two materials [88].

$$\frac{1}{E'} = \frac{3}{4} \left[\left(\frac{1 - v_1^2}{E_1} \right) + \left(\frac{1 - v_2^2}{E_2} \right) \right] \tag{5.71}$$

The elastic energy releases during the process when each asperity is compressed and stretched. The mean elastic energy of a pair of asperity can express as:

$$U_i = w_i \delta_i \tag{5.72}$$

$$U_{asperity\ contact} = \sum_{i=1}^{n} U_i \tag{5.73}$$

Figure 5.16 presents the stressed deformation of asperity contacts, and Figure 5.17 shows the vibration manner of asperity collisions.
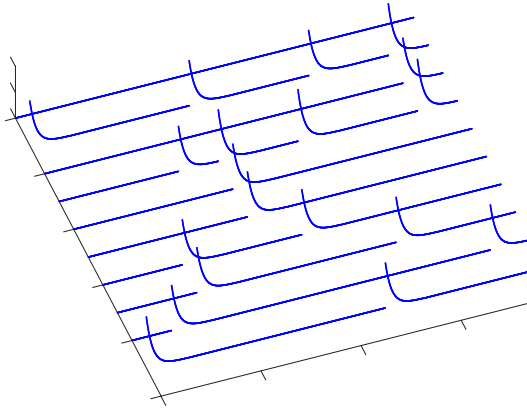
Figure 5.15 Stress deformations of asperities   Figure 5.16 Vibration manner of asperities
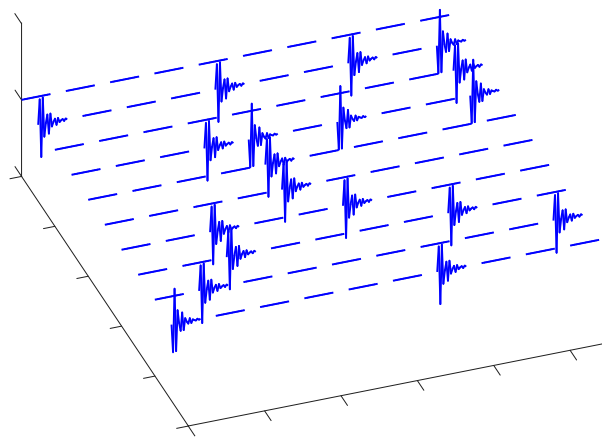
For more detailed understanding of the asperity collisions, asperity contact can be also represented as a spring has a unique stiffness coefficient as shown in Figure 5.17.
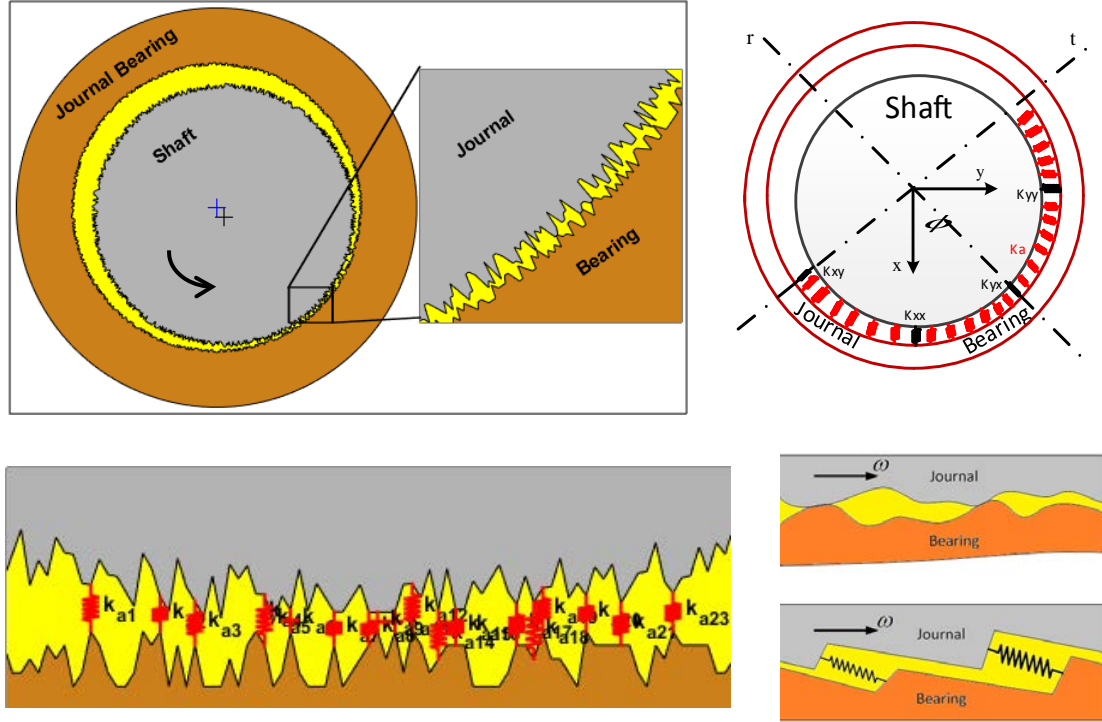
Figure 5.17 Vibration caused by asperity collisions

The stiffness of a single asperity contact pair is built and calculated based on shoulder-shoulder asperity contact [100], as seen in Figure 5.18.
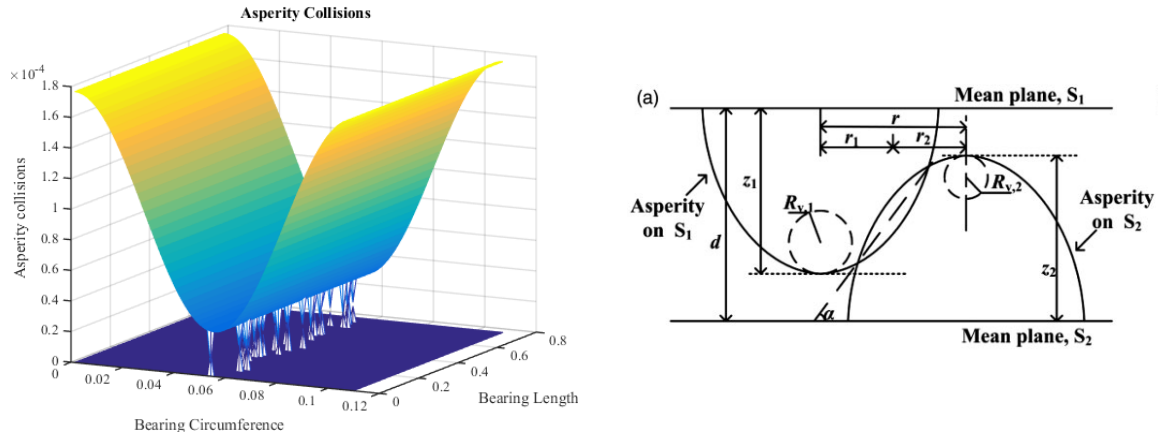
Figure 5.18 Shoulder-shoulder asperity contact [100]

$$w = w_1 \cos \alpha \qquad (5.74)$$

$$w_1 = z_1 + z_2 - d - \frac{r^2}{2R_s} \qquad (5.75)$$

$$\cos\alpha = \left(1 + \frac{r^2}{R_s^2}\right)^{-1/2} \qquad (5.76)$$

$$R_s = R_{v,1} + R_{v,2} \qquad (5.77)$$

where d is the separation of two surfaces, r is the tangential offset of two contact asperities, $R_{v,1}$ and $R_{v,2}$ are the radii of asperity summits and in contrast, z_1 and z_2 are the heights of summits, f is the contact force and f_n, and f_t are its normal and tangential components, is the contact angle, w, w_1 are interferences in different directions.

The Jackson and Green (JG) elastic-plastic contact model was employed to fit contact force piecewise on single asperity scale as

$$f^* = \begin{cases} w_*^{3/2} & 0 < w_* \leq 1.9 \\ \left[\exp\left(-\frac{1}{4}w_*^{5/12}\right)\right]w_*^{3/2} + \frac{4H_G}{CS_y}\left[1 - \exp\left(-\frac{1}{15}w_*^{5/9}\right)\right]w_* & w_* \geq 1.9 \end{cases} \qquad (5.78)$$

where f^* is the ratio of f to the critical force fc and w^* is the ratio of w to the critical interference w_c. From the JG contact model, w_c and fc are provided as

$$w_c = \left(\frac{\pi CS_y}{2E'}\right)^2 R_{v,s} \qquad (5.79)$$

$$f_c = \frac{4}{3}E'R_{v,s}^{1/2}w_c^{3/2} \qquad (5.80)$$

where the equivalent radius of asperity summit $R_{v,s}$ is defined by

$$R_{v,s} = \frac{R_{v,1}R_{v,2}}{R_{v,1} + R_{v,2}} \qquad (5.81)$$

S_y is the yield strength. C is related to, the Poisson ratio of the softer contact material, by

$$C = 1.295\exp(0.736v) \qquad (5.82)$$

E' is the combined Young's modulus for the two contact surfaces

$$\frac{1}{E'} = \frac{1-v_1^2}{E_1} + \frac{1-v_2^2}{E_2} \qquad (5.83)$$

where E_1, E_2 and v_1, v_2 are Young's moduli and Poisson ratios of two contact surfaces, respectively.

It is noteworthy that hardness geometric limit H_G which is defined in JG contact model, changes with the contact geometry and the material property following the formula

$$\frac{H_G}{S_y} = 2.84 - 0.92\left(1 - cos\left(\frac{\pi^2 Ce_y}{2} w_*^{1/2}\left(\frac{w_*}{1.9}\right)^{B/2}\right)\right) \tag{5.84}$$

where

$$e_y = \frac{S_y}{E'} \tag{5.85}$$

$$B = 0.14\,exp(\,23e_y\,) \tag{5.86}$$

Accordingly, the normal force f_n of single asperity contact pair is obtained

$$f_n = f\,cos\,\alpha \tag{5.87}$$

$$f_n = \begin{cases} \frac{4}{3}E'R_{v,s}^{1/2}w^{3/2}\left(1+\frac{r^2}{R_s^2}\right)^{1/4} & 0 < w_* \le 1.9 \\[4mm] fc\left(1+\frac{r^2}{R_s^2}\right)^{5/2}\left[\begin{array}{l} exp\left(\frac{-w_*^{5/12}}{4}\right)w_*^{3/2} \\[2mm] +\frac{4}{C}\left(2.84-0.92\left(1-cos\left(\frac{\pi^2 Ce_y}{2}w_*^{1/2}\left(\frac{w_*}{1.9}\right)^{B/2}\right)\right)\right) \\[2mm] \left(1-exp\left(\frac{-w_*^{5/9}}{25}\right)\right)w_* \end{array}\right] & w_* \ge 1.9 \end{cases} \tag{5.88}$$

The normal stiffness k_n of single asperity pair is calculated by

$$k_n = \frac{df_n}{dw_*}\times\frac{dw_*}{dw}cos\,\alpha = \frac{df_n}{dw_*}\times\frac{cos\,\alpha}{w_c(\,r\,)} \tag{5.89}$$

$$k_n = \begin{cases} 2E'R_{v,s}^{1/2}w^{1/2}\left(1+\frac{r^2}{R_s^2}\right)^{-1/4} & 0 < w_* \le 1.9 \\[4mm] w_c^{-1}\left(1+\frac{r^2}{R_s^2}\right)^{1/2}fc\left[\begin{array}{l} \dfrac{3\lambda w_*^{1/2}}{2}-\dfrac{5\lambda w_*^{11/12}}{48}-\dfrac{4\varepsilon(\gamma-1)}{C} \\[3mm] +\dfrac{4\varepsilon\gamma w_*^{5/9}}{45C}+\dfrac{46\kappa(B+1)(\gamma-1)sin\,\kappa}{25C} \end{array}\right] & w_* \ge 1.9 \end{cases} \tag{5.90}$$

$$\lambda = exp\left(\frac{-w_*^{5/12}}{4}\right) \tag{5.91}$$

$$\gamma = exp\left(\frac{-w_*^{5/9}}{25}\right) \tag{5.92}$$

$$\kappa = \left((10/19)^{B/2}\ \pi^2 Ce_y w_*^{(B+1)/2}\right) \tag{5.93}$$

$$\varepsilon = \left((23\cos\kappa)+48\right)/25 \tag{5.94}$$

While the contact occurs, the stiffness of the asperity pair is calculated and summed as the multi-asperity normal stiffness as

$$k_{an} = \frac{1}{A}\sum_{q=1}^{N} k_{an,q}(d) \tag{5.95}$$

where $k_{an,q}(d)$ is the stiffness of the number q contact pair at surface separation d, N is the total number of contact pairs and A is the nominal contact area [100].
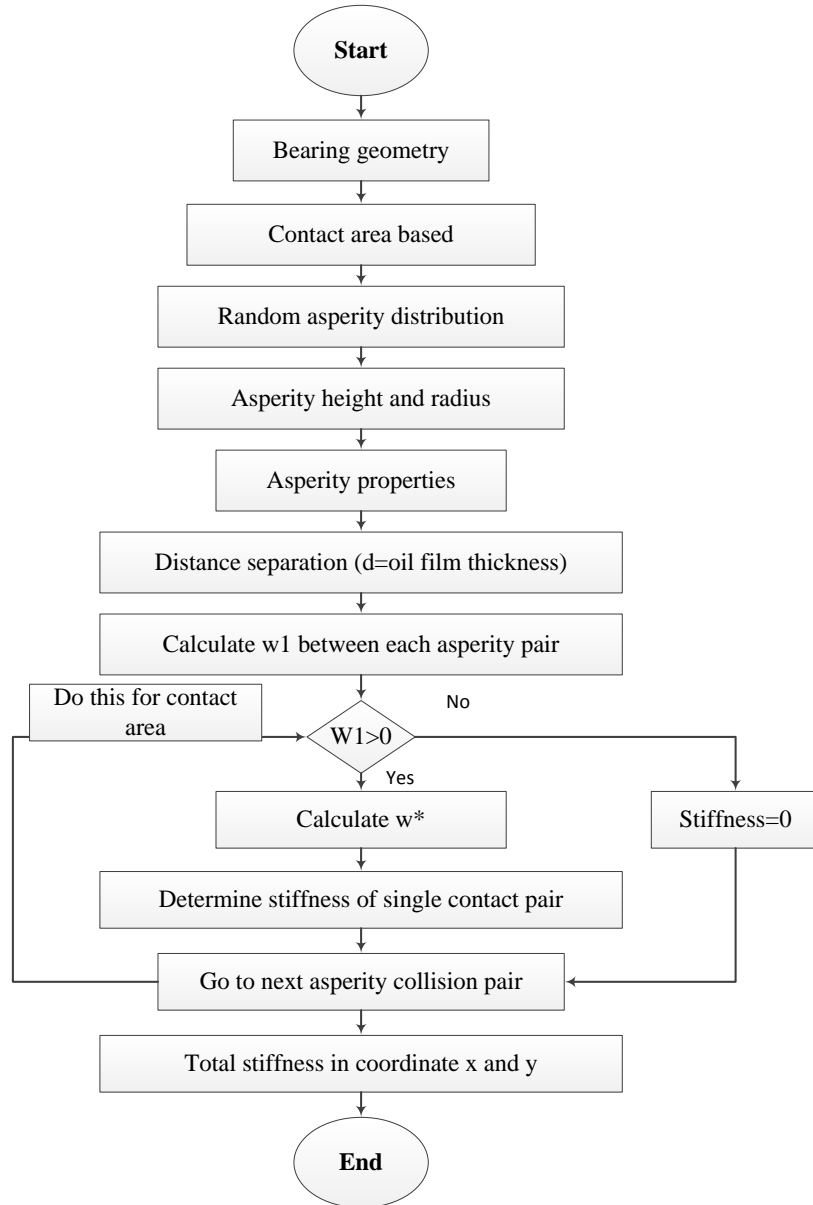
Flowchart 5.2 Asperity contact stiffness

This excitation leads to generate random forces cause corresponding high frequency vibration responses [28]. Figure 5.17 shows that asperity contact can be expressed as a spring has a unique stiffness coefficient.

5.3.3.2 Asperity Compression Excitation

Based on Reynolds Equation, at zone load, the oil pressure distributes over the bearing circumference. The maximum pressure is at minimum oil film (smallest gap between the shaft and the bearing). Pressure on an asperity causes compress it at load zone and decompress it at out of load zone.
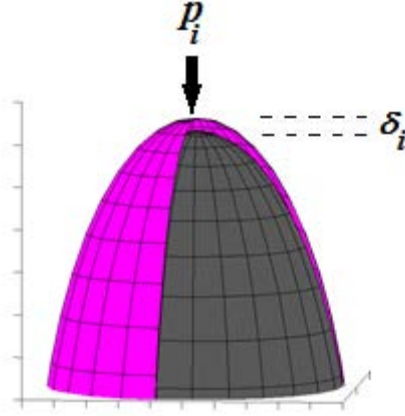
Figure 5.19 A compressed asperity by fluid pressure

The pressure distribution of a journal bearing is given by:

$$p_{\theta} = \frac{6\mu v r}{c^2} \frac{\varepsilon(2 + \varepsilon cos\theta) sin\theta}{(2 + \varepsilon^2)(1 + \varepsilon cos\theta)^2} \tag{5.96}$$

To simplify the modelling of asperity compressed, all the asperities are assumed to be as a roller or bar. By using Stress-strain relation could calculate the deflection caused by oil pressure.

$$\frac{\delta_i}{h_i} = \frac{p_{\theta_i}}{E} \tag{5.97}$$

$$\delta_i = \frac{h_i}{E} \frac{6\mu v r}{c^2} \frac{\varepsilon(2 + \varepsilon cos\theta) sin\theta}{(2 + \varepsilon^2)(1 + \varepsilon cos\theta)^2} \tag{5.98}$$

Elastic energy of compressed asperities can express as:

$$U_i = w_i \delta_i \tag{5.99}$$

$$U_{fluid\ pressure-asperity} = \sum_{i=1}^{n} U_i \tag{5.100}$$
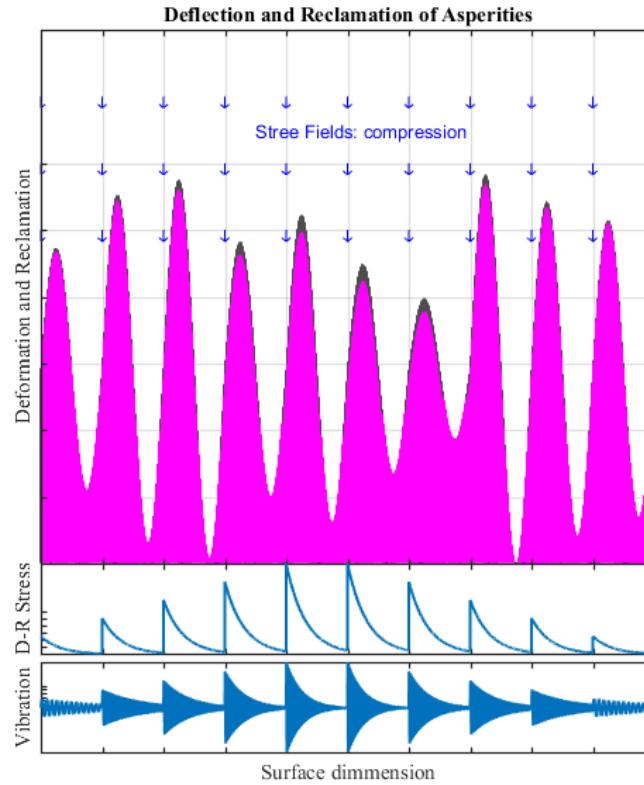
Figure 5.20 Fluid pressure causes asperity vibration

5.3.3.3 Asperity Churn Excitation

For high speeds and high oil viscosities but low radial loads, a bearing operates under hydrodynamic lubricant regime in which the bearing surfaces are separated by oil film and under this condition wear is minimal. However, the fluid shearing forces are high and consequently can cause high friction in the forms of heat generation and vibration. This type of vibration can be understood to be the effect of fluid shearing which causes an alternation between surface asperity deformation and reclamation because the shearing stress fields are not uniform i.e. random turbulent close to bearing surfaces. Even though of the separation, the vibration still exists which might be caused by churning the asperities. To simplify the modelling of asperity churns, all the asperities are assumed to be as a cantilever beam. As seen in Figure 5.21, F is the shear force due to the unidirectional or laminated oil flows, l is the length of an asperity and δ if the maximum deflection of the asperity.
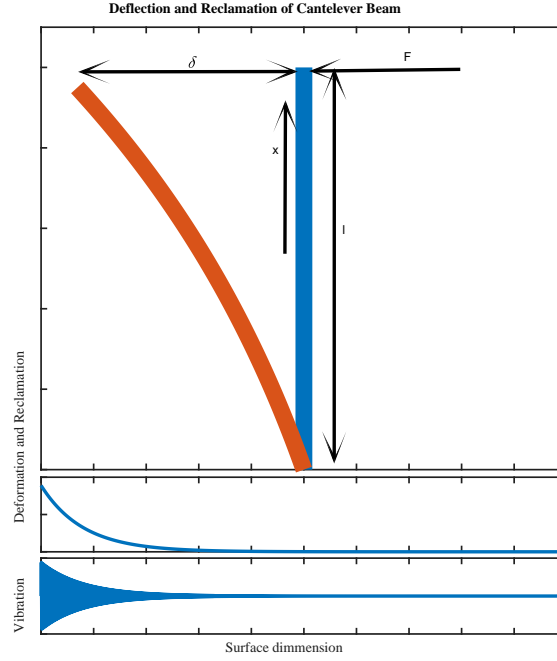
Figure 5.21 Cantilever beam deformation

The curvature of elastic curve of an asperity surface at a top point may be expressed as [101]

$$\frac{\frac{d^2 y}{dx^2}}{\left[1+\left(\frac{dy}{dx}\right)^2\right]^{3/2}} = \frac{M(x)}{EI} \tag{5.101}$$

In the case of the elastic curve of a beam, the slop $\frac{dy}{dx}$ is very small. Thus it is negligible, the Equation can be expressed as

$$\frac{d^2 y}{dx^2} = \frac{M(x)}{EI} \tag{5.102}$$

The product EI is known as the flexural rigidity. Assuming the shape of the asperities looks like beam, so the flexural rigidity is constant. By integration, the Equation becomes

$$EI\frac{dy}{dx} = \int_0^l M(x)\,dx + C_1 \tag{5.103}$$

Integrating the Equation to obtain the deflection of the asperity

$$y = \delta = \frac{1}{EI} \int_0^l \left[\int_0^l M(x) \, dx + C_1 \right] dx + C_2 \tag{5.104}$$

The cantilever beam is an extremely useful model for asperity churning. The fundamental assumptions of a straight cantilever beam analysis can have extended to asperity churning of most any shape and size. Shear forces (F) of oil flow which applied on asperities give amount of deflection (δ). The ratio between the force and deflection in each asperity is referred to as the stiffness of the asperity churning. The linear relationship between the force and deflection of a cantilever beam, as long as the deflection is small and the beam material does not yield is expressed as:

$$\delta(x) = \frac{Fx^2}{6EI}(3l - x) \tag{5.105}$$

Here, E is the elastic modulus of the spring material, I is the area moment of inertia of the beam cross section, l is the length of the beam, and F is the force applied on the end of the beam. The deflection amount depends on the geometry of the beam as well as the material stiffness of the beam. For a deflection at the end of the beam perpendicular to the beam axis, the force can be expressed as:

$$\delta_{max} = \frac{Fl^3}{3EI} \tag{5.106}$$

This equation is only valid if the stress in the spring does not exceed the elastic limit of the metal. If the material should start to yield, the elastic modulus is no longer a constant.

Elastic energy of the defection converted to heat, acoustic emission or vibration can express as:

$$U_i = w_i \delta_i \tag{5.107}$$

$$U_{asperity\ churn} = \sum_{i=1}^{n} U_i \tag{5.108}$$

Figure 5.22 shows the vibration modes and maximum deflections of asperities while the oil flows at zone load.
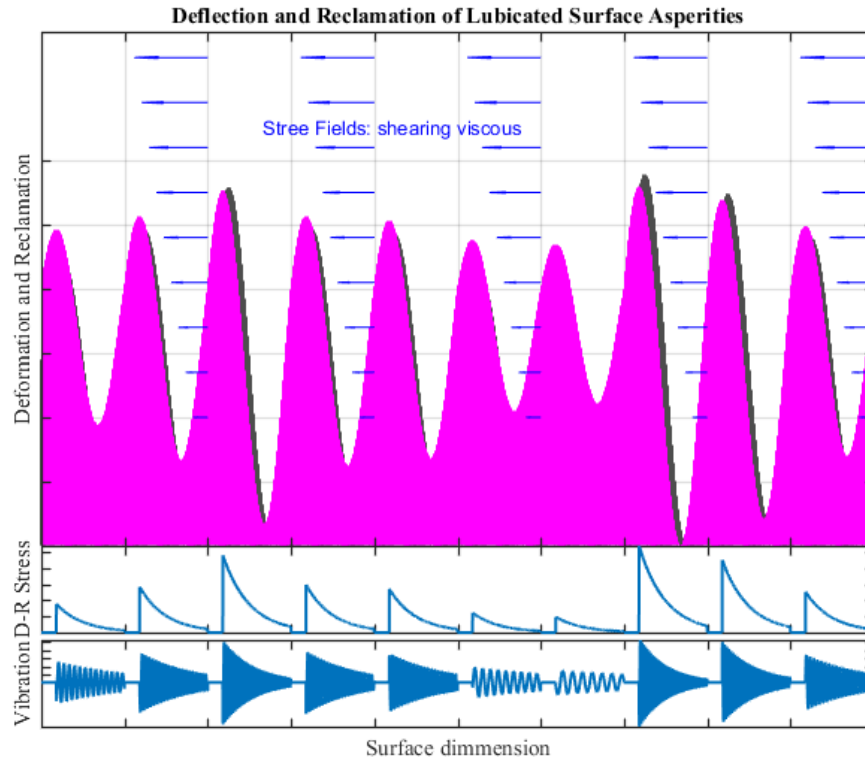
Figure 5.22 Asperity churns

The surface asperities in the fluid field endure both compression and shear forces. Figure 5.23 presents the total elastic energy of asperities.

$$U_{total} = U_{asperity\ churn} + U_{fluid\ pressure-asperity} \tag{5.109}$$

Deflection and Reclamation of Lubicated Surface Asperities
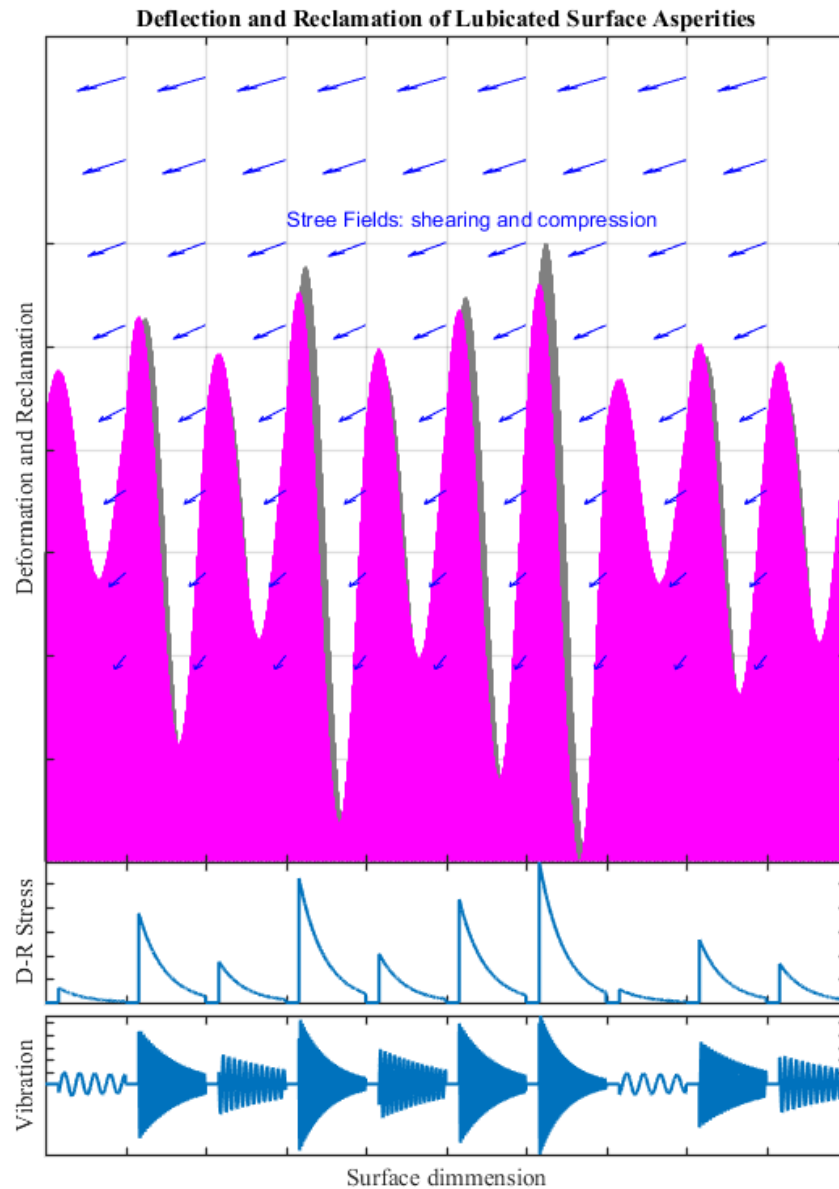
Figure 5.23 Total elastic energy of asperity churns and compress

5.3.3.4 Combined Asperity Excitations

In the mixed lubrication regime, vibration is caused mainly by asperity-asperity collisions and asperity churns. Figure 5.24 illustrates both such sources of vibration in the journal bearing.
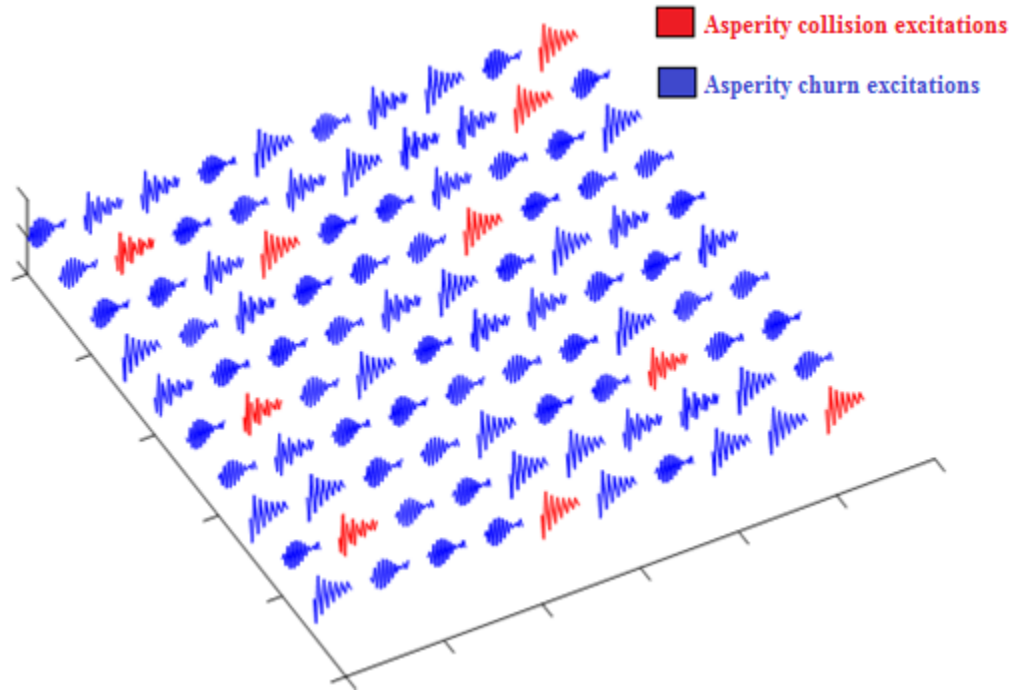
Figure 5.24 Vibration by both asperity collisions and asperity churns

5.3.3.5 Signal Processing for Reseponses to the Combined Asperity Excitations

According the Equation (5.109) above, the frequency response will be wide band frequency as shown in Figure 5.25.
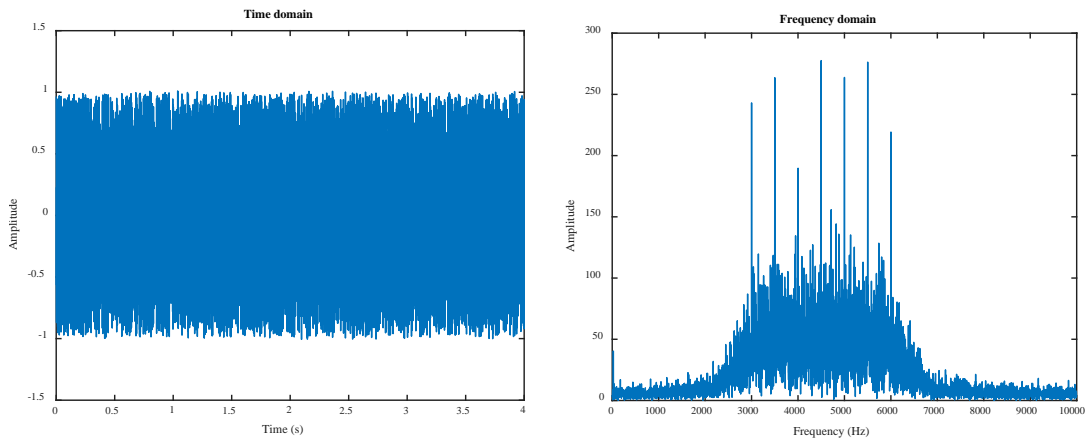
Figure 5.25 Wide frequency band of asperity vibrations

The conventional dynamic vibration model of journal bearing is combined with the influences of rotor unbalance, hydrodynamic force and radial load [9, 10]. However, according to the hydrodynamic lubrication and friction generation mechanisms, vibration responses of a journal bearing can be modelled to take into account two more fault related

excitations namely micro asperity collisions and churns. As illustrated in Figure 5.23, the micro peaks on the lubricated surfaces can bend when they enter into the high pressure zones and recover elastically in the low pressure zones. Similarly, the bending deformation and restoration will happen for the asperity collisions as illustrated in Figure 5.14. Thereby, the conventional dynamic models [102, 103] for journal bearings can be extended to be in the form of

$$m_s \ddot{x} + \overbrace{k[p(x), \omega, \mu]x}^{\text{Hydrodynamic}} + \overbrace{\sum_{i=1}^{n} \tilde{k}_i \Gamma[p(x), \omega, \mu]x}^{\text{Asperity churns}} + \overbrace{\sum_{i=1}^{n} \tilde{k}_i \Psi[p(x), \omega, \mu]x}^{\text{Asperity collisions}} = \overbrace{F_r}^{\text{Static radial load}} + \overbrace{\sum_{i}^{n} A_i \cos(i\omega t + \alpha_i)}^{\text{Unbalance+misalignment}} \quad (5.110)$$

m_s is the mass of the shaft; $\tilde{k}_i$ denotes the bending stiffness of an arbitrary micro asperity; k is the stiffness coefficients due to hydrodynamic pressure effect which includes inherent surface defects and journal elastic deformations of micro asperities and main load zones. Obviously, the unbalance and eccentricity often cause low frequency vibrations appearing at the shaft rotation orders: $i\omega$. Particularly, the oil whirl and whip phenomena due to the average unsteady flow will be at about 0.4ω [8]. On the other hand, due to the micro-scale and random distributions of asperities and dynamic pressures, their vibration responses would appear at high frequency range and high randomness. Moreover, these periodic and random excitations will be coupled due to the self-excitation mechanism, which can lead to nonlinear modulation contents. Especially, these vibrations can be further influenced nonlinearly by structural resonances, making the measured responses highly complicated and nonlinear.

5.4 Equation of Motion

In designed operating conditions, mainly there is not any asperity contact, the journal spins inside the bearing and the oil film completely separates their surfaces. By decreasing the oil film thickness, metal to metal contact occurs and asperity stiffness affects the motion.

Figure 5.26 (a) presents only external forces and fluid forces. Figure 5.26 (b) shows how asperity collisions generate vibration.
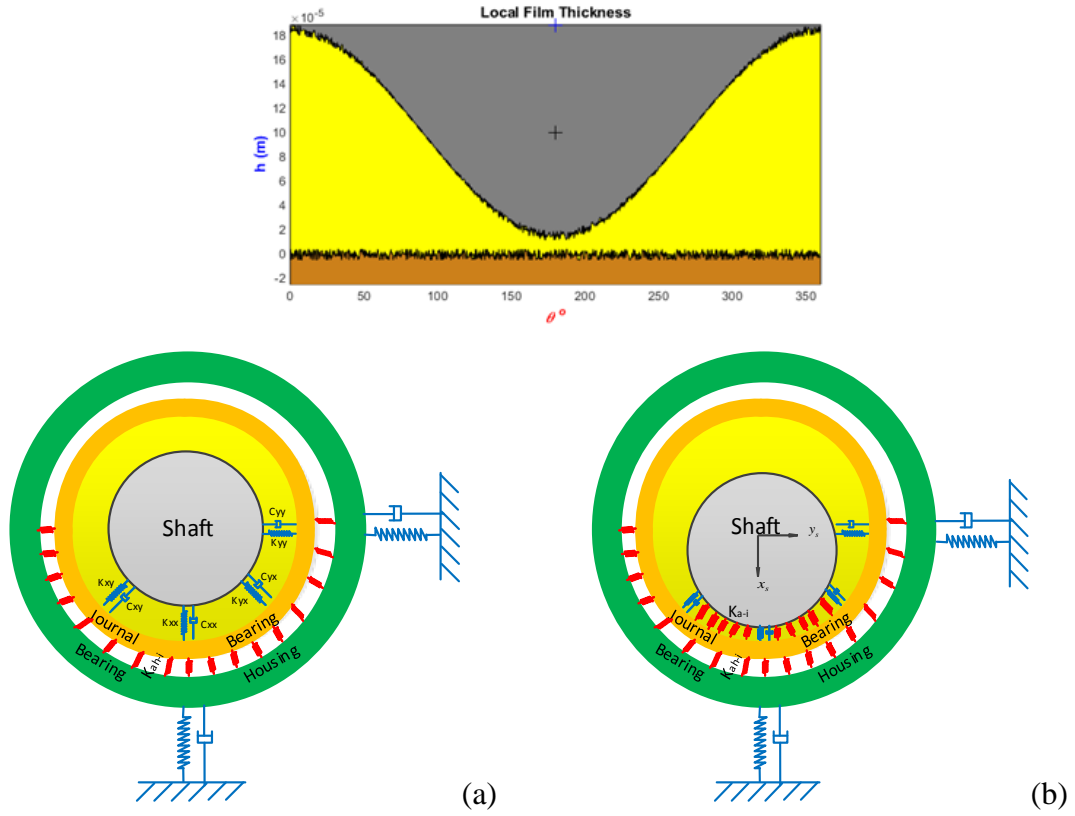
Figure 5.26 Vibration model. a) Considers fluid coefficients (hydrodynamic regimes). b) Considers fluid coefficients and asperity contact (boundary regimes)

The free body diagrams and vibration model for internal and external excitation can be represented as in Figure 5.27.
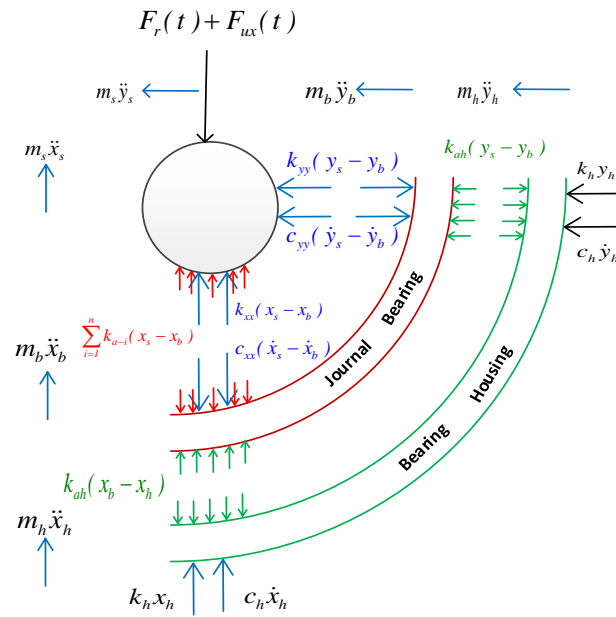
Figure 5.27 Free body diagram of a journal bearing

$$m_s \ddot{x}_s + c_{xx}(\dot{x}_s - \dot{x}_b) + k_{xx}(x_s - x_b) + c_{xy}(\dot{y}_s - \dot{y}_b) + k_{xy}(y_s - y_b)$$

$$+ \sum_{i=1}^{n} c_{a\_i}(\dot{x}_s - \dot{x}_b) + \sum_{i=1}^{n} k_{a\_i}(x_s - x_b) = F_r(t) + F_{ux}(t) \tag{5.111}$$

$$m_b \ddot{x}_b - c_{xx}(\dot{x}_s - \dot{x}_b) - k_{xx}(x_s - x_b) - c_{xy}(\dot{y}_s - \dot{y}_b) - k_{xy}(y_s - y_b)$$

$$- \sum_{i=1}^{n} c_{a\_i}(\dot{x}_s - \dot{x}_b) - \sum_{i=1}^{n} k_{a\_i}(x_s - x_b) + c_{xah}(\dot{x}_b - \dot{x}_h) + k_{xah}(x_b - x_h) = 0 \tag{5.112}$$

$$m_h \ddot{x}_h - c_{xah}(\dot{x}_b - \dot{x}_h) - k_{xah}(x_b - x_h) + c_h \dot{x}_h + k_h x_h = 0 \tag{5.113}$$

$$m_s \ddot{y}_s + c_{yy}(\dot{y}_s - \dot{y}_b) + k_{yy}(y_s - y_b) - c_{yx}(\dot{x}_s - \dot{x}_b) - k_{yx}(x_s - x_b)$$

$$+ \sum_{i=1}^{n} c_{a\_i}(\dot{y}_s - \dot{y}_b) + \sum_{i=1}^{n} k_{a\_i}(y_s - y_b) = F_{uy}(t) \tag{5.114}$$

$$m_b \ddot{y}_b - c_{yy}(\dot{y}_s - \dot{y}_b) - k_{yy}(y_s - y_b) + c_{yx}(\dot{x}_s - \dot{x}_b) + k_{yx}(x_s - x_b)$$

$$- \sum_{i=1}^{n} c_{a\_i}(\dot{y}_s - \dot{y}_b) - \sum_{i=1}^{n} k_{a\_i}(y_s - y_b) + c_{yah}(\dot{y}_b - \dot{y}_h) + k_{yah}(y_b - y_h) = 0 \tag{5.115}$$

$$m_h \ddot{y}_h - c_{yah}(\dot{y}_b - \dot{y}_h) - k_{yah}(y_b - y_h) + k_h y_h + c_h \dot{y}_h = 0 \tag{5.116}$$

$$[M] = \begin{bmatrix} m_s & 0 & 0 & 0 & 0 & 0 \\ 0 & m_b & 0 & 0 & 0 & 0 \\ 0 & 0 & m_h & 0 & 0 & 0 \\ 0 & 0 & 0 & m_s & 0 & 0 \\ 0 & 0 & 0 & 0 & m_b & 0 \\ 0 & 0 & 0 & 0 & 0 & m_h \end{bmatrix} \tag{5.117}$$

$$[K] = \begin{bmatrix} k_{xx} + \sum_{i=1}^{n} k_{xa\_i} & -k_{xx} - \sum_{i=1}^{n} k_{xa\_i} & 0 & k_{xy} & -k_{xy} & 0 \\ -k_{xx} - \sum_{i=1}^{n} k_{xa\_i} & k_{xx} + \sum_{i=1}^{n} k_{xa\_i} + k_{xah} & -k_{xah} & -k_{xy} & k_{xy} & 0 \\ 0 & -k_{xah} & k_{xah} + k_{xh} & 0 & 0 & 0 \\ -k_{yx} & k_{yx} & 0 & k_{yy} + \sum_{i=1}^{n} k_{ya\_i} & -k_{xx} - \sum_{i=1}^{n} k_{ya\_i} & 0 \\ k_{yx} & -k_{yx} & 0 & -k_{yy} - \sum_{i=1}^{n} k_{ya\_i} & k_{yy} + \sum_{i=1}^{n} k_{ya\_i} + k_{yah} & -k_{yah} \\ 0 & 0 & 0 & 0 & -k_{yah} & k_{yah} + k_{yh} \end{bmatrix} \tag{5.118}$$

$$[C] = \begin{bmatrix} c_{xx} + \sum_{i=1}^{n} c_{xa\_i} & -c_{xx} - \sum_{i=1}^{n} c_{xa\_i} & 0 & c_{xy} & -c_{xy} & 0 \\[2ex] -c_{xx} - \sum_{i=1}^{n} c_{xa\_i} & c_{xx} + \sum_{i=1}^{n} c_{xa\_i} + c_{xah} & -c_{xah} & -c_{xy} & c_{xy} & 0 \\[2ex] 0 & -c_{xah} & c_{xah} + c_{xh} & 0 & 0 & 0 \\[2ex] -c_{yx} & c_{yx} & 0 & c_{yy} + \sum_{i=1}^{n} c_{ya\_i} & -c_{xx} - \sum_{i=1}^{n} c_{ya\_i} & 0 \\[2ex] c_{yx} & -c_{yx} & 0 & -c_{yy} - \sum_{i=1}^{n} c_{ya\_i} & c_{yy} + \sum_{i=1}^{n} c_{ya\_i} + c_{yah} & -c_{yah} \\[2ex] 0 & 0 & 0 & 0 & -c_{yah} & c_{yah} + c_{yh} \end{bmatrix} \quad (5.119)$$
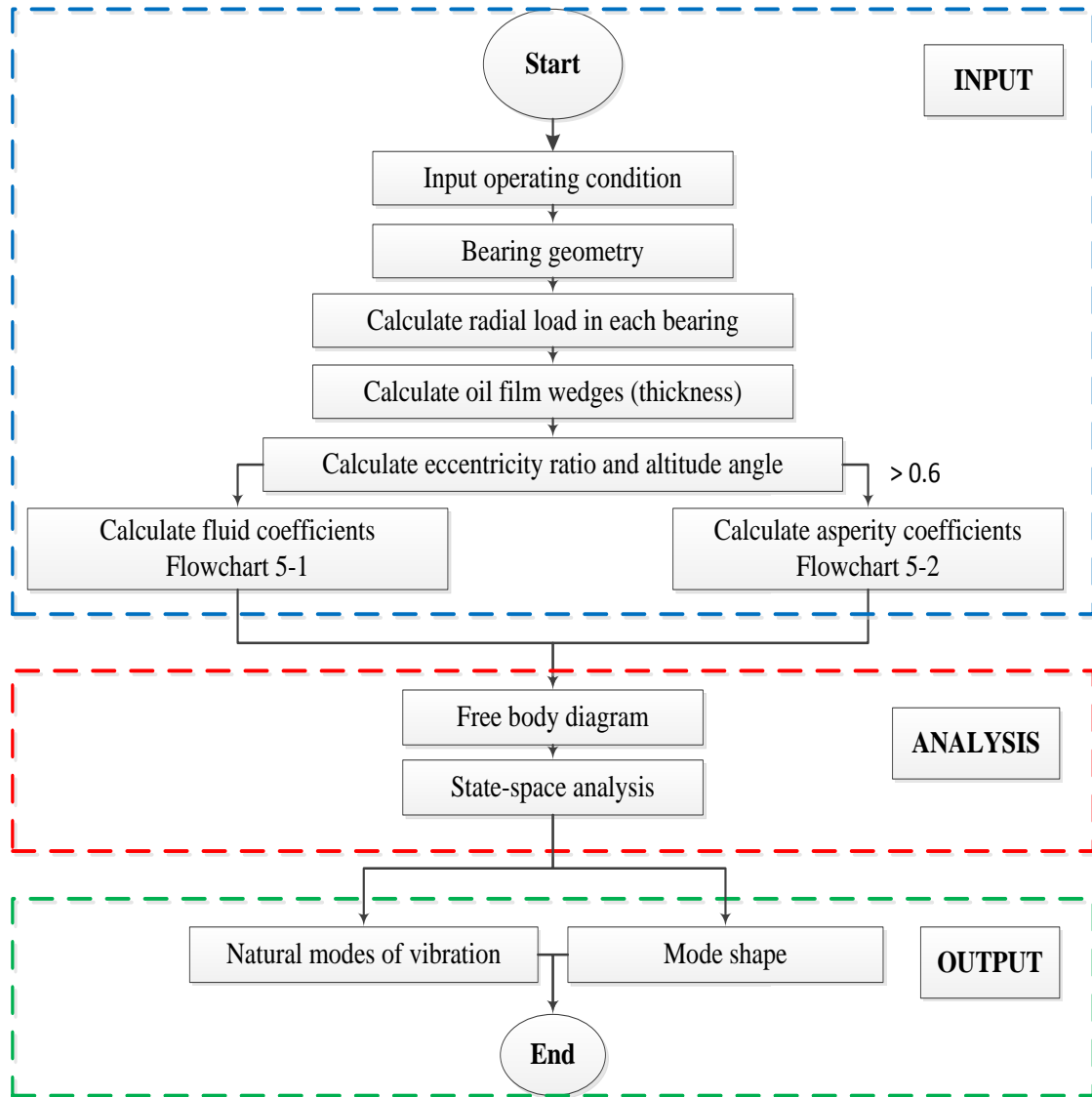
Flowchart 5.3 Mathematical model of journal bearing vibrations

5.5   State Space Representation

Representing the equations of motion of the system are complex with second order differential equations. The concept of the state space of a dynamic system refers to a minimum set of variables. It changes the form of the equations with second order differential equations to first order differential equations. The first order form of equations of motion is known as state space form.

State space has been used to estimate the linear system, and its equations are presents as

$$\dot{x}(t) = Ax(t) + Bu(t)$$
$$y(t) = Cx(t) + Du(t)$$

$$\begin{bmatrix} \dot{x}_1 \\ \vdots \\ \dot{x}_n \end{bmatrix} = A \begin{bmatrix} x_1 \\ \vdots \\ x_n \end{bmatrix} + B \begin{bmatrix} u_1 \\ \vdots \\ u_n \end{bmatrix}$$

$$\begin{bmatrix} y_1 \\ \vdots \\ y_n \end{bmatrix} = C \begin{bmatrix} x_1 \\ \vdots \\ x_n \end{bmatrix} + D \begin{bmatrix} u_1 \\ \vdots \\ u_n \end{bmatrix}$$

(5.120)

where x is the state vector of the system, u is the input scalar, y is the output scalar. The matrices A (system matrix) and B (input matrix) present the relationship between the state and input variables whereas the matrices C and D describe the relationship between the state and the output variables.

$$A = \begin{bmatrix} [0] & [I] \\ [K]/-[M] & [C]/-[M] \end{bmatrix}$$

(5.121)

$$B = \begin{bmatrix} [0] & [0] \\ [0] & [M^{-1}] \end{bmatrix}$$

(5.122)

In the state space formulation, the six second order differential equations of motions are converted to twelve first order differential equations.

$x_1 = x_s$	Postion of	Shaft	Mass	x	direction
$x_2 = x_b$	Postion of	Bearing	Mass	x	direction
$x_3 = x_h$	Postion of	House	Mass	x	direction
$x_4 = y_s$	Postion of	Shaft	Mass	y	direction
$x_5 = y_b$	Postion of	Bearing	Mass	y	direction
$x_6 = y_h$	Postion of	House	Mass	y	direction
$x_7 = \dot{x}_s$	Velocity of	Shaft	Mass	x	direction
$x_8 = \dot{x}_b$	Velocity of	Bearing	Mass	x	direction
$x_9 = \dot{x}_h$	Velocity of	House	Mass	x	direction
$x_{10} = \dot{y}_s$	Velocity of	Shaft	Mass	y	direction
$x_{11} = \dot{y}_b$	Velocity of	Bearing	Mass	y	direction
$x_{12} = \dot{y}_h$	Velocity of	House	Mass	y	direction

$$(5.123)$$

The relationship between the first and second derivatives:

$$\dot{x}_1 = \dot{x}_s = x_7$$
$$\dot{x}_2 = \dot{x}_b = x_8$$
$$\dot{x}_3 = \dot{x}_h = x_9$$
$$\dot{x}_4 = \dot{y}_s = x_{10}$$
$$\dot{x}_5 = \dot{y}_b = x_{11}$$
$$\dot{x}_6 = \dot{y}_h = x_{12}$$
$$\dot{x}_7 = \ddot{x}_s$$
$$\dot{x}_8 = \ddot{x}_b$$
$$\dot{x}_9 = \ddot{x}_h$$
$$\dot{x}_{10} = \ddot{y}_s$$
$$\dot{x}_{11} = \ddot{y}_b$$
$$\dot{x}_{12} = \ddot{y}_h$$

$$(5.124)$$

Rewriting the three equations for $\ddot{x}_s, \ddot{x}_b, \ddot{x}_h, \ddot{y}_s, \ddot{y}_b, \ddot{y}_h$ in terms of the twelve states x_1 through x_{12} and adding the three equations defining the position and velocity relationships:

$$\dot{x}_1 = \dot{x}_s = x_7$$

$$\dot{x}_2 = \dot{x}_b = x_8$$

$$\dot{x}_3 = \dot{x}_h = x_9$$

$$\dot{x}_4 = \dot{y}_s = x_{10}$$

$$\dot{x}_5 = \dot{y}_b = x_{11}$$

$$\dot{x}_6 = \dot{y}_h = x_{12}$$

$$\dot{x}_7 = \ddot{x}_s = \begin{bmatrix} c_{xx}(x_7 - x_8) + k_{xx}(x_1 - x_2) + c_{xy}(x_{10} - x_{11}) + k_{xy}(x_4 - x_5) \\ + \sum_{i=1}^{n} c_{a\_i}(x_7 - x_8) + \sum_{i=1}^{n} k_{a\_i}(x_1 - x_2) \end{bmatrix} / -m_s$$

$$\dot{x}_8 = \ddot{x}_b = \begin{bmatrix} -c_{xx}(x_7 - x_8) - k_{xx}(x_1 - x_2) - c_{xy}(x_{10} - x_{11}) - k_{xy}(x_4 - x_5) \\ - \sum_{i=1}^{n} c_{a\_i}(x_7 - x_8) - \sum_{i=1}^{n} k_{a\_i}(x_1 - x_2) + c_{ah}(x_8 - x_9) + k_{ah}(x_2 - x_3) \end{bmatrix} / -m_b$$

$$\dot{x}_9 = \ddot{x}_h = \begin{bmatrix} -c_{ah}(x_8 - x_9) - k_{ah}(x_2 - x_3) + c_h x_9 + k_h x_3 \end{bmatrix} / -m_h$$

$$\dot{x}_{10} = \ddot{y}_s = \begin{bmatrix} c_{yy}(x_{10} - x_{11}) + k_{yy}(x_4 - x_5) - c_{yx}(x_7 - x_8) - k_{yx}(x_1 - x_2) \\ + \sum_{i=1}^{n} c_{a\_i}(x_{10} - x_{11}) + \sum_{i=1}^{n} k_{a\_i}(x_4 - x_5) \end{bmatrix} / -m_s$$

$$\dot{x}_{11} = \ddot{y}_b = \begin{bmatrix} -c_{yy}(x_{10} - x_{11}) - k_{yy}(x_4 - x_5) + c_{yx}(x_7 - x_8) + k_{yx}(x_1 - x_2) \\ - \sum_{i=1}^{n} c_{a\_i}(x_{10} - x_{11}) - \sum_{i=1}^{n} k_{a\_i}(x_4 - x_5) + c_{ah}(x_{11} - x_{12}) + k_{ah}(x_5 - x_6) \end{bmatrix} / -m_b \qquad (5.125)$$

$$\dot{x}_{12} = \ddot{y}_h = \begin{bmatrix} -c_{ah}(x_{11} - x_{12}) - k_{ah}(x_5 - x_6) + c_h x_{12} + k_h x_6 \end{bmatrix} / -m_h$$

Rewriting the equations above in matrix form as:

$$\begin{bmatrix} \dot{x}_1 \\ \dot{x}_2 \\ \vdots \\ \dot{x}_{11} \\ \dot{x}_{12} \end{bmatrix} = \begin{bmatrix} \begin{bmatrix} 0 & 0 & \cdots & 0 \\ 0 & 0 & 0 & \vdots \\ \vdots & 0 & \ddots & 0 \\ 0 & \cdots & 0 & 0 \\ & [K]/-[M] & \end{bmatrix} & \begin{bmatrix} 1 & 0 & \cdots & 0 \\ 0 & 1 & 0 & \vdots \\ \vdots & 0 & \ddots & 0 \\ 0 & \cdots & 0 & 1 \\ & [C]/-[M] & \end{bmatrix} \end{bmatrix} \begin{bmatrix} x_1 \\ x_2 \\ \vdots \\ x_{11} \\ x_{12} \end{bmatrix} + \begin{bmatrix} \begin{bmatrix} 0 & \cdots & 0 \\ \vdots & \ddots & \vdots \\ 0 & \vdots & 0 \end{bmatrix} & \begin{bmatrix} 0 & \cdots & 0 \\ \vdots & \ddots & \vdots \\ 0 & \vdots & 0 \end{bmatrix} \\ \begin{bmatrix} 0 & \cdots & 0 \\ \vdots & \ddots & \vdots \\ 0 & \vdots & 0 \end{bmatrix} & [1/M] \end{bmatrix} \begin{bmatrix} u_1 \\ u_2 \\ \vdots \\ u_{11} \\ u_{12} \end{bmatrix} \qquad (5.126)$$

$$\begin{bmatrix} y_1 \\ y_2 \\ \vdots \\ y_{11} \\ y_{12} \end{bmatrix} = \begin{bmatrix} 1 & 0 & \cdots & \cdots & 0 \\ 0 & 1 & 0 & \iddots & \vdots \\ \vdots & 0 & \ddots & 0 & \vdots \\ \vdots & \iddots & 0 & 1 & 0 \\ 0 & \cdots & \cdots & 0 & 1 \end{bmatrix} \begin{bmatrix} x_1 \\ x_2 \\ \vdots \\ x_{11} \\ x_{12} \end{bmatrix} + [0] \begin{bmatrix} u_1 \\ u_2 \\ \vdots \\ u_{11} \\ u_{12} \end{bmatrix} \qquad (5.127)$$

The most basic analysis one can perform on a dynamic system is to solve for its eigen values (natural frequencies) and eigenvectors (mode shapes).

Start by postulating that there is a set of initial conditions such that if the system is released with that set, the system will respond in one of its natural modes of vibration. To that end, we set the forcing function to zero and write the homogeneous state space equations of motion;

$$\dot{x} = Ax \tag{5.128}$$

Defining motion in a principal mode as;

$$\begin{aligned} x_i &= x_{mi}e^{\lambda_i t} \\ \dot{x}_i &= \lambda x_{mi}e^{\lambda_i t} \end{aligned} \tag{5.129}$$

where λ_i is the ith eigenvalue (the natural frequency of the ith mode of vibration).

x_i is the states vector at the ith frequency.

x_{mi} is the ith eigenvector (the mode shape for the ith mode).

Substituting Equation (5.129) into the state equation Equation (5.128);

$$\lambda x_{mi} = Ax_{mi} \tag{5.130}$$

The eigenvalues and eigenvectors of the system can be calculated based on:

$$(\lambda I - A)x_{mi} = 0 \tag{5.131}$$

Where the eigenvector for the ith mode, $x_{mi} = [x_s, x_b, x_h, y_s, y_b, y_h, \dot{x}_s, \dot{x}_b, \dot{x}_h, \dot{y}_s, \dot{y}_b, \dot{y}_h]$

and the corresponding natural frequency can be calculated from the eigen value:

$$f_i = \sqrt{\lambda_i} / 2\pi \tag{5.132}$$

5.6 Multiple-Input Multiple-Output

Multiple-input multiple-output (MIMO) is a system with more than one input and/or more than one output. This is in contrast to systems that have only a single input and a single output (SISO). A state space system is represented as shown in Figure 5.28. The scalar inputs $u_n(t)$ are fed into state space function and the outputs $y_n(t)$ are scalar. A the system

matrix, B the mass influence matrix, C provides the relationship matrix between the state and the output variables and D the direct transmission matrix.

$$u_1(t) \rightarrow \boxed{\begin{array}{l} \dot{x}(t) = Ax(t) + Bu(t) \\ y(t) = Cx(t) + Du(t) \end{array}} \rightarrow y_1(t)$$

$Input \quad u_1(t), u_2(t), \dots, u_{12}(t) \rightarrow$ system $\rightarrow y_1(t), y_2(t), \dots, y_{12}(t) \quad Output$
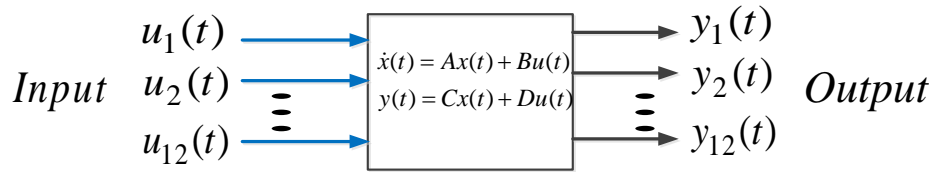
Figure 5.28 Block diagram of MIMO state space system

5.7 Model Results

Based on journal bearing parameters and state space technique, Eigen values have been calculated that determine the nature frequencies of the system. As the result of Eigen analysis, the natural frequencies of the shaft and the bearing are around 6 kHz and 13 kHz.

The result bellow, in Figure 5.29, presents vibration response of a journal bearing due to multi operating conditions. The operating conditions, speed 1500 rpm, under six different radial loads (1, 5, 10, 20, 40 bar) and three different oil viscosities (5, 15, 46). The vibration model has been simplified based on the value of eccentricity ration. At low eccentricity ratio, the excitation force is only correlated to fluid. At high eccentricity ratio, the excitations become more significant and correlation to both fluid and asperity forces, when the oil film thickness becomes much smaller than the size of the surface roughness.
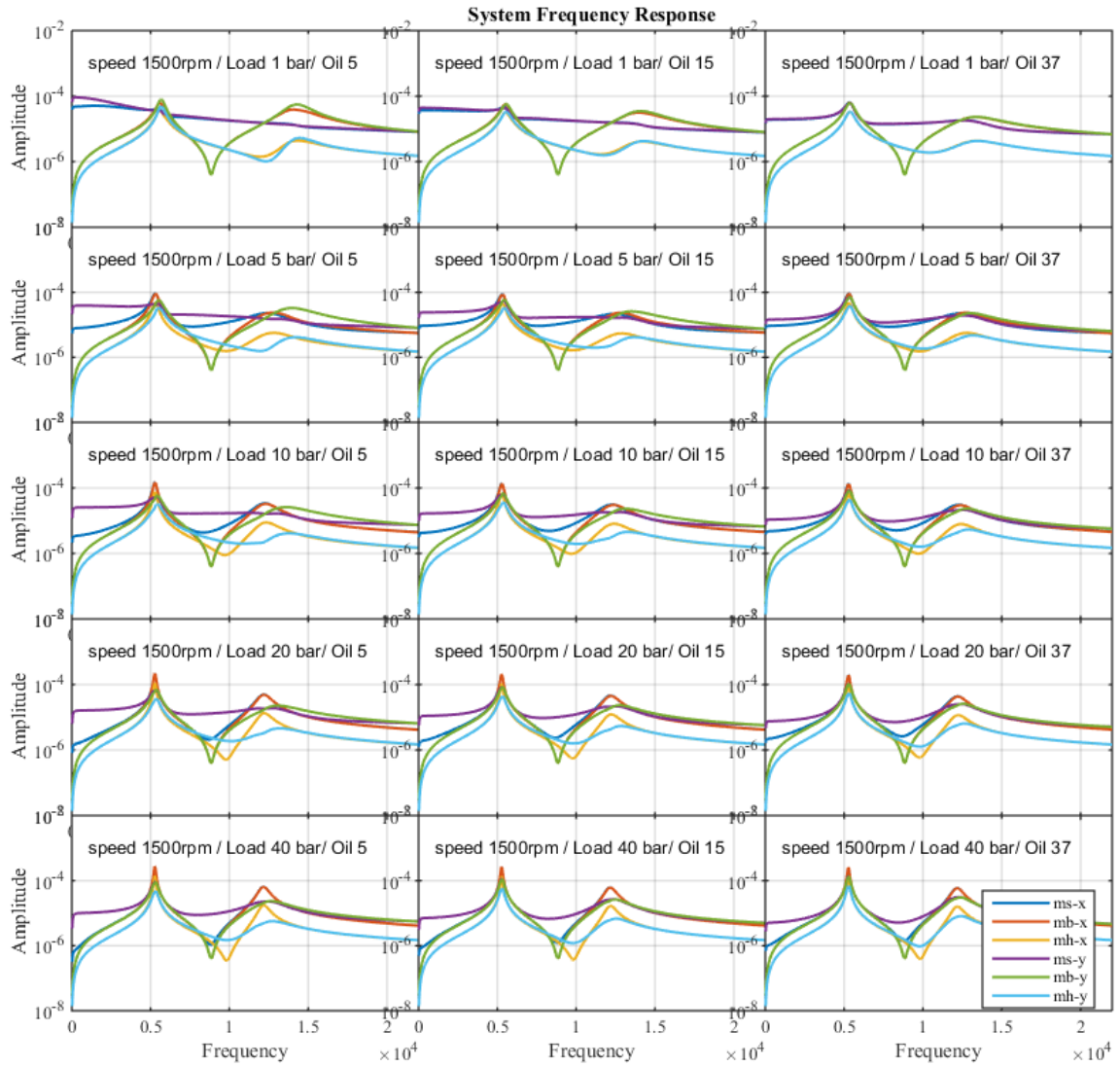
Figure 5.29 Natural frequency modes of wide operating conditions

Figure 5.30 presents six modes, each mode shows the vibration shapes of the shaft, bearing and house masses in X any Y axis. This also, presents the nature mode of vibration under different loads and oil viscosities. Figure 5.31 presents natural frequency for each mode under different operating conditions. Natural frequencies increase while the load increase and oil viscosity decrease.
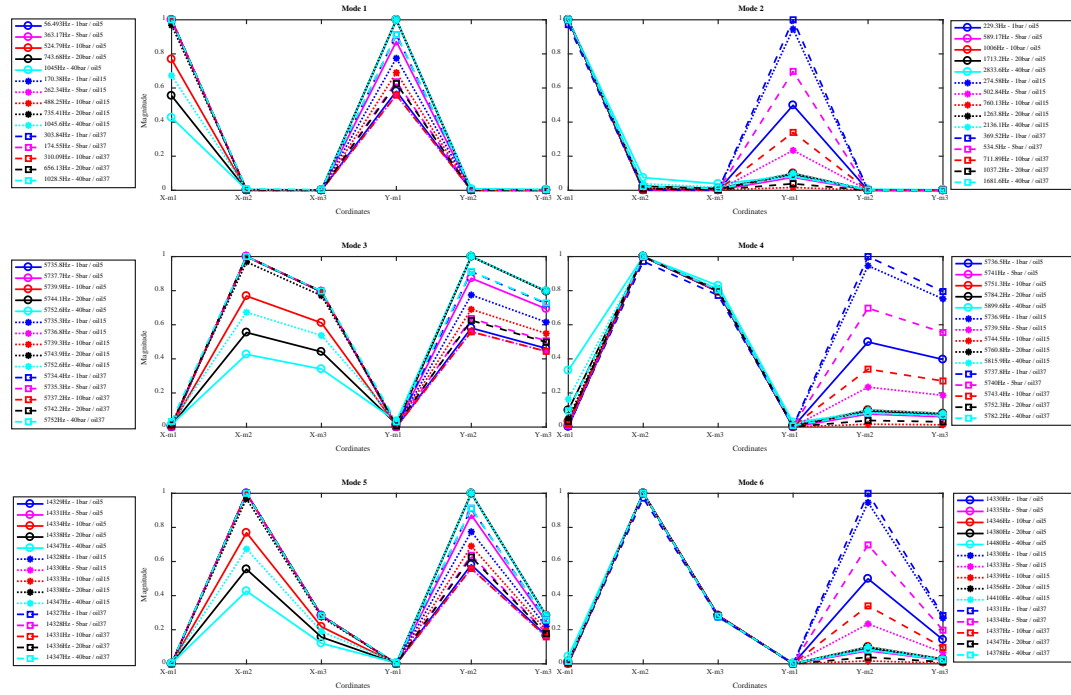
Figure 5.30 Natural modes of vibration
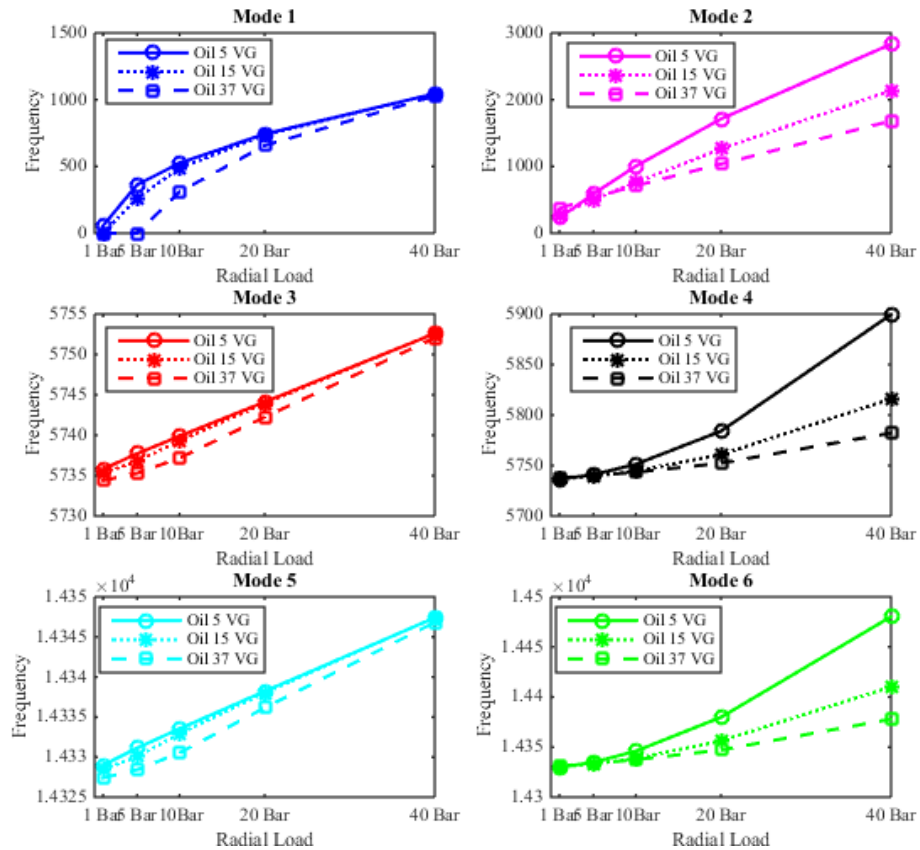
Figure 5.31 Natural frequency Vs radial load for three different oil viscosities
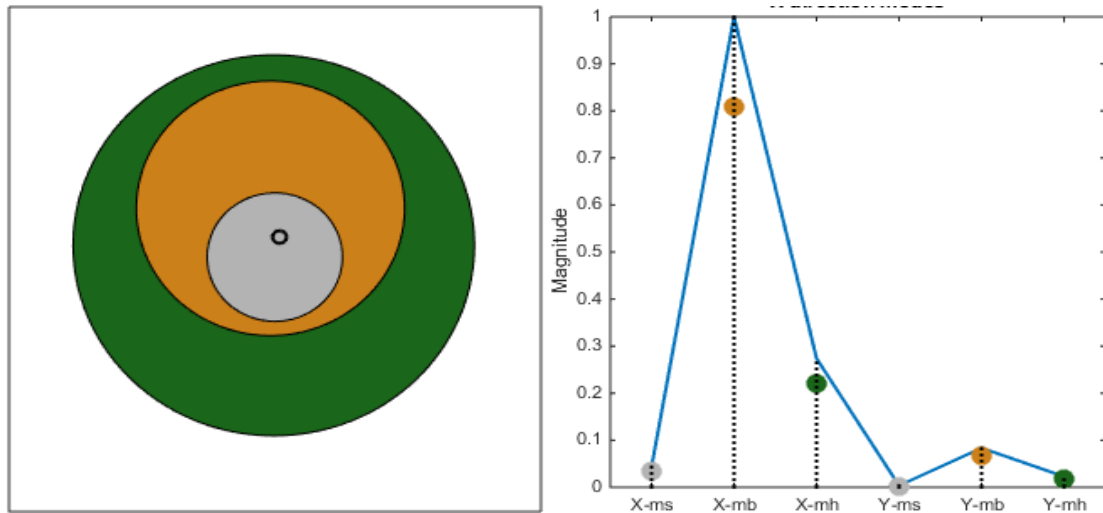
Figure 5.32 Vibration response of mode 6 at 1500 rpm and under 40 bar

5.8 Summary

A mathematical model is established for carrying out an in-depth of bearing vibration responses. This model considers not only conventional fluid forces but also asperity collision and churn effect, allowing explaining high frequency responses of the lubricated journal bearing to be the effect of micro asperity elastic deformations. The model with six degrees of freedom are solved by using the state space technique, each Eigen value and volume of a certain mass in one direction present natural and shape modes, respectively. The natural frequencies of the system are found to be around 6 kHz and 13 kHz. Additionally, as a result of asperity collisions which increase with higher radial loads or lower viscous oil, the natural frequencies of the journal bearing can shift higher.

CHAPTER SIX

TEST SYSTEMS AND METHODS

To verify and evaluate theoretical analysis and fault detection methods proposed, this chapter describes the test rig construction that includes the setup of journal bearing bench, instrumentation and other facilities with specifications of mechanical and electrical components, measurement instrumentations and devices. In addition, different test procedures are also depicted with respect to different bearing fault cases to be tested.

6.1 Introduction

To fulfil the aim and objectives planned, the research began with designing and building a bearing test rig to gain basic understandings of journal vibrations along with their operating characteristics. Moreover, the rig is capable to verify and evaluate techniques developed for fault detection and diagnosis.

The rig consists of an AC motor, a DC generator, a hydraulic system of radial load, two self-aligning spherical journal bearings and measurement instrumentation systems, including a data acquisition, an encoder, thermocouples, a pressure sensor, displacement laser sensors and accelerometers. In this configuration and selection, the bearing undertakes minimal misalignment effect when it operates under different loads, speeds and oil conditions. Simultaneously, bearing vibrations on its housing can be measured at high sampling rate together with other critical operating parameters.

Preliminary experiments were conducted to ensure all equipment and instrumentation to operate as expected and to obtain good measurement repeatability and reliability. Preliminary experiment results showed that all the equipment including the driving, the loading, the data acquisition and the measurement system perform adequately. The test rig is displayed in Figure 6.1 and Figure 6.2.

The motor speed is controlled by a Siemens Micro Master Controller so the drive shaft can be run at different speeds. Also, a manual hydraulic pump is used to apply a defined radial load.
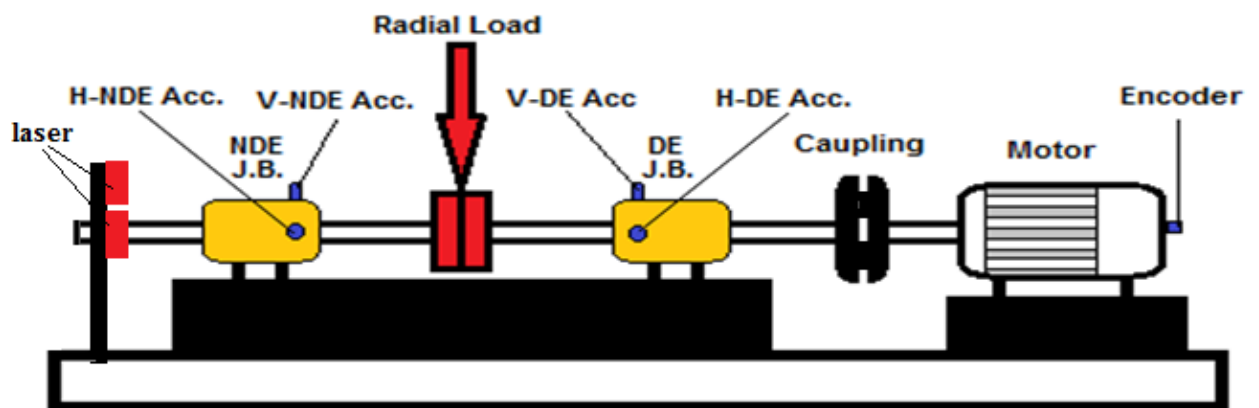
Figure 6.1 Test rig components
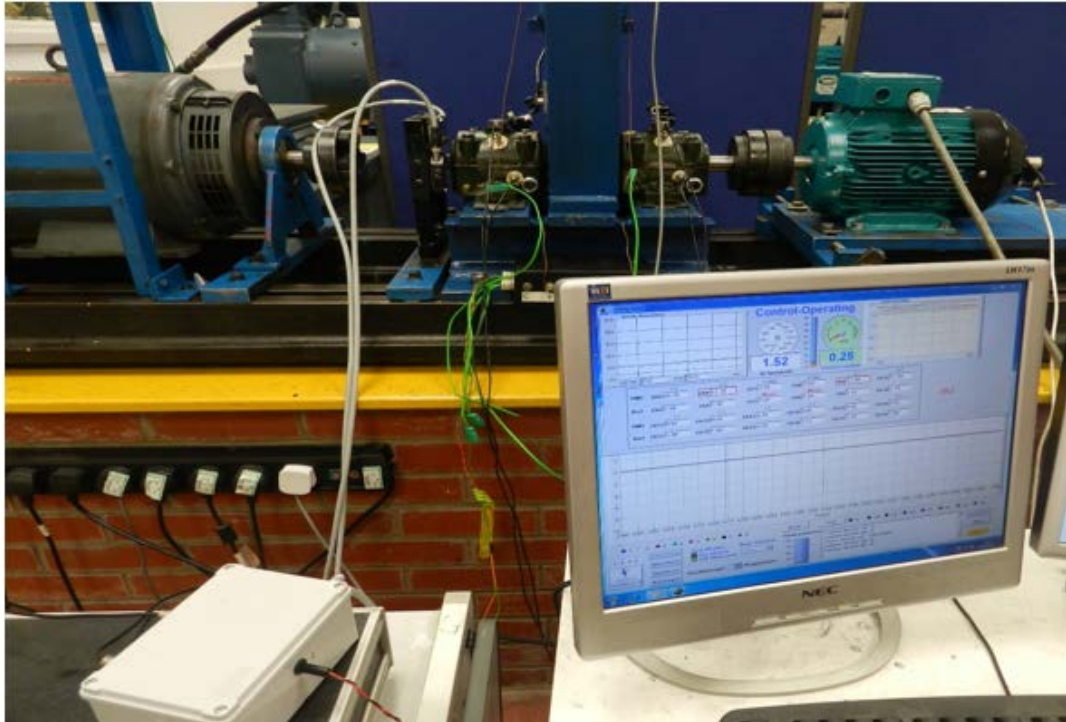
Figure 6.2 Self-journal bearing test system

6.2 Mechanical Components

6.2.1 Self-Aligning Spherical Journal Bearings

The self-aligning spherical journal bearing is shown in the Figure 6.3. The two SA35M self-aligning spherical journal bearings to be tested is set up at the drive end (DE) and non-drive end (NDE) of the drive train.
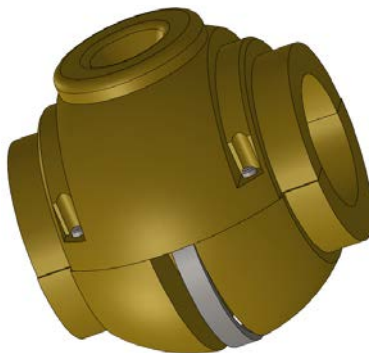
(a)   (b)

(c)

Figure 6.3 (a) Plane bearing. (b) Journal inside bearing. (c) Self-aligning journal bearing components.

The specification of the tested journal bearing is shown in Table 6.1.

Table 6.1 Self-aligning journal bearing specification [28]

Self-aligning spherical journal bearing		Bearing code	SA35 M/S4170
Diameter of bearing (hole)	35 mm	Lubrication system	Ring
Length of bearing	76 mm	Maximum load	10 kN

At high loads and speeds, the required clearance between the journal and bearing diameter should be 0.0381mm for each mm of diameter [69].

For the self-aligning spherical journal bearing lubrication, Arvis recommended to use Shell Tellus Oil 37, Shell Rotella "S" Oil 10W or an equivalent for ambient temperatures 0°C to 30°C and for ambient temperatures 30°C to 60°C to use Shell Tellus Oil 33. Shell Rotella 'S' Oil 20/20W or an equivalent.

During the journal bearing assembly, a pair of washers and a pair of rubber seals should be installed to prevent axial movement and oil leakage.

6.2.2 Alternating Current Motor

The test rig was driven by a Brook electric inductions motor, maximum speed 2870 rpm. Different motor speeds are controlled by a controller panel. Table 6.2 Specification of the test rig motor [104] shows the specifications of the test rig motor.

Table 6.2 Specification of the test rig motor [104]

Manufacturer	**Brook Crompton**
Type	WU-DA112MM
Phase	3 Phase
Pole number/rpm	2 pole/2870 rpm
Power	4kWatt
Shaft diameter	28mm
Frame size	132

6.2.3 Direct Current Generator

Siemens DC is used to generator torsion loads adjusted by the Siemens controller panel. The maximum power is 9.9 kW at speed of 2850 rpm, supply voltage 400V and current of 28A. DC generator is used to study the effective of torque loads on the test rig.

6.2.4 Control Panel

Ac motor speeds and Dc generator torque loads can be controlled by Siemens Micro Master Controller. Also, it is easy to use and deliver torque and speeds accurately by a control screen that includes number of steps, time of operation (minute), AC motor speed (%) and DC torsion load (%).

Figure 6.4 Siemens micro master controller

6.2.5   Hydraulic System

A hydraulic hand pump is used to apply a radial load on the shaft centre between DE and NDE journal bearings. A manual hydraulic pump with a pressure gauge is used to pressurize a hydraulic ram frame on two roller bearings linked on the shaft centre, shown in Figure 6.5. Table 6.3 show the specifications of the hydraulic pump and hydraulic ram.

Table 6.3 Specification of hydraulic hand pump [105]

Manufacturer	Enerpac	
Type	P391	
Speed	Single	
Maximum Operating Pressure	700	Bar
Cylinder Stroke	25.4	Mm
Usable Oil Capacity	901	cm3

Table 6.4 Specification of hydraulic ram [106]

Manufacturer	Steerforth	
Type	Single acting	
Stoke	200	mm
Bore diameter	40	mm
Rod diameter	27	mm
Outside diameter	50	mm
Piston diameter	30	mm
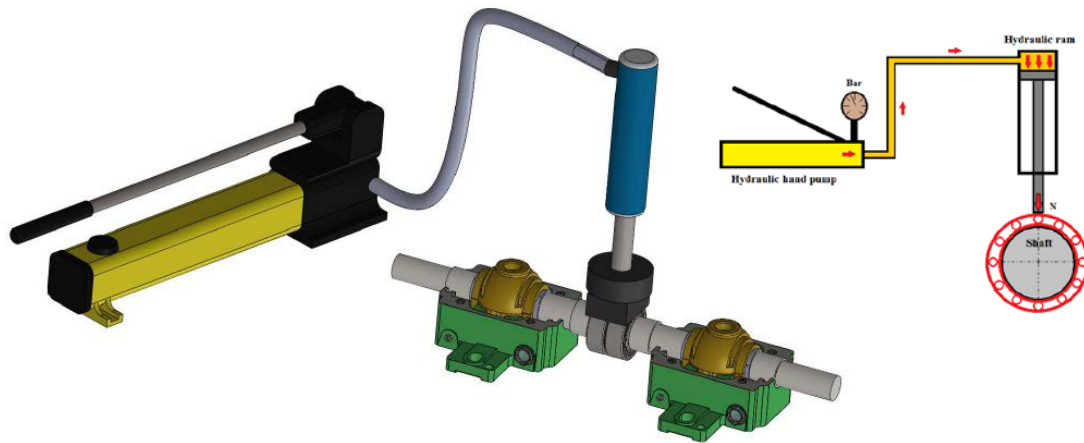
Figure 6.5 Hydraulic system on test rig of journal bearing

By considering the geometry of hydraulic ram and bearing, Figure 6.6 presents the conversion of the pressure units which applied by hand bump into force on journal bearing. Also, fitting line in Figure 6.6 obtained flowing Equation which is a short way to convert pressure in bar unit of hand bump into force in Newton unit on a bearing.

$$y = 63x - 2.3 \times 10^{-13} \tag{6.1}$$

where x is a hydraulic hand bump pressure (bar), and y is the radial force applied to bearing (N)
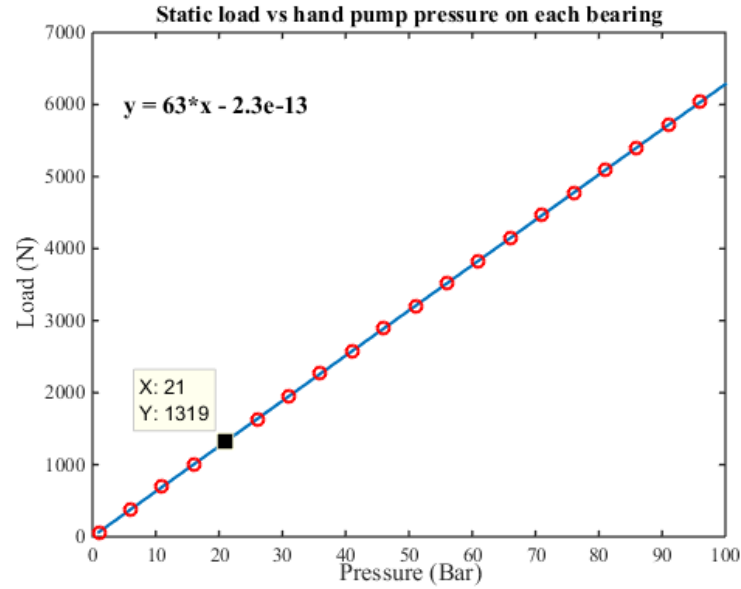
Figure 6.6 Transform bar pressures of hydraulic hand pump to Newton radial load

6.2.5.1 Load Ratio

The load ratio is the relation between load applied to maximum load which is variable dependons on rotational speed. For example, the perentage of 30 bar (~2000 N) equals 50% at 600 rpm, 33% at 900 rpm, 25% at 1200rpm and 20% at 1500 rpm. Figure 6.9 presents the ratio of each applied radial load, conversion between bar and Nwton, and load capacity at different speeds.
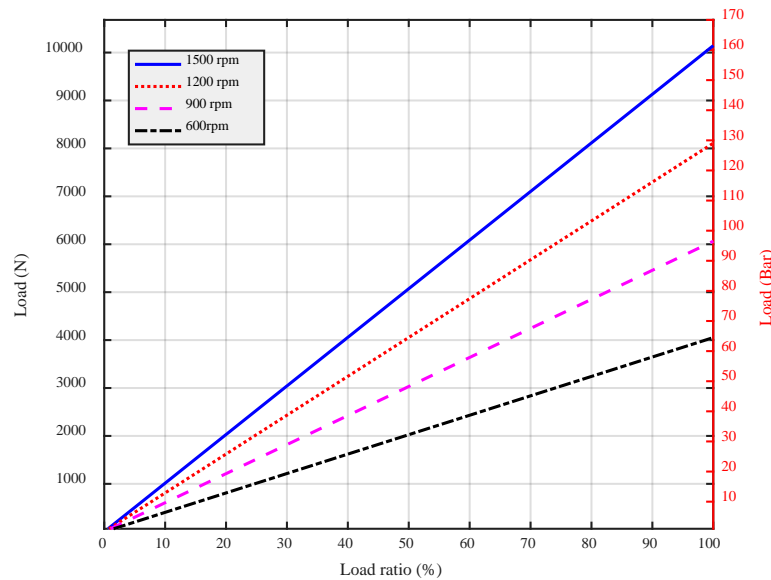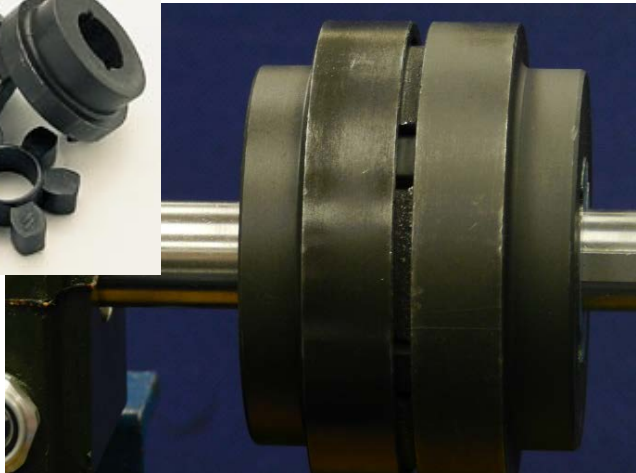
Figure 6.7 Transform bar pressures of hydraulic hand pump to newton radial load

6.2.6   Hard Rubber Coupling

A hard rubber coupling (HRC) is used to connect the electrical motor drive shaft to the bearing testing shaft. The specification of the HRC130H is in Table 6.5.

Table 6.5 Hard rubber coupling specification [28] [107]

Manufacturer	Fenner	
Type	HRC130H	
Size	130	
Outer diameter	130	mm
Diameter of hub	108	mm
Length of hub	18	mm
Width of rubber	36	mm

6.2.7   Loading Bearing

Two cylindrical roller bearings [108] are used to support radial load. They are located in-between two tested journal bearings as shown in Figure 6.5. Table 6.7 presents the specification of these bearings. Furthermore, their fault frequencies are calculated based on parameters in Table 6.6.

Table 6.6 Fault frequencies of loaded bearing based on different rotating speeds

Number of Rollers (Nb)	No.		12			
Roller Diameter (Db)	mm		13			
Pitch circle diameter (Dp)	mm		66.5			
Shaft frequency (fr)	Hz		25	20	15	10
Outer Race Fault Frequency (Hz)	$f_o = f_r \dfrac{N_b}{2}(1 - \dfrac{D_b}{D_p})$		120.7	96.5	72.4	48.3
Inner Race Fault Frequency (Hz)	$f_i = f_r \dfrac{N_b}{2}(1 + \dfrac{D_b}{D_p})$		179.3	143.5	107.6	71.7
Ball Fault Frequency (Hz)	$f_b = f_r \dfrac{D_p}{(2D_b)}(1 - (\dfrac{D_b}{D_p})^2)$		61.5	49.2	36.89	24.6
Cage Fault Frequency (Hz)	$f_c = f_r \dfrac{1}{2}(1 - \dfrac{D_b}{D_p})$		10.06	8.05	6.03	4.02

Table 6.7 Cylindrical roller bearing specification [108]

Manufacturer	SKF	
Type	N 308	
Limiting Speed	9500	rpm
Ref Speed	8000	rpm
Dynamic Load	93	kN
Static Load	78	kN
Width	23	mm
Outside Dia	90	mm
Inside Dia	40	mm
Clearance	Standard	
Mass	0.769	kg

6.3 Measurement Instrumentations

6.3.1 Accelerometers

For vibration measurements, cost-effective accelerometers are used seen in Figure 6.8. Figure 6.9 shows the positions of the accelerometers on journal bearing house. Accelerometers CA-YD-182A have a linear frequency response ranging from 1 Hz to 10,000 Hz, which may be sufficiently wide to perceive vibrations due to the collisions of asperities. Moreover, the high sensitivity 2.00 mV/ms^{-2} of the accelerometer allows the small amplitude of vibrations due to the collisions to be measured.

As illustrated in the Figure 6.9, accelerometers were mounted vertically and horizontally to the NE and NDE bearing housings via a threaded bronze stud base that is glued to the bearing house. Especially, the accelerometer attached horizontally is close to the load zones and can produce high quality signals regarding to lubrication conditions of the bearing operations. In the meantime, the vertical sensors are used because they may also produce good signals to the lubrication process due to the effect of structural resonances.

Figure 6.8 Accelerometer sensors
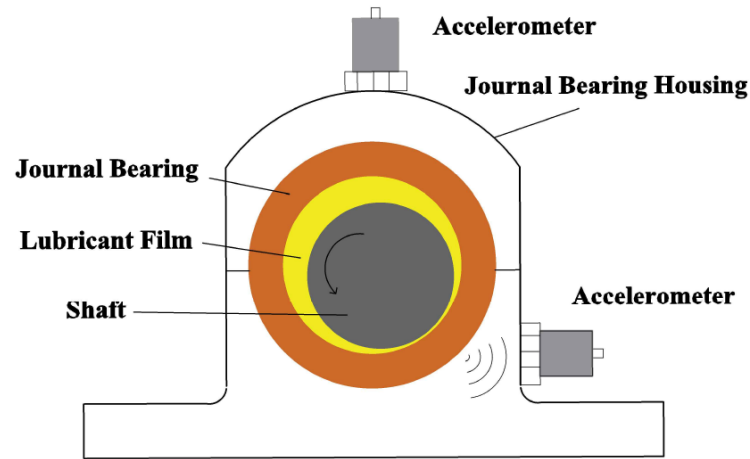
Figure 6.9 Accelerometer positions

6.3.2 Shaft Encoder

In the test rig, a shaft encoder, as depicted in Table 6.8, is installed onto the end of the motor shaft. It produces a 100-pulse train per rotation while the shaft rotates. By counting the time intervals between pulses, the rotating speed can be obtained as the measure of the bearing operating speed.

Table 6.8 Encoder specification [109]

Manufacturer	HENGSLER	
Type	RI 32	
Mounting	Round flange	
Number of pulses	100 per rev.	
Shaft diameter	5 mm	
Maximum speed	6000 rpm	
Operating temperature	-10-60ºC	
Supply voltage	DC 5V±10%	

6.3.3 Pressure Sensor

A pressure sensor is known as a gauge or a relative pressure sensor. It is used to measure pressure relative to the barometric pressure, by opening the back of the sensing element. In the test rig, this sensor is used to measure radial load which applied by the hydraulic hand pump. It acts as a transducer by generating a signal as a function of the pressure forced [110]. The manufactory's specifications are listed in Table 6.9.

Table 6.9 Pressure sensor specifications [110]

Manufacturer	RS	
Type	Gauge sensor	
Minimum pressure reading	0bar	
Minimum pressure reading	40bar	
Accuracy	±0.25 %	
Supply voltage	3-12 V	
Minimum Operating Temperature	-20o C	
Maximum Operating Temperature	+135o C	

6.3.4 Data Acquisition System

A data acquisition system is used for online and offline monitoring by recording voltages of the sensors data such as temperature, vibration and load. DAS system YE6232B, is employed to record all input mode (V/IEPE) at a sampling rate of 96 kHz. The data acquisition system specification is shown in Table 6.10.

Table 6.10 Data Acquisition System (DAS) Specification

Manufacturer	Sinocera	
Type	YE6232B V/IEPE Input	
Channels	16	
A/D bits	24bit($\sum$-Δ)	
Input Mode	V/IEPE	
IEPE Power Supply	4mA/+24VDC	
Signal Frequency Range	DC-30kHZ(-3dB±1dB)	
Accuracy	±0.5%	
Sample Rate (Max.)	96kHz/CH, Parallel	
Interface	USB2.0	
Trigger Modes	Signal Trigger	
Dimensions (mm)	236W×88H×277D	
Weight	4 Kg	
Power Supply	AC: 220V 50Hz 110V 60Hz	

6.3.5 Laser Sensor

The optoNCDT1402 laser sensor from Micro-Epsilon is installed for measuring the vertical displacement and position of the shaft. The sensor uses the principle of optical triangulation, i.e. a visible, modulated point of light is projected onto the target surface. Moreover, it is suitable for rapid processes. The diffuse element of the reflection of the light spot is imaged by a receiver optical element positioned at a certain angle to the optical axis of the laser beam onto a high-sensitivity resolution element (CCD), in dependency on distance [111].
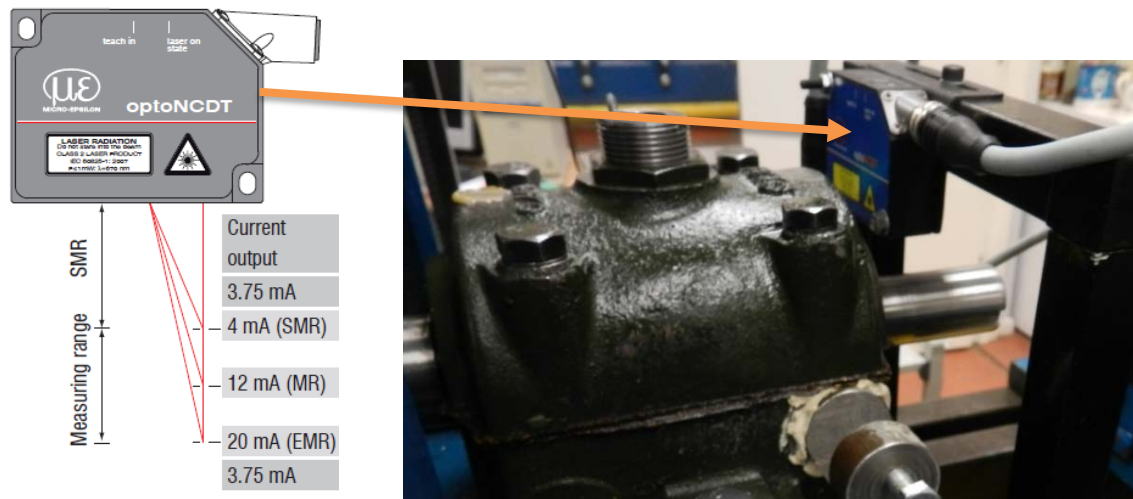
Figure 6.10 Laser sensor (optoNCDT1402) [111]

Table 6.11 Laser Sensor Specification [111]

Manufacturer	Micro-Epsilon
Model	optoNCDT1402
Measurement range	5 … 25 mm
Linearity	5 … 9 µm
Vibration	10 … 1000 Hz
Measurement value output	4 … 20 mA

6.3.6   Particular Oil Analysis Device

The LNF (LaserNetFinesTM) is a particle counter technology device. It is providing particle counts, abnormal wear classification and ferrous wear measurement. The Q230 series is fast, accurate and easy to use. Viscosities up to 320cSt can be processed without dilution due to the wide dynamic range. The LNF calculates free water in ppm, and differentiates contaminants silica, metal and fibre.

Figure 6.11 Particle counter technology device Q230

6.4 Summary

Test rig has been established to be able to measure a self-aligning spherical journal bearing with different the state of the art technologies. All the mechanical and electrical components which are used for testing the journal bearing are showed in this chapter. In addition, the measurement instruments, the accelerometer, the encoder, the pressure sensor, the data acquisition and the laser sensor are descried with their key specifications that meet the requirement of the configured bearing system. Alongside, other devices involved are also briefed in order to evaluate the results of fault detection of the journal bearing.

CHAPTER SEVEN

MONITORING ABNORMAL OPERATING CONDITIONS

This chapter presents the identification of optimal bearing operating conditions based on vibration analysis. Firstly, it describes the exploitation of a hierarchical cluster approach to the separation of different operations over a wide speed and load conditions based on vibration spectrum patterns. Then a more advanced analysis is investigated by applying using MSB to the raw vibration signals, which allows the instable operations and excessive viscous friction operations to be identified because MSB analysis shows more details of the vibration mechanisms.

7.1 Introduction

Journal bearings are used to support radial load and considered as the best element for absorbing vibrations, resisting shock and extending service life. However, high radial load, low rotating speed, and weakness of oil film may lead the journal bearings to work in adverse operating conditions, resulting in early failures. Based on the analytic studies and experimental verifications, it has been demonstrated that popular vibration monitoring can detect abnormal wide operating conditions.

Journal bearing vibration is not only caused by a rotor system which mainly occurred at hydrodynamic lubricant regime but also asperity churns and collisions occurred at mixed and boundary lubricant regimes. Under mixed and boundary regimes, asperity-asperity and fluid-asperity interactions are the sources of self-excitation, which result in high responses at structure resonances. In this chapter, clustering and MSB techniques have been used to detect mis-operating conditions and monitor journal bearing lubrication conditions.

A hierarchical clustering method is applied to the spectrum to select frequency bands that allow the separation different lubrication regimes. Thereby, the boundary lubrication can be identified as a reference for detecting abnormal lubrication condition.

Modulation signal bispectrum (MSB) is an advanced technique used to analyse complicated vibration signals which are induced by a combination of the information content with another content in a nonlinear modulation way. The interaction between periodic responses in journal bearing such as journal rotations and system responses produces modulation signals.

7.2 Vibration Response Mechanisms

In addition to low frequency vibrations due to shaft frequency, oil whirl and whip instabilities within journal bearings [112], high frequency vibration responses can also be induced by various bearing lubrication regimes. As investigated in Chapter 5, they can appear in different lubricating regimes: hydrodynamic lubrication (HL), mixed lubrication (ML), and boundary lubrication (BL) as categorised by the well-known Stribeck curve. According to these categories bearing lubrication states can be determined according to the unit less bearing parameter or modulus values:

$$BM = \mu N / p \tag{7.1}$$

where μ is dynamic viscosity of lubricant, N is rotational speed of the shaft and p is the pressure in bearing loading area (W / lD), W is the radial load, l is the bearing length and D journal diameter.
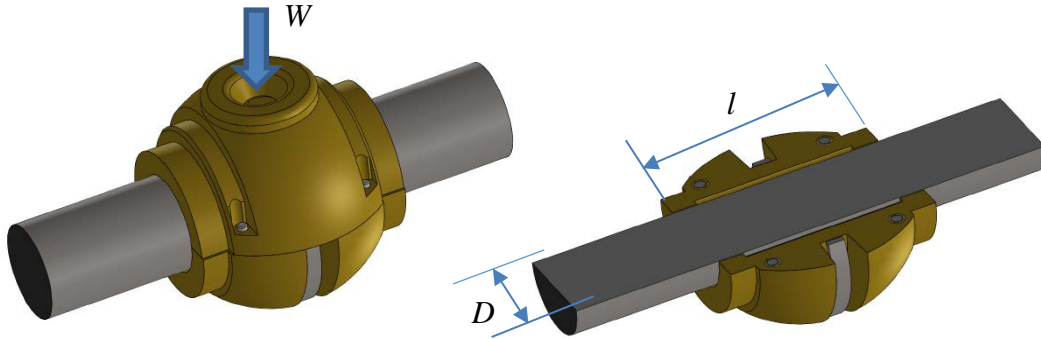
Figure 7.1 Project area of journal bearing

Boundary lubrication (BL) is mostly an unwanted operating regime for hydrostatic or hydrodynamic bearings, because it generates friction, wear, and quickly damages the bearing. Unfortunately, during a bearing's operating lives, they face boundary lubrication, during start-up, shutdown, low excitation speed, weak lubrication system and high radial load. Bearings operating in this regime have extensive metal-to-metal contacts and asperity collisions because of little hydrodynamic lubrication. Consequently, it shows high rate of wear, which will company with vibration energy release [81]. In the meantime, similar to the effect of fluid shearing, the alternation of deformation and reclamation by the collision of asperities also produces vibration energy.

The overall vibration excitation power is thus proportional to both the normal load and the velocity. Similar to the fluid shearing induced vibrations, vibration responses due to direct asperity collisions will also be wide bands, due to the randomness of asperities. However, it may induce discrete impulsive responses for the collisions and the removal of large asperities.

ML occurs during the transition between the BL and HL. At mixed lubricated surfaces, thin film lubrication is formed and sliding surfaces are partially separated, as lower friction levels are achieved. The vibration excitation power can be the combination of that of HL and BL. It means that bearing load, velocity and viscosity all play effects on the vibration responses. In other words, low and very high bearing modulus values means that journal bearing operates at abnormal operations and should be avoided.

7.3   Vibration Monitoring Based On Spectrum Clustering

7.3.1   Spectrum Clustering

It is difficult to obtain a full understanding of high frequency vibration contents because they are very detailed in modelling the interactions between fluid and mechanical dynamics as discussed in Section 7.2. To understand and differentiate the complicated vibration responses from different lubrication regimes, cluster technique (discussed in section 3.5) has been applied on vibration signals of DE and NDE journal bearings.

7.3.2   Test Facilities and Procedure

A journal bearing test rig is constructed as shown in Figure 7.2 (described in Chapter 6). To simulate lubricant degradation during services, three types of common lubrication oils, denoted as Oil-15 VG, Oil-37 VG and Oil-46 VG respectively, were tested under a number of load and speed conditions. These operating conditions achieve a consecutive increase and wide ranges of bearing modulus values.
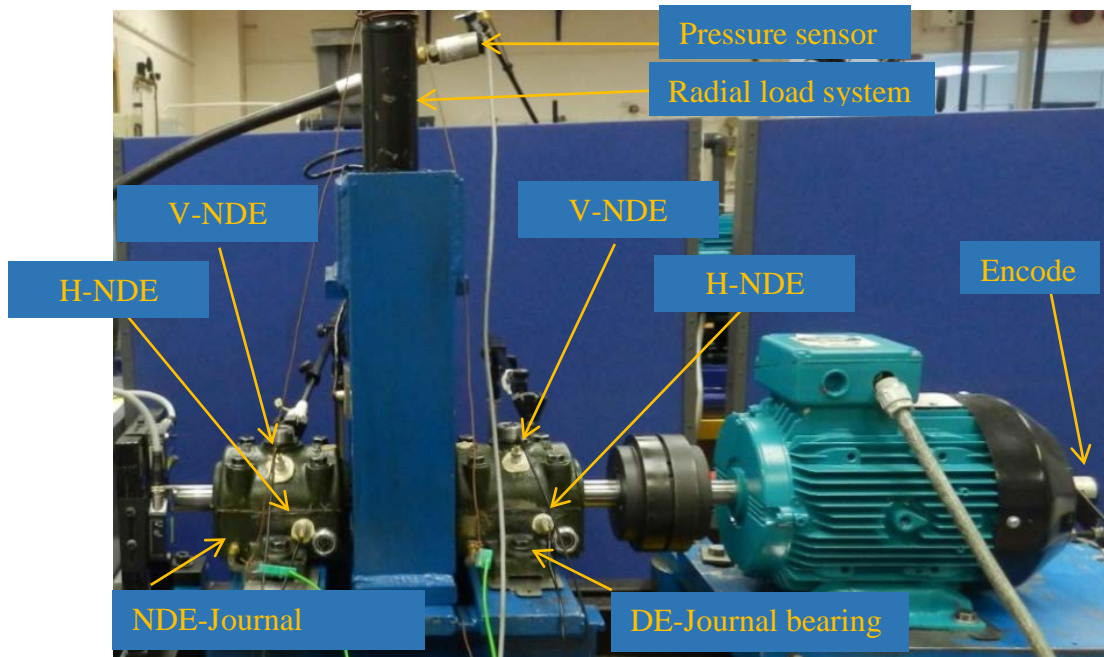

Figure 7.2 Self-aligning journal bearing components

Table 7.1 shows the operating conditions of each lubricant verse their bearing modulus values. Twenty-three tests have been done for each oil, starting by high modulus of operating parameters and finishing by low modulus. Figure 7.3 shows three sets of speed and three sets of radial load these sets depend on viscosity of lubricants.

Table 7.1 Variable operating condition vs. bearing modulus of different oil

| Test No.	Speed (rpm)	Load (bar)	Oil 15 Bearing Modulus x 10-6		Oil 37 Bearing Modulus x 10-6		Oil 46 Bearing Modulus x 10-6	
				ε		ε		ε
1	450	5	0.6538	0.52	1.613	0.33	2.005	0.28
2	360	5	0.5230	0.56	1.290	0.38	1.604	0.33
3	300	5	0.4358	0.58	1.075	0.41	1.337	0.37
4	450	10	0.3269	**0.64**	0.806	0.48	1.002	0.43
5	210	5	0.3051	**0.65**	0.753	0.49	0.936	0.44
6	360	10	0.2615	**0.68**	0.645	0.52	0.802	0.48
7	300	10	0.2179	**0.70**	0.538	0.56	0.668	0.51
8	150	5	0.2179	**0.70**	0.538	0.56	0.668	0.51
9	453	20	0.1634	**0.74**	0.403	**0.61**	0.501	0.57
10	210	10	0.1525	**0.75**	0.376	**0.62**	0.468	0.58
11	360	20	0.1305	**0.76**	0.323	**0.64**	0.401	**0.61**
12	450	30	0.1090	**0.78**	0.269	**0.67**	0.334	**0.64**
13	300	20	0.1090	**0.78**	0.269	**0.67**	0.334	**0.64**
14	150	10	0.1090	**0.78**	0.269	**0.67**	0.334	**0.64**
15	360	30	0.0872	**0.80**	0.215	**0.70**	0.267	**0.67**
16	450	40	0.0817	**0.81**	0.202	**0.71**	0.251	**0.68**
17	210	20	0.0763	**0.82**	0.188	**0.72**	0.234	**0.69**
18	300	30	0.0726	**0.82**	0.179	**0.73**	0.223	**0.70**
19	360	40	0.0654	**0.83**	0.161	**0.74**	0.200	**0.71**
20	300	40	0.0545	**0.84**	0.134	**0.76**	0.167	**0.74**
21	150	20	0.0545	**0.84**	0.134	**0.76**	0.167	**0.74**
22	210	30	0.0508	**0.85**	0.125	**0.77**	0.167	**0.74**
23	210	40	0.0381	**0.85**	0.094	**0.80**	0.117	**0.78**
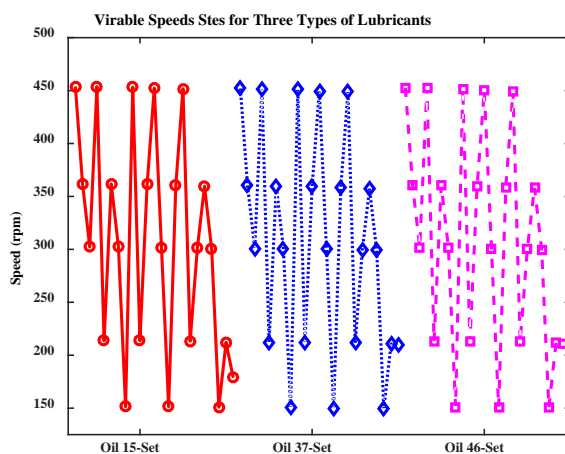
Figure 7.3 Rotating speed sets
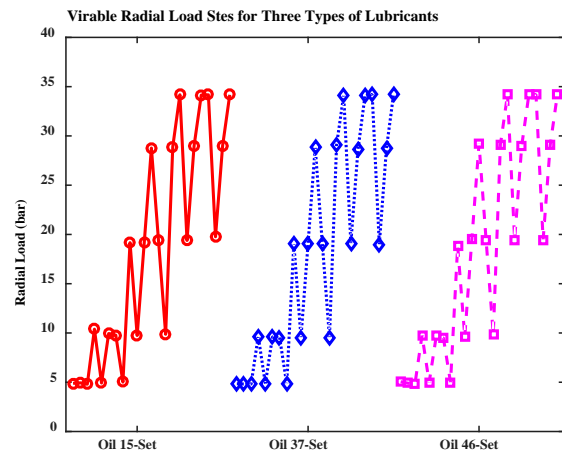
Figure 7.4 Radial load sets

Eccentricity is a function of operating conditions and eccentricity ration equals eccentricity over radial clearance. Thus, if the eccentricity ratio is too high there is a risk of metal-to-

metal contact. And if it is too low (journal is nearly centred) then the machine could more easily become unstable. Most journal bearings operate at steady state eccentricity ratio of about 0.6-0.8 [92]. Thus considering that the minimum value of eccentricity ratio is 0.6 which is the point separates between mis-operating conditions and acceptable operating conditions. Therefore, any bearing modulus of the operating condition greater than 0.4×10^{-6} ($\varepsilon < 0.6$) considers that journal bearing is working at safe conditions (hydrodynamic or mixed regimes). In contrast, low bearing modulus means the journal bearing is working at risky conditions (boundary regime).According to bearing design standard, the operation with low BM values are more likely to be BL or ML regimes as shown by the test conditions below the horizontal dashed line in Figure 7.5, whereas the high BM values are hydrodynamic lubrication (HL). In this way, characteristics of vibration responses can be examined under different lubrication conditions so that they can be based to differentiate abnormal lubrications such as BL and ML from HL. In general, most of test cases for Oil-15 have smaller BM values compared with other two, which have higher chances operating under BL and ML. In addition, each of the 23 tests runs for each type of oil, starting with operating conditions under large BM values to avoid possible wear influences on high BM operations.
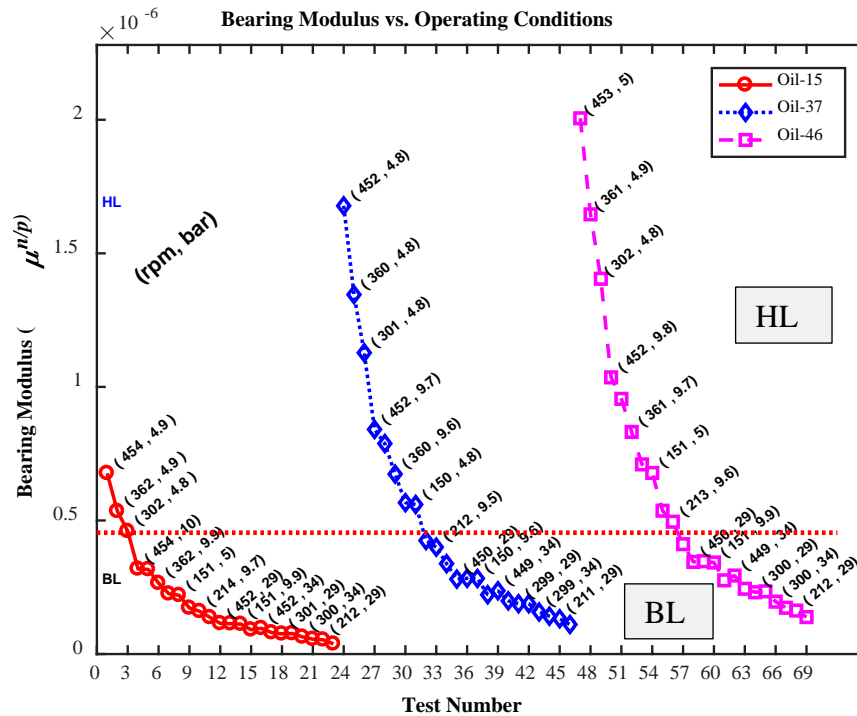

Figure 7.5 Bearing modulus vs. operating conditions of different oils

7.3.3   Results and Discussion

The test obtained 3×23=69 vibration datasets, each 23 datasets corresponding to an oil case. In order to use vibration responses for lubrication regime identification, the data sets were processed with both the common time and frequency analysis and the advanced wavelet analysis, in which, both raw data and feature parameters based cluster techniques were applied to separate the different test samples. Particularly, the discrete wavelet analysis was used to attempt to highlight the responses from asperity collisions that may induce impulsive responses. Unfortunately, it was not successful in separating the 69 tests to obtain a result that was in accordance with the bearing modulus. As an alternative, the common spectrum analysis produced results which can be observed to confirm bearing modulus. Therefore, the analysis is made on the results obtained using the commonly used spectrum analysis techniques. Moreover, it has also found that the horizontal vibration response is higher than that of the vertical one. This can be explained by the fact that the sensor at the horizontal direction is closer to the load zone and hence the horizontal vibration signal has higher signal to noise ratio in reflecting bearing lubrication conditions. Following this, the vibration responses from horizontal sensors are the main focuses.

Firstly, the spectrums of the data sets are examined to find if any frequency bands can give clear differences in different test runs. Figure 7.6 and Figure 7.7 show a spectrum comparison of the horizontal vibration at the DE and NDE bearings between different type of oils for higher and lower BM values. It can be seen that they have distinctive peaks at a number of discrete peaks below the frequency of 2000Hz. These low frequency displays can come easily from remote interference excitations such as the unbalances, eccentricity and motor bar/slot component excitations, therefore they are not considered in this study. In the meantime, the high frequency vibrations from asperity collisions and fluid shearing effects are the main concerns. By inspecting the spectra in the high frequency range above 2000Hz, it can be found that:

1. Clear differences exist between higher and lower BM values, showing that the fluid shearing induced vibration responses are different from that of asperity collisions.
2. The differences between different oils vary significantly from frequency bands to bands, indicating that high complicity of vibration responses due to combined excitation mechanisms.

These characteristics of vibration responses mean that there is a close connection between vibration responses and lubrication conditions. However, the connection is very nonlinear

and cannot be resolved directly with common linear methods such as threshold based approaches.
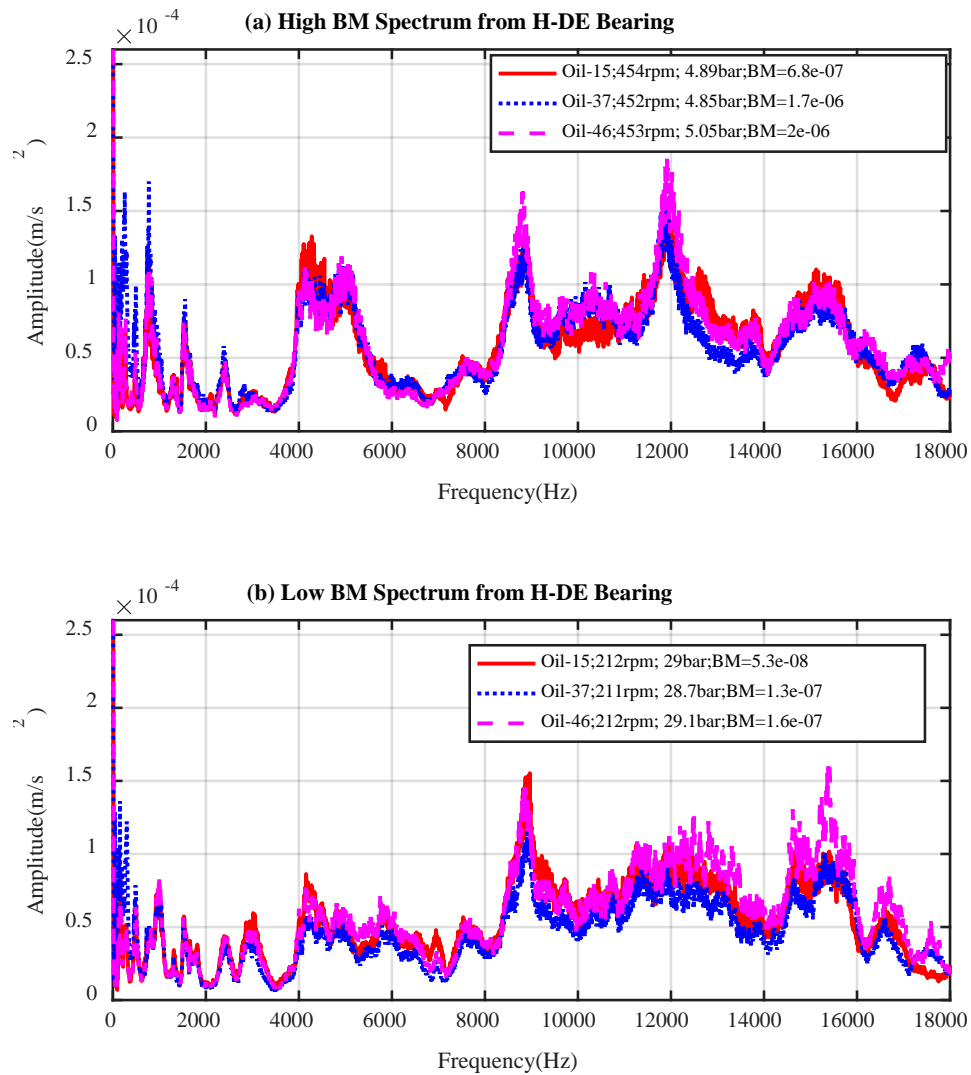

Figure 7.6 Spectrum comparison of H-DE vibrations under different oils and operating conditions
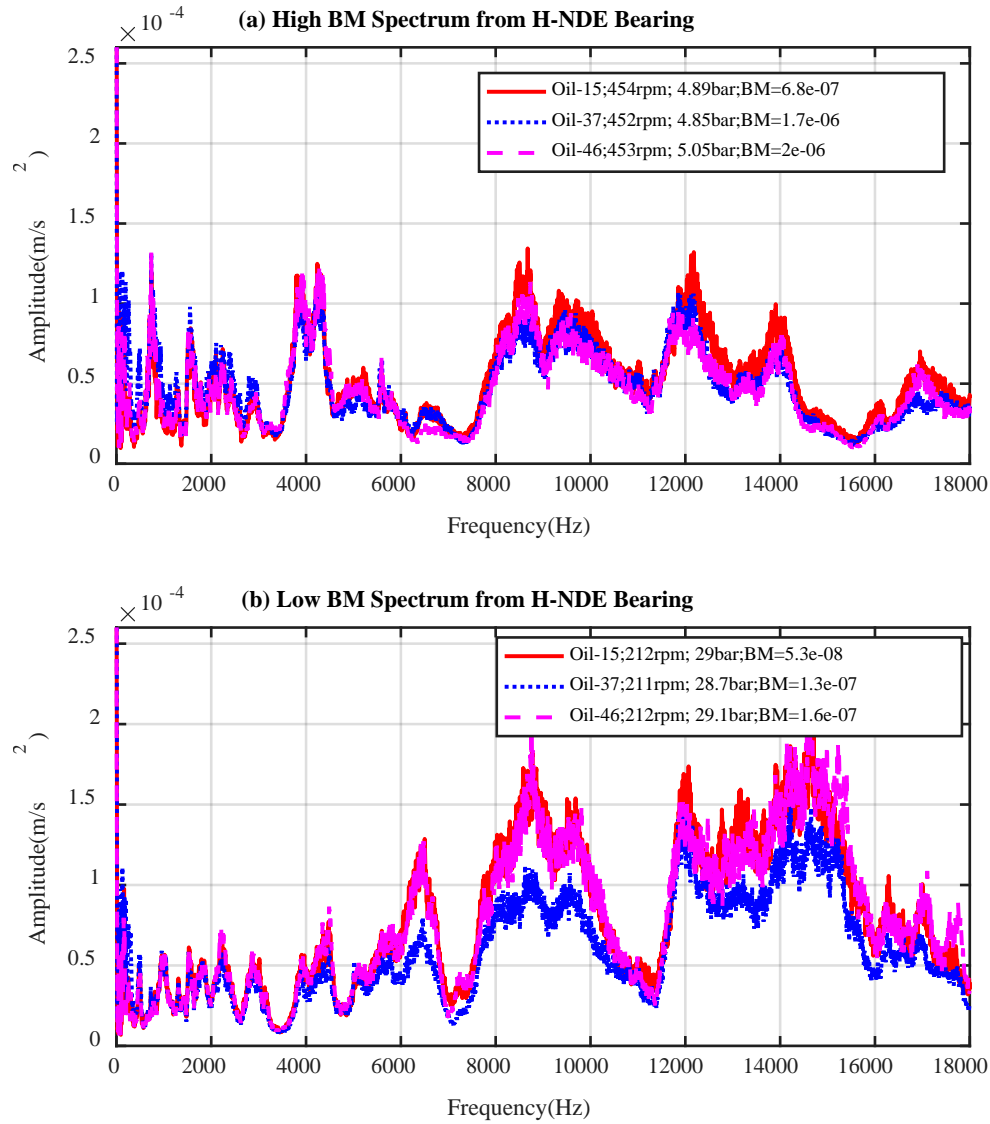
Figure 7.7 Spectrum comparison of H-NDE vibrations under different oils and operating conditions

To connect the vibration responses to different lubrication conditions, an agglomerative hierarchical clustering approach is employed to attempt to group the 3×23 data so that they can correspond to both their BM values and oil types respectively. In the clustering method, correlation measures are used to show the similarity between different spectrum segments and the Ward's minimum variance algorithm is used to merge two clusters. However, it has found that it is difficult to obtain a consistent result by applying it to the conventional feature values from the time domain, the frequency domain and the wavelet coefficients. Therefore, the spectrum values in different frequency bands are directly used for cluster analysis. By tuning the centre frequency from 4,000Hz with bandwidth step of 1000Hz, it has found that the spectral amplitudes between 9,000Hz and 12,000Hz produced more

consistent results. Through fine tuning, it results in cluster results as shown in Figure 7.8. It can be seen from the dendrogram in Figure 7.8 (a) that the data set can be grouped into two subclasses illustrated by red and cyan colours, which are subsequently denoted as '1' and '2' respectively for ease of discussion. Once subclasses are presented according to oil types and BM values, which is shown in Figure 7.8 (b), it can be seen that nearly all of the tests for Oil-15 are classified as '2' corresponding to the BM values which are lower than the designing threshold, whereas for Oil-46 most tests are classified as '1' which corresponds to the BM values higher than the design threshold. In addition, the tests for Oil-32 are classified into two subgroups of similar sizes, each corresponding to HL and ML respectively. Moreover, according to the connection between the subgroups and the BM values, the vibration responses associated with subgroup '2' can be used to show the effects of asperity collisions. Thereby it allows the abnormal lubrication conditions associated with the mixed and boundary lubrication to be detected.
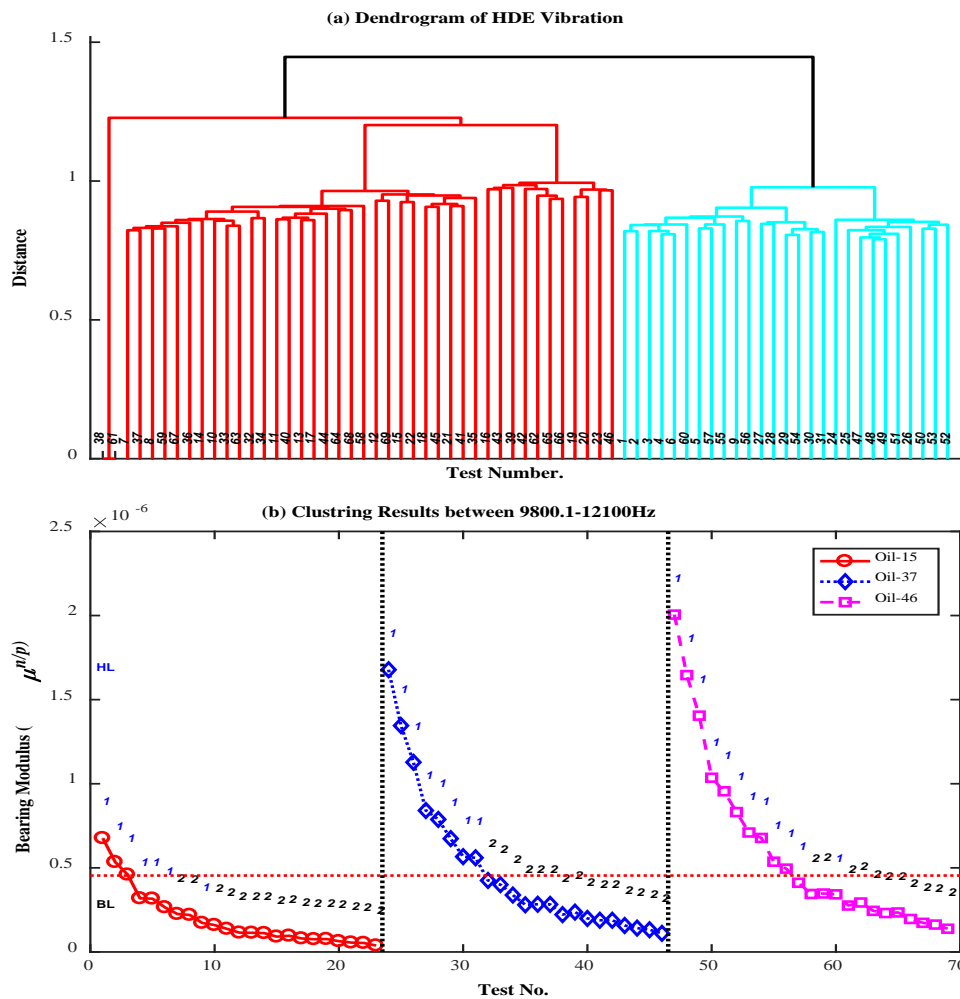

Figure 7.8 Clusters of vibration spectrum from H-DE journal bearing

In the same way, the vibration spectrum datasets from the NDE bearing can be also clustered to produce consistent results. As shown in Figure 7.9, the results are very similar to that of the DE bearing. However, it is obtained from a slightly different frequency band. This may be due to slight differences in vibration transmission paths between two bearings, which are likely caused by the discrepancy of accelerometer frequency responses at resonance ranges.
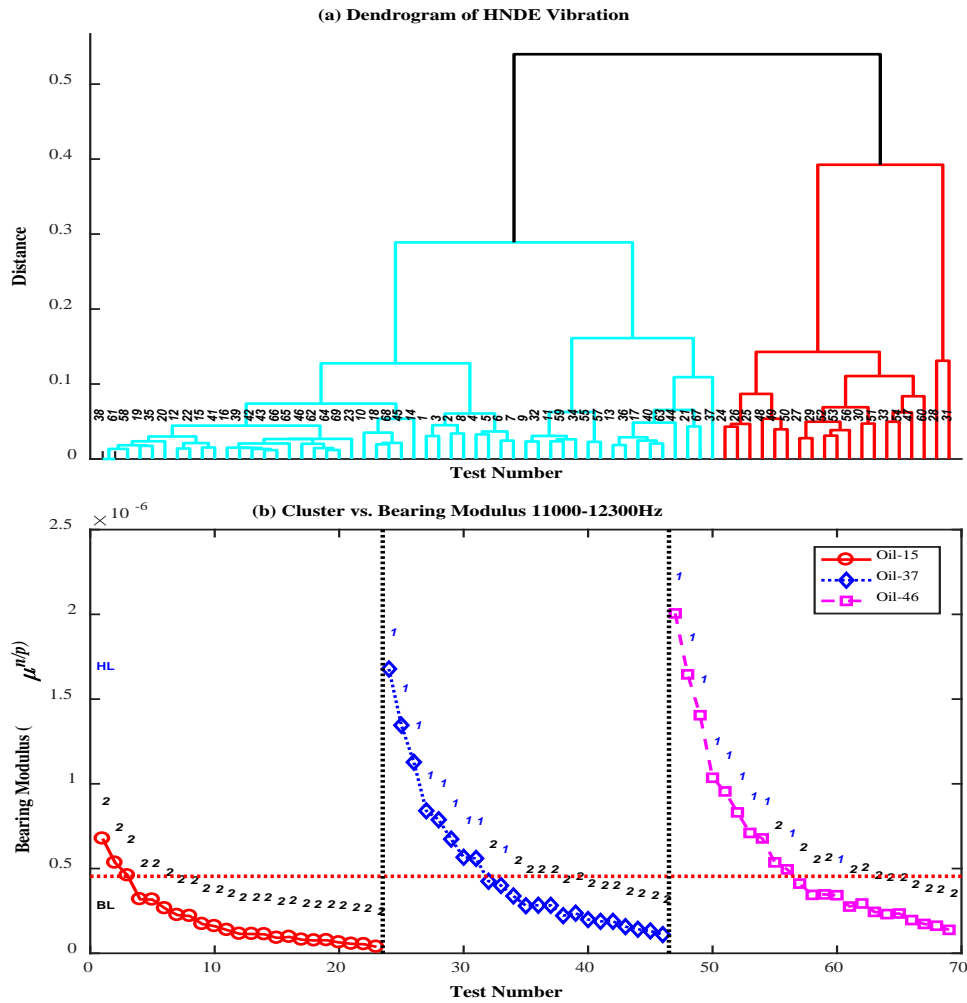
Figure 7.9 Clusters of vibration spectrum from H-NDE journal bearing

7.4 Vibration Monitoring Using Modulation Signal Bispectrum Technique

7.4.1 Test Procedure

A self-aligning spherical journal bearing, SA35M has been tested under different operating conditions on the test rig shown in Figure 7.2 (described in Chapter 6). In order to realise different lubrication conditions, three types of lubricants: 5VG, 15VG and 46VG were

tested under three shaft speeds: 1500rpm, 1200rpm and 900 rpm and four radial loads: 1bar, 5bar, 10bar and 20 bar. These different viscosities, rotation speeds and radial loads will lead the journal bearing working under different lubricant regimes, which, are expected to be separated based on external vibration analysis.

7.4.2 Time Domain Features

Figure 7.10 presents time domains of (3(speeds)×4(loads)×3(oils)) different operating conditions. Obviously, high speeds have more power of amplitudes than low speed. Also, applying high redial loads, causes more vibration because of surface to surface contact. Lastly, it is not easy to see the differences when changing lubrication viscosity.

RMS values are proportional with speeds and loads, but do not show significant difference between lubrication types. In theory, low speed causes more friction, especially at high load, but in RMS results show that high speed always has high vibration. Thus in this study, RMS values are not good parameters to present the bearing condition at different lubricant regimes, nor to obtain optimum operating conditions. In contrast, even though kurtosis decreases while speed increases, it acts nonlinearity while changing load or lubricant viscosity. Thus, kurtosis values are not suitable to present vibration in journal bearing, shown in Figure 7.11.
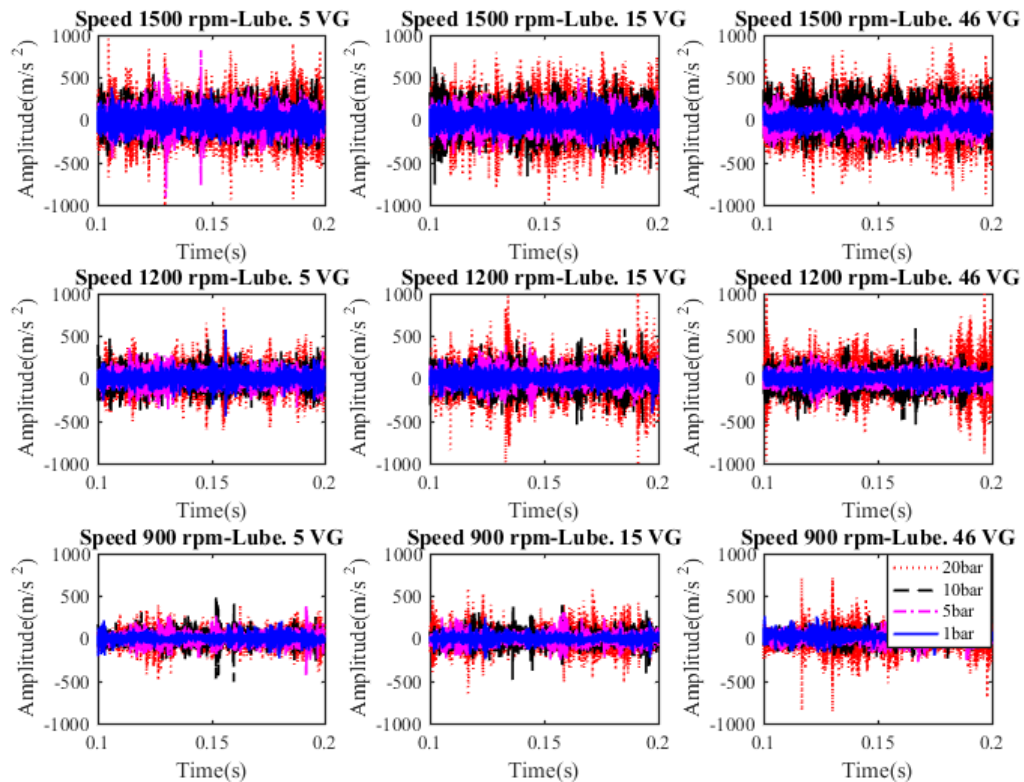

Figure 7.10 Time domain of vibration signals of different operating conditions
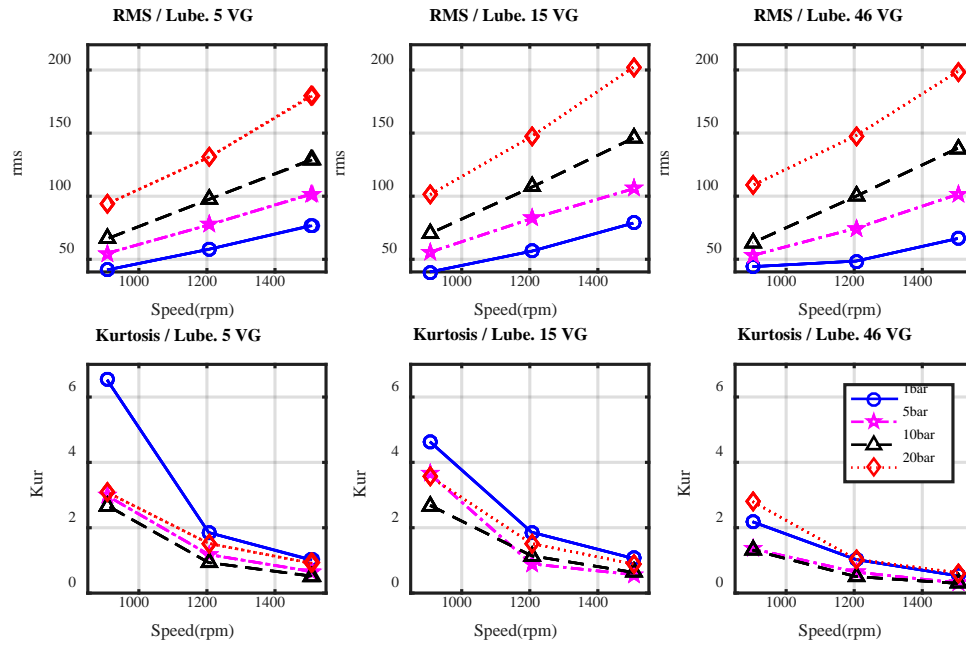
Figure 7.11 RMS and kurtosis values of vibration signals of different operating conditions

7.4.3   Frequency Domain Features

Investigate the Load Changes:

Whilst increasing the load, the distance between the shaft and bearing becomes very small. Thus, the opportunity of asperity collisions to occur increases. Spectrums show that the frequency magnitude bands between 8,000 Hz up to 10,500 Hz increase randomly, which might be present with metal-to-metal contact. On the other hand the modulated frequency magnitude between 3.500Hz to 7,500 Hz decreases and become wider because the information signal decrease when applying high load and the shaft becomes more stable, as show in Figure 7.12.

Investigate the Viscosity Changes:

While lubrication viscosity rises, two possibilities will occur based on the radial load. At low load, high viscosity lubricant causes more shear force on the other hand low viscosity oil causes more fluctuating of the shaft. Spectrum magnitude band of the coupled signal between 3,500 Hz to 7,500 Hz increase while the viscosity decrease due to information signal which is shaft frequency and its harmonics. While viscosity increase the shear force increase especially at high speed, shaft frequency might clearly present it. At high load, the

gap became very small, so the high viscosity will not move easily between the surfaces. Due to this, the spectrum increases while the oil viscosity increase, see Figure 7.12.

Investigate the Speed Changes:

Spectrums of different speeds always have linear behaviour, high speed has high spectrum at high or low loads or different viscosities. Figure 7.12 presents spectrums of all cases of differed operating conditions.
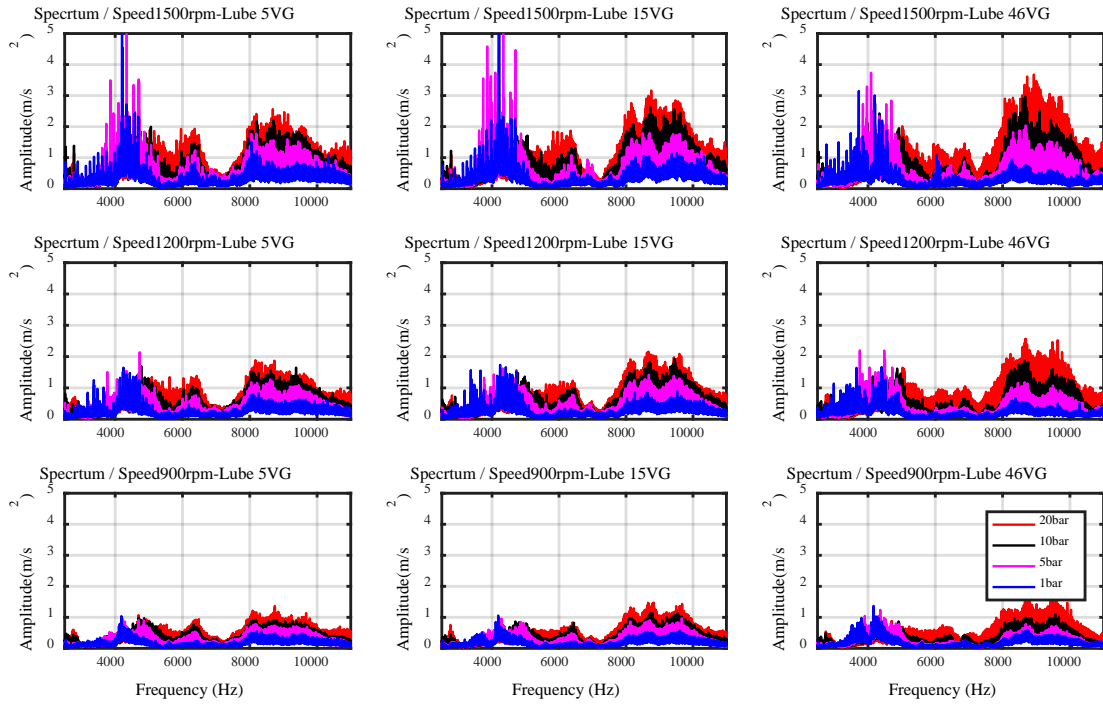
Figure 7.12 Spectrum of different operating conditions

7.4.4 Results and Discussion

Modulation Signal Bispectrum Analysis

To avoid the influences of low frequency vibrations from other interfering sources such as the driving motors, MSB of Equation (3.13) was calculated in a high frequency range for the carrier $f_c = 2.5kHz \square 11kHz$ whereas the modulator $f_x = 0Hz \square 50kHz$ in order to catch the shaft rotational component up to the second harmonics.

Figure 7.13 shows MSB magnitude results for different loads and viscous values at the speed of 1500rpm. Each subplot was obtained with a frequency resolution Δf of 0.7324Hz and through 80 averages to ensure a stable result and the MSB magnitudes remain the same when further average was added.

It can be found in Figure 7.13 that MSB shows distinctively two patterns. The first is that more discrete components are the main characteristic for the low radial loads. Particularly, as these components are associated with $f_x = 0.4kf_r , nf_r$ (f_r is the journal speed in Hz), it shows that the bearing operates with high oscillations in such frequencies relating to oil whirls due to instable hydrodynamic effects and misaligned rotors due to mechanical unbalances.

The second MSB pattern is that the magnitudes are more continuous shapes across the modulator frequency and in different bands of the carrier frequency. As it appears in high load conditions, it indicates the overwhelming effect of the micro churns and collisions due to highly pressured oil films.
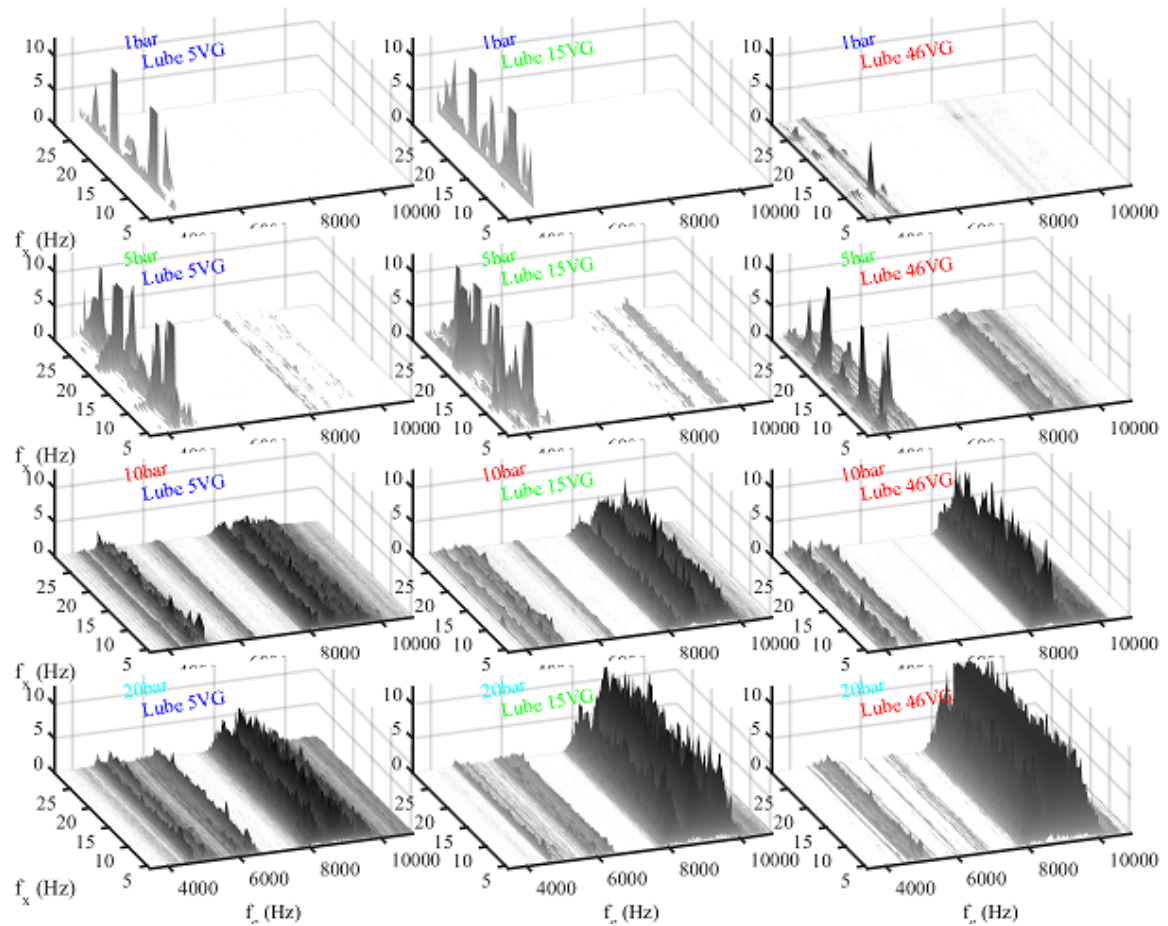

Figure 7.13. MSB magnitude for different loads and viscosity at 1500rpm

Moreover, two distinctive carrier frequency bands can be observed in Figure 7.13. The low frequency band ranges from 5.5kHz and 7.5kHz whereas the high frequency band is 8kHz to 10.5kHz. For high loads, MSB magnitudes in the high bands exhibit an increase with the

viscosity, showing more occurrences of the asperity churns as the oil becomes more viscous. However, MSB magnitudes in the low band show a decrease with the increase of viscous values. This may indicate more the effect of asperity collisions can be reduced as the oil viscosity is higher.

Overall, MSB magnitudes bring forward distinctive characteristics of vibration contents relating to lubrication conditions, providing useful information for diagnostics. For more results of spectrum, see Appendix C.

Detection of Instable Operations based on Modulation Signal Bispectrum Analysis

To quantify MSB results for accurate detection and diagnosis, entropy measures were calculated to show the difference between the two distinctive patterns. As shown in Figure 7.14, entropy values can clearly separate the low load from high load for all the operating speeds. As discussed earlier, the low load operations exhibit clear periodic oscillations due to instable oil whirl, which may induce high vibration to the whole rotor system, they are therefore regarded as abnormal lubrication. As shown in Figure 7.14, such abnormal cases have very low entropy values, which can be easily differentiated from the high load cases which have much high entropy values. In addition, the Figure also shows that the higher speed operation of 1500rpm shows more whirls compared with that of 1200rpm. Especially the 900rpm shows little such instable oscillations.
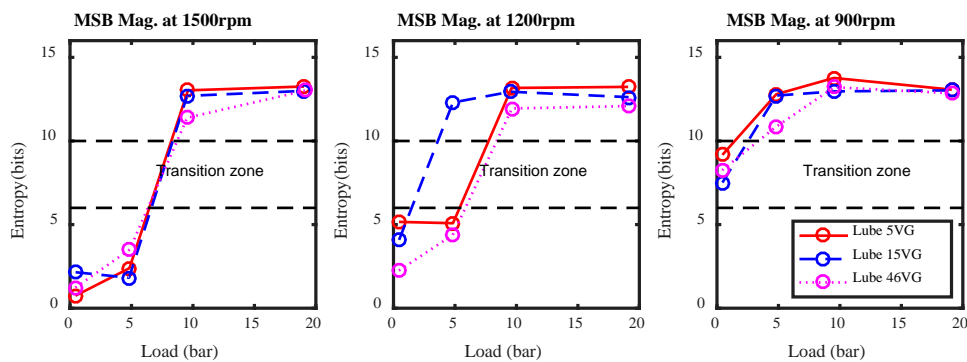

Figure 7.14. MSB magnitude entropy

Detection of High Friction Operations based on Modulation Signal Bispectrum Analysis

Based on the high amplitudes in the low frequency band from 5.5kHz and 7.5kHz as shown in Figure 7.15, it is possible to differentiate the low viscosity from others as it happens with

more asperity collisions under high radial loads, and thereby more wear occurs, which corresponds to the asperity contact friction.
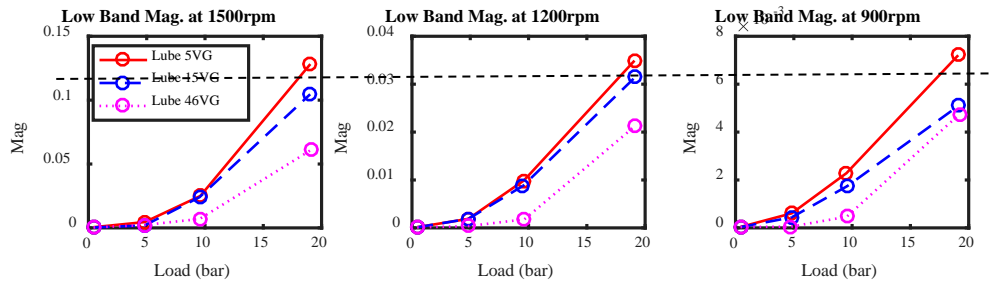

Figure 7.15 Averaged MSB magnitudes in the low frequency bands
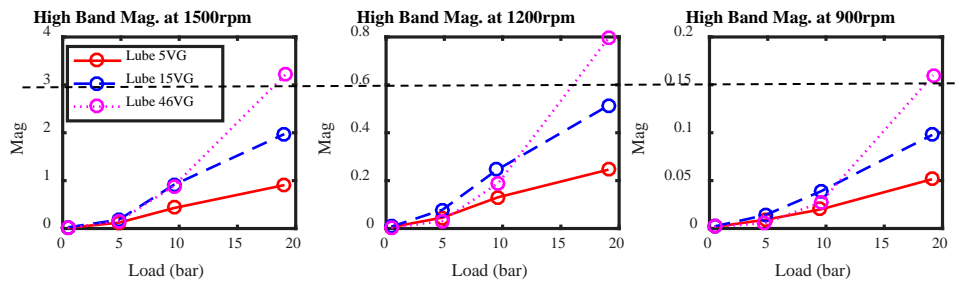
Figure 7.16 Averaged MSB magnitudes in the high frequency bands

Based on the higher amplitudes in the high frequency band from 8kHz and 10.5kHz it is possible to differentiate the high viscosity case from others as it happens with more asperity churns under high loads, and thereby more frictional losses, corresponding to more to the fluid friction.

Therefore, load conditions such as 10 bars for all three oils and 20 bars for only VG 15 oils are regarded as acceptable operations. This viscosity dependency diagnostic shows that vibration is sensitive to detect oil changes.

7.5   Summary

Abnormal operating conditions are one of the problems that cause journal bearing to fail. Based on the analytic studies and experimental verifications, it has been demonstrated that popular vibration monitoring can detect abnormal oils and operations in wide operating conditions.

Through a hierarchical clustering approach, the similarity and difference between the spectra of test samples can be recognised step by step in a relatively narrow frequency band. Furthermore, it obtains a classification result in the frequency band around 10 kHz that allows different oils and operating conditions to be separated in consistent with lubrication regimes.

The successful diagnosis is achieved based on modulation signal bispectrum analysis which allows the nonlinear vibration responses of journal bearings to be characterised into two distinctive patterns to correspond to the instable lubrication and the asperity interactions respectively. Furthermore, the MSB magnitudes in different frequency bands can be based to differentiate the asperity interactions between asperity collisions and the asperity churns. A higher magnitude in the lower frequency band can indicate the excessive asperity contacts due to lowering viscosities. Meanwhile a higher magnitude in the higher frequency band indicates the extreme fluid frictions.

High frequency vibration responses are mainly from two frictional effects in a journal bearing. The surface asperity collision in the boundary lubrication explain main vibration responses, whereas fluid shearing induced asperity deformation and recovery in the hydrodynamic lubrication regime can also be an effective vibration generation mechanism. Analytic and experimental studies show that these vibration responses in the high frequency range are complicated and difficult to separate according to the oil types and lubrication regimes.

CHAPTER EIGHT

MONITORING OIL STARVATION

This chapter presents the study of monitoring the oil starvation of journal bearings based on vibration analysis. In particular, MSB analysis of vibration responses from different levels of lubricant oil in the reservoir shows that vibration characteristics are different in terms of frequency bands and magnitudes, which can be based on to differentiate between degrees of oil starvation.

8.1 Introduction

The journal bearings are designed to be operated under fully oil film which completely separates between bearing and journal surfaces. This thick oil film reduces wear and friction at the contact points. While the oil film is not thick enough to separate the surfaces, asperity collisions have a high chance of occurring. Thus, any problem affecting the oil film thickness might be a reason for metal-to-metal contact occurring especially during applying a radial load. Unfortunately, some bearings forces to be operated under oil starvation conditions which are common reasons of journal bearing failure. One of the possible reasons of starved conditions is an oil leak from rubber seals or gaskets. Due to a limited amount of lubrication or high lubricant viscosity, starvation can occur [41]. Another reason of starved condition is that the oil film is not thick due to journal rotating speed and bearing load to cover the full bearing width. Under starved conditions journal eccentricity ratio is different from optimum conditions, the oil film thickness and shape change [113].

For that reason, the oil leakage might cause catastrophic damage in industry. Consequently, appropriate level of oil keeps journal bearings operating efficiently and provides a long service life. An effective test has been studied by simulating the oil leakage fault by reducing the oil level of a bearing's reservoir. To further investigate the vibration based diagnostic performance, this study focus on examining vibration responses to lubrication oil levels and developing features for diagnosing oil starvation in journal bearings. The vibration signals were collected at different speeds under different radial loads.

8.2 Test Facilities and Procedure

To examine the performance of vibration based oil level detection method, a self-aligning spherical journal bearing, SA35M, was tested on a test rig as shown in Figure 6.2. The bearing was lubricated with oil 37 VG. The maximum recommended volume of oil in the reservoir is 100ml. In order to simulate oil starvation, the test was started with a full lubrication level of 100ml which was subsequently reduced by 20ml at each successive test. Table 8.1 details the operating conditions and lubrication status. According to the size and lubricant used, the eccentricity ratio ($\varepsilon = e/c$) was also calculated, showing that the bearing was operating under acceptable lubrication regimes.

The vibration was measured by a 10kHz wide band accelerometer. In addition, the vertical and horizontal displacements of the shaft were measured by a pair of laser displacement

sensors. It can be seen that the distance between the journal and bearing becomes smaller with the successive reduction in oil levels, indicating that the hydrodynamic films become thinner and more asperity collusions occur due to oil starvation.

Table 8.1. Test conditions

4 oil levels: Baseline 100%, 80%, 60%, and 40%				
Speeds:	1500rpm	1200rpm	900rpm	600rpm
eccentricity ratio:	ε	ε	ε	ε
Load 1 bar	0.10	0.12	0.16	0.23
Load 2 bar	0.19	0.23	0.28	0.37
Load 5 bar	0.37	0.42	0.48	**0.56**
Load 10 bar	**0.51**	**0.56**	**0.61**	**0.67**
Load 20 bar	**0.64**	**0.67**	**0.71**	**0.76**

Figure 8.1 Oil level eye (100%, 80%, 60% and 40%)

8.3 Vibration Characteristics in the Time and Frequency Domain

A comparison was made between raw vibration signals for different oil levels and operating conditions. It was found that the vibration amplitudes exhibited a significant increase with operating conditions. To quantify the differences, the root mean squared (RMS) values were calculated and shown in Figure 8.3.The RMS values increase with the decrease in oil levels, along with an increase in speed and load. This change agrees with the characteristics of the two excitation mechanisms. Therefore, it can be effective to indicate the lubrication conditions using vibration responses.
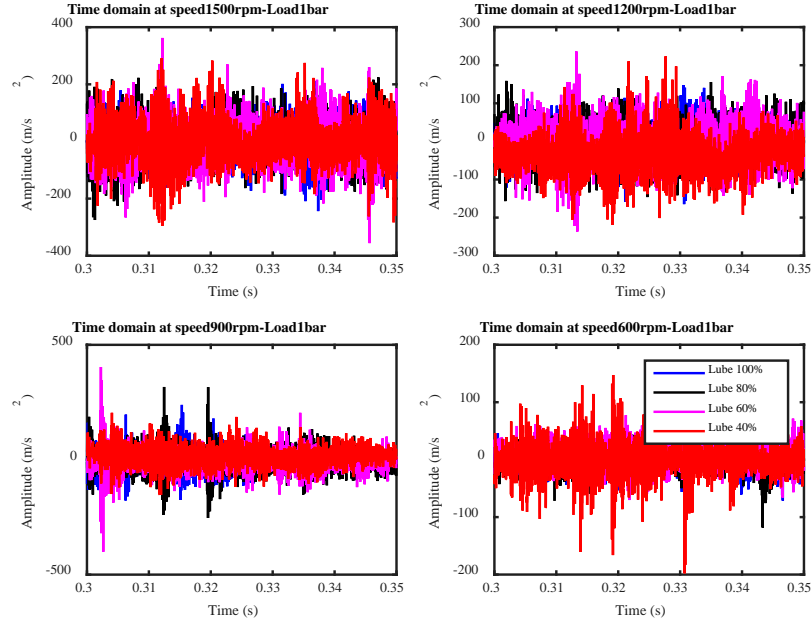
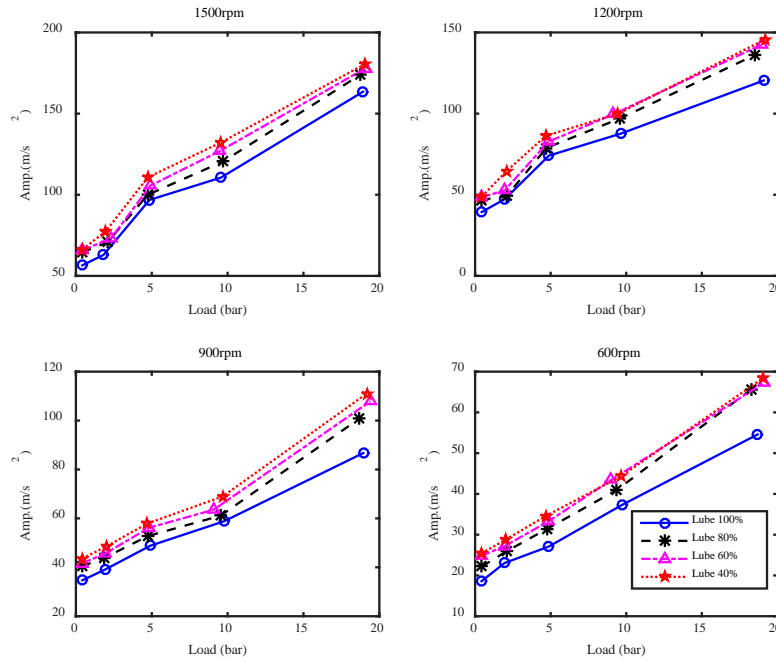Figure 8.2. Time domain of different oil levels

Figure 8.3. RMS of vibrations for different operating conditions and oil levels

However, as shown by the RMS, some of the oil level conditions cannot be separated adequately. In addition, vibrations of low frequencies can be affected by other sources such as that of the driving motors and couplings, leading to an unreliable diagnosis. To refine the results, spectrum analysis was carried out to find an optimal frequency band for making a better separation.
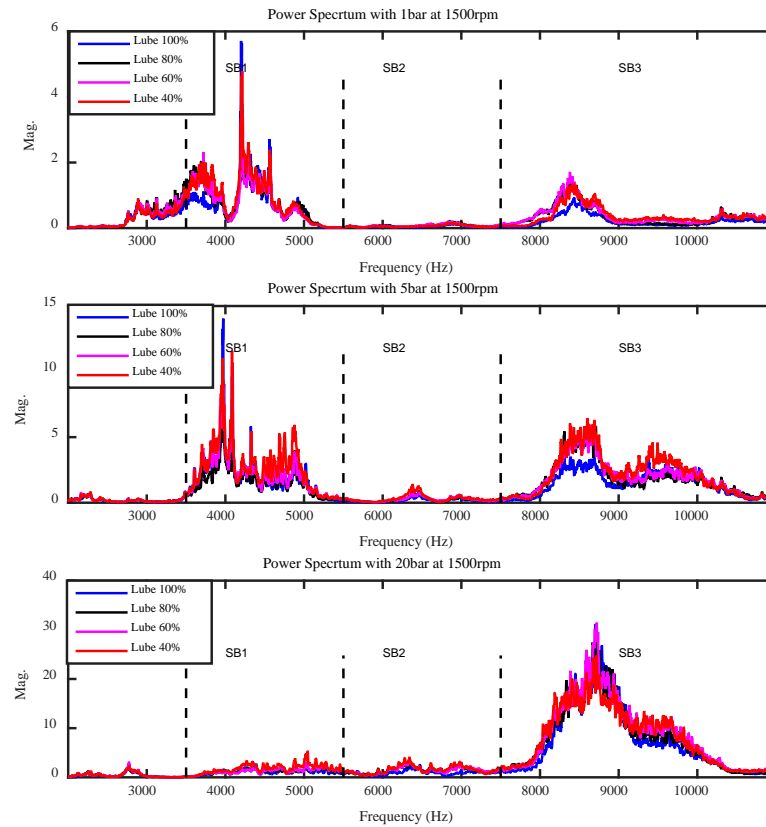
Figure 8.4. Spectrum characteristics of vibrations for different oil levels and operations
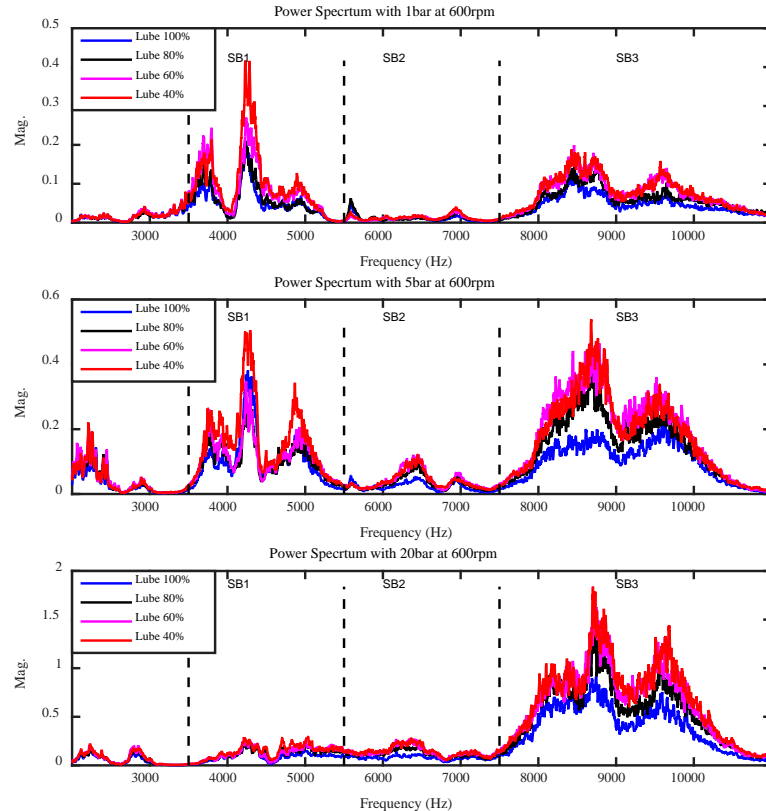

Figure 8.5. Spectrum characteristics of vibrations for different oil levels and operations

Figure 8.4 and Figure 8.5, the spectrum in the high frequency range can be regarded to have three sub-bands: SB1 for 3.5kHz-5.5kHz, SB2 for 5.5kHz-7.5kHz and SB3 for 7.5kHz-11kHz, according to the distinction of the spectral amplitudes. In each band, spectrum exhibit continuous profiles due to the random excitations of asperity churns and collisions. In addition, these profiles are also magnified by the nonlinear transfer paths of structural resonances. Nevertheless, the amplitude in each band increases with the speed and loads showing they can be a good indication for operating conditions. Moreover, these amplitudes are also sensitive to change in oil levels therefore the averages of the spectral amplitudes were extracted for differentiating the oil levels. For more results of spectrum, see Appendix D. Figure 8.6, Figure 8.7 and Figure 8.8 present the averaged amplitudes for different operating conditions along with different oil levels. They show the two high frequency bands SB2 and SB3 give more consistent separation for the oil levels in that they agree more with the excitation mechanisms. Especially, SB2 band can provide nearly full separation for all the test cases which are more reliable, compared with that of RMS values. SB3 band however, can show better differences from the base line oil level. However, due to its high nonlinear effects, the separation between different levels is not as good as that of SB2. More interestingly, the amplitude of the lower frequency band of SB1 shows a very nonlinear behaviour with loads, which is inconsistent with the understanding of vibration mechanisms.
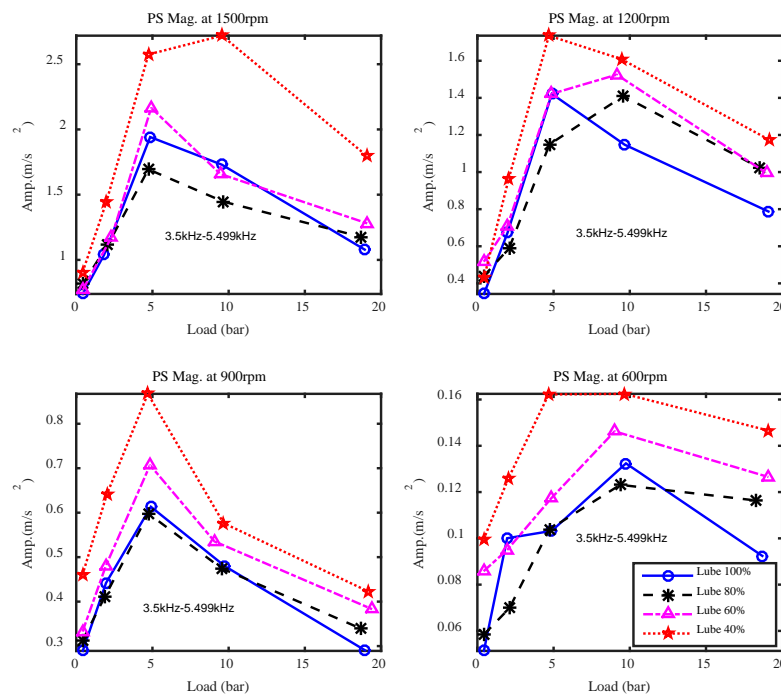

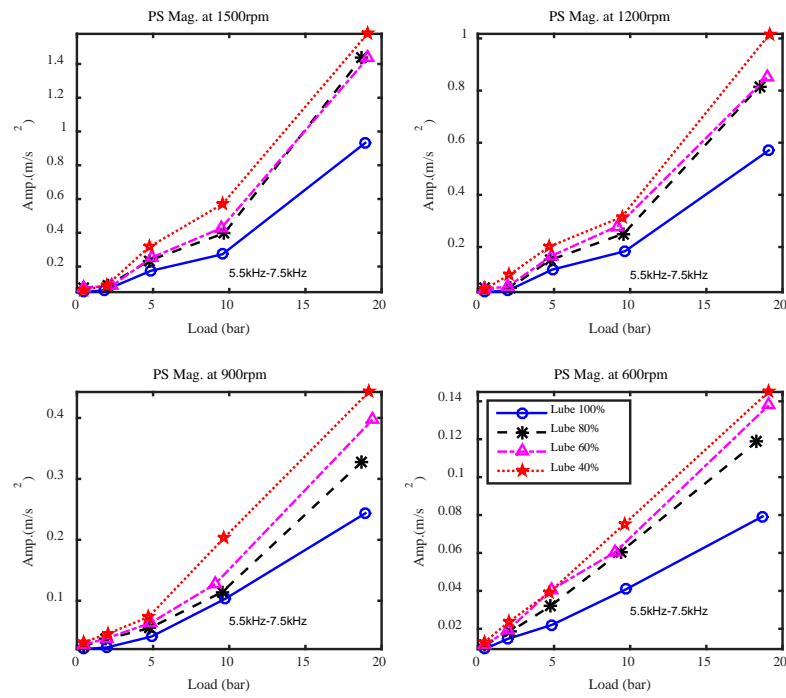Figure 8.6. The spectral magnitudes of vibrations in frequency band SB1

Figure 8.7. The spectral magnitudes of vibrations in frequency band SB2

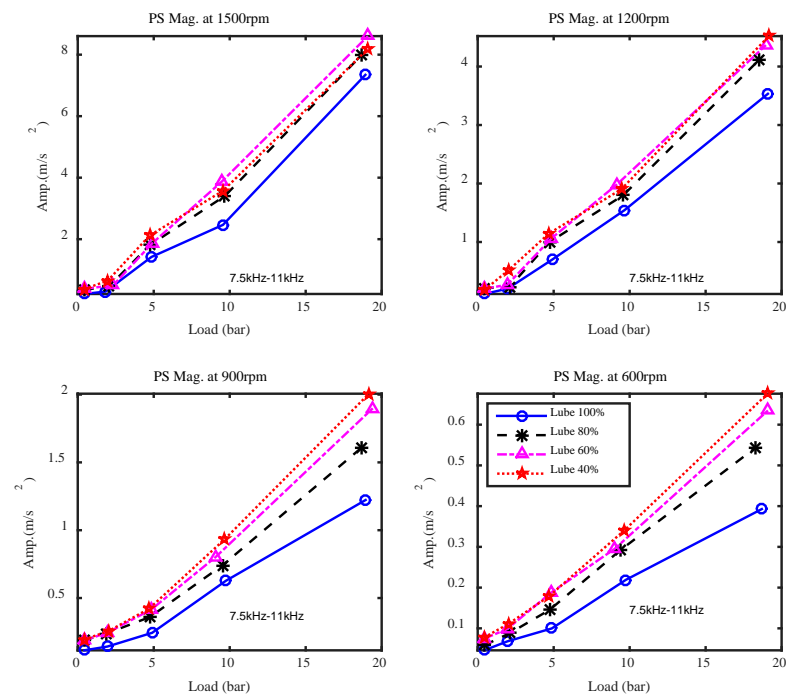Figure 8.8. The spectral magnitudes of vibrations in frequency band SB3

8.4   Shaft Positions

The leaser sensor measured the distance of the shaft movement at different oil levels. This measuring is an evidence of the oil film thickness becoming smaller when leakage occurs and surfaces almost hit each other.
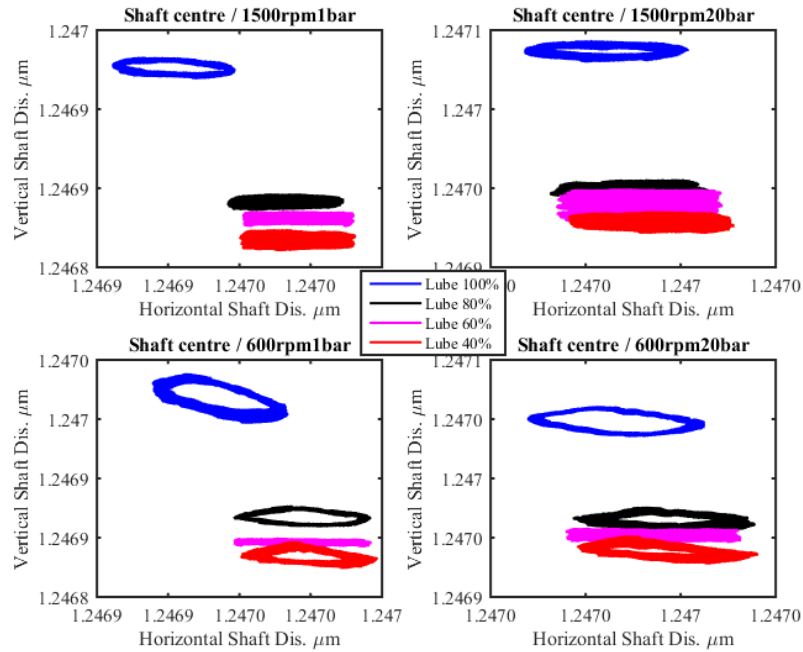

Figure 8.9. Shaft displacements
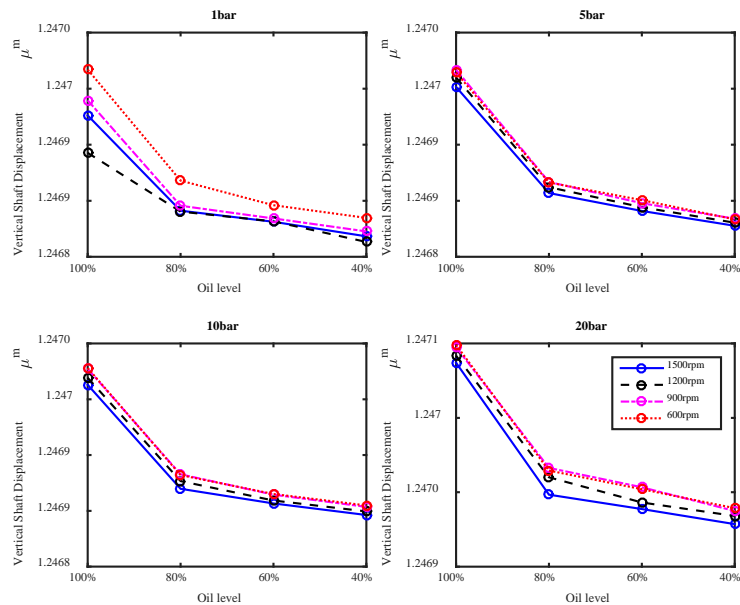
Figure 8.10 Shaft centre during oil film loses its thickness by leaser sensor

8.5 Modulation Signal Bispectrum Analysis

Modulation signal bispectrum (MSB) analysis was carried out to attain a better understanding of the vibration mechanisms as it is more effective in characterising the nonlinear behaviours embedded signals[37, 63]. Particularly, it can suppress components and thereby highlights the modulating deterministic components so that more stable results can be obtained for characterising the vibrations. Figure 8.11 and Figure 8.12 present the MSB magnitude results in the low frequency band of SB1 from 3.5kHz to 5.5kHz at rotational speeds 1500 and 600 rpm (other speeds see Appendix D).

Figure 8.11. MSB magnitudes of SB1vibrations at high speed (1500rpm)

Figure 8.12. MSB magnitudes of SB1 vibrations at low speed (600rpm)

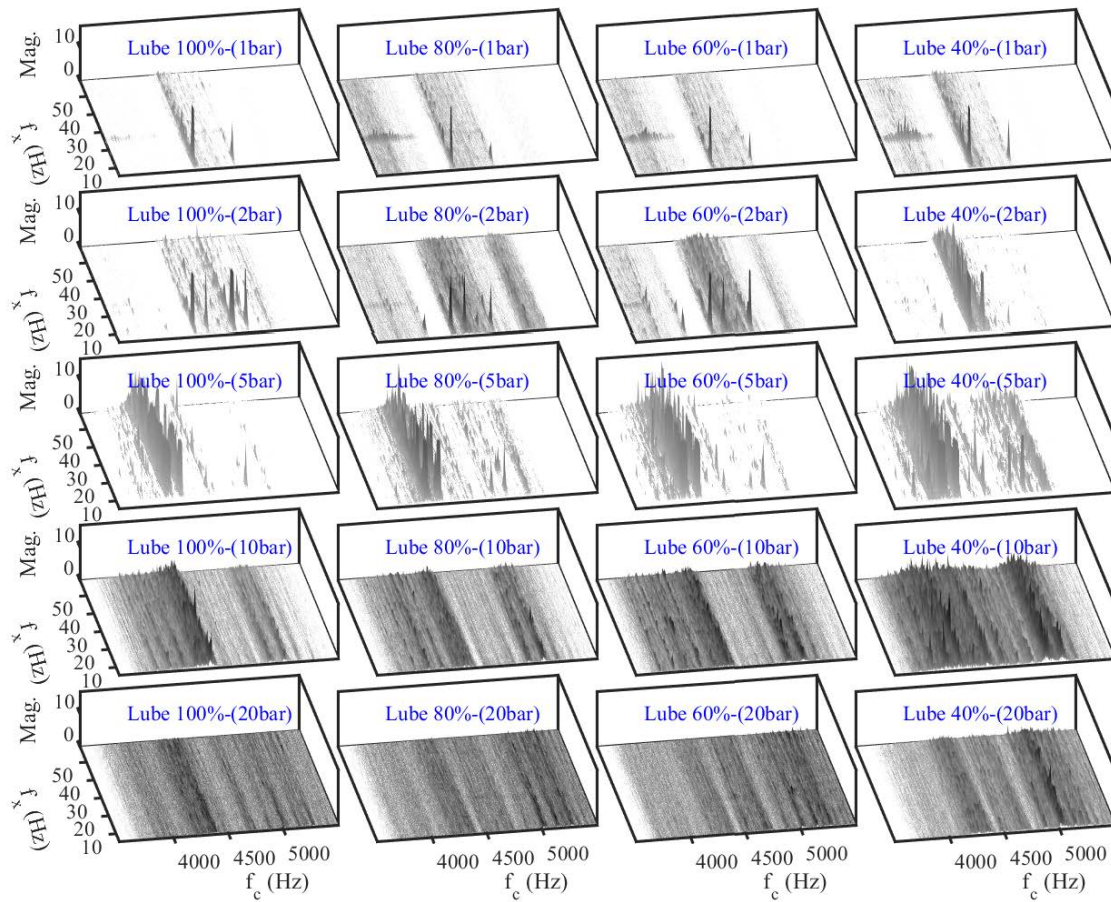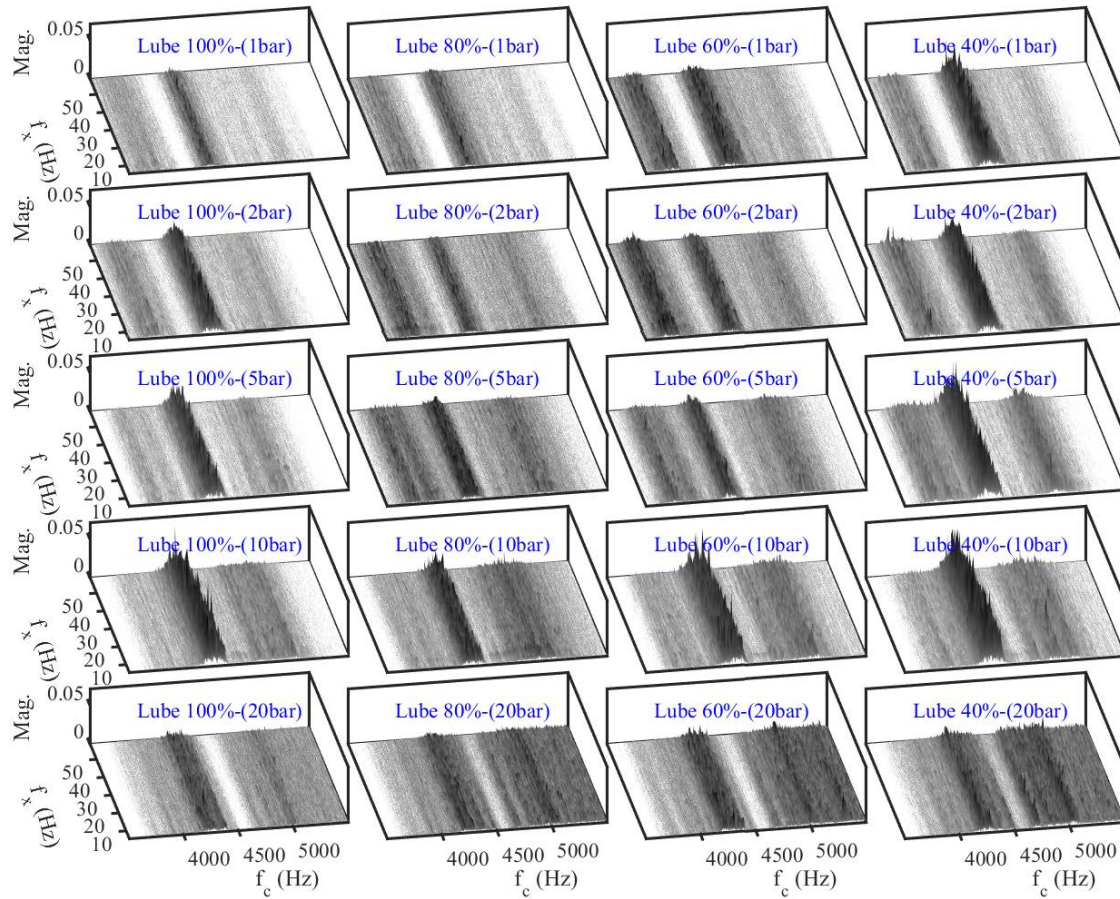It can be seen that MSB shows significant modulation components for the low load operations (lower than 5 bars). Particularly, for the results at the speed of 1500rpm, MSB peaks at bifrequencies (10, 4500) Hz and at (20, 4500) Hz cases can be accounted by oil whirls and peaks at bifrequency (25, 4500) Hz is from the effect of rotor eccentricity. In other words, the random excitations of asperity churns and collisions are marked. Conversely, for the high load operations, MSB magnitudes show much more random patterns, which can reflect more the effect of random excitations. Based on this analysis, it can be understood that the magnification of vibration in this band is more dominated by the instability of hydrodynamic interactions. Therefore, this band produces less agreeable results for differentiating the oil levels and operating conditions. However, this band can be particularly useful to detect the instability operations at the low load cases, which can be very negative to the entire rotor system.

8.6 Summary

Based on the vibration mechanisms established and experimental studies, the vibration signals collected under different operating conditions and lubricant levels can be separated adequately for the purpose of condition monitoring. Journal bearing vibration responses are induced by the combination of the conventional hydrodynamic effect and the asperity churns and collisions between the lubricated rough surfaces the combination of which can be characterised by modulation bispectrum analysis. The hydrodynamic effect can interfere with the asperity effect in the low frequency range SB1 (3.5kHz to 5.5kHz), resulting in good detection of the instability but an inconsistent diagnosis of oil levels. Meanwhile, the structural resonances in the high frequency range SB2 and SB3 (5.5kHz to 11kHz) can better reflect the excitations and result in a more agreeable separation of different levels under wide operating conditions.

CHAPTER NINE

MONITORING WORN BEARINGS

This chapter presents the monitoring of worn journal bearings based on vibration analysis techniques. Firstly, worn bearings have been effectively created by applying high radial load to journal bearings. Then, MSB analysis of the vibration responses from different degree of wears shows that different degrees of worn bearings can be detected based on vibration characteristics of frequency bands and magnitudes.

9.1   Introduction

Direct contact between the shaft and journal bearing causes quick wear and high temperature even though the journal bearing surfaces are fine and made of materials that have low coefficients of friction. Also, it is well known that in journal bearings, friction occurs not only in boundary regime but, in all lubrication regimes [114]. Journal bearings do not suddenly fail as a rolling element but wear happens extremely slowly. Operation condition such as low rotational speed, high load and low lubricant viscosity are some of the most important factors that produce wear [114]. Furthermore, vibration in bearings that are caused by unbalance or misalignment can cause excessive wear [65] [114]. Using a lubricant to reduce the amount of friction and to absorb vibrations, as well as to reduce unwanted heat. A thin layer of oil mainly at low speed and high load is an indicator of metal to metal contact will occur. In contrast, too much thickness of oil especially at high rotational speed and low load is an indicator that shaft instability will occur.

In this test, vibration signals analysed to detect bearing situation after two stages of wear that accelerated by increasing direct contact. Also, oil particular is analysed by Q230 (more details see section 6.3.6) to provide evidence about worn bearing had been occurred. The goal of this chapter is to investigate the effect of wear (changes in radial clearance) on bearing vibration signals.

9.1.1   Friction and Wear in Journal Bearing

Wear of bearings may be defined as the removal of surface material. Also, the friction between shaft and journal bearing causes wear on the bearing material surface. In time, due to friction between the surface components, wear appears and changes the micro (roughness) and macro geometry [82]. Studies conducted in the last five decades show that the lifetime of tribological systems is influenced by the choice of the key factors that control wear: operational conditions and material properties [82]. In the HL regime the separation between the surfaces is sufficient to prevent asperity contact and is characterized by low values of the wear rate (10^{-15} to 10^{-9} mm^3/N·m) [82].

In BL, the operational conditions become severe (high loads and high temperatures) and sliding contact occurs between unlubricated surfaces then the values of wear rate may become 10^{-5} to 10^{-1} mm^3/N·m [82].

During applying a high radial load, vibration signals have maximum power due to friction and wear, which was proven in Chapter 7.

9.1.2 Oil Film with Different Worn Bearing

The main aim of changing geometry by wear, is to change the lubricant thickness, thus the lubricant regime changes form one regime into another. By changing bearing clearance, the effective system of fluid damping and stiffness coefficients alter. Also, the effects of asperity collision stiffness coefficients are changed as well. To model the worn zone, the worn track created by the journal in the bearing is centred to the minimum oil film thickness [115] as shown in the following Figure 9.1.
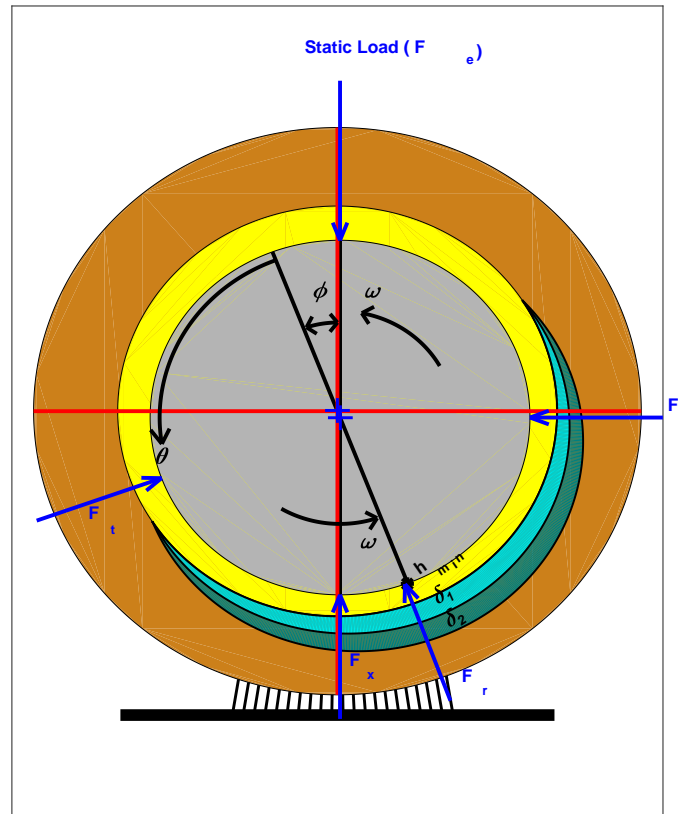
Figure 9.1 Two stages of worn Journal bearing

9.2 Test Facilities and Procedure

A self-aligning spherical journal bearing has been tested. The test was divided into five steps, even steps for collecting data and odd steps for simulating wear, as shown in Figure 7.2. For avoiding any changing in transmission bath of the signals, wear was created without uninstall journal bearing and measurement devises. Thus the simulated wears

shown in red dashed box in Schematic 9.1. Wear has been generated by applying high redial load during (40 bar) the shaft rotated at 600 rpm and the bearing contained very low level of lubricant.

To investigate the vibration signals of journal bearing three datasets were collected: one before simulated wear and the other two after wear stage 1 and wear stage 2, as shown in blue dashed box in Schematic 9.1. Each set of data had different operating conditions: four different speeds 1500, 1200, 900 and 600 rpm and three different loads: 2, 10 and 20 bar were applied. In this test, the journal bearing contained lubricant 37 VG.

Besides capturing vibration signals for different worn bearings, new lubricant and after each simulated wear step (after blue dashed box in Schematic 9.1) were analysed by using Q230 devise shown in Figure 6.11, section 6.3.6.
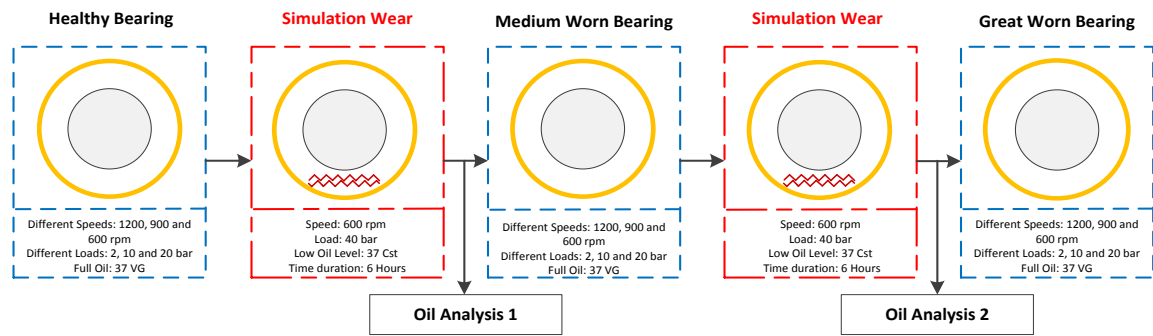
Schematic 9.1 Test procedure

9.3   Results and Discussion

9.3.1   Oil Analysis

The purpose of oil particular analysis is to provide evidence that wear has occurred and to count the particles in the oil as a result of wear. It is obvious from Figure 9.2 that the oil colour of wear at stage 2 darker than wear at stage 1. Table 9.1 presents particular counts, types and shapes. New oil has 7,216 part/1ml, wear 1 oil has 124,715.7 part/1ml and wear 2 oil has 682,374.8 part/1ml. as a result of the oil analysis, the particulars in lubricant increased while stage of wear increases. Thus, this analysis will be considered as evidence that wear happened and it became sever after step 4. Also, Figure 9.3 shows a worn bearing after the test. Furthermore Table 9.1 presents a number of particulars in the lubrication at no wear and after wears. Also, it shows the shapes of these particulars.
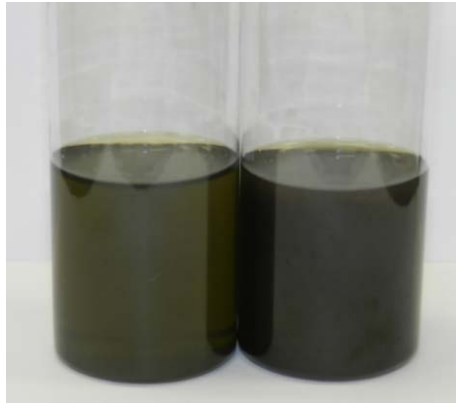
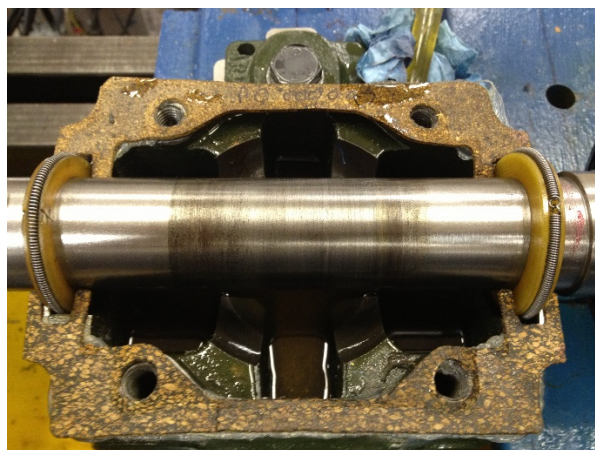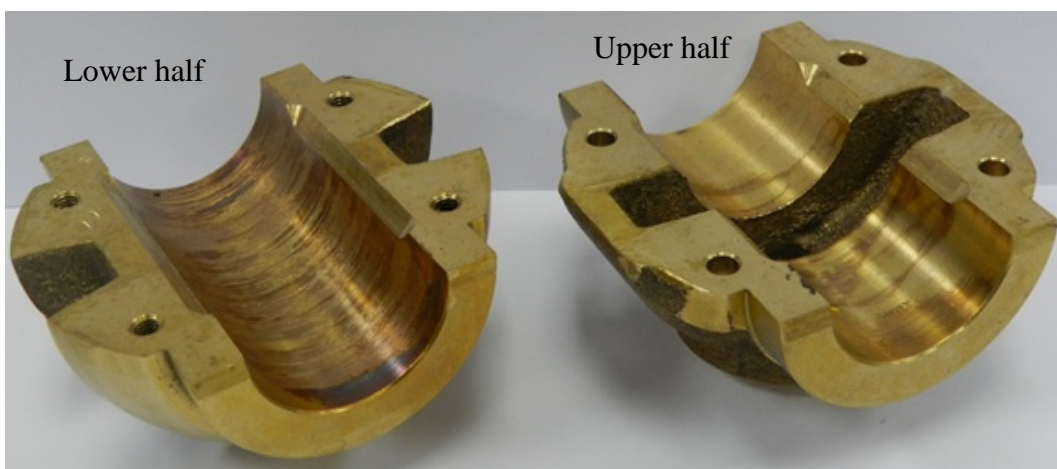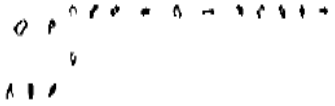Figure 9.2 Lubrication specimens
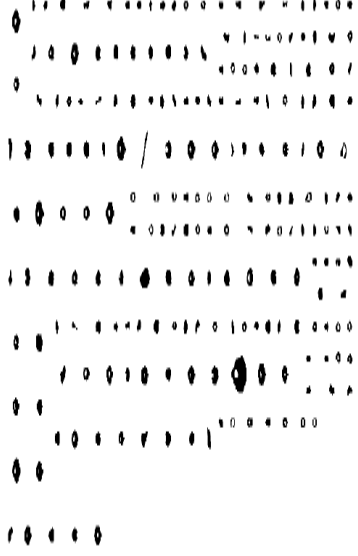
Figure 9.3 Worn journal bearing

Table 9.1 Lubricant analysis of new oil and two oil specimens after two steps of worn bearing

No wear	Wear 1	Wear 2
ISO 4406 (1999)	**ISO 4406 (1999)**	**ISO 4406 (1999)**
Part/1 ml	Part/1 ml	Part/1 ml
>4um(c): 7,216.0 20	>4um(c): 124,715.7 24	>4um(c): 682,374.8 27
>6um(c): 1,774.3 18	>6um(c): 27,744.2 22	>6um(c): 139,748.4 24
>14um(c): 51.0 13	>14um(c): 555.3 16	>14um(c): 1,084.4 17

Max Diameter Method	(Part/ml)	Max Diameter Method	(Part/ml)	Max Diameter Method	(Part/ml)
Cutting Wear	5.0	Cutting Wear	8.8	Cutting Wear	18.8
Severe Sliding Wear	3.8	Severe Sliding Wear	27.5	Severe Sliding Wear	88.8
Fatigue Wear	5.0	Fatigue Wear	140.1	Fatigue Wear	252.5
Non Metallic Wear	7.5	Non Metallic Wear	83.8	Non Metallic Wear	172.5
Unclassified Wear	0.0	Unclassified Wear	6.3	Unclassified Wear	3.8

9.3.2 Time Domain Analysis

Due to the simple design of a journal bearing, time domain features of vibration signals are good for the overall investigation. RMS values of vibration signals are good indicators to track journal bearing situation, but it will not provide any information on which component causes vibration [56].

In Figure 9.5 shows the contented power in the vibration signature by measuring RMS of raw data in Figure 9.4. RMS results present that worn journal bearing has less vibration energy, this is proven, by the worn bearing having more gaps between surface and oil film thickness, as in Figure 9.1. A worn bearing reduces vibration by dropping asperity collisions, but that does not mean more wear will in turn increase journal bearing lives.

The vibration sources in a journal bearing are mechanical problems and asperity collisions (as study in Chapter 5), and these two sources are inversely proportional. Frequency domain and MSB release that not always wear is good for journal bearing.
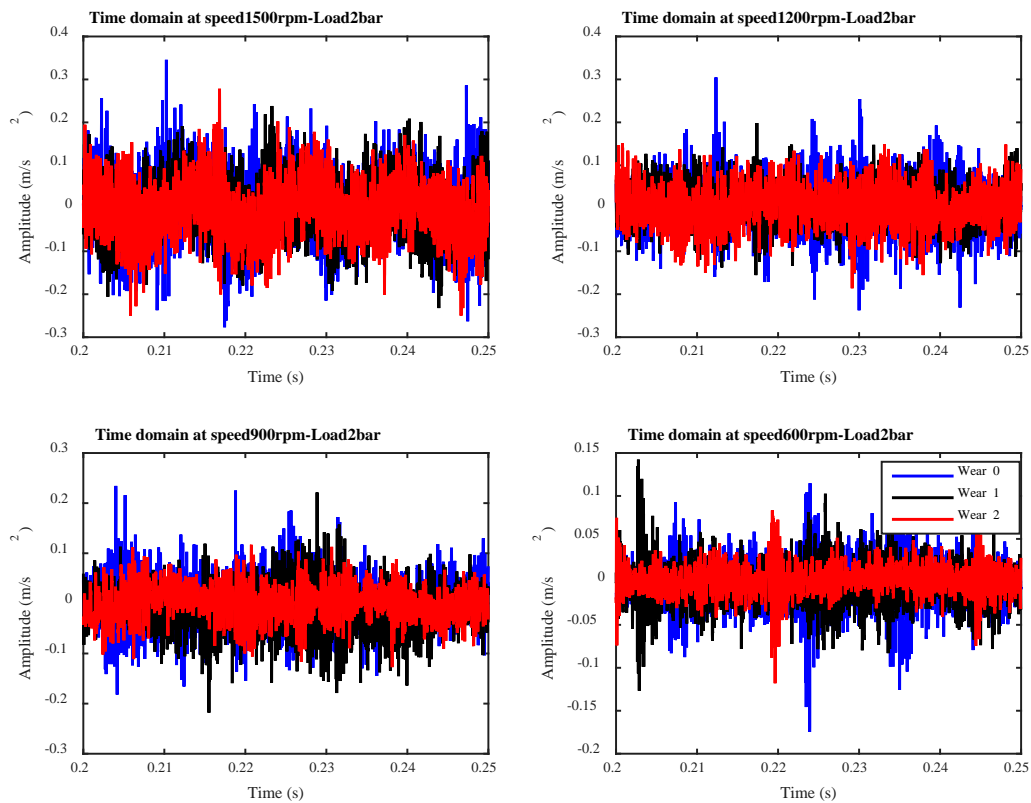
Figure 9.4 Time domain of vibration data at different clearances
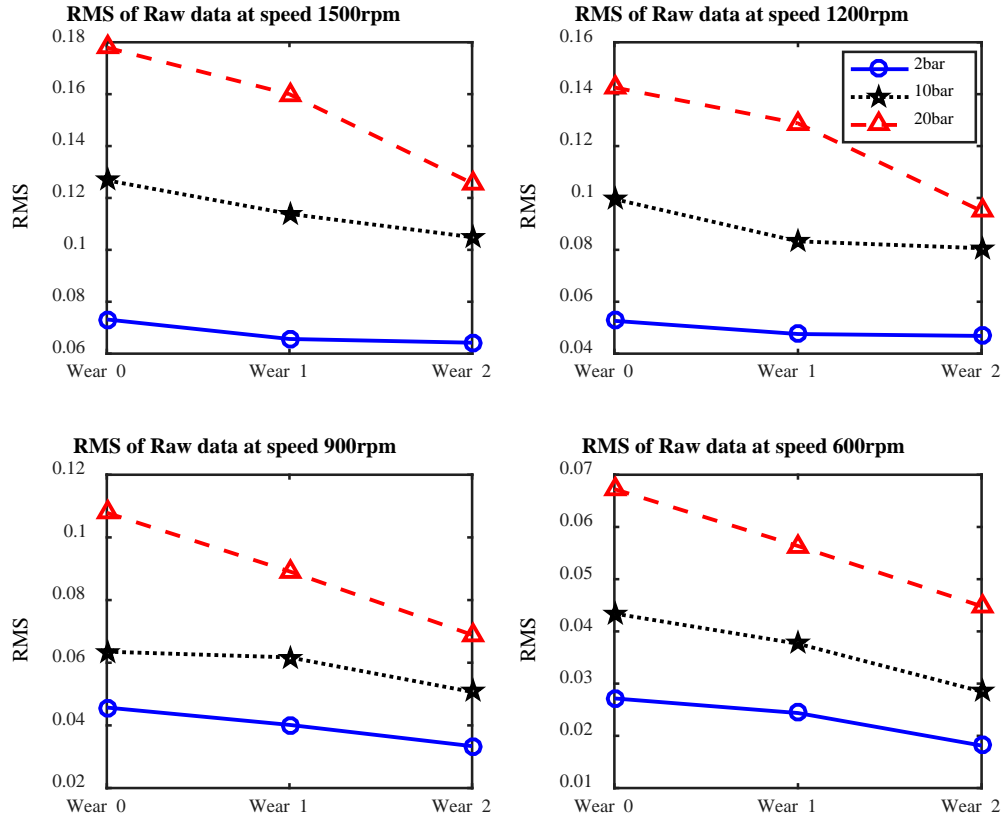
Figure 9.5 RMS values of raw data of different levels of wear

9.3.3 Spectrum Analysis

Figure 9.6 shows the power spectrum of health and different degrees of worn bearing at speed 1500 rpm and load 2, 10 and 20 bar. Spectrum signatures show two frequency bands and these two bands are inversely proportional. Low band, from 3000 Hz up to 5000 Hz releases more power of spectrum at massive worn bearing than healthy bearing, and it has more components related to shaft frequency especially at low load. Thus this band might relate to mechanical problems. In contrast, the high frequency band 8000 Hz to 11000 Hz reveals more power of health bearing than worn bearing, these bands might be related to asperity collisions and churns.
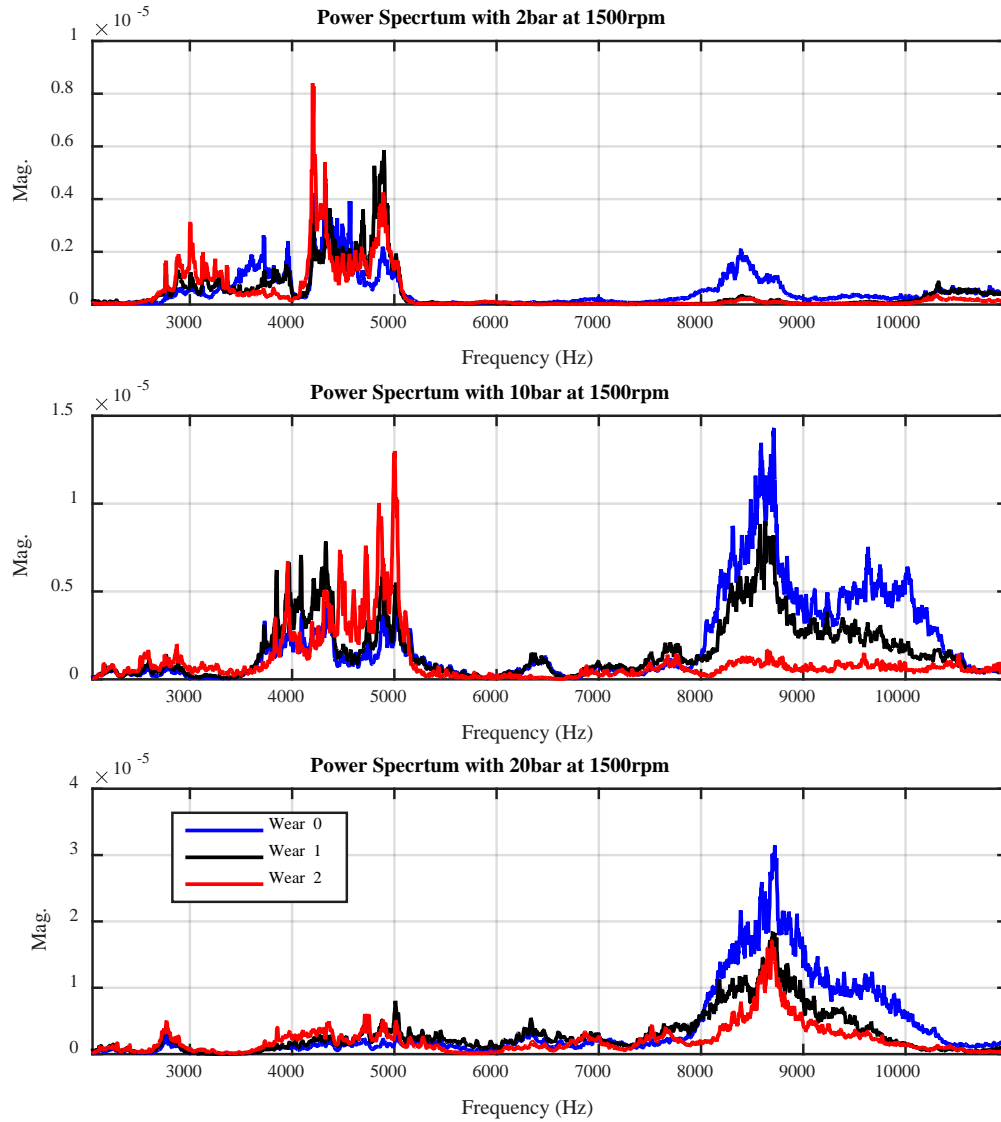
Figure 9.6 Power spectrum of different levels of wear

9.3.4 Modulation Signal Bispectrum Analysis

MSBs (frequency-frequency analysis) present the components of the vibration signal signatures. At a low frequency band from 4kHz to 5kHz, mean magnitude of MSB increases due to shaft frequency components, in Figure 9.7 and Figure 9.12. Vibrations of a large stage of worn bearing which offers more space between surfaces are associated with increasing mechanical problems and reducing asperity collisions, as a result of that vibration power increases. Also, entropy values (randomness measurement) increase when the gap between surfaces becomes bigger, in Figure 9.9.

Figure 9.7 MSB of worn bearing in the frequency band 4000-5000 Hz

Figure 9.8 Mean values of MSB Mag. in the frequency band 4000-5000 Hz of different operating conditions

Figure 9.9 Entropy values of MSB Mag. in the frequency band 4000-5000 Hz

In contrast, high frequency band from 7kHz to 11kHz, mean magnitude of MSB decreases because a worn bearing has more space to separate between surfaces and reducing asperity contacts, in Figure 9.10 and Figure 9.11. Furthermore, worn bearing has less values of entropy as shown in Figure 9.12. (Other operating conditions see APPENDIX E).
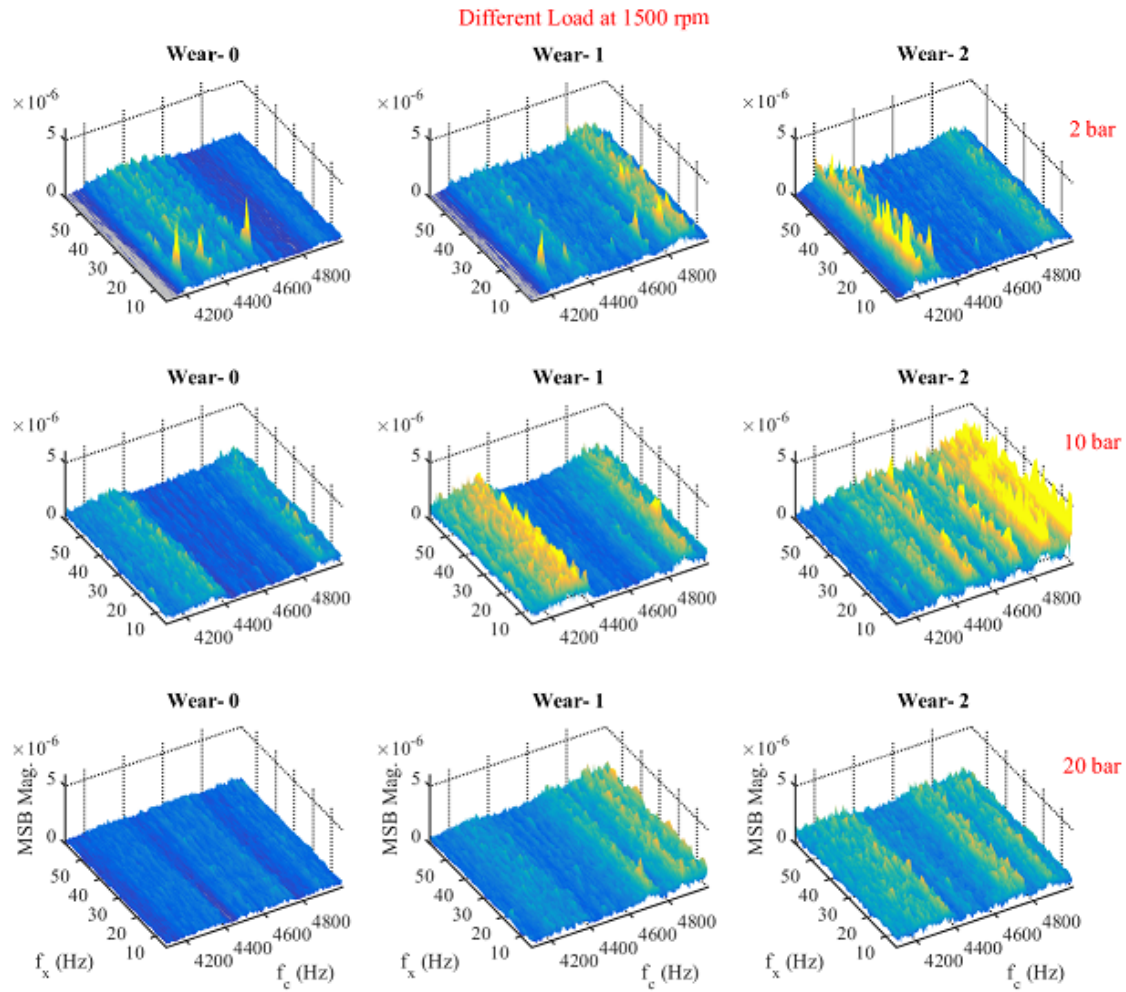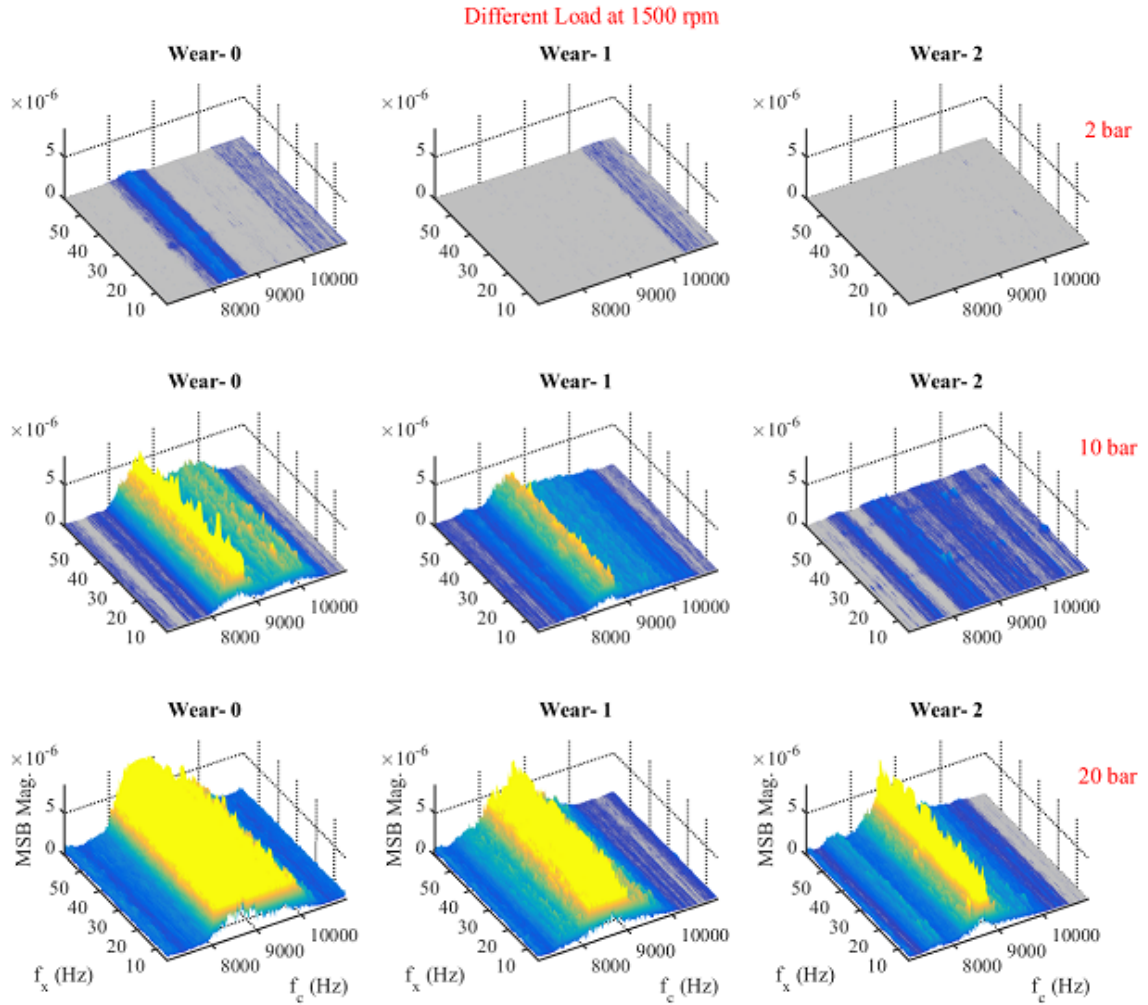
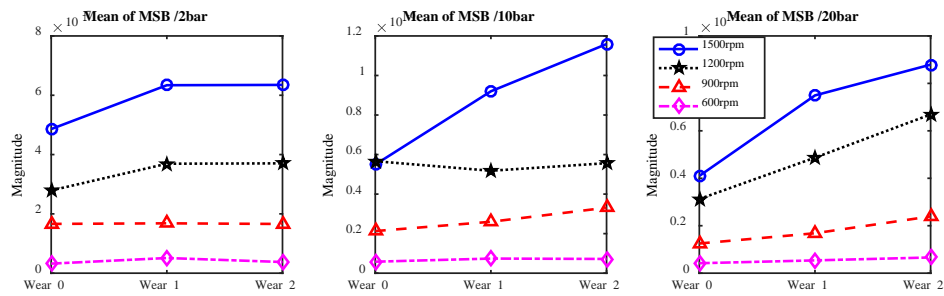Figure 9.10 MSB of worn bearing in the frequency band 7000-11000 Hz
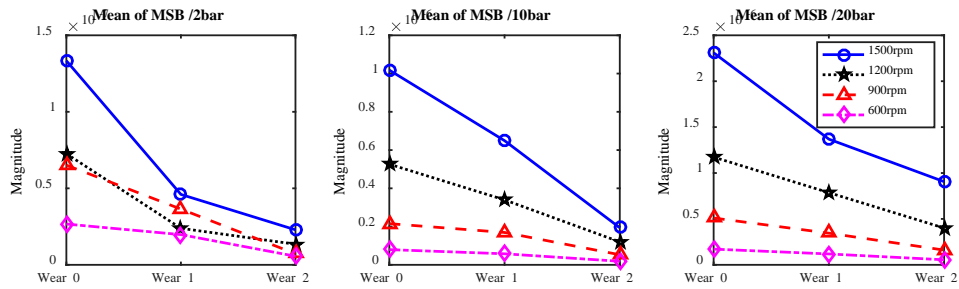
Figure 9.11 Mean values of MSB Mag. in the frequency band 7000-11000 Hz of different operating conditions
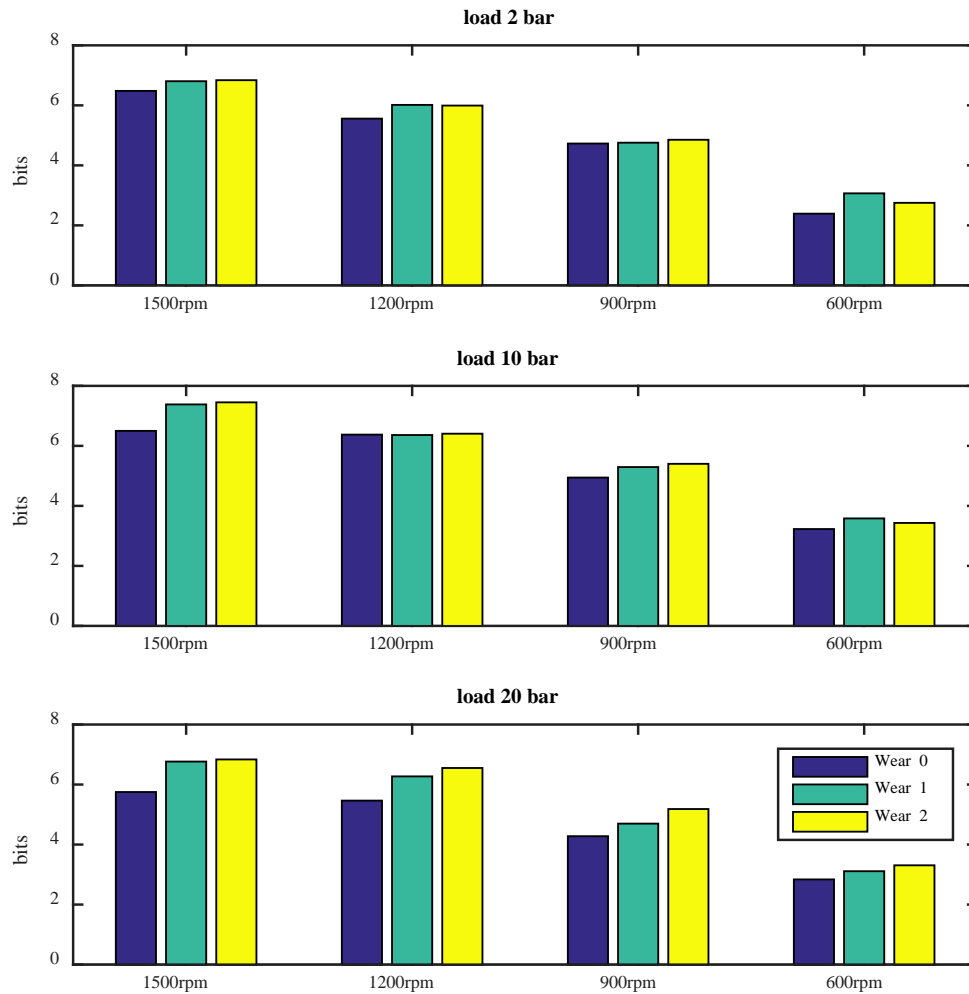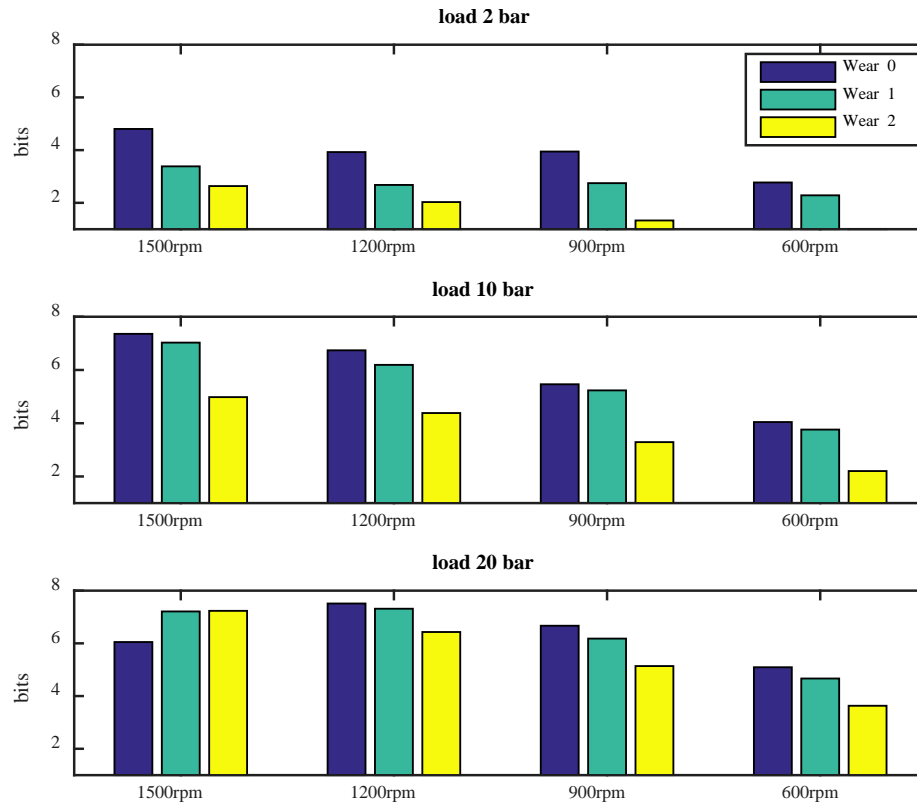
Figure 9.12 Entropy values of MSB Mag. in the frequency band 7500-11000 Hz

9.4   Summary

Journal bearings are designed to use lubricant oil film to reduce asperity collision by keeping two surfaces separate. Lubrication can reduce friction but it cannot be avoided completely. Thus if the wear happens the geometry of bearing will change and this wear will change bearing's clearance. Two different stages of worn bearing have been studied. RMS values of raw data are a good indication; they illustrate that worn bearing releases less vibration. This result presents only over all vibration power which is a combination of different vibration sources such as mechanical and asperity collisions. MSB technique can decompose the vibration signal into two main sources of vibrations in journal bearing. Low frequency band combined with harmonics of shaft frequency which increase at worn bearing and cause more fluctuating of the shaft. On the hand, high frequency band has less combination with shaft frequency and this band might relate to asperity contact. In this band vibration decreases at worn bearing because the space between surfaces is great.

CHAPTER TEN

ACHIEVEMENTS, CONCLUSIONS, NOVELTIES AND RECOMMENDATIONS FOR FURTHER WORK

This chapter presents achievements conclusions drawn by the research. Then it presents a summary of the novels and contributions. Finally, critical recommendations have been given for further studies in the direction of vibration analysis based bearing monitoring.

10.1 Review of Aims, Objectives and Achievements

The aim of this research was to develop a predictive maintenance techniques based on vibration analysis, which was fulfilled by establishing mathematical models of journal bearing vibrations, identifying effective signal processing methods, and evaluating detection and diagnosing common bearing faults based a laboratory test system.

The main aim of this research was:

Condition monitoring of journal bearings for predictive maintenance management based on high frequency vibration analysis

The main objectives of this thesis and the corresponding key achievements are detailed below.

Objective 1: To review maintenance management strategies and discuss condition monitoring techniques and their applications to journal bearings.

Achievement 1: The theory of maintenance and management strategies, maintenance optimisation and some common approaches of them have been discussed in Section 2.2, Section2.3 and Section 2.4. Chapter two in Section 2.5 to 2.8 described the condition based maintenance, its construction, condition monitoring techniques and its applications. Also, the journal bearing monitoring techniques was reviewed in Section 2.9. These bring forward that reliable and accurate monitoring techniques need to be developed to realise an optimised maintenance.

Objective 2: To review and evaluate potential vibration signal processing techniques and their parameters of detecting and diagnosing journal bearing faults.

Achievement 2: The concept of signal processing was discussed in Chapter 3. And different signal types were presented in Section 3.2. Chapter three in Section 3.4 to Section 3.8 presented the vibration response of journal bearing in time domain, frequency domain, time-frequency domain and frequency-frequency domain. Also, it has focused to show the idea of modulation signals and MSB technique which used to decompose noise.

Objective 3: To understand the fundamentals of journal bearing components, operating characteristics and their failure modes.

Achievement 3: The types and functions of journal bearings were discussed in Section 4.2. Vital fundamental of a self-aligning spherical journal bearing was which the case of this research expansively described in Section 4.3 to Section 4.7 which has included more details about its components, material and lubricant selections and lubricant regimes. Different failure modes of the journal bearing were discussed in Section 4.8.

Objective 4: To establish a mathematical model of journal bearing vibrations to take into account fluid churns and asperity collusions and any likely excitations that correlates with bearing health conditions.

Achievement 4: The operational principle of a journal bearing was examined in Section 5.2, which help to propose new vibration excitations due to asperity collisions and churns. These identified excitations interact nonlinearly with conventional fluid and unbalance excitations, and structural dynamics, resulting in complicated vibration responses that exhibit nonlinear modulations. Also, Chapter Five in Section 5.3 presented different sources of vibration in a journal bearing. A vibration model with a six degree-of-freedom was established in MATLAB based on operating conditions, in Section 5.4. Natural frequencies and modal shapes have been examined considering fluid and asperity forces by using a state-space approach in Sections 5.5, 5.6 and 5.7.

Objective 5: To design and build a comprehensive tests rig to test journal bearings with different faults under different lubrication regimes.

Achievement 5: The test rig has been installed and developed to examine the self-aligning spherical journal bearing vibration responses in Chapter Six. The details about the test rig components, sensors, instrumentations and accessory devises are also included in this Chapter in Section 6.2 and Section 6.3.

Objective 6: To investigate journal bearing vibrations under different operating conditions to discover key characteristics using both conventional methods and the state of the techniques such as clustering and MSB analyses

Achievement 6: Monitoring abnormal operating conditions have been successfully achieved by two approaches. Firstly clustering signatures of vibration signal spectra are found to be successfully differentiate between boundary and hydrodynamic lubricant regimes in Section 7.3. Moreover, modulation signal bispectrum analysis identified the

critical operating parameters which cause more vibrations in Section 7.4, Especially, MSB is found to provide much more detailed information of bearing operating process.

Objective 7: To detect and diagnose lubricant starvation of a journal bearing under different operating conditions with proposed techniques.

Achievement 7: The time domain and the frequency domain of vibration signals of different oil levels in the journal bearing presented initial results of oil starvation detection, in Section 8.3. However, it confirmed that MSB analysis of vibration responses are more effective to monitor the oil starvation of journal bearing in Section 8.5.

Objective 8: To detect and diagnose worn bearings under different operating conditions using proposed methods.

Achievement 8: A worn bearing has been effectively simulated and diagnosed. RMS values of raw data were a good indication; they show that a worn bearing releases less vibration in Section 9.3.2. MSB technique can decompose the vibration signal into two main sources of vibrations shaft fluctuation and asperity collisions in Section 9.3.4., which results in an even better separation of the worn bearing

10.2 Conclusion

In conclusion, concepts of general maintenance techniques and condition based maintenance are described in Chapter two. In addition to that vibration based condition monitoring which is described in Chapter three is applied to investigate the vibration signals obtained from different operating parameters, bearing starvation and worn journal bearing. Based on theoretical study and experimental evaluation, it has found that vibration of a journal bearing is influenced by a number of factors including radial load, shaft speed and lubricant characteristics.

High frequency vibration responses are mainly from two frictional effects in a journal bearing. The surface asperity collision in the boundary lubrication explain the main vibration responses, whereas fluid shearing induced asperity deformation and recovery in the hydrodynamic lubrication regime can also be an effective vibration generation mechanism. Analytic and experimental studies show that these vibration responses in the

high frequency range are complicated and difficult to separate according to the oil types and lubrication regimes.

A mathematical model is used to successfully calculate natural frequencies of the journal bearing. This model considers both conventional fluid forces and asperity contact forces. The natural frequencies of the system are around 6 kHz and 13 kHz. Furthermore, the natural frequencies gradually increase while the radial load increase and oil viscosity decrease.

Abnormal operating conditions are one of the problems that cause a journal bearing to fail. Based on the analytic studies and experimental verifications, it has been demonstrated that popular vibration monitoring can detect abnormal oils and operations in wide operating conditions.

Through a hierarchical clustering approach, the similarity and difference between the spectra of test samples can be recognised step by step in a relatively narrow frequency band. Finally, it obtains a classification result in the frequency band around 10kHz that allows different oils and operating conditions to be separated in consistent with lubrication regimes.

This successful diagnosis is achieved based on modulation signal bispectrum analysis which allows the nonlinear vibration responses of journal bearings to be characterised into two distinctive patterns to correspond to the instable lubrication and the asperity interactions respectively. Furthermore, the MSB magnitudes in different frequency bands can be based to differentiate the asperity interactions between asperity collisions and the asperity churns. A higher magnitude in the lower frequency band can indicate the excessive asperity contacts due to lowering viscosities. Meanwhile a higher magnitude in the higher frequency band indicates the extreme fluid frictions.

Based on the vibration mechanisms established and experimental studies, the vibration signals collected under different operating conditions and lubricant levels can be separated adequately for the purpose of condition monitoring. Journal bearing vibration responses are induced by the combination of the conventional hydrodynamic effect and the asperity churns and collisions between the lubricated rough surfaces the combination of which can be characterised by modulation bispectrum analysis. The hydrodynamic effect can interfere with the asperity effect in the low frequency range (3.5kHz to 5.5kHz), resulting in good

detection of the instability but an inconsistent diagnosis of oil levels. Meanwhile, the structural resonances in the high frequency range (5.5kHz to 11kHz) can better reflect the excitations and result in a more agreeable separation of different levels under a wide variety of operating conditions.

A journal bearing is designed to use lubricant oil film to reduce asperity collision by keeping two surface separation. Lubrication can reduce friction but it can avoid it completely. Thus if the wear happened the geometry of bearing will change and wear will change the bearing's clearance. RMS values of raw data are good indication; they present that a worn bearing releases less vibration. This result presents only vibration power caused by solid friction, even though the sources of vibration in a journal bearing are mechanical and asperity collisions. MSB technique can present two main sources of vibrations in journal bearing. Low frequency band combined with harmonics of shaft frequency which increase with a worn bearing and cause more fluctuating of the shaft. On the other hand, a high frequency band has less combination with shaft frequency and this band might relate to asperity contact. Vibration decreases with a worn bearing because the space between surfaces is greater.

A worn bearing means that the bearing gradually increases its radial clearance and its geometry is changed. Due to that, thick oil film will be formed which avoids asperity contact but increases the shafts fluctuation. MSB technique successfully presents two main sources of vibrations in journal bearing: fluctuating shaft and asperity collisions. Mean values of low frequency band of MSB shows the instability of the shaft inside the worn bearing. In contrast, mean values of a high frequency band of MSB present asperity collision vibration which has less effect at worn bearing. More clearance leads to less metal to metal contact but this is not always it is good for a journal bearing.

10.3 Research Contribution to Knowledge

The researches carried out have brought a number of new understandings on the subject of vibration condition monitoring for accurate detection and diagnosis of conditions and faults in journal bearings. For convenience, key contributions to knowledge in this thesis are outlined below:

Contribution 1: An improved mathematical model has been provided to give in-depth and novel understanding the bearing vibration responses. The approach in Chapter 5 is that the excitations of asperity collisions and churns were introduced into the vibration analysis of

the journal bearing. Furthermore, this modelling allows the modulation phenomena with conventional excitations and structural resonances which are more correlated with bearing conditions.

Contribution 2: Through a clustering approach, it successfully differentiates the similarity and differences between high frequency spectrum signatures of abnormal operating conditions and successfully differentiates between boundary and hydrodynamic lubricant regimes (Chapter 7, Section 7.3).

Contribution 3: Based on high frequency vibration responses, modulation signal bispectrum analysis, MSB entropy and MSB magnitude, abnormal operating conditions of journal bearings can have been online and offline monitored (Chapter 7, Section 7.4).

Contribution 4: Common faults of journal bearings such as oil starvation and worn bearings had been firstly detected and diagnosed online and offline by utilising high frequency vibration responses and modulation signal bispectrum analysis under wide operating conditions (Chapters 8 and Chapter 9), respectively.

10.4 Novel Feature Summary

This section presents a number of significant progressions in developing on-line vibration based condition monitoring for a journal bearing; these are novel and not implemented by previous researchers. The following are the highlighted novel points.

First Novelty: In this research, the approach of utilising high frequencies of journal bearing vibration signal for monitoring is novel. Most of previous researchers focused only on low frequency of vibration. The evaluation and confirmation of the feasibility of high frequency vibrations for diagnostics improves the diagnostic performance significantly (Chapters 7, 8 and 9).

Second Novelty: In the mathematical model (Chapter 5), the excitations of asperity collisions and churns are introduced into the vibration analysis of journal bearing for the first time. This novel modelling allows the modulation phenomena with conventional excitations and structural resonances which are more correlated with bearing conditions to be explained.

Third Novelty: In Chapter 7, abnormal operating conditions can be on-line monitored by using the state of the art MSB technique and cluster analysis, which are reported firstly in by this research.

Fourth Novelty: Common faults including oil starvation and worn bearings have been firstly detected and diagnosed online using MSB vibration technique under wide operating conditions and severities., comparatively, they are conventionally diagnosed offline by expensive oil analysis techniques (Chapter 8, Chapter 9), respectively.

10.5 Future Work Recommendations for Journal Bearing Monitoring

In the following research aspects might be taken into consideration in the future.

- **Recommendation 1:** To investigate the characteristic of bearing vibration response by adding sold contaminants into the lubricant. These contaminates are a realistic presentation of two and three body abrasive wear particles.

- **Recommendation 2:** To investigate the journal bearing surface when scratched. Hardness material of three body abrasive wear might cause markers on the surface of bearing, shaft or both.

- **Recommendation 3:** To diagnose the vibration response of a wiped journal bearing. At starting up, heavy shaft wipe some bearing surface because of small separation.

- **Recommendation 4:** To determine remaining life time by monitoring the vibration signals during long time running.

- **Recommendation 5:** To develop a measurement and analysis system for journal bearing condition monitoring. To investigate the orbit of the shaft spin inside the bearing by using either a wireless sensor fitted on shaft or displacement sensor fitted on bearing.

- **Recommendation 6:** To investigate the characteristic of bearing vibration response by analysing current and voltage. Friction and surface faults might affect either motor current or voltage.

REFERENCES

[1]   Gulati, R., Maintenance and reliability best practices. 2012: Industrial Press.

[2]   Crespo-Marquez, A. and B. Iung, A review of e-maintenance capabilities and challenges. Journal of systemics, cybernetics and informatics, 2008. 1(6): p. 62-66.

[3]   Sethiya, S., Condition Based Maintenance (CBM). Secy. to CME/WCR/JBP, 2006.

[4]   Saxena, A., Knowledge-Based Architecture for Integrated Condition Based Maintenance of Engineering Systems. 2007, Citeseer.

[5]   IAEA, Implementation Strategies and Tools for Condition Based Maintenance at Nuclear Power Plants. 2007.

[6]   Bengtsson, M., On condition based maintenance and its implementation in industrial settings. 2007, Mälardalen University.

[7]   Laakso, K., T. Rosqvist, and J.L. Paulsen, The use of condition monitoring information for maintenance planning and decision-making. 2002: Technical Report. NKS-80.

[8]   Sullivan, G., et al., Operations & Maintenance Best Practices. 2002.

[9]   Al-Najjar, B., On establishing cost-effective condition-based maintenance: Exemplified for vibration-based maintenance in case companies. Journal of Quality in Maintenance Engineering, 2012. 18(4): p. 401-416.

[10]   Swanson, L., Linking maintenance strategies to performance. International Journal of Production Economics, 2001. 70(3): p. 237-244.

[11]   on a fuzzy analytic hierarchy process. International Journal of Production Economics, 2007. 107(1): p. 151-163.

[12]   Bengtsson, M., Condition Based Maintenance Systems: An Investigation of Technical Constituents and Organizational Aspects. 2004: Citeseer.

[13]   Barnes, J., Bayesian Methods for Online Condition Monitoring, in Engineering in the Faculty of Science and Engineering. 2006, University of Manchester Manchester.

[14]   Clemens, P., Fault tree analysis. JE Jacobs Severdurup, 2002.

[15]   Bowles, J.B. and C.E. Peláez, Fuzzy logic prioritization of failures in a system failure mode, effects and criticality analysis. Reliability Engineering & System Safety, 1995. 50(2): p. 203-213.

[16]   Lawson, D., Failure mode, effect and criticality analysis, in Electronic Systems Effectiveness and Life Cycle Costing. 1983, Springer. p. 55-74.

[17]   Deshpande, V. and J. Modak, Application of RCM to a medium scale industry. Reliability Engineering & System Safety, 2002. 77(1): p. 31-43.

[18]   Kennedy, I. Holistic Condition Monitoring. in 1st Seminar on Advances in Maintenance Engineering. 1998. University of Manchester.

[19]   Roberts, J. Total Productive Maintenance (TPM) http://et.nmsu.edu/~etti/fall97/manufacturing/tpm2.html. 1997.

[20]   Butcher, S.W., Assessment of condition-based maintenance in the Department of Defense. Logistics Management Institute, USA, McLean, VA, 2000: p. 1-70.

[21]   OSIsoft, Condition-based Maintenance (CBM) Across the Enterprise. 2007: San Leandro, CA.

[22]   Kazama, T. and Y. Narita, Mixed and Fluid Film Lubrication Characteristics of Worn Journal Bearings. Advances in Tribology, 2012. 2012.

[23] Prajapati, A., J. Bechtel, and S. Ganesan, Condition based maintenance: a survey. Journal of Quality in Maintenance Engineering, 2012. 18(4): p. 384-400.

[24] Jardine, A.K.S., D. Lin, and D. Banjevic, A review on machinery diagnostics and prognostics implementing condition-based maintenance. Mechanical Systems and Signal Processing, 2006. 20(7): p. 1483-1510.

[25] Moosavian, A., H. Ahmadi, and A. Tabatabaeefar, Condition monitoring of engine journal-bearing using power spectral density and support vector machine. Elixir Mech. Engg, 2012. 43: p. 6631-6635.

[26] Veldman, J., W. Klingenberg, and H. Wortmann, Managing condition-based maintenance technology: a multiple case study in the process industry. Journal of Quality in Maintenance Engineering, 2011. 17(1): p. 40-62.

[27] Joshi, P., et al., Application of the condition based maintenance checking system for aircrafts. Journal of Intelligent Manufacturing, 2012. 23(2): p. 277-288.

[28] Raharjo, P., An Investigation of Surface Vibration, Airbourne Sound and Acoustic Emission Characteristics of a Journal Bearing for Early Fault Detection and Diagnosis. University of Huddersfield, May 2013.

[29] Mobley, R.K., Maintenance fundamentals. 2011: Butterworth-Heinemann.

[30] Mobley, R.K., An introduction to predictive maintenance. 2002: Butterworth-Heinemann.

[31] Mayuram, K.G.M.M., Lubrication of Journal Bearings Theory and Practice. Indian Institute of Technology Madras.

[32] Geng, T., et al. Ultrasonic monitoring of lubricating conditions of hydrodynamic bearing. in DAMAS; IOP Publishing. 11-13 July 2011, Oxford, UK

[33] Adams, M.L., Rotating machinery vibration: from analysis to troubleshooting. 2009: CRC Press.

[34] Jayaswal, P., A. Wadhwani, and K. Mulchandani, Machine fault signature analysis. International Journal of Rotating Machinery, 2008. 2008.

[35] Scheffer, C. and P. Girdhar, Practical machinery vibration analysis and predictive maintenance. 2004: Elsevier.

[36] Gu, F., et al., Fault severity diagnosis of rolling element bearings based on kurtogram and envelope analysis. 2014.

[37] Gu, F., et al., A Novel Method for the Fault Diagnosis of a Planetary Gearbox based on Residual Sidebands from Modulation Signal Bispectrum Analysis. 2014.

[38] Muszynska, A., Vibrational diagnostics of rotating machinery malfunctions. International Journal of Rotating Machinery, 1995. 1(3-4): p. 237-266.

[39] Chandra, N.H. and A. Sekhar, Fault detection in rotor bearing systems using time frequency techniques. Mechanical Systems and Signal Processing, 2016. 72: p. 105-133.

[40] Werner, U., Vibrations caused by noncircular shaft journals—a mathematical model for rotordynamic analysis of electrical motors with sleeve bearings. Journal of Mechanical Science and Technology, 2013. 27(2): p. 337-351.

[41] Damiens, B., et al., Starved lubrication of elliptical EHD contacts. Journal of tribology, 2004. 126(1): p. 105-111.

[42] Nelson, F., Rotor dynamics without equations. International Journal of COMADEM, 2007. 10(3): p. 2.

[43] Kim, M., et al., Experimental identification of abnormal noise and vibration in a high-speed polygon mirror scanner motor due to mechanical contact of plain journal bearing. Microsystem technologies, 2010. 16(1-2): p. 3-8.

[44] Raharjo, P., et al., Vibro-Acoustic Characteristic of A Self Aligning Spherical Journal Bearing due to Eccentric Bore Fault. 2012.

[45]   Raharjo, P., et al., Vibro-Acoustic Characteristic of A Self Aligning Spherical Journal Bearing due to Eccentric Bore Fault. CM and MFPT, 12-14 June, 2012, London, UK., 2012.

[46]   Raharjo, P., et al., Early Failure Detection and Diagnostics of Self-Aligning Journal Bearing through Vibro-acoustic Analysis. CM and MFPT, 22 – 24 June, 2010, Ettington Chase, Stratford-upon-Avon, England, 2010.

[47]   Carden, E.P. and P. Fanning, Vibration based condition monitoring: a review. Structural health monitoring, 2004. 3(4): p. 355-377.

[48]   Hassin, O., Different Signal Processing Techniques for Predicting the Condition of Journal Bearings. 2013.

[49]   Mandal, M. and A. Asif, Continuous and discrete time signals and systems: CD. 2007.

[50]   Yüksekkaya, M.E., Characteristics of Mechanical Noise during Motion Control Applications. 2010: INTECH Open Access Publisher.

[51]   Osama Hassin, et al., Journal bearing lubrication monitoring based on spectrum cluster analysis of vibration signals in CMADEM 2015. 2015.

[52]   Shin, K. and J. Hammond, Fundamentals of signal processing for sound and vibration engineers. 2008: John Wiley & Sons.

[53]   Mobley, R.K., An Introduction to Predictive Maintenance.

[54]   Baydar, N., et al., Detection of incipient tooth defect in helical gears using multivariate statistics. Mechanical Systems and Signal Processing, 2001. 15(2): p. 303-321.

[55]   Wang, W., et al., The application of some non-linear methods in rotating machinery fault diagnosis. Mechanical Systems and Signal Processing, 2001. 15(4): p. 697-705.

[56]   Lebold, M., et al. Review of vibration analysis methods for gearbox diagnostics and prognostics. in Proceedings of the 54th meeting of the society for machinery failure prevention technology, Virginia Beach, VA. 2000.

[57]   Katiyar, S. and P. Arun, A review over the applicability of image entropy in analyses of remote sensing datasets. arXiv preprint arXiv:1405.6133, 2014.

[58]   Kahirdeh, A., A Diagnosis Feature Space for Condition Monitoring and Fault Diagnosis of Ball Bearings. 2014.

[59]   Brian S. Everitt, S.L., Morven Leese and Daniel Stahl, Cluster Analysis. 5th ed. 2011, United Kingdom: John Wiley & Sons, Ltd.

[60]   Artés, M., Application of cluster analysis to machine fault diagnosis using vibration signal processing. Machine Design Fundamentals, 2007: p. 377-380.

[61]   Bebis, Short Time Fourier Transform.

[62]   Gu, F., et al., Electrical motor current signal analysis using a modified bispectrum for fault diagnosis of downstream mechanical equipment. Mechanical Systems and Signal Processing, 2011. 25(1): p. 360-372.

[63]   Gu, F., et al., A new method of accurate broken rotor bar diagnosis based on modulation signal bispectrum analysis of motor current signals. Mechanical Systems and Signal Processing, 2015. 50: p. 400-413.

[64]   Gu, F., et al., A Novel Method for the Fault Diagnosis of a Planetary Gearbox based on Residual Sidebands from Modulation Signal Bispectrum Analysis. COMADEM 2014 16th-18th Sep. Brisbane, Australia., 2014.

[65]   Nazar, N., Job Training Mechanical Technician Course, module 3, Bearings. 2011.

[66]   Industries, T., Gear Box Bronze Bush.

[67]   Bowman, Wrapped Standard Bearings.

[68]   ARVIS, FLS RANGE.

[69]   Arvis. Arvis Bearing Catalogue, Criptic Arvis Ltd, Croft Grange Works, 16 BridgePark Road, Thurmaston, LE4 8BL, Leicester, UK.; Available from: http://www.arvis.co.uk/products.php?product=26.

[70]   Johnson, M., Lubricant selection: Bearings, gear drives and hydraulics. Tribology & lubrication technology, 2008. 64(4): p. 18-28.

[71]   Neale, M.J., Lubrication and reliability handbook. 2001: Newnes.

[72]   Frene, J., et al., Hydrodynamic lubrication: bearings and thrust bearings. Vol. 33. 1997: Elsevier.

[73]   Shigley, J.E. and C.R. Mischke, Mechanical engineering design. 2001, Boston, Mass; London: McGraw Hill.

[74]   Tomanik, E. and A. Ferrarese. Low friction ring pack for gasoline engines. in ASME 2006 Internal Combustion Engine Division Fall Technical Conference. 2006. American Society of Mechanical Engineers.

[75]   Kopeliovich, D., Engine Bearings and how they work. Cedar Grove, NJ 07009, USA.

[76]   Lu, X. and M.M. Khonsari, On the lift-off speed in journal bearings. Tribology Letters, 2005. 20(3-4): p. 299-305.

[77]   Albers, A., et al., Monitoring lubrication regimes in sliding bearings-using acoustic emission analysis. Practicing Oil Analysis, 2006. 5.

[78]   Khonsari, M.M. and E.R. Booser, Applied tribology: bearing design and lubrication. 2001, Chichester; New York: John Wiley & Sons.

[79]   Mayuram, K.G.M.M., SLIDING CONTACT BEARINGS. Indian Institute of Technology Madras

[80]   Anderson, D.W. Basics of Lubrication. 2008.

[81]   Towsyfyan, H., et al., Characterization of Acoustic Emissions from Mechanical Seals for Fault Detection. NDT 11 Sep 2014, Manchester, UK.

[82]   Cracaoanu, I., Effect of macroscopic wear on friction in lubricated concentrated contacts. 2010: University of Twente, Thesis.

[83]   Scott, R. Journal Bearings and Their Lubrication.

[84]   Kiral, Z. and H. Karagülle, Simulation and analysis of vibration signals generated by rolling element bearing with defects. Tribology International, 2003. 36(9): p. 667-678.

[85]   Ray D. Kelm, P.E., Journal Bearing Analysis. Danbury, TX.

[86]   Kiral, Z., SIMULATION AND ANALYSIS OF VIBRATION SIGNALS GENERATED BY ROLLING ELEMENT BEARINGS WITH DEFECTS in the Graduate School of Natural and Applied Sciences july 2002, Dokuz Eylul University Izmir.

[87]   Muszynska, A., Free, forced, and self-excited vibration. December 1997.

[88]   Stachowiak, G. and A.W. Batchelor, Engineering tribology. 2013: Butterworth-Heinemann.

[89]   Harnoy, A., Bearing design in machinery: engineering tribology and lubrication. 2002: CRC press.

[90]   Andres, L.S., Hydrodynamic fluid film bearings and their effect on the stability of rotating machinery. 2006, DTIC Document.

[91]   Rho, B.-H., D.-G. Kim, and K.-W. Kim, Noise analysis of oil-lubricated journal bearings. Proceedings of the Institution of Mechanical Engineers, Part C: Journal of Mechanical Engineering Science, 2003. 217(3): p. 365-371.

[92] Tiwari, R., Analysis And Identification In Rotor-Bearing Systems. 2010, Department of Mechanical Engineering Indian Institute of Technology Guwahati 781039.

[93] Javorova, J., B. Sovilj, and I. Sovilj-Nikic, On the derivation of dynamic force coefficients in fluid film bearings. 2009, Monograph of FTS "Machine design", Novi Sad.

[94] Sleeve Bearings - Oil Whirl - VibrationSchool.com. 8 Nov 2015

[95] Kamesh, P., Oil-whirl instability in an automotive turbocharger. 2011, University of Southampton.

[96] Freeman, P., Lubrication and Friction. 1962: Published by Sir Isaac Pitman & Sons.

[97] Singhal, S., A Simplified Thermohydrodynamic Stability Analysis of the Plain Cylindrical Hydrodynamic Journal Bearings. 2004, Louisiana State University.

[98] Li, C., et al., Multi-scale autocorrelation via morphological wavelet slices for rolling element bearing fault diagnosis. Mechanical Systems and Signal Processing, 2012. 31: p. 428-446.

[99] Fan, Y., F. Gu, and A. Ball, Modelling acoustic emissions generated by sliding friction. Wear, 2010. 268(5): p. 811-815.

[100] Zhao, B., et al., A modified normal contact stiffness model considering effect of surface topography. Proceedings of the Institution of Mechanical Engineers, Part J: Journal of Engineering Tribology, 2014: p. 1350650114558099.

[101] Todd, J., Deflection of Beams, in Structural Theory and Analysis. 1981, Springer. p. 142-160.

[102] De Castro, H.F., K.L. Cavalca, and R. Nordmann, Whirl and whip instabilities in rotor-bearing system considering a nonlinear force model. Journal of Sound and Vibration, 2008. 317(1): p. 273-293.

[103] Wang, J. and M. Khonsari, Effects of oil inlet pressure and inlet position of axially grooved infinitely long journal bearings. Part II: Nonlinear instability analysis. Tribology International, 2008. 41(2): p. 132-140.

[104] Brook. AC electric motors, UK. 2015; Available from: http://www.brookcrompton.com/pages/products.html.

[105] Enerpac. pressure hydraulic tools. 2016; Available from: http://www.enerpac.com/en/industrial-tools/hydraulic-pumps-and-valves/hydraulic-manual-pumps.

[106] Steerforth. Hydraulic Components, , Ramparts,UK. 2011; Available from: http://www.steerforth.co.uk/product_info.php/hfrt-displacement-hydraulic-cylinders-hydraulic-rams-p-4048.

[107] Swan. Industrial Distribution. Available from: http://www.swanind.co.uk/cgi-bin/trolleyed_public.cgi?action=showprod_HRC130H.

[108] SKF. Roller Bearing Available from: http://www.skf.com/uk/products/bearings-units-housings/roller-bearings/cylindrical-roller-bearings/single-row-cylindrical-roller-bearings/single-row/index.html?designation=N%20308%20ECM.

[109] Hangsrler. HENGSTLER INCREMENTAL ENCODERS. Available from: http://www.theencodercompany.co.uk/assets/uploads/pdf/IE0512.pdf.

[110] RS. Gauge Pressure Sensor, 40bar Max Pressure, 3 → 12 V dc. Available from: http://uk.rs-online.com/web/p/pressure-sensors/7974977/.

[111] Micro-Epsilon. optoNCDT1402 laser sensor Available from: http://www.micro-epsilon.co.uk/download/manuals/man--optoNCDT-1402--en.pdf.

[112] Peng, C. and L. Bo, Vibration Signal Analysis of Journal Bearing Supported Rotor System by Cyclostationarity. Shock and Vibration, 2014. 2014.

[113] Tanaka, M., Journal bearing performance under starved lubrication. Tribology international, 2000. 33(3): p. 259-264.

[114] Yan, R. and R.X. Gao, An efficient approach to machine health diagnosis based on harmonic wavelet packet transform. Robotics and Computer-Integrated Manufacturing, 2005. 21(4): p. 291-301.

[115] Chasalevris, A. and F. Dohnal, A Journal Bearing With Variable Geometry for the Reduction of the Maximum Amplitude During Passage Through Resonance. Journal of Vibration and Acoustics, 2012. 134(6): p. 061005.

[116] Looseness - Bearing - VibrationSchool.com. 17 Nov 2015

APPENDIXS

The following section contains the appendixes of the additional results.

I.   APPENDIX A

Vibration sources of a journal bearing [116]

Bearing looseness
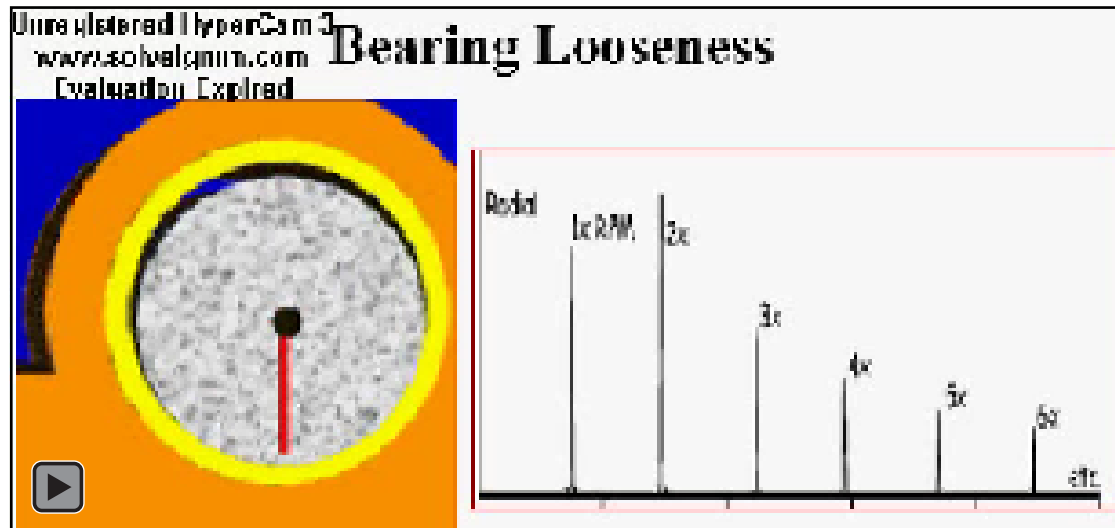
Angular `misalignment
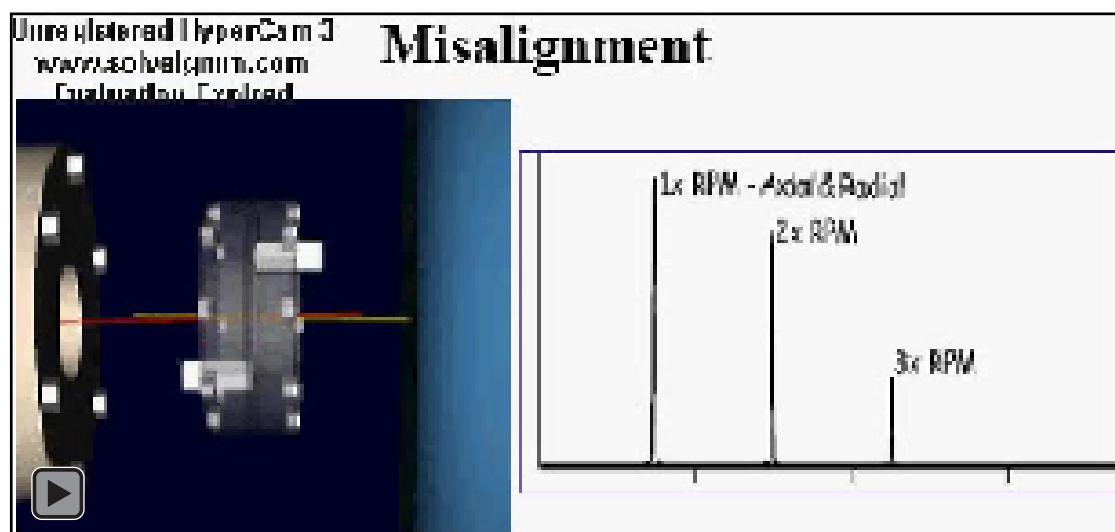
Rotor unbalance
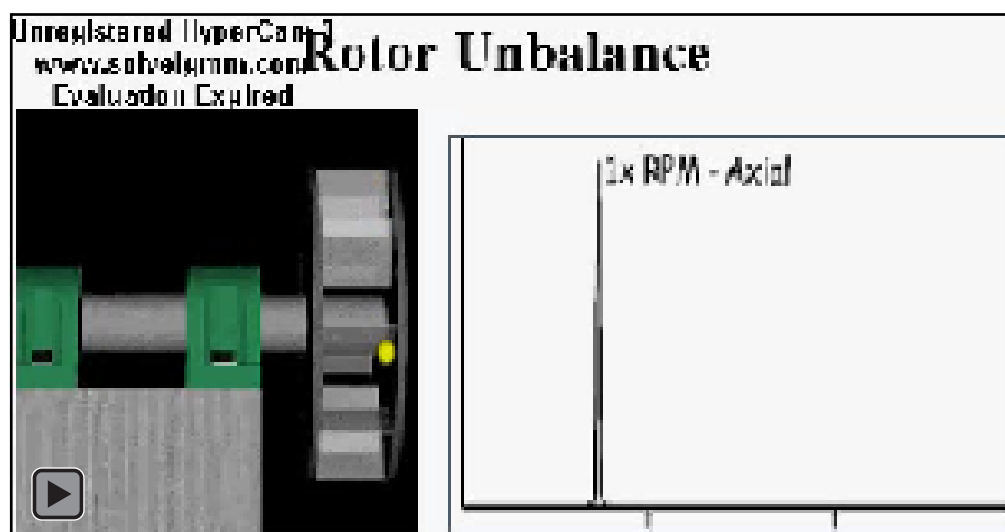
Oil whirl
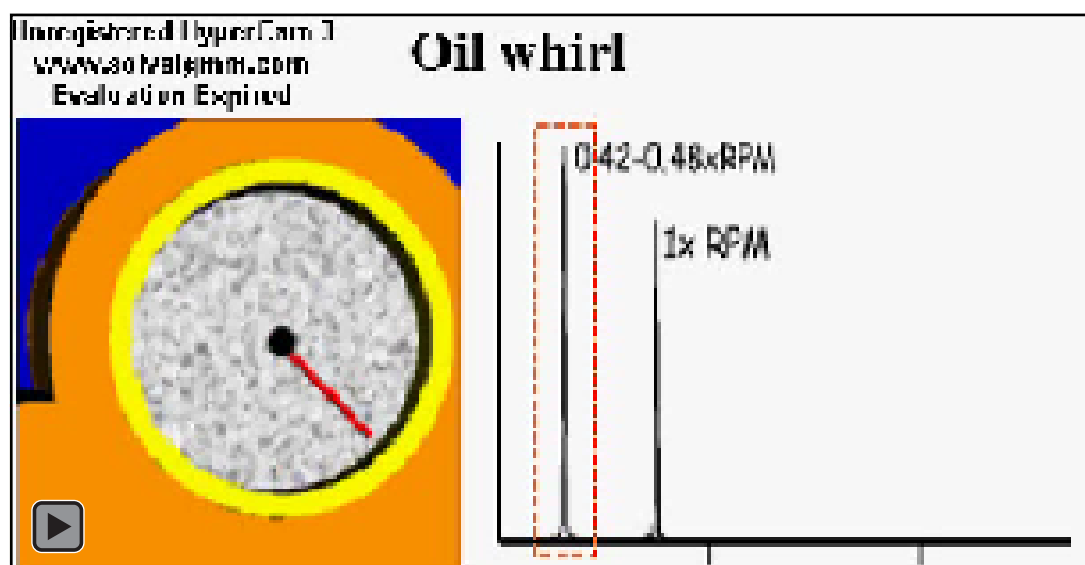
Asperity churns
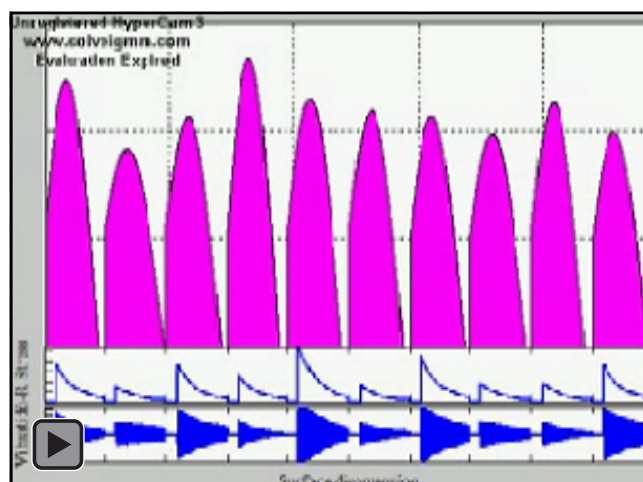
Asperity collisions
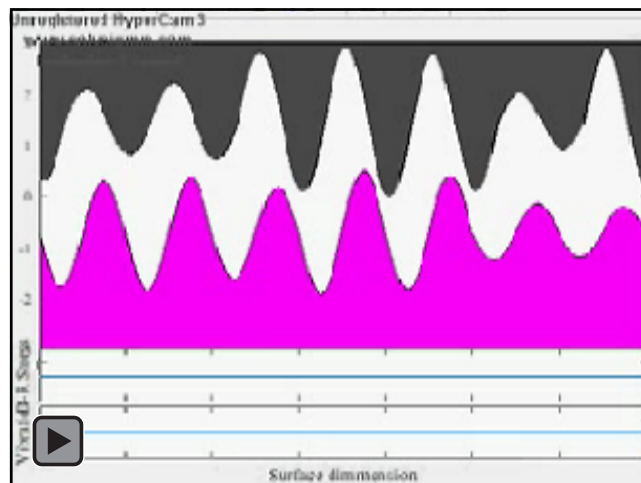
Natural frequency modes and shapes
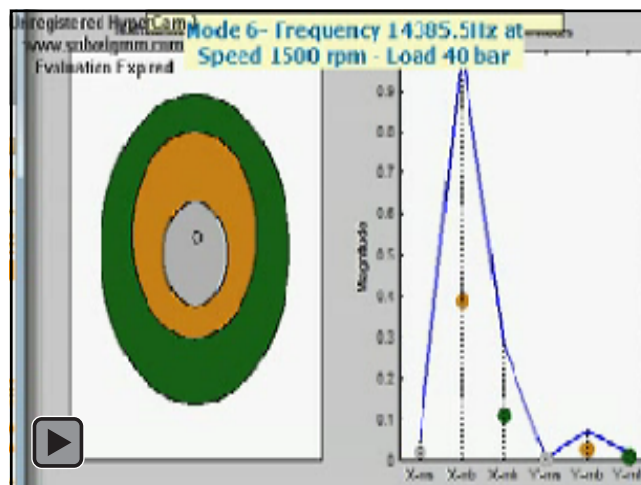
Different operating conditions
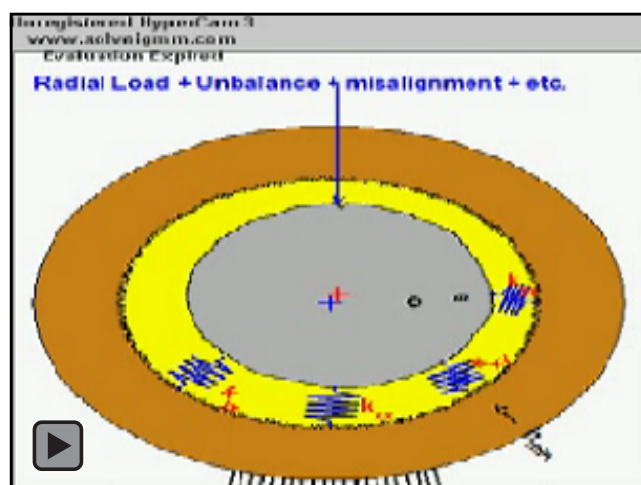
II. APPENDIX B

The journal bearing test rig
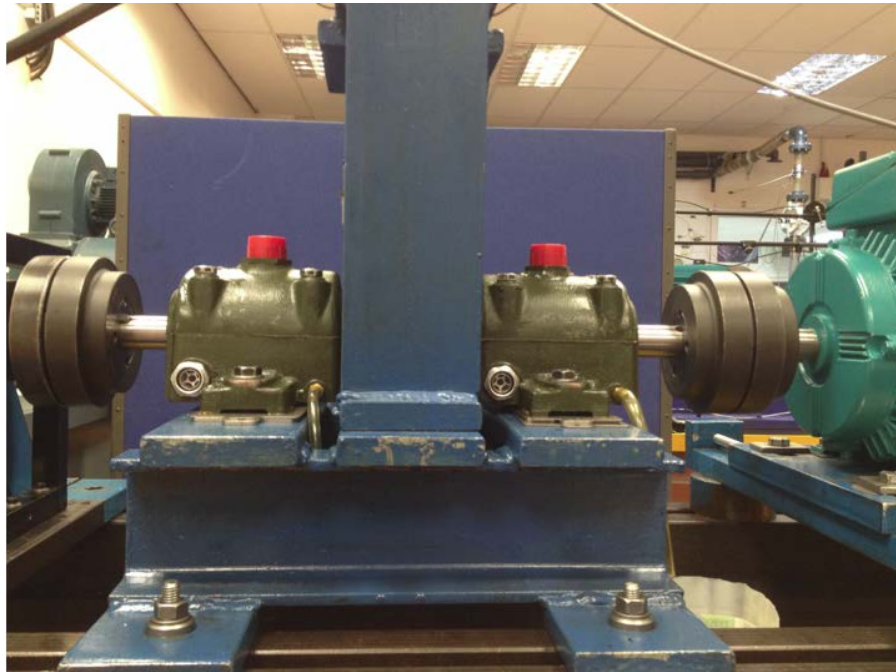
Accelerometers and laser sensors

Self-aligning spherical journal bearing dimension

FAN BEARINGS SAROE RANGE DIMENSIONS   **ARVIS**

DIMENSIONS
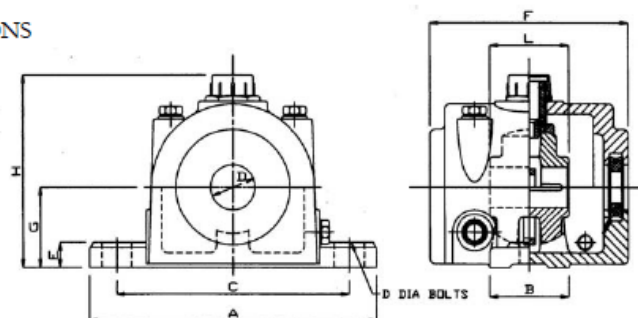
METRIC

D mm	Code	Mark	A	B	C	D	E	F	G	H	L
25	SA25M	S4165	184	51	149	M10	16	127	50.8	130	50.8
30	SA30M	S4169	222	64	178	M12	25	152	57.2	143	63.5
35	SA35M	S4169	222	64	178	M12	25	152	57.2	143	76.2
40	SA40M	S4169	222	64	178	M12	25	152	57.2	143	76.2
45	SA45M	S4175	292	89	216	M16	32	184	82.5	183	88.9
50	SA50M	S4175	292	89	216	M16	32	184	82.5	183	101.6
55	SA55M	S4181	330	102	241	M16	38	229	101.6	214	114.3
60	SA60M	S4181	330	102	241	M16	38	229	101.6	214	127
65	SA65M	S4181	330	102	241	M16	38	229	101.6	214	127
70	SA70M	S4187	368	127	286	M20	44	254	120.6	259	146.1
75	SA75M	S4187	368	127	286	M20	44	254	120.6	259	146.1
80	SA80M	S4193	419	140	349	M20	51	292	133.4	283	165.1
90	SA90M	S4193	419	140	349	M20	51	292	133.4	283	177.8
100	SA100M	S4199	445	165	362	M24	51	330	139.7	292	203.2
115	SA115M	S4207	511	216	410	M30	51	400	152.4	318	254
125	SA125M	S4207	511	216	410	M30	51	400	152.4	318	254

IMPERIAL

D inch	Code	Mark	A	B	C	D	E	F	G	H	L
1	SA16E	S4165	7 ¼	2	5 ⅞	M10	⅝	5	2	5 ¼	2
1 ¼	SA20E	S4169	8 ¾	2 ½	7	M12	1	6	2 ¼	5 ⅝	2 ½
1 ½	SA24E	S4169	8 ¾	2 ½	7	M12	1	6	2 ¼	5 ⅝	3
1 ¾	SA28E	S4175	11 ½	3 ½	8 ½	M16	1 ¼	7 ¼	3 ¼	7 ¼	3 ½
2	SA32E	S4175	11 ½	3 ½	8 ½	M16	1 ¼	7 ¼	3 ¼	7 ¼	4
2 ¼	SA36E	S4181	13	4	9 ½	M16	1 ½	9	4	8 ⅝	4 ½
2 ½	SA40E	S4181	13	4	9 ½	M16	1 ½	9	4	8 ⅝	5
2 ¾	SA44E	S4187	14 ½	5	11 ¼	M20	1 ¾	10	4 ¾	10 ¼	5 ½
3	SA48E	S4187	14 ½	5	11 ¼	M20	1 ¾	10	4 ¾	10 ¼	5 ¾
3 ¼	SA52E	S4193	16 ½	5 ½	13 ¼	M20	2	11 ½	5 ¼	11 ⅛	6 ½
3 ½	SA56E	S4193	16 ½	5 ½	13 ¼	M20	2	11 ½	5 ¼	11 ⅛	7
4	SA64E	S4199	7 ½	6 ½	14 ½	M24	2	13	5 ½	11 ½	8
4 ½	SA72E	S4207	20 ⅛	8 ½	16 ⅛	M30	2	15 ¾	6	12 ½	10
5	SA80E	S4207	20 ⅛	8 ½	16 ⅛	M30	2	15 ¾	6	12 ½	10

ARVIS

Criptic Arvis Ltd, Bridge Park Rd, Thurmaston, Leicester, LE4 8BL. Tel +44(0) 116 2609700 Fax: +44(0) 116 26401

Self-aligning spherical journal bearing information

FAN BEARINGS SAROE RANGE   **ARVIS**

### SILENT RUNNING- HIGH SPEEDS-SUITABLE FOR FANS

FEATURES.
Self aligning.
DO NOT suddenly fail as a rolling element but wear extremely slowly and replacement can be planned.
EASY Replacement of shells without dismantling the whole unit and its connected drives.
A ring oiling bearing will run trouble free for years with very little maintenance.
A full range of Imperial and metric units available from stock.

SELF ALIGNING   CONSTANT LUBRICATION
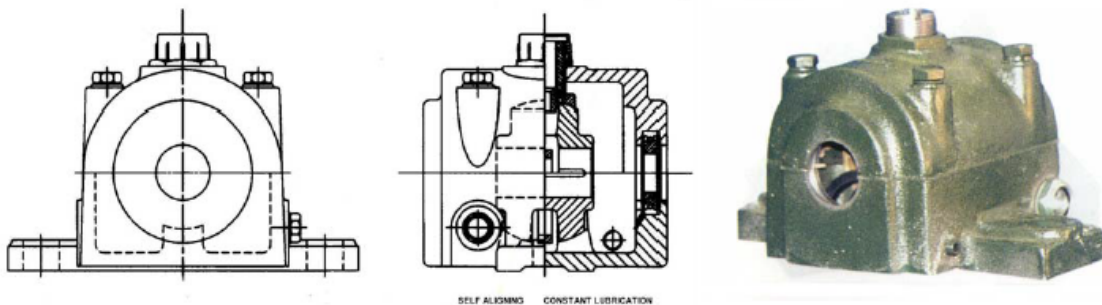
Imperial and metric sizes available from stock

These units have split bearings, housings and seals. A gasket between chair and cap prevents oil leakage at this point. The split seals at each end grip and rotate with the shaft and prevent any escape of oil along the shaft.

Provision is made in the cap to enable the gunmetal bearings to be correctly adjusted in the housing seating

The oil level gauge and drain plug are fitted as standard and can be fitted on the opposite side to the illustration at extra cost.

Special collars can be fitted inside the housings to take up thrust. These are not split and have to be arranged on the shaft before fitting the bearings. The chamfer on these collars must be away from the bearing face.

Suitable for high speeds · Designed for fans and similar applications. Quiet in operation · Compensate for misalignment occurring after erection.

SHAFT LIMITS - The bearings are accurately bored to BS4500: Section 1.1:1990 ISO 2861:1988, E8 limits. For general use standard bright mild steel shafts or turned shafting to h8 limits can be used.

For more selective uses where high loads and speeds are required the shaft journals should have a ground or lapped finish and the clearance between the journal and bearing diameter should be 0.0015in for each inch of diameter (0.0381mm for each mm of diameter).

LUBRICATION

For ambient temperatures O°C to 30°C use Shell Tellus Oil 37, Shell Rotella "S" Oil 10W or an equivalent. For ambient temperatures 30°C to 60°C use Shell Tellus Oil 33. Shell Rotella 'S' Oil 20/20W or an equivalent.

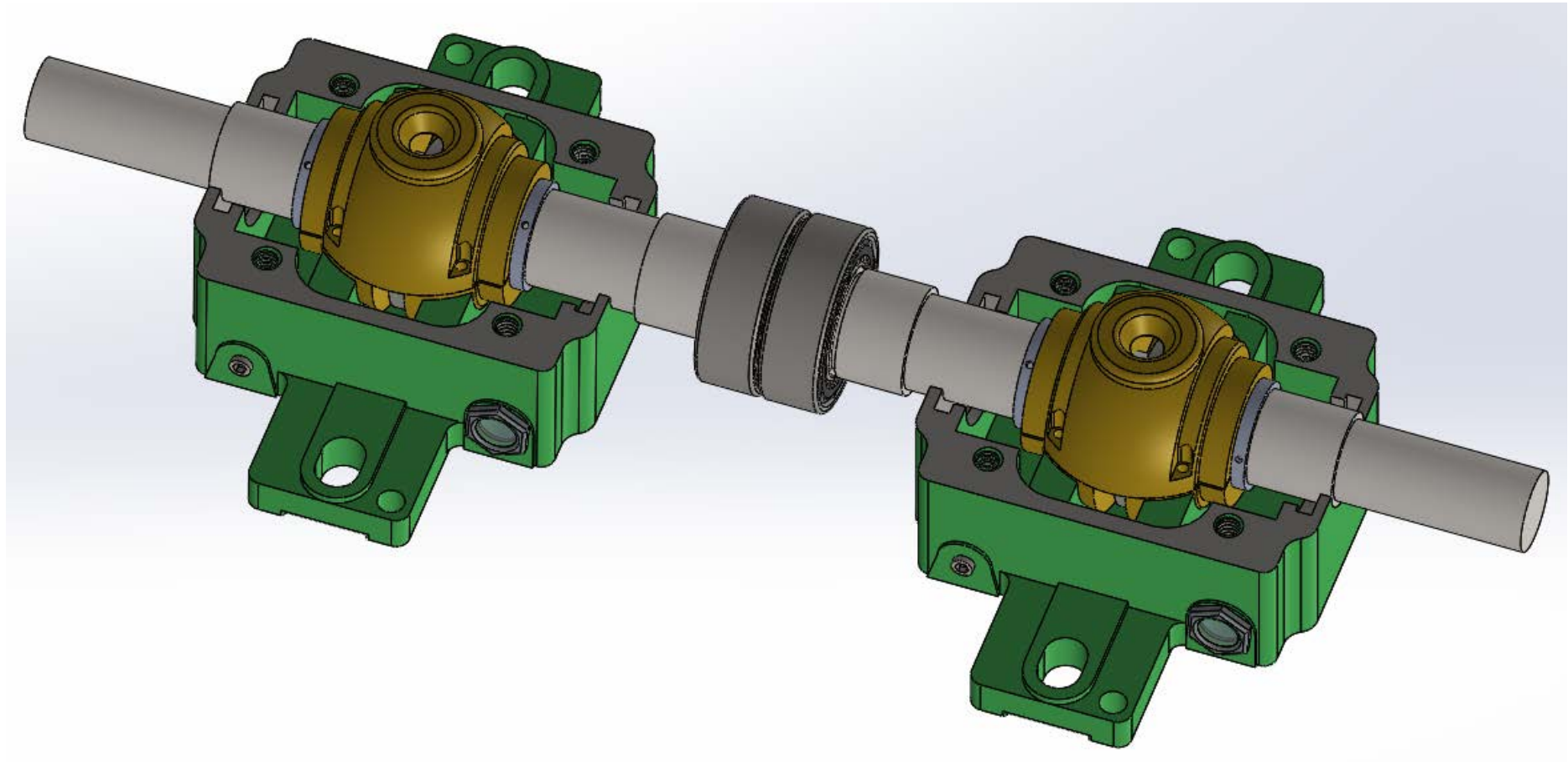Self-aligning spherical journal bearing sold works sections

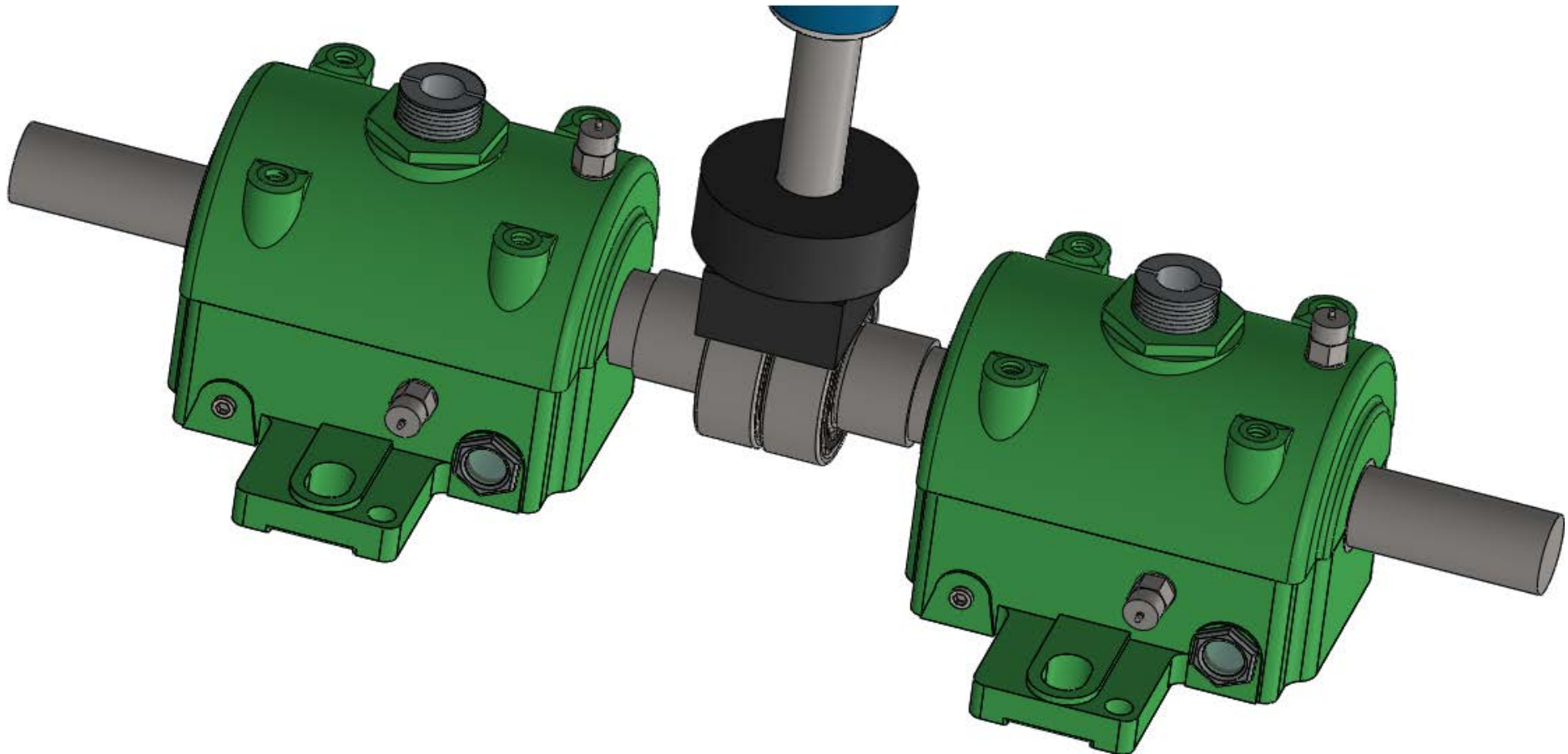Self-aligning spherical journal bearing sold works sections
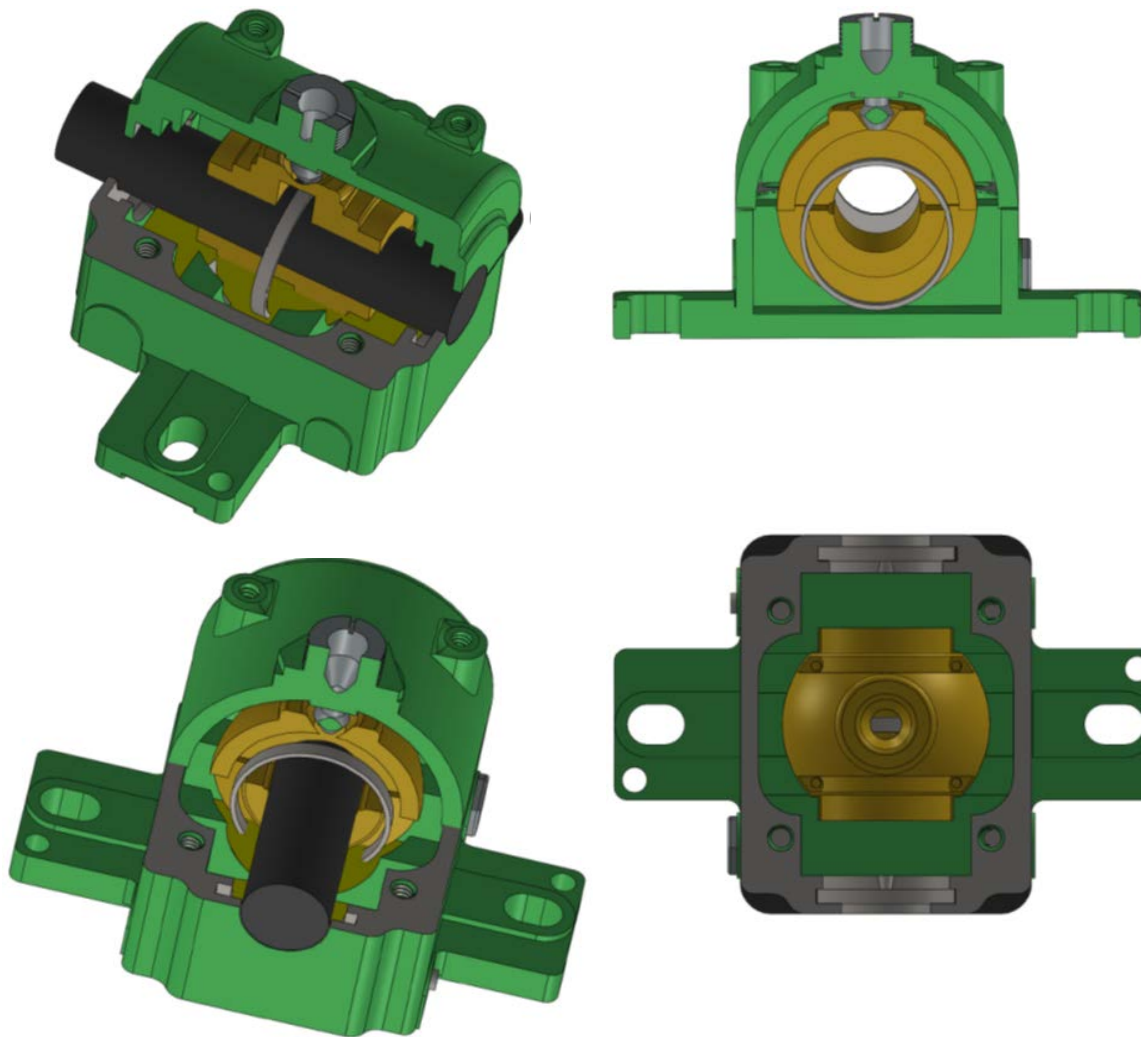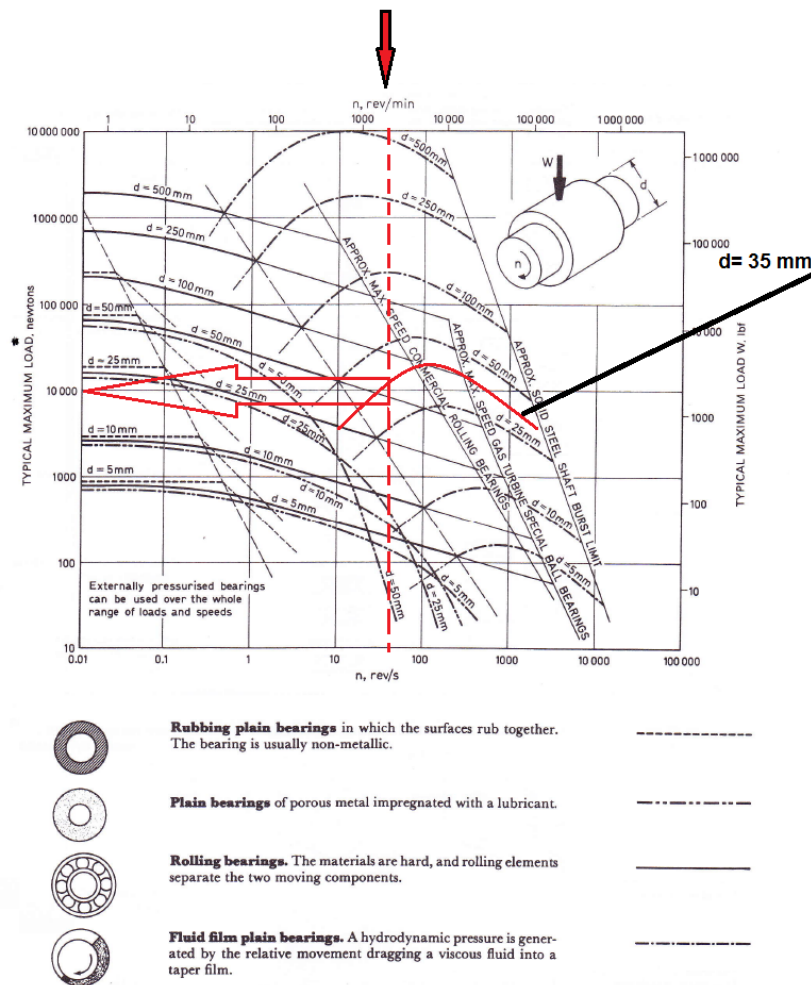
The shaft dimension
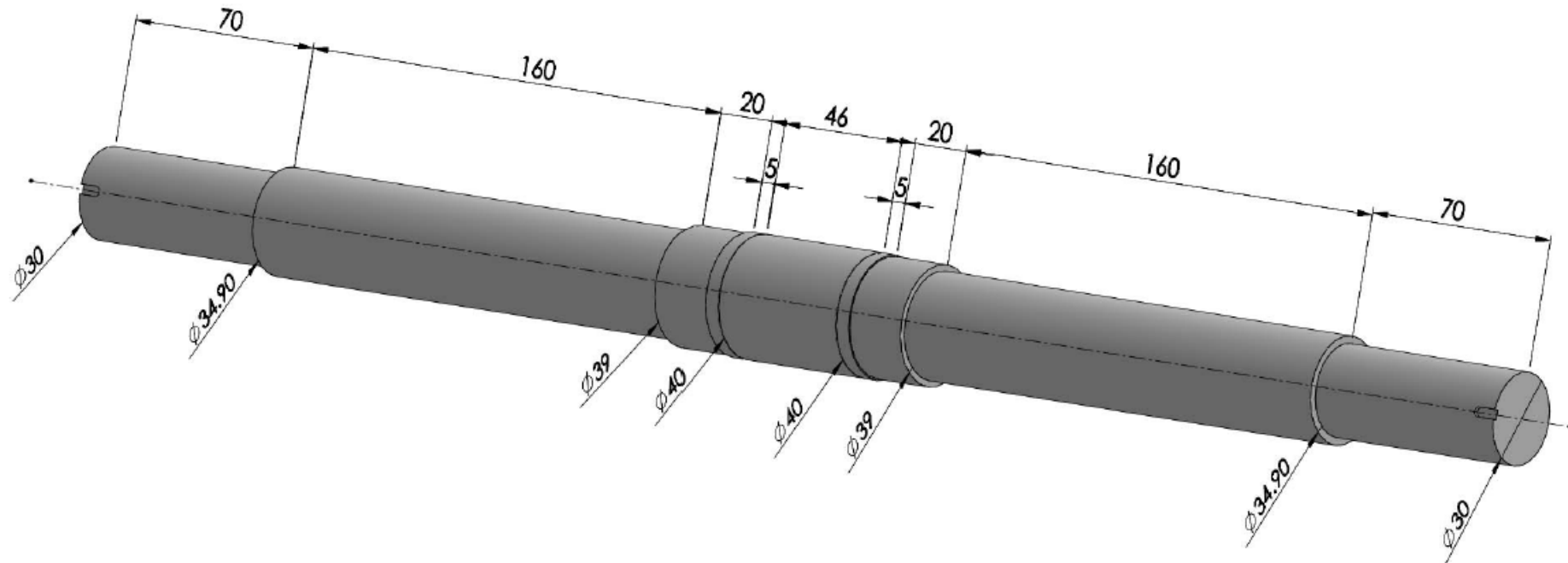
Assembly test rig

Accelerometers positions on bearing houses

Journal bearing design guide
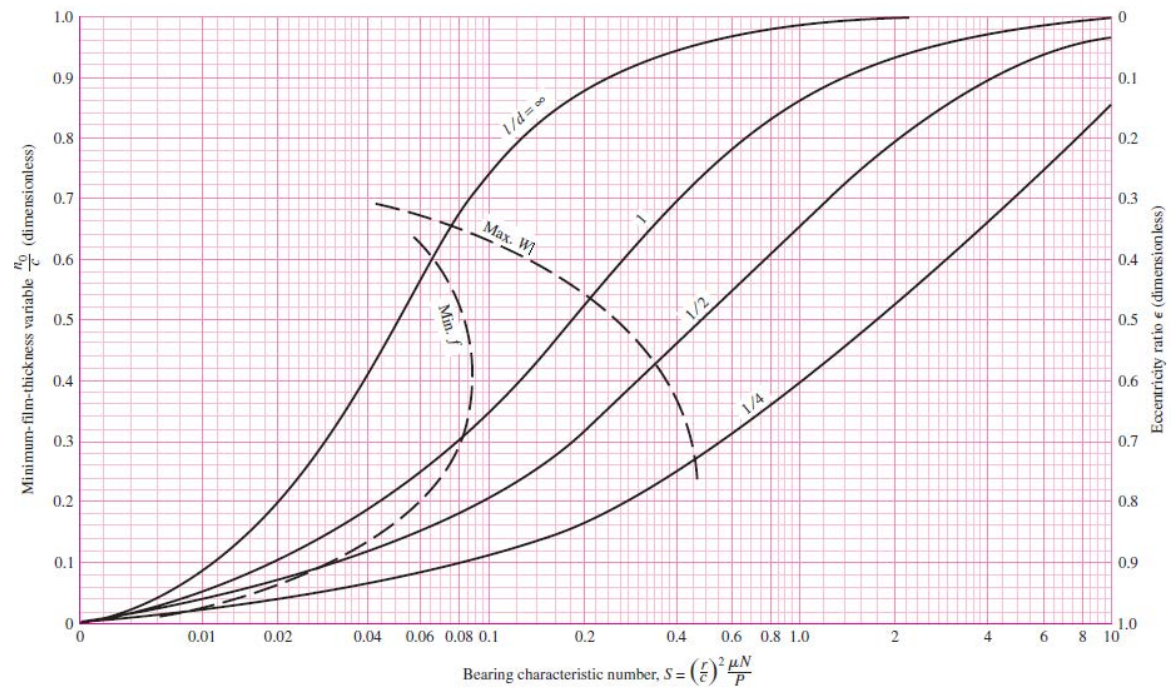

Load capacity base on speed, diameter of bearing [78]

Chart for minimum film-thickness variable and eccentricity ratio. The left boundary of the zone defines the optimal h0 for minimum friction; the right boundary is optimum h0 for load. (Raimondi and Boyd.) [73].

Sensors specifications

Qualification Certification

Type: IEPE Accelerometer
Model: CA-YD-182A
Serial No. 72582

SINOCE
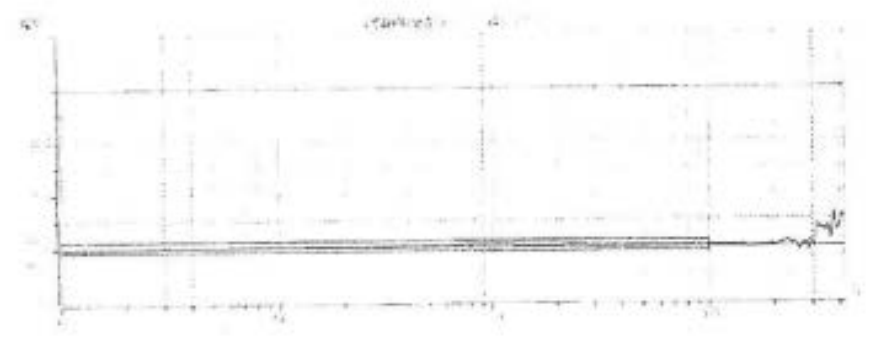
Voltage Sensitivity: 2.05 mV/ms^{-2}
Transverse Sensitivity: < 5 %
Accelerometer Limit: 2500 ms^{-2}
Capacitance: ------- pF
Resistance: ≤100 Ω
Polarity: +
Temperature Range: -40 to +120 ℃

Excitation Current: 2 to 10 mA
Power Supply: 12 to 24 VDC
Output base: 6 to 8 VDC
Mounting: M5
Frequency Range: 1 to 10, 000 Hz
Weight: 10 g
Output Connector: M5

Test Ambient:

Temperature: 19℃ Humidity: 65%

Checker: _____   Date: 2013.11.04

Frequency Response

Qualification Certification

Type: **IEPE Accelerometer**
Model: **CA-YD-182A**
Serial No. **72590**

Voltage Sensitivity: **1.99** mV/ms^{-2}

Transverse Sensitivity: **< 5** %

Accelerometer Limit: **2500** ms^{-2}

Capacitance: -------- pF

Resistance: **≤100** Ω

Polarity: **+**

Temperature Range: **-40 to +120** ℃

Excitation Current: **2 to 10** mA

Power Supply: **12to 24** VDC

Output base : **6to8** VDC

Mounting: **M5**

Frequency Range: **1 to 10, 000** Hz

Weight: **10** g

Output Connector: **M5**

Test Ambient:

Temperature:19℃   Humidity:**65%**

Checker: _____

Date: **2013.11.04**

Frequency Response

III.   APPENDIX C

Additional results from monitoring oil starvation (Chapter 7).
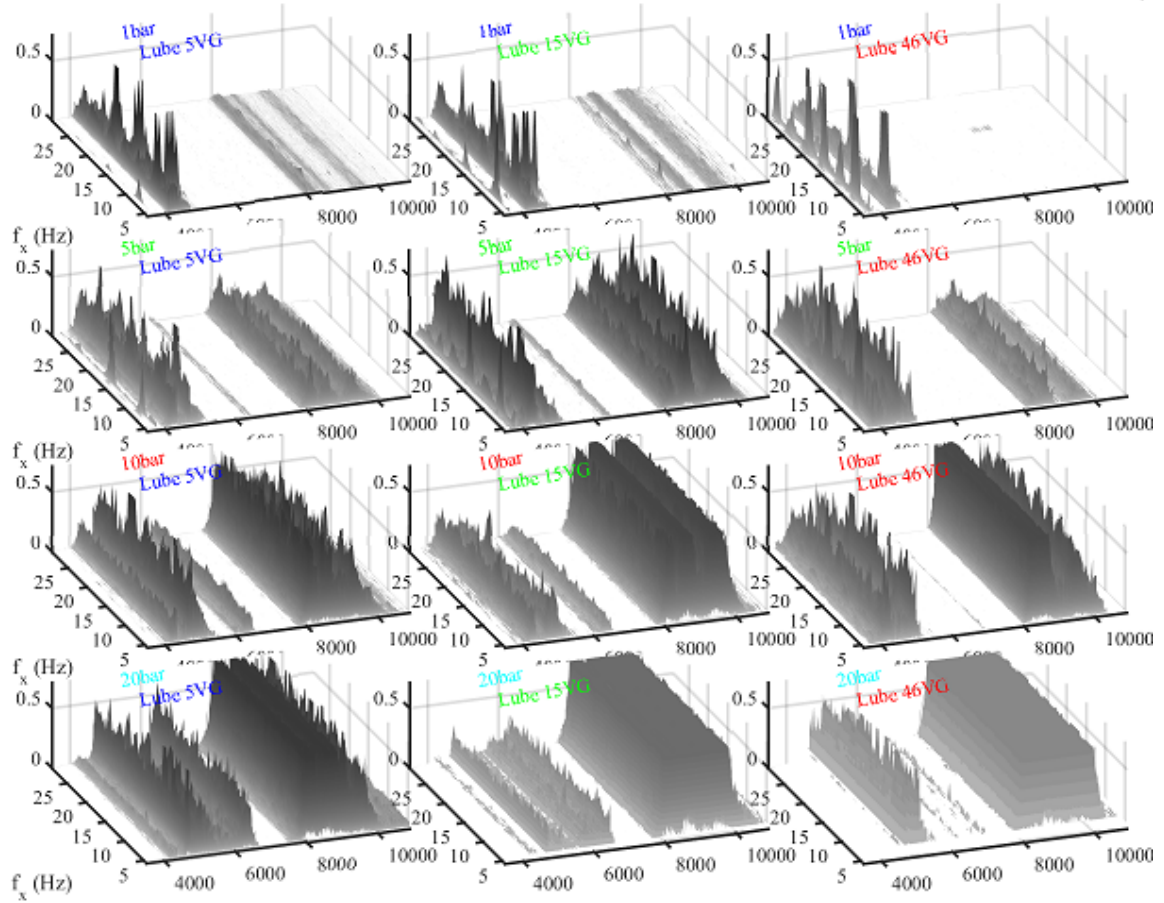
MSB magnitude for different loads and viscosity at 1200rpm
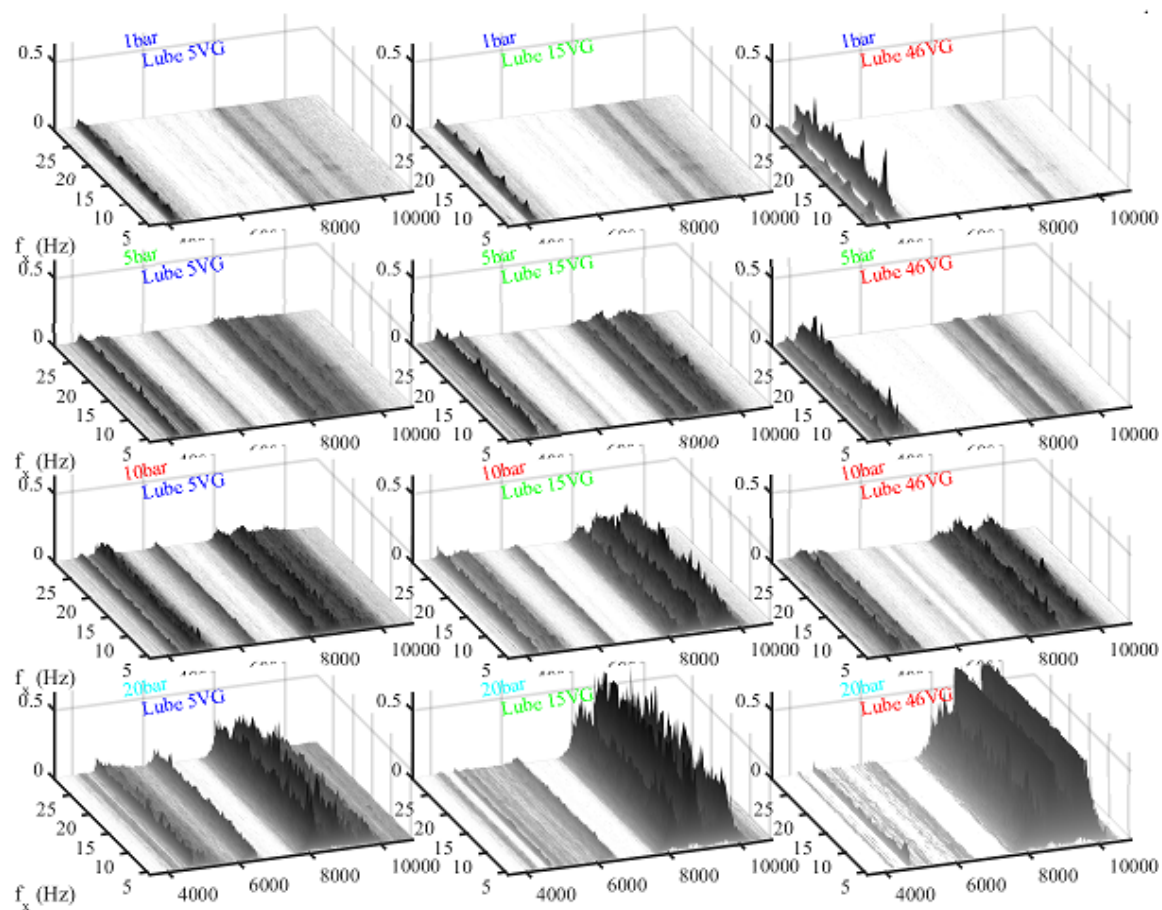
MSB magnitude for different loads and viscosity at 900rpm
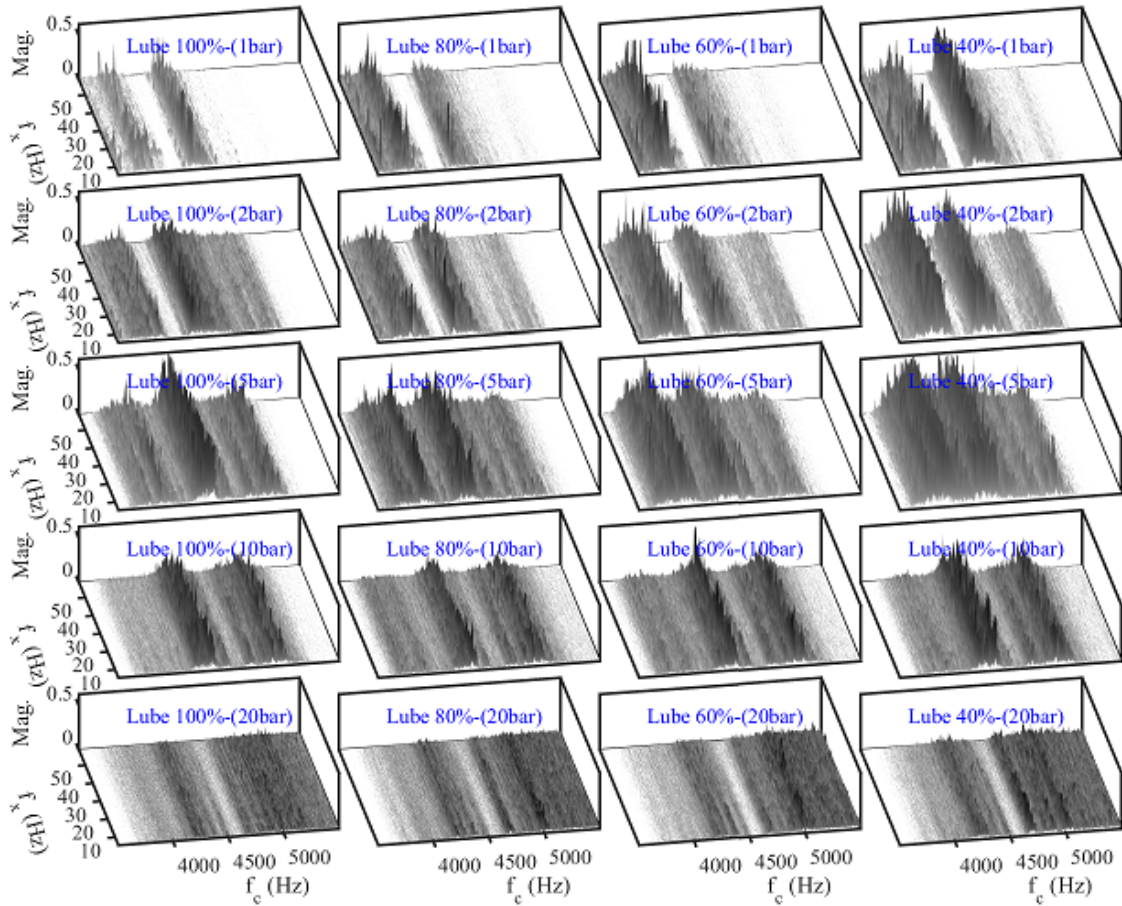
IV. APPENDIX D

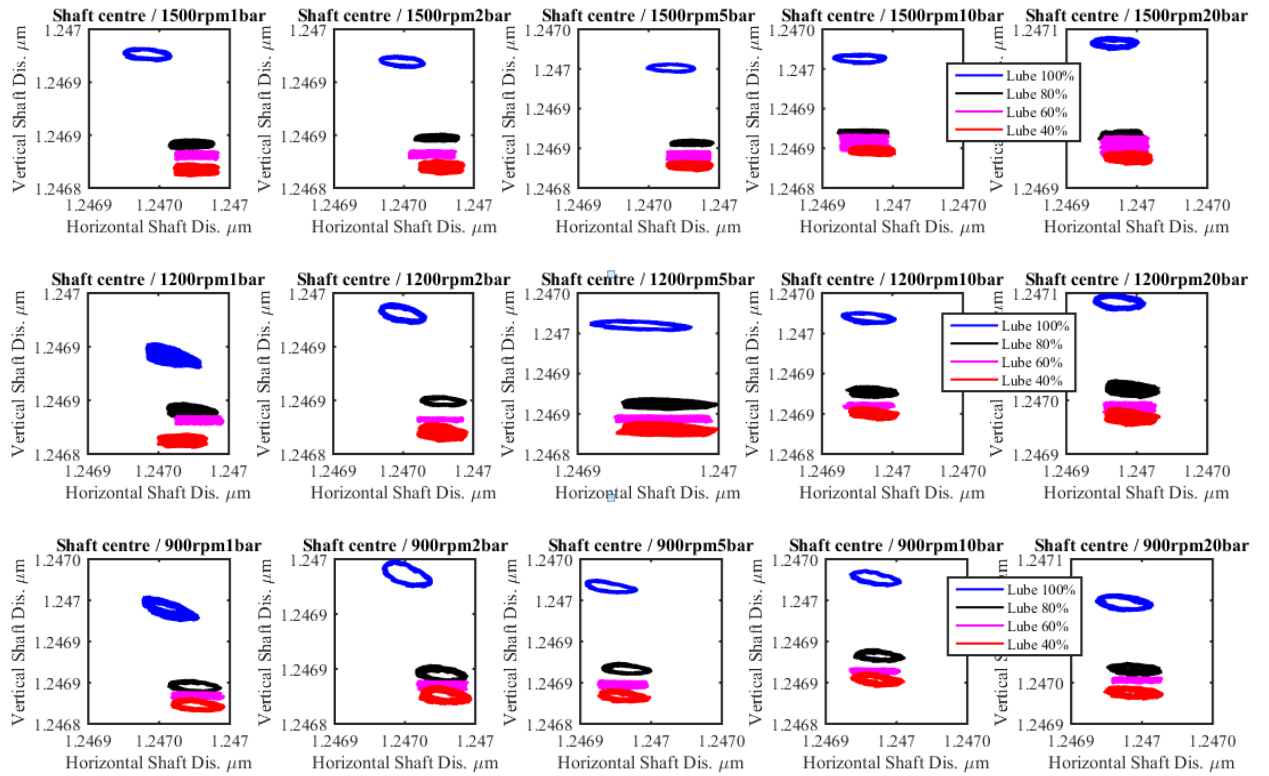Additional results from monitoring oil starvation (Chapter 8).
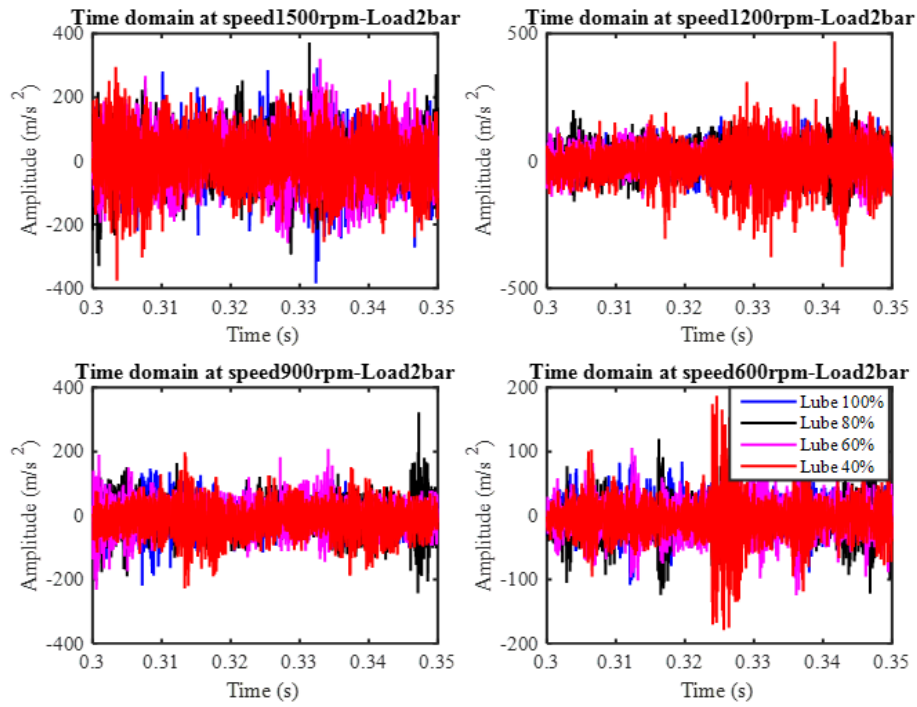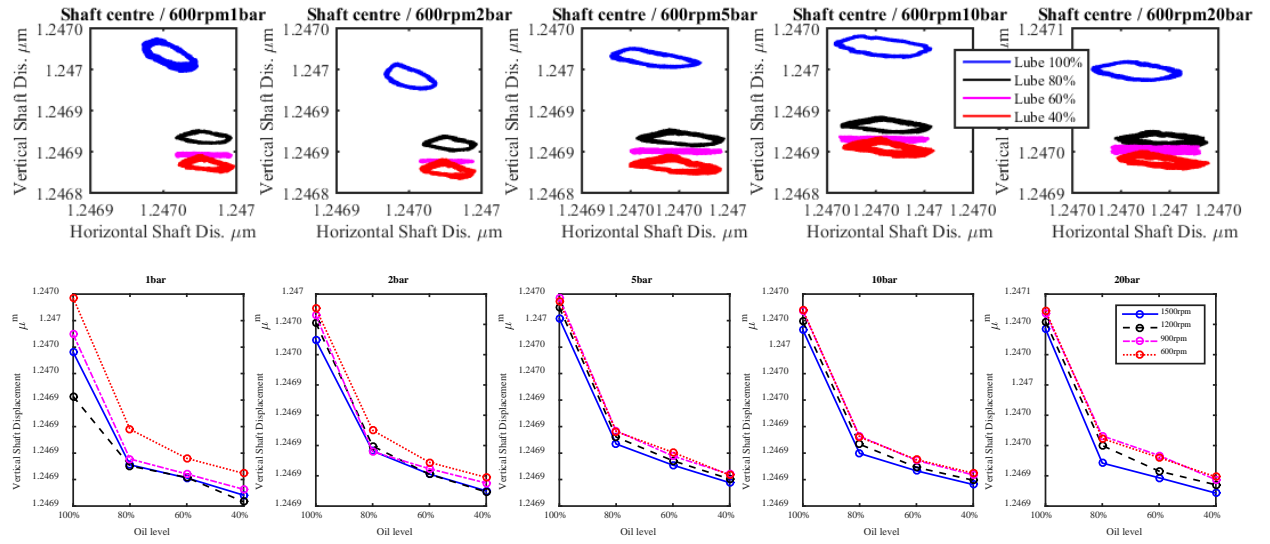

Time domain at different speeds under 2 bar
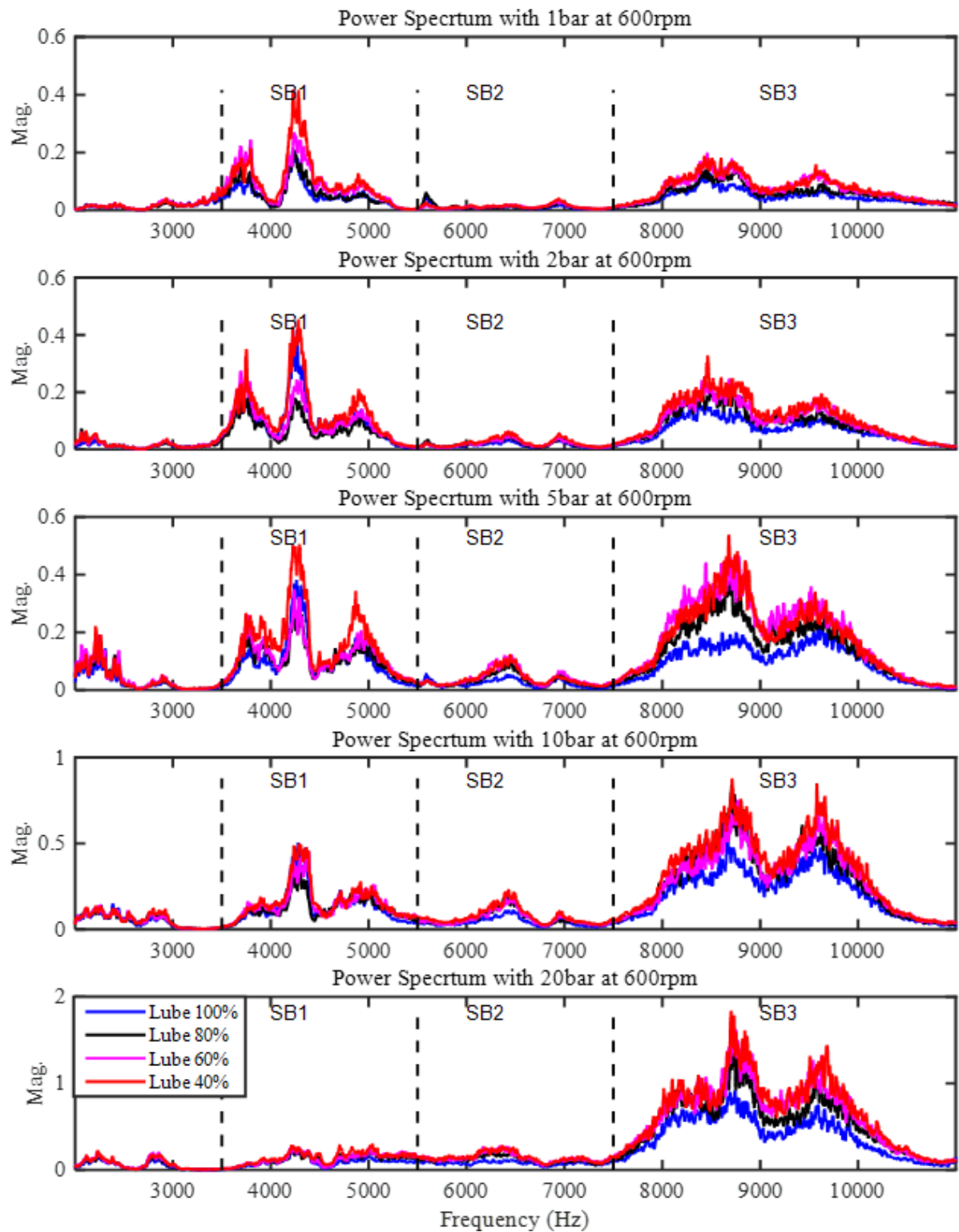
Spectrum at 600 rpm under different loads and oil levels

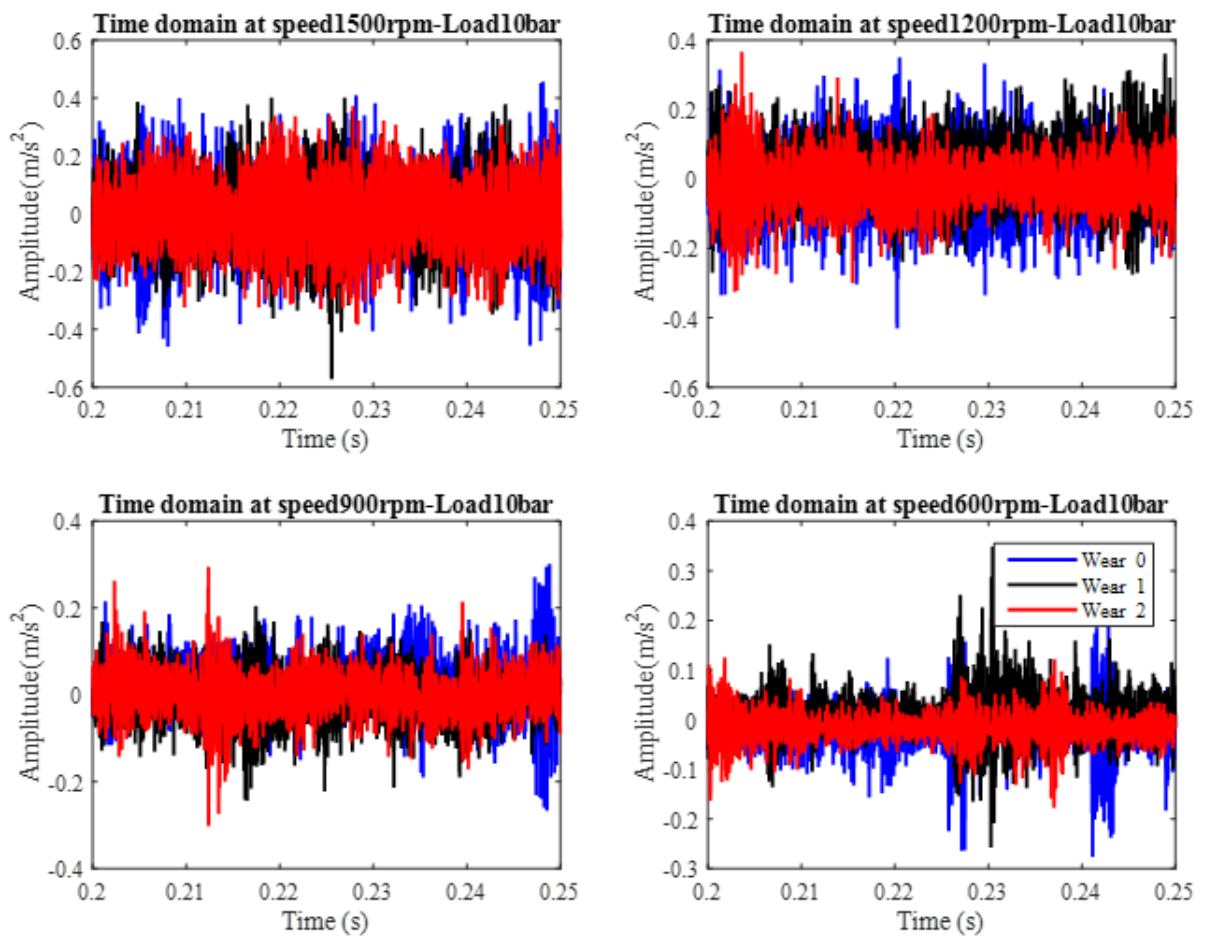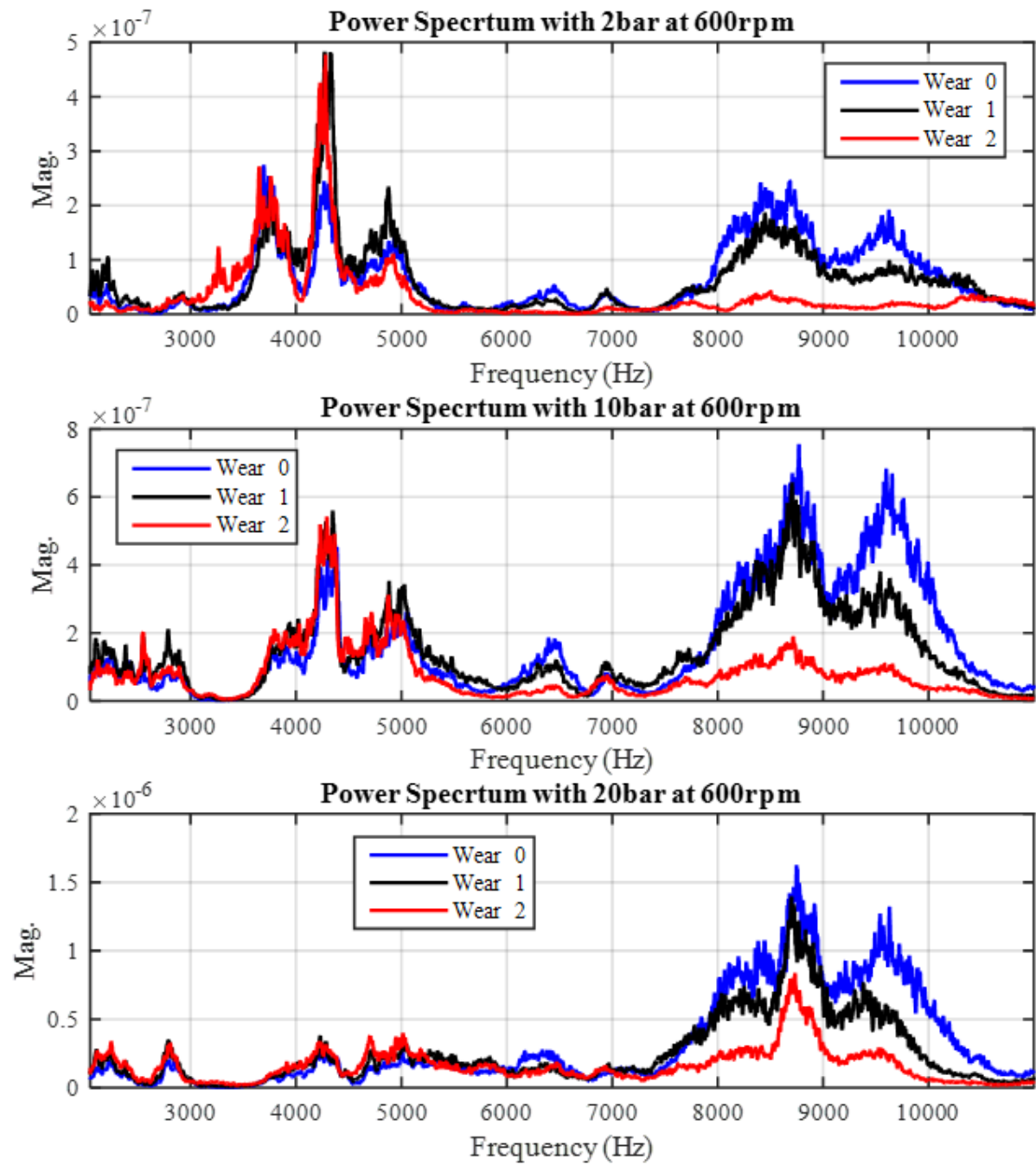MSB Magnitudes of SB1 vibrations at speed 900rpm

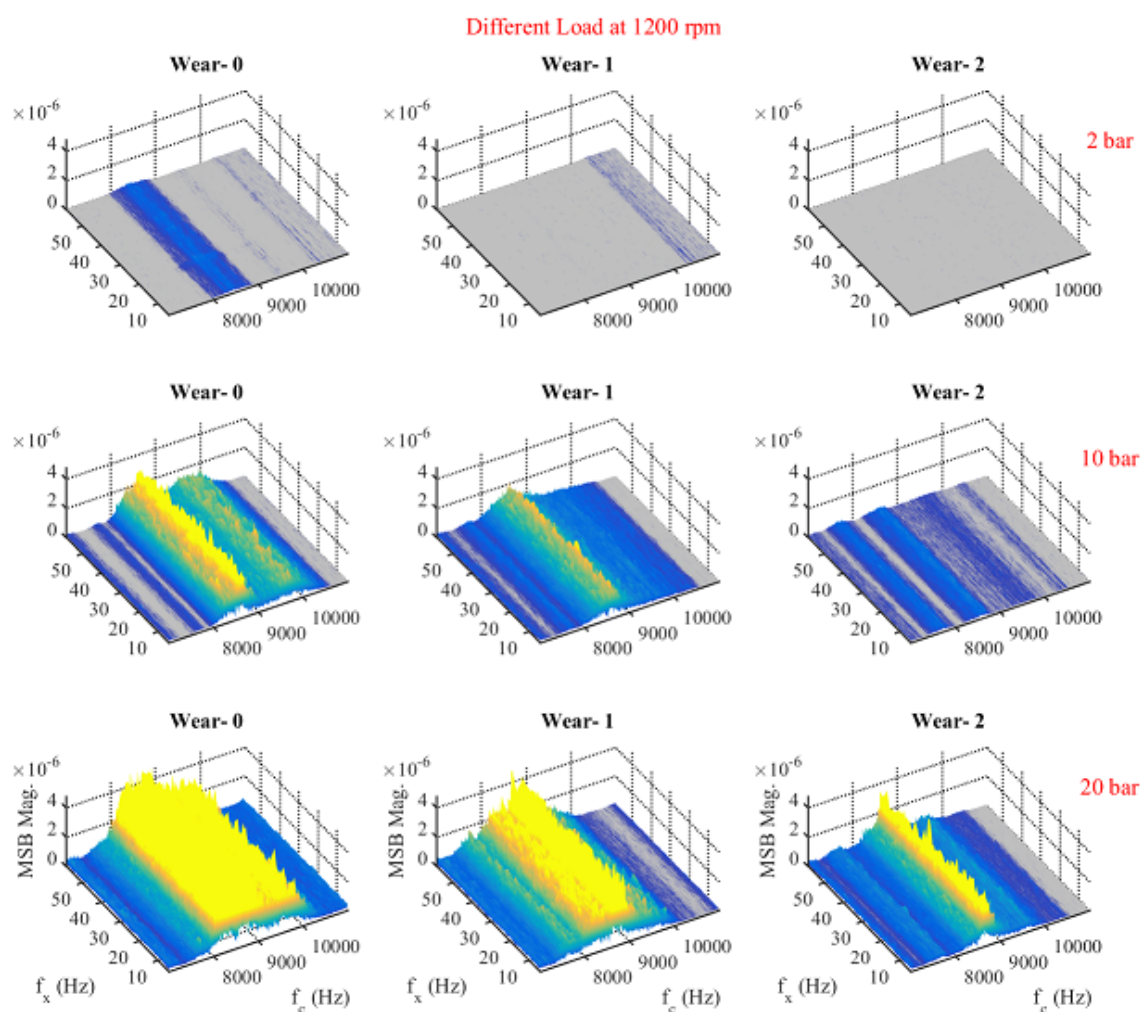Shaft position during a test

V.   APPENDIX E

Additional Results from worn bearing tests (Chapter 9).

Time domain at different speeds under 10 bar

Spectrum at 600 rpm under different loads of worn bearing

MSB Magnitudes of vibrations at speed of 1200rpm

my education has not finished,

today a new stage of it is opened

(Osama Hassin)